

**DENSITY TRANSITION BASED SELF-FOCUSING OF A SHORT PULSE
LASER IN PLASMA**

THESIS SUBMITTED TO
LOVELY PROFESSIONAL UNIVERSITY

FOR THE AWARD OF
DOCTOR OF PHILOSOPHY

IN
PHYSICS

BY
MANZOOR AHMAD WANI

(Reg. No. 11312810)

SUPERVISED BY

DR. NITI KANT

FACULTY OF TECHNOLOGY AND SCIENCES

**LOVELY PROFESSIONAL UNIVERSITY
PUNJAB**

NOVEMBER, 2016

DECLARATION

I hereby declare that the thesis entitled, **DENSITY TRANSITION BASED SELF-FOCUSING OF A SHORT PULSE LASER IN PLASMA** has been prepared by me under the guidance of Dr. Niti Kant, Associate Professor of Physics, Lovely Professional University. This work is entirely my original work and all ideas and references have been duly acknowledged. It does not contain any work for the award of any other degree or fellowship previously at any University.

Manzoor Ahmad Wani

Regd. No. 11312810

Department of Physics,

Lovely Professional University,

Phagwara, Punjab

Date:

CERTIFICATE

This is to certify that Manzoor Ahmad Wani has completed his Ph. D. thesis entitled, **DENSITY TRANSITION BASED SELF-FOCUSING OF A SHORT PULSE LASER IN PLASMA** for the award of Ph. D. of the Lovely Professional University under my guidance and supervision. To the best of my knowledge, the present work is the result of his original investigation and study. No part of the dissertation has ever been submitted for any other degree or fellowship previously at any university.

The thesis is fit for the submission and the partial fulfilment of the conditions for the award of Ph. D Physics.

Dr. Niti Kant
Associate Professor,
Department of Physics,
Lovely Professional university,
Phagwara-144402

Date:

ABSTRACT

In this thesis we have studied the **DENSITY TRANSITION BASED SELF-FOCUSING OF A SHORT PULSE LASER IN PLASMA** using Wentzel-Kramers-Brillouin (WKB) and paraxial approximations through parabolic wave equation approach. In chapter-3, self-focusing of Hermite-cosh-Gaussian (HchG) laser beam in plasma under density transition has been investigated theoretically by a ponderomotive mechanism. The results obtained indicate that HchG beams give freedom to additional source parameters mode index (m) and decentered parameter (b), changing the nature of self-focusing significantly. In this chapter it is observed that strong self-focusing occurs as the HchG beam propagates deeper inside the plasma as spot size shrinks due to highly dense plasmas. Further, increase in plasma density and decentered parameter ($b \leq 1$) results in enhancement of self-focusing of laser beam in plasma.

In chapter-4, density transition based self-focusing of cosh-Gaussian laser beam in plasma with linear absorption has been studied. The effect of density ramp on the self-focusing of laser has been studied at various values of absorption levels and decentered parameter. By choosing optimized laser and plasma parameters, the combined effect of density ramp, decentered parameter (characteristic of cosh-Gaussian beam) and linear absorption on beam width parameter has been investigated. The results show that the plasma density ramp, decentered parameter and linear absorption coefficient are in such a way that they change the nature of self-focusing / defocusing of the laser beams significantly. The absorption weakens the self-focusing effect and density transition sets an early and stronger self-focusing of cosh-Gaussian laser beam in plasma.

In chapter-5, investigation of relativistic self-focusing of Hermite-cosine-Gaussian laser beam in collisionless plasma has been studied and enhancement in self-focusing is observed. Depending up on the values of optimized laser and plasma parameters, the variation of dimensionless beam width parameter as a function of normalized propagation distance has been observed. The results obtained indicate that the laser beam focuses faster and earlier with smaller spot size. The spot size can be controlled by optimizing laser plasma parameters. The decentered parameter and laser intensity has a significant role in improving self-focusing of HcosG laser beam in plasma.

In chapter-6, nonlinear propagation of Gaussian laser beam in an inhomogeneous plasma under plasma density ramp has been studied. The results reveal that the amplitude of oscillation decreases considerably with the distance. The oscillatory behavior of beam width parameter becomes slow with increase in relative plasma density and intensity of laser beam. The saturation behavior of the beam width parameter shows that the laser beam evolves differently when propagates through underdense plasma. Further, after initial focusing of the laser beam, the relativistic mass effect is more pronounced in the region of high plasma density. Therefore, the plasma density ramp enhances the self-focusing effect to a greater extent.

In chapter-7, self-focusing/defocusing of chirped Gaussian laser beam in collisional plasma with linear absorption has been investigated. The results indicate that the laser beam is defocused due to strong diffraction and absorption effects at higher oscillation frequencies. It is further, revealed that initially the amplitude of beam width parameter is too large and continuously diverges in the collisional plasma. The chirp parameter minimizes the divergence and consequently, an earlier self-focusing of laser beam is observed. Apart from electron acceleration, the chirp can also be used to study the self-focusing / defocusing of laser beam in plasma. Thus, the chirp parameter is important for the self-focusing / defocusing of laser beam in plasma and plays a vital role in laser plasma interaction.

In chapter-8, self-focusing of a laser beam in the rippled density magnetoplasma has been studied. Effect of magnetic field and normalized ripple wave number on self-focusing of a laser beam has been analyzed at various optimized laser and plasma parameters. The results revealed that the magnetic field of a few MG increases the self-focusing capacity of laser beam strongly in rippled density plasma. Further, there is a strong coupling between the magnetic field and laser field. Due to the presence of suitable wavelength of density ripple in plasma, stronger and earlier self-focusing is achieved.

In chapter-9, self-focusing of Hermite-cosine-Gaussian (HcosG) laser beam in plasma under density transition has been investigated. The results obtained reveal that the density transition and decentered parameter (b) enhance the self-focusing of HcosG laser beams to a greater extent. It is noticed that the introduction of plasma density ramp makes a remarkable contribution in the process of self-focusing and it could produce ultrahigh laser irradiance over distances much greater than the Rayleigh length. Moreover, due to increase in the value of intensity of laser

beam, self-focusing enhances and shifts towards lower values of normalized distance of propagation.

PREFACE

The density transition based self-focusing of a short pulse laser in plasma is studied. In this work, we apply plasma density ramp and investigate its effects on the self-focusing of laser beam in plasma. As the phenomenon of self-focusing of laser beam in a nonlinear medium like plasma is widely studied by researchers and scientists as the converged beam has a lot of energy at a focused point. In the present study a high powerful laser beam gets focused as it propagates deeper and deeper in to the plasma so that an amount of energy generated in such a process can be visualized. In many useful applications like laser driven accelerators, laser driven fusion, x-ray lasers etc., high energy is required and hence, self-focusing is very useful in these cases. We have focused our attention on enhancing the self-focusing effect by using density transition and proper selection of various laser and plasma parameters. The enhancement in self-focusing of laser beam has been observed and reported in the present study.

Manzoor Ahmad Wani

Dated:

TABLE OF CONTENTS

S. No	Title	Page No.
01.	Declaration	[II]
02.	Certificate	[III]
03.	Abstract	[IV-V]
04.	Preface	[VI]
05.	Table of contents	[VII-IX]
06.	List of Figures	[X-XIII]
07.	Chapter – 1 Introduction and Overview	[1-7]
	1.1 Introduction 1.2 Self-focusing of laser beam in plasma 1.2.1 Ker- induced Self-focusing 1.2.2 Plasma Self-focusing 1.2.3 Thermal Self-focusing 1.2.4 Relativistic Self-focusing 1.2.5 Ponderomotive Self-focusing 1.3 Importance of Self-focusing 1.4 Importance of plasma density ramp	
08.	Chapter – 2 Review of Literature 2.1 Literature Review	[8-27]
09.	Chapter – 3 Self-focusing of Hermite – cosh – Gaussian laser beam in plasma under density transition 3.1 Introduction 3.2 Field distribution of HchG laser beams 3.3 Non – linear dielectric constant 3.4 Self-focusing	[28-47]

	3.5 Results and Discussion 3.6 Conclusion	
10.	Chapter – 4 Density transition based self-focusing of cosh – Gaussian laser beam in plasma with linear absorption 4.1 Introduction 4.2 Field distribution of cosh - Gaussian beams 4.3 Non – linear dielectric constant 4.4 Self-focusing equations 4.5 Results and Discussion 4.6 Conclusion	[48-64]
11.	Chapter – 5 Investigation of relativistic self-focusing of Hermite – cosine – Gaussian laser beam in collisionless plasma 5.1 Introduction 5.2 Field distribution of Hermite-cosine–Gaussian (HcosG) beam 5.3 Non – linear dielectric constant 5.4 Self-focusing equations 5.5 Self-trapped condition 5.6 Results and Discussion 5.7 Conclusion	[65-79]
12.	Chapter – 6 Nonlinear propagation of Gaussian laser beam in an inhomogeneous plasma under plasma density ramp 6.1 Introduction 6.2 Non – linear dielectric constant 6.3 Self-focusing equations 6.4 Results and Discussion 6.5 Conclusion	[80-89]
13.	Chapter – 7 Self-focusing/Defocusing of chirped Gaussian laser beam in collisional plasma with linear absorption	[90-106]

	7.1 Introduction 7.2 Self-focusing of chirped Gaussian laser beam 7.3 Results and Discussion 7.4 Conclusion	
14.	Chapter – 8 Self-focusing of a laser beam in the rippled density Magnetoplasma 8.1 Introduction 8.2 Non – linear dielectric constant 8.3 Self-focusing equations 8.4 Results and Discussion 8.5 Conclusion	[107-125]
15.	Chapter – 9 Self-focusing of Hermite – cosine – Gaussian laser beam in plasma under density transition 9.1 Introduction 9.2 Field distribution of Hermite – cosine – Gaussian (HcosG) beam 9.3 Nonlinear dielectric constant 9.4 Self-focusing equations 9.5 Numerical results and Discussion 9.6 Conclusion	[126-139]
16.	Chapter – 10 Summary and Conclusion	[140-143]
17.	Chapter – 11 References	[144-158]
18.	Biodata	[159-160]
19.	Appendix / List of Publications	[161-162]
20.	Published Papers	[163]

LIST OF FIGURES

Figures	TITLE	Page No.
Figure 3.1 (a)	Dependence of f on ξ for various values of ω_{p0}/ω . The other parameters are $b = 0$ and $d = 5$.	[43]
Figure 3.1 (b)	Dependence of f on ξ for various values of ω_{p0}/ω . The other parameters are $b = 1$ and $d = 5$.	[44]
Figure 3.2 (a)	Dependence of f on ξ for various values of b . The other parameters are $\omega_{p0}/\omega = 0.02$ and $d = 5$.	[45]
Figure 3.2 (b)	Dependence of f on ξ for various values of b . The other parameters are $\omega_{p0}/\omega = 0.03$ and $d = 5$.	[46]
Figure 3.3	Dependence of f on ξ for various values of b . The other parameters are $\omega_{p0}/\omega = 0.04$ and $d = 5$.	[47]
Figure 4.1	Dependence of f on ξ for various values of k'_i and ω_{p0}/ω at $b = 0$.	[60]
Figure 4.2	Dependence of f on ξ for various values of k'_i and ω_{p0}/ω at $b = 1$	[61]
Figure 4.3	Dependence of f on ξ for various values of k'_i and ω_{p0}/ω at $b = 2$.	[62]
Figure 4.4	Dependence of f on ξ for $\omega_{p0}/\omega = 0.2$, $k'_i = 2$ and for various decentered parameter (b) values.	[63]
Figure 4.5	Dependence of f on ξ for $\omega_{p0}/\omega = 0.5$, $b = 1$ and for various values of k'_i	[64]
Figure 5.1	Dependence of $\rho_0(r_0\omega_{p0}/c)$ on αE_0^2 for $m_0/M = 0.02$ and $\gamma = 1.25$	[75]
Figure 5.2	Dependence of f_1 and f_2 on ξ for various values of b . The other parameters are $\omega_{p0}/\omega = 0.6$, $\alpha E_0^2 = 1.5$, $m_0/M = 0.02$, $r_0\omega/c = 50$, $\gamma = 1.25$	[76]

Figure 5.3:	Dependence of f_1 and f_2 on ξ for various values of αE_0^2 . The other parameters are $\omega_{p0}/\omega = 0.4$, $b = 0.5$, $m_0/M = 0.02$, $r_0\omega/c = 50$, $\gamma = 1.25$	[77]
Figure 5.4	Dependence of f_1 and f_2 on ξ for various values of b . The other parameters are $\omega_{p0}/\omega = 0.6$, $\alpha E_0^2 = 2$, $m_0/M = 0.02$, $r_0\omega/c = 50$, $\gamma = 1.40$	[78]
Figure 5.5	Dependence f_1 and f_2 on ξ for various values of ω_{p0}/ω . The other parameters are $\alpha E_0^2 = 1.2$, $m_0/M = 0.02$, $r_0\omega/c = 50$, $\gamma = 1.25$ and $b = 0.5$	[79]
Figure 6.1	Dependence f on ξ for various values of ω_{p0}/ω . The other parameters are $d = 10$, $\varepsilon_2 E_0^2 = 10$, $\rho^{-2} = 0.04$.	[87]
Figure 6.2	Dependence f on ξ for various values of $\varepsilon_2 E_0^2$. The other parameters are $\omega_{p0}/\omega = 0.4$, $d = 15$, $\rho^{-2} = 0.08$	[88]
Figure 6.3	Dependence f on ξ for various values of ρ^{-2} . The other parameters are $\varepsilon_2 E_0^2 = 10$, $\omega_{p0}/\omega = 0.8$, $d = 10$	[89]
Figure 7.1	Dependence of f on ξ for various values of v/ω_0 . The other parameters are: $\omega_p/\omega_0 = 0.4$, $\alpha E_0^2 = 0.4$ and $b = 0$	[101]
Figure 7.2 (a)	Dependence of f on ξ for various values of b . The other parameters are: $\omega_p/\omega_0 = 0.4$, $\alpha E_0^2 = 0.4$ and $v/\omega_0 = 0$	[102]
Figure 7.2 (b)	Dependence of f on ξ for various values of negative chirp. The other parameters are same as taken in the figure 7.2 (a).	[103]
Figure 7.3	Dependence of f on ξ for various values of ω_p/ω_0 . The other parameters are: $v/\omega_0 = 0.002$, $\alpha E_0^2 = 0.4$ and $b = 0.002$	[104]

Figure 7.4	Dependence of f on ξ for various values of αE_0^2 . The other parameters are: $\nu/\omega_0 = 0.002$, $\omega_p/\omega_0 = 0.4$, and $b = 0.002$	[105]
Figure 7.5	Dependence of f on ξ for various values of intensity. The other parameters are: $\nu/\omega_0 = 0.002$, $\omega_p/\omega_0 = 0.6$, and $b = 0.002$	[106]
Figure 8.1	Dependence of f on ξ for various values of α_0 . The other parameters are: $d = 59$, $\omega_{p1}/\omega = 0.4$, $\omega_{p2}/\omega = 0.15$ and $\omega_c/\omega = 0.12$.	[120]
Figure 8.2	Dependence of f on ξ for various values of λ . The other parameters are: $d = 59$, $\omega_{p1}/\omega = 0.4$, $\omega_{p2}/\omega = 0.15$, $\omega_c/\omega = 0.12$ and $\alpha_0 = 0.3$.	[121]
Figure 8.3	Dependence of f on ξ for various values of ω_{p1}/ω . The other parameters are: $d = 59$, $\omega_c/\omega = 0.12$, $\omega_{p2}/\omega = 0.15$ and $\alpha_0 = 0.3$	[122]
Figure 8.4	Dependence of f on ξ for various values of ω_{p2}/ω . The other parameters are: $d = 59$, $\omega_c/\omega = 0.12$, $\omega_{p1}/\omega = 0.4$ and $\alpha_0 = 0.2$	[123]
Figure 8.5	Dependence of f on ξ for various values of ω_c/ω . The other parameters are: $d = 59$, $\omega_{p1}/\omega = 0.4$, $\omega_{p2}/\omega = 0.15$ and $\alpha_0 = 0.3$	[124]
Figure 8.6	Dependence of f on ξ for various values of d . The other parameters are: $\omega_{p1}/\omega = 0.4$, $\omega_{p2}/\omega = 0.15$, $\alpha_0 = 0.3$ and $\omega_c/\omega = 0.12$	[125]
Figure 9.1 (a)	Dependence of f_1 and f_2 on ξ for various values of ω_{p0}/ω . The decentered parameter is fixed at $b = 0$ and the other parameters are $\alpha E_0^2 = 2$, $m/M = 0.02$, $r_0\omega/c = 50$ and $d = 10$	[136]
Figure 9.1(b)	Dependence of f_1 and f_2 on ξ for various values of ω_{p0}/ω . The	[137]

	decentered parameter is fixed at $b = 1$ and the other parameters are same as taken in Figure 9.1 (a)	
Figure 9.2	Dependence of f_1 and f_2 on ξ for various values of decentered parameter b . The other parameters are: $d = 10$, $\alpha E_0^2 = 2$, $m/M = 0.02$, $r_0 \omega / c = 50$ and $\omega_{p0} / \omega = 0.5$	[138]
Figure 9.3	Dependence of f_1 and f_2 on ξ for various values of αE_0^2 . The decentered parameter is fixed at $b = 1.5$ and the other parameters are same as taken in Figure 9.2	[139]

CHAPTER-1

INTRODUCTION AND OVERVIEW

1.1 INTRODUCTION

After the discovery of self-focusing of light by Askaryan in 1962 [1], the process of self-focusing of laser beam in plasma is of great importance for various applications like plasma based charged accelerators [2, 3], laser-driven fusion [4], x-ray lasers [5-7], laser electron acceleration [8-12], fast igniter concept of inertial confinement fusion [13-15], ionospheric modification [16-19] etc. So laser beams have always been an interesting area of research for many years which has inspired theoretical and experimental interest [2-12]. To preserve such an efficient interaction of laser beams with the plasmas, it is necessary for these beams to propagate in plasma over extended distances without loss of energy. Further, for the above mentioned applications and to guide the laser beam, preformed plasma channels are necessary so that due to natural diffraction the beam in vacuum expands infinitely. Due to recent advances in such laser pulse technology, we are able to focus the laser beam to extremely higher intensities ordering 10^{20} W/cm². The investigators choose the propagation of different kind of laser beams profile like Gaussian beams [20], cosh-Gaussian beams [21], Hermite-Gaussian beams [22], Hermite-cosh-Gaussian beams [23-25], Hypergeometric Gaussian subfamily beams [26], cos-Gaussian beam [27] etc. in the plasma. The study of such pulses makes feasibility to analyze an important nonlinear phenomenon like self-focusing. Further, the relativistic nonlinear optical effects are arisen that are most important phenomena to study relativistic self-focusing, thermal self-focusing and ponder motive self-focusing. When the laser power is greater than its critical value, the relativistic effect becomes dominant. However, when it is smaller then the beam diffraction dominates over relativistic self-focusing [105, 144].

There is an increasing interest in these days in investigating the interaction of laser radiations with plasmas. Therefore the study of various phenomena's like self-focusing, self-phase modulation and various instabilities are of prime importance as these phenomena's significantly govern the experiments on various advanced physical events like plasma based charged accelerators, laser driven fusion etc. When a highly powerful laser beam passes through partially

ionized plasma it changes its refractive index, which has a linear as well as a nonlinear component. It is the ponderomotive force which makes the electrons to move away out of an axis region and changes the electron density distribution. This further changes the refractive index of plasma medium and hence leads to process of self-focusing [138]. The ponderomotive and relativistic nonlinear effects arise due to the interaction of free electrons of the ionized plasma with the propagating laser radiation. While as the interaction of unionized atoms leads to atomic nonlinearities. The relativistic nonlinearity leads to self-focusing and the ponderomotive nonlinearity leads to plasma density perturbation which in turn is believed to affect the focusing properties of the laser pulse. Further, when the plasma electrons are set to relativistic quiver motion due to intense laser beam, the ponderomotive nonlinearity sets in and leads to electron density perturbation inside the plasma. This perturbation is caused due to $\mathbf{V} \times \mathbf{B}$ force which is exerted by the radiation field on the free plasma electrons. Such nonlinear relativistic effects of the laser beam as it enters through partially stripped plasma have been studied in great detail. However, the effects produced by ponderomotive nonlinearity along with these effects have not been included in many studies. Since both the nonlinearities are in such a way that they change the beam propagation through plasmas, so it is important to study their combined effect [55].

Most of the investigations about the process of self-focusing have been done in unmagnetized plasmas and have neglected the effect of magnetic field. Their self-generation in laser produced plasmas influences the self-focusing and propagation of laser beams by modifying the dielectric permittivity of plasma [139, 140]. However taking in to account the relativistic electron mass variation, field aligned magnetic perturbations and static density in magnetized plasma, the electromagnetic filamentation instability is investigated [141]. The laser beam evolution in cold, magnetized and underdense plasma is studied by using dependent expansion source method. The transverse magnetic field reduces the critical power which is a basic need for the beam to self-focus [142]. Further, in the Gaussian laser beam evolution in collisional warm magnetoplasma, self-focusing strength is increased. The oscillation period of beam width parameter decreases due to increase in collision frequency. With this the self-focusing occurs faster in comparison to the stationary oscillation regime without the collision frequency [143]. With the availability of high power laser systems and an increasing interest in laser induced fusion generation, most of the investigators have used the fundamental Gaussian beam and simplest class of relativistic case of

reference. This makes it possible to inquire the fascinating nonlinear process such as self-focusing. Furthermore, the interaction of lasers with semiconductors has been considered an important and captivating field for many decades. The nonlinear phenomena's are also due to the semiconductors [20] which act like a medium. The fact that self-focusing is being observed in semiconductors is of great pertinence to possibilities of optical limiting devices and various practical applications. In the equilibrium condition, the temperature of the free carriers and that of the crystal is almost same so that the net exchange of energy between them is zero. In the steady state, with the application of electric field, the free carriers gain energies and results in higher temperature than that of the crystal [63]. This change in carrier temperature leads to corresponding change in the effective mass of carriers which plays a captivating and an important role for self-focusing in semiconductors [24]. Thus, the interaction of lasers with semiconductors continues to be a front line area of research.

Most of the electromagnetic beams have a non-uniform distribution of irradiance along the wave-front. This non-uniform distribution of irradiance has been taken in to account in harmonic generation. It is well known that these beams show the phenomenon of self-focusing/defocusing. Also, for non-uniform irradiance distribution and for a given power of the beam, it is found that the average of the power of the electric vector in the wave-front is much higher than that for uniform irradiance distribution. Hence, in the case of non-uniform irradiance, the magnitude of the generated harmonic is higher. This provides a strong motivation for the study of the growth of the harmonics in plasma when self-focusing is taken in to account [145]. Therefore, the propagation of electromagnetic waves having non-uniform intensity distribution through plasmas is a problem of considerable importance. Since, at low power densities diffraction causes divergence of the wave while as this picture is changed drastically at high power densities. Furthermore, in laser plasma interactions which involve high intensities, a laser beam can overcome natural diffractive defocusing and can remain focused via its own nonlinear interaction with the plasma [144]. The self-focusing effect can be produced due to the relativistic mass increase of electrons, change in the refractive index and also due to density perturbation caused by radiation or thermal pressure [20, 106].

1.2 SELF FOCUSING OF LASER BEAM

The process of self-focusing of laser beams in plasmas has been considered a subject of extensive study over the last few decades [146]. It has wide applications in energy fusion driven by lasers, laser wake-field acceleration, beat wave accelerator, x-ray lasers etc. When a Gaussian laser beam propagates in non-linear medium like plasma, the intensity is greatest on the axis of the medium and the index of refraction would be greater on the axis than off the axis of medium. Due to such induced refractive index variations the wave front of the laser acquires a curvature and hence tends to focus. The process is known as self-focusing. In other words it is a nonlinear process that has been produced by change in the refractive index of materials when made visible to electromagnetic radiations. It is frequently observed when generated radiation (by femto second laser) propagates through many solids, liquids and gases. It is also caused by the intensity dependent refractive index, $\partial\eta/\partial|E|^2 > 0$ which arises due to relativistic mass effect, ponderomotive force, non-uniform ohmic heating [147] and subsequent plasma diffusion. At an instant when relativistic nonlinearity arises, it requires very high laser intensity so that the electron quiver velocity becomes comparable to the velocity of light in vacuum ($v \sim c$) [146]. Because of the various mechanisms that produce refractive index variations, in turn result in self-focusing. There are two main cases in self-focusing which are as follows.

1.2.1 Kerr-induced self-focusing: This type of self-focusing is brought about by the modification in refractive index of the materials when electromagnetic radiations are made incident up on them. Optical Kerr-effect is non-linear process which occurs when an intense electromagnetic radiation interacts with the nonlinear medium, and produces a variation in the refractive index (η) as $\eta = \eta_0 + \eta_2 I$, where η_0 is the linear part and η_2 is the non-linear part of the refractive index [148]. I is called radiation intensity. If the radiation power is greater than the critical power then self-focusing arises and critical power is given by $P_{cr} = \alpha \lambda^2 / 4\pi n_0 n_1$, where λ is the wavelength of the radiation and α is a constant that depends on the spatial initial distribution of the beam.

1.2.2 Plasma self-focusing: The first quantitative field of study for self-focusing of laser radiation was developed for dielectric materials i.e. non-ionized solids, liquids and gases. In advance laser technology, the most interesting area is the observation of self-focusing of laser

beams in plasmas. The process of self-focusing is caused by the change in refractive index of the medium, when laser beam propagates through it. There are two dominating contributions [149]. One is the relativistic mass increase of electrons that comes from the quiver motion of electron in the electrical field of the refractive index. It decreases the beam spot size with beam energy focused inward. Another resulting from excitation of electron plasma wave is the force of the beam. The interplay and evaluation of such processes is not a simple task, but the outset relationship for critical power [105, 144]

$$P_{cr} = \frac{m_e \omega^2 c^5}{e^2 \omega_p^2} \approx 17 \left(\frac{\omega}{\omega_p} \right)^2 \text{ GW}$$

Where, ω is the radiation angular frequency of incident laser, m_e is the mass of electron, c the speed of light and e the electronic charge. The self-focusing can be thermal, relativistic and ponderomotive.

1.2.3 Thermal self-focusing: It arises when the density of perturbation is caused by radiation or thermal pressure, respectively. It is because of collision heating of plasma, due to induced hydrodynamic expansion that leads to an increase in refractive index and hence further heating. It could initiate the process of self-focusing which decreases the filament size and increases the intensity in the filament.

1.2.4 Relativistic self-focusing: This is the nonlinear mechanism for the modification of the refractive index for plasma. Relativistic self-focusing arises due to the mass increase of electrons, which change the refractive index n_{rel} as $n_{rel} = \left(1 - \omega_p^2 / \omega^2\right)^{1/2}$, where, ω_p the relativistic plasma frequency.

1.2.5 Ponderomotive self-focusing: The ponderomotive nonlinearity is important to self-focusing. It is due to expulsion of the electrons from the focal spot. Ponderomotive self-focusing is generated in plasma due to ponderomotive force which makes the electrons to move away out of the region having higher intensity, leaving behind a region of lowered electron density and increased refraction index and hence induces a focusing effect. Since the refraction index of plasma depends on the electron density n_e and critical density n_c . It is given as $n = \left(1 - n_e / n_c\right)^{1/2}$

the depletion of electrons at the place where intensity is large raises the refraction index, slows down the phase velocity of the light wave and causes the wave-fronts to acquire curvature so that the light is focused towards the original region of enhanced intensity. So, the light wave energy propagates normal to the curved wave front. So an initial section of the beam with a slightly higher intensity than its surroundings will become more intense as the beam propagates.

1.3 IMPORTANCE OF SELF FOCUSING

The self-focusing effect plays a captivating and crucial role in a number of applications like those of laser-driven fusion, plasma based charged accelerators, x-ray lasers, harmonic generation, electron acceleration in wake-field, inertial confinement fusion etc. It is very undesirable in those applications where compression of fuel pellets can be prevented and provides a method of obtaining high flux densities which are necessary to study laser plasma interactions [35]. It further imposes a restriction on the power which can be transmitted through an optical medium and often leads to damage in optical materials [28]. So, it can be considered as a limiting factor in designing the high-power laser systems. Further, the ponderomotive force which expels radially the electrons of an intense laser beam, lead to cavitation in plasma [48]. In case of collisional plasmas with nonlinear absorption, the nonlinearity in absorption cancels the effect of divergence. The relativistic mechanism manifests itself for intense pico-second laser pulses and makes the study very important. The laser propagates in a periodically focused manner if the laser power is above the critical power and undergoes divergence, if it is below the critical power [105]. The relativistic self-focusing effect is produced due to relativistic mass change. If in plasma, the frequency becomes greater than the natural frequency of electron oscillations, then the electrons will be forced to move away out of the beam field. The focused beam then exerts a radial ponderomotive force on electrons and makes them to move away out of the beam, producing a lower density region which results in focusing of the radiation [28]. Remarkable self-focusing effects have been observed recently with femto second laser beams propagating in the atmosphere and light filaments in the air. From such air filaments (permitting spectroscopy), a broad spectrum of radiation from ultraviolet to mid-infrared is generated in the atmosphere. The entire absorption spectrum can be determined by a single pulse from a portable femto second laser. Another exciting possibility of the use of these filaments containing plasmas is to guide lightning away from sensitive sites.

1.4 IMPORTANCE OF PLASMA DENSITY RAMP

The plasma density ramp or density transition in plasma occupies a crucial and captivating role in laser-plasma interactions as it is used to overcome the defocusing of laser beam [64]. A highly powerful laser beam that undergoes through underdense plasma acquires a very lower spot size due to relativistic effect and hence regular and repeated self-focusing or defocusing of the beam takes place. In order to make the self-focusing effect a bit stronger, density ramp is considered [77, 92, 97, 99]. It is because in the density ramp region, the laser beam detects a narrowing channel and hence in this environment, the oscillation amplitude contracts while as frequency of laser beam increases. Again, electron density being an increasing function of the propagation distance, the dielectric constant of plasma decreases rapidly as the laser beam deepens in to the plasma. With the result, the laser beam gets more focused and hence self-focusing effect is enhanced [22, 85]. Further, to abstain the laser from defocusing and to observe better and maximum focusing nature, the length of the density ramp is to be increased in an underdense plasma [64]. So, plasma density ramp has a captivating role in making the self-focusing effect stronger. The gas jet plasma based experiments observe such a kind of plasma density ramp. The magnetic fields along with the density ramp have also been found to increase the focusing capacity of beam [65, 91, 93, 102]. In other words, the magnetic field is found to act like a catalyst for self-focusing phenomenon [65]. This scheme forms a basis for various laser-driven applications as the laser beam not only is focused but propagates up to a long distance without divergence.

CHAPTER-2

REVIEW OF LITERATURE

2.1 LITERATURE REVIEW:

The study of self-focusing of laser light in plasma is a captivating field and has become a subject of considerable interest. As these phenomena's occupy an important place in a large number of applications like x-ray lasers, harmonic generation, laser driven plasma based accelerators and inertial confinement fusion. So laser beams have always been an interesting area of research for many years.

Askaryan (1962) [1] was the first who discussed the self-focusing of laser beam in plasma by considering the energy momentum flux density of the beam. The whole plasma has been expelled and the pressure thereof was balanced by the plasma pressure profile acting against the centre of the laser beam. Askaryan was able to compare the required optical intensities for compensating the gas dynamic pressure.

Hora (1969) [28] studied the self-focusing process by a ponderomotive mechanism and treated it in terms ponderomotive acceleration. It occurs due to light intensity gradient. The radiation focusing takes place within the first minimum of diffraction. It then adjusts a lower limit for the usual lasers having laser power of the order of 1MW. But this is possible only if a temperature of about 10eV is authenticated.

Litvak (1970) [29] studied the self-focusing in magnetoactive plasma for the case of longitudinal propagation. The nonlinearity mechanisms for the magnetoactive plasma have been studied and expressions are obtained for the nonlinear corrections to the refractive index due to heating, and nonlinear motion of a single electron. They have obtained the necessary condition for self-focusing and determined the characteristic parameters for self-focusing of the beam.

Sodha et al. (1971) [30] investigated theoretically the propagation and focusing of an electromagnetic wave in inhomogeneous dielectrics. They concluded that the focusing length is enhanced in a medium where the dielectric constant is a decreasing function of axial distance of propagation and vice-versa.

Sodha et al. (1973) [31] studied the nonlinearity in the dielectric constant of strongly ionized plasma and concluded that the non-linearity comes because of the heating and redistribution of the electrons. The energy loss gained from the field is due to thermal conduction. This self-induced non-linearity causes self-focusing and oscillatory waveguide propagation of the beam even though the non-linear dielectric constant does not fall in the saturating range. In a typical case of 10^{10} W laser, the axial intensity is enhanced by a factor of 25 and has been predicted in a length scale of 0.6cm.

Sodha et al. (1974) [32] investigated the process of self-focusing/defocusing of laser beam operating in the TEM_{01} mode. They concluded that the cylindrical symmetry and the power of irradiance increases inside the medium and gets concentrated around the points of maximum irradiance in different directions. Further they observed that a figure of eight is being made by the polar representation of maximum irradiance in the transverse plane.

Sodha et al. (1974) [33] investigated the process of self-focusing of a cylindrically symmetric electromagnetic pulse in collision-less and collisional plasmas. They considered the ponderomotive force and the non-uniform heating as a source of non-linearity. They further considered that the pulse duration is larger than the characteristic time of non-linearity. They found that the beam is focused in a moving filament. But in collisional plasmas and due to relaxation effects, the peak of the pulse is shifted to higher values. However, in case of collision-less plasmas, the pulse is severely distorted because of self-focusing and the peak shift is not significant.

Sodha and Nayyar (1975) [34] observed that the electromagnetic energy gets converged in the x-direction and vice-versa as the refractive index decreases with increasing temperature in the TEM_{01} mode. They also found that in the case of geometric-optics, the thermal self-focusing / defocusing of beam occurs in TEM_{00} and TEM_{10} cylindrical modes.

Siegrist (1976) [35] used the constant shape paraxial-ray approximation to discuss the propagation of intense laser beams in plasmas. It is further found that the stationary self-focusing behavior of each mechanism is treated separately and similar with several orders of magnitude difference in critical power. Further, in stationary self-focusing due to the combined mechanisms,

the occurrence of relativistic effects is prevented by the complete saturation of ponderomotive self-focusing.

Nayyar (1978) [36] studied the self focusing in strongly ionized plasma by consideration of a non-Gaussian beam that operates in TEM₀₁ mode. It is found that the focusing effects are observed in Y-direction when the incident power of beam becomes larger than the critical power. Whereas, beam divergence takes place in X-direction. However, in the reverse case the normalized beam width parameter f_2 first increases in Y-direction and after penetrating a certain depth inside the medium, it attains a broadened maximum and then starts decreasing with the propagation distance. The beam continues to diverge in the X-direction and the extent of self focusing is reduced by the absorption.

Nayyar and Soni (1979) [37] reported that in collisional plasma, the non-linear dependence of the dielectric constant is due to inhomogeneous heating of energy carriers and in collision-less plasma, it is due to ponderomotive force. Further they found that the beam gets focused at different points in different planes and hence exhibits the effect of astigmatism. In certain power regions they have considered, the beam either converges or diverges in both directions. While in some other regions of the power spectrum, one dimension of the beam focuses while the other defocuses. The beam then propagates in an oscillatory waveguide mode.

Askar'yan et al. (1981) [38] studied the nonlinear defocusing of a focused beam and observed a fine beam from the focus zone. They have used a single-mode, unmodulated neodymium laser with energy of 1J and with a millisecond pulse and a YAG-Nd laser in operating single and high frequency millisecond-pulse repetition modes and experimentally explained the defocusing nature of the beam in the weakly absorbing nonlinear medium.

Mori et al. (1988) [39] found that initially relativistic self focusing occurs initially due to filamentation and then by an extreme and unexpected ponderomotive mechanism at the boundary of channel walls. It is less intense for single frequency illumination and more for resonant double frequency.

Kurki et al. (1989) [40] have obtained the steady-state asymptotic solution of beam propagation in a localized solitary waveform in slab geometry and also presented the solutions for the beam profile where it is oscillatory in nature, which correspond to the fact or condition of being present the steady-state solution of a multiple-beamlet profile.

Cicchitelli et al. (1990) [41] have shown that the electromagnetic beams in vacuum do have a longitudinal component that can be proved experimentally from the polarization independence of the energy of electrons from the focus of a laser (Lax, Louisell, and Knight (LLK)). They have developed the LLK paraxial approximation to a Maxwellian exact solution for a Gaussian beam and included the exact longitudinal field components of the laser beam.

Cohen et al. (1991) [42] investigated the dynamics of ponderomotive self-focusing in plasmas. They calculated the space-time evolution of non-linear coherent beam and the parameters under consideration have dominant non-linearity in terms of the ponderomotive force and the plasma response is quite hydrostatic. It can be important both for high-power laser applications including inertial-confinement fusion and for heating of magnetically confined plasmas with intense, pulsed free electron lasers.

Brandi et al. (1993) [43] investigated the high-irradiance propagation of a laser beam in plasma whose optical index has a non-linear relationship with light intensity through both theoretical and numerical analysis. The nonlinear effects examined include expulsion of electrons and decrease of the plasma frequency. The defocusing and focusing effects are assumed to remain cylindrical and for plasma supposed homogeneous medium are along the propagation direction.

Chen et al. (1993) [44] derived a set of three dimensional equations for the propagation of an intense laser pulse of arbitrary strength $a = eA/mc^2$ in cold underdense plasma. In different limits, these equations can be reduced to certain previous one dimensional model. Chen *et al.* found that for $|a| < 1$, an approximate set of equations from the averaged Lagrangian is obtained. They solved the axisymmetric two dimensional model equations numerically to show the effect of dispersion in the self focusing process.

Bulanov et al. (1995) [45] studied that an ultra-short, relativistically strong pulse can be self-focused in plasma with strong magnification of its amplitude and channelling in a narrow channel shaped like a “bullet”. Plasma turbulence occurs in the region occupied by the pulse and behind it and leads to electron heating. It is found that a regular longitudinal electric field is produced in the wake of a wide pulse shorter than the plasma wave period and behind the shape edge of a long pulse. The transverse nonuniformity of the pulse causes the formation of horseshoe structures that is used to focus and accelerate electrons and protons. Hence fast and strong modulation of the pulse occurs by the induced focusing of the EM radiation.

Gibbon et al. (1996) [46] experimentally studied the self-channeling and relativistic self-focusing of a terawatt laser pulse in the range of $(0.7TW \leq P \leq 15TW)$ by using paraxial envelope model. The model described the laser propagation and the plasma response is being described by the ponderomotive force. They have shown that a laser intensity of 5–15 times may be obtained in vacuum when P lies in the $(1.25 - 4) \times P_c$ range.

Asthana et al. (2000) [47] studied relativistic self-focusing when Gaussian beam is incident normally on a plane interface of a linear medium and a non-linear, non-absorbing plasma with an intensity dependent dielectric constant. They considered non-linearity to arise from the relativistic variation of mass and the Lorentz force on electrons and followed WKB and paraxial approximation to analyze the relativistic self-focusing of transmitted laser radiation for the arbitrary magnitude of non-linearity. They found that as the upper critical power increases, minimum beam radius and focal length decreases so that the refraction at the interface has an effect on self-focusing.

Belafhal and Ibnchaikh (2000) [23] have studied the relative intensity distribution of the Hermite-cosh-Gaussian beams for the propagation in the free space. They also reported the normalized intensity plots of the Hermite-cosh-Gaussian beam profiles for the propagation through an aperture lens for various values of the truncation parameter for different mode indices.

Hafizi et al. (2000) [48] found that the ponderomotive force associated with an intense laser beam expels electrons radially and can lead to cavitations in plasma. Relativistic effects as

well as ponderomotive force which acts in such a way that it expels electrons and hence modifies the refractive index. They derived an equation for the laser spot size, using the source-dependent expansion method with Laguerre-Gaussian Eigen functions, and reduced to quadrature. The envelop equation is valid for arbitrary laser intensity within the long pulse, quasi-static approximation and neglects instabilities. The significant contraction of the spot size and an increase in intensity is possible when the laser power surpasses the critical power.

Osman et al. (2000) [49] proposed an investigation of the behavior of a laser beam having finite diameter in plasma. They studied it with respect to the forces and optical properties leading to the self-focusing in non-relativistic regime. The fugacious setting of ponderomotive nonlinearity in a collision less plasma results in the focusing of plasma wave at high laser intensities. Further, they considered the relativistic effects to compute an expression for the relativistic self-focusing for Nd glass radiation, at different plasma densities. Furthermore, a numerical program in c⁺⁺ has been developed to examine or to investigate the deepness of self-focusing.

Liu and Tripathi (2000) [50] investigated the laser frequency up-shift, ring formation in tunnel ionizing gases and self-defocusing in plasmas. In their work a high-intensity laser produces rapid tunnel ionization of gas and the refractive index decreases by increasing plasma density which in turn causes frequency up-shift and super-continuum generation. However, refractive index decreases due to tunnel ionization when the laser intensity profile peak is on the axis and thus causes defocusing of the laser. This defocusing reduces the rate of ionization and frequency up-shift.

Feit et al. (2001) [51] studied the description of powerful beam self focusing in plasma. They emphasized on the total electron evacuation under the effect of ponderomotive forces. They displayed a method which showed that a laser beam can be self channeled in underdense plasma if the laser intensity is high enough to yield cavitations. It is studied that cavitation results in suppression of filamentation and the possibility to channel power well above the nominal critical power of self focusing for a distance of many Rayleigh lengths.

Faure et al. (2002) [52] discussed experimentally pulse duration effects on self-focusing of lasers in underdense plasmas. It was shown by them that the nominal critical power P_c for relativistic self-focusing in particular is not the only parameter that describes the pulse duration in comparison to plasma particle motion. However, using time resolved shadowgraphs, it has been displayed by them that a pulse does not self-focus relativistically if its duration is excessively short. This is due to divergence by the longitudinal wake that has been generated by the laser pulse itself. However, the phenomenon of self-focusing can occur for powers much less than the critical power. This is because of the radial expansion of ions that creates a channel which combines with relativistic effect and makes the laser pulse to focus.

Nitikant and Sharma (2004) [53] have seen the pulse slippage effect on resonant second harmonic generation. In their work they found that process of second harmonic generation is enhanced resonantly by the application of a magnetic wiggler. The laser gives an oscillatory velocity to electrons at $(2\omega_1, 2k_1)$ and exerts a longitudinal ponderomotive force. The electrons at the second harmonic acquire an oscillatory velocity and the wiggler magnetic field beats to produce a transverse second harmonic current at $(2\omega_1, 2k_1 + k_0)$. It then drives the second harmonic electromagnetic radiation whose amplitude saturates. The so created beam then stumbles out of the main beam.

Sharma et al. (2004) [54] extended the formalism of self-focusing of electromagnetic waves to include nonlinear absorption by the medium. Further they employed a complex eikonal which does not need any approximation about the relative magnitudes of the real and imaginary parts of the dielectric constant or their dependence on the irradiance of the beam. They found that the nonlinearity in absorption tends to cancel the effect of divergence on account of diffraction. The beam-width and attenuation depends on distance of propagation

Jha et al. (2004) [55] studied the propagation characteristics and modulation instability of a laser beam propagating through partially stripped plasma. They found that the ponderomotive non linearity tends to defocus the laser beam as against the nonlinear relativistic self-focusing phenomenon. Also the current density perturbation arising due to ponderomotive nonlinearity, when combined with relativistic nonlinearity tends to increase the modulation instability of the

laser beam. However the peak growth rate is enhanced and also increases the range of unstable wave numbers in comparison to the case where ponderomotive nonlinearity is neglected.

Kant and Sharma (2004) [56] studied that second harmonic in plasma is generated by a Gaussian beam when magnetic wiggler of suitable period is present. For a particular value of the Wiggler period, the phase matching conditions are satisfied. The intensity of the second harmonic pulse is enhanced by self-focusing of the primary pulse. It then experiences a repeated and regular focusing in plasma channel which is formed by the primary wave.

Kant and Sharma (2005) [57] reported that a laser pulse focuses near the axis when incident on a cylindrical dielectric fibre perpendicular to the axis of the fibre. The focusing effect is enhanced for a given radius of the fibre and for a laser of specific intensity. However, in the axial region the tunnel ionization is produced due to high intensity of the laser. Further, the optical breakdown of the dielectric results in electron-hole pair production and plasma formation in the form of capillary and the plasma tends to self-defocus the laser.

Prakash et al. (2005) [58] investigated the focusing and defocusing of a beam in a medium which is depicted by built in radial inhomogeneity. They used the paraxial approximation and nonlinearity having saturating nature. Using an eikonal and parabolic equation for wave propagation, they found that the beam width and an axis irradiance depends on the distance of propagation. Further they concluded that the media in which an electromagnetic beam is guided by inhomogeneity in refractive index with a small cross section over long path lengths are ideal for achieving highly efficient nonlinear interactions.

Varshney et al. (2005) [59] presented an investigation of relativistic self-focusing of laser radiation in inhomogeneous plasma by using paraxial approximation. The nonlinearity in the dielectric constant appears on account of the relativistic mass variation for an arbitrary magnitude of intensity. For a circularly polarized wave, the nonlinear dielectric constant has been used in analyzing the laser-beam propagation. The dependence of the beam width parameter variation, the self-trapping condition and the critical power have been examined. Depending on the plasma inhomogeneity and the initial intensity, the laser beam behaves in such a way that it

likely acquires a constant value whose numerical estimation is done for typical values of the laser–plasma interaction.

Saini and Gill (2006) [60] presented the dynamics of combined effects of nonlinearity and spatial diffraction. They used the variation approach and observed the phenomenon of cross-focusing where focusing of one beam width parameter results in defocusing of another beam width parameter and vice-versa. However no stationary self-trapping is observed but oscillatory self-trapping occurs far below the threshold and the regularized phase is always negative in collision-less magneto-plasma.

Kumar et al. (2006) [61] discussed the nonlinear effects due to relativistic decrease of the plasma frequency and the ponderomotive expulsion of electrons. From the fluid equations they obtained have been used to study the amplitude variation of the excited electron plasma wave. It is observed that the inclusion of ponderomotive nonlinearity is significant on the excitation of plasma wave. This affects the number of energetic electrons and their energy ranges on account of wave particle interaction.

Sodha and Sharma (2006) [62] investigated the mutual focusing/defocusing of Gaussian electromagnetic beams in collisional plasma. In their work, they have considered the mutual focusing/defocusing in singly ionized collisional plasma which is initially in thermal equilibrium and the ionosphere with singly charged ions. They started from the expression of the electron temperature in terms of the irradiance of the waves and derived expressions for the electron density and the dielectric function. The power loss by electrons to heavy particles is supposed to be more larger than that due to thermal conduction. The dominant nonlinearity considered here is the radial redistribution of the electron density on account of the radial dependence of the electric field of the waves and consequently of the electron temperature. Using this expression for the dielectric function, the coupled wave equations corresponding to different beams have been solved in the paraxial approximation, yielding a system of coupled second-order differential equations for the beam-widths. They also solved coupled equations for the widths of two beams numerically for some typical cases and correspondingly the critical curves for the two beams have also been obtained. They have also considered specifically effect of one beam on the critical

curve of the other beam. They presented their results in the form of graphs for plasmas in thermal equilibrium and also for day-time mid-latitude ionosphere at a height of 150 km.

Gupta and Suk (2007) [63] studied the self-focusing and spot size behavior in semiconductor plasma. They have shown that enhancement in focusing is possible by beating of two co-propagating laser beams that can promote a large amplitude plasma wave in a resonant manner inside a narrow gap semiconductor. The medium is made highly nonlinear by the ponderomotive force of the electrons due to the plasma beat wave. As a result, the incident laser beam becomes self-focused.

Gupta et al. (2007) [64] found that a high- power laser beam propagating through underdense plasma under plasma density ramp acquires a very lower spot size due to relativistic self-focusing. Further away from the focus, it is the nonlinear refraction that weakens and the waist size of the laser increases. The density transition is introduced in order to abstain the laser from defocusing. This causes the reduction in the laser spot size close to the axis of propagation. In the absence density ramp, the laser is de-focused beyond the Rayleigh length due to the supremacy of the diffraction effect and in the presence of an upward plasma density ramp, as the plasma density increases, it occurs sooner and becomes stronger.

Gupta et al. (2007) [65] observed the focusing by taking in to account both density transition and magnetic field. They found that the magnetic field acts in such a way so as to increase the rate of self-focusing. This scheme forms a basis for various laser-driven applications as the laser beam not only is focused but propagates over a long distance without divergence.

Agarwal and Sodha (2007) [66] analyzed the linear absorption effect and initial curvature on focusing/defocusing in an inhomogeneous nonlinear medium by following paraxial approximation. It has been found that the lower and higher values of the beam width go on decreasing with increase in absorption along with propagation distance. This continues till the beam becomes very weak and diverges in a steep manner. Its penetrating power also decreases with increasing absorption in an overdense medium. Depending up on the initial values of beam width and axial irradiance, the beam initially converges and then goes in the oscillatory divergence, self-focusing or smooth divergence mode. The greatest value of the penetrating

power occurs in the range $-0.7 < (\partial f/\partial z)_{\text{at } z=0} < 0.4$ and outside these limits, it falls in a sharp manner.

Faisal et al. (2008) [67] developed the energy balance equation for electrons and equations which express the pressure gradient balance of electrons and ions to the force produced by space charge field. They also solved equation for initial time profile at $z=0$ of the pulse to obtain f as a function of normalized distance and time profile. It is seen by them that in the initial period the beam suffers steady divergence because of the nonlinearity that does not build up to sufficient extent. Later, the behavior changes to oscillatory divergence, then oscillatory convergence, and again oscillating divergence and finally smooth divergence. This is explained by the fact that focusing is dependent on the rate of change of nonlinearity with the irradiance, rather than on the magnitude of the nonlinearity. They used both Gaussian as well as sine time profile of the pulse for investigation.

Patil et al. (2008) [25] studied the HchG laser beam propagation by considering a non-degenerate germanium containing neutrality of space charge. They applied the parabolic wave equation approach and used the paraxial approximation to obtain the analytical solutions by following the inequality $R_n < R_d$, where, R_n and R_d are the self-focusing length and diffraction length respectively. The so examined behavior of beam width parameter showed that the process of self-focusing occurs for various decentered parameter values.

Kaur and Sharma (2009) [68] observed that a laser beam propagates in a regularly and repeatedly focused manner above the critical power of the laser. However, the beam follows divergence below this power. At significantly greater powers, the laser beam converges till the saturation effect of nonlinearity puts an end to self-focusing and diffraction succeeds. The density ripple causes self-focusing length to rise and the spot size variation depends on the wave number of the ripple.

Verma and Sharma (2009) [69] developed a theoretical model to study the self-focusing effect. They found that after the passage of laser beam, the plasma expands and creates a channel with minimum electron density on the axis. The second pulse of lower duration and much lower

intensity is capable of heating the electrons, hence raising the ionization rate and suppressing the recombination ratio. This leads to significant enhancement of the plasma channel lifetime. The formation of the channel by the first pulse requires a time delay of $\sim 5-10$ ns between the two pulses to allow radial ambipolar diffusion of the plasma. The second laser pulse undergoes periodic focusing in such a channel leading to a strong heating rate of the electrons. The second pulse then self-focuses, enhances the heating rate and lengths the lifetime of the plasma channel.

Parashar (2009) [70] investigated the self- focusing effect on third harmonic generation in a gas embedded with atomic clusters. The results obtained reveal that the effectiveness of third harmonic is sensitive to the ratio of electron density inside the clusters to critical density. As the clusters expand under hydrodynamic pressure caused by the laser, efficiency is maximum at an instant when this ratio is three for clusters on the laser axis as these clusters contribute maximum to harmonic generation. The efficiency is also greatly enhanced by self-focusing. Since laser spot size varies in a periodic manner with the propagation distance. Due to competition between self-focusing and diffraction effects, it was found that the efficiency of harmonic generation also shows a similar behavior.

Takale et al. (2009) [71] used the parabolic wave equation approach for entire theoretical formulation and completed the numerical computation of TEM_{op} Hermite-Gaussian laser beam by following Runge-Kutta method. They obtained the differential equations for beam width parameters under paraxial approximation and observed perfectly synchronized periodic oscillations of beam width parameters in transverse directions in small scale spatial manipulations in optical trap.

Bonabi et al. (2009) [72] analyzed the Gaussian beam propagation in underdense plasma by considering density transition. The outcomes they have obtained indicate that the laser beam becomes highly focused and penetrates deep into the plasma medium by reduction of diffraction effect. In their work, they introduced a unique ramped density profile which increased self-focusing effect for intense laser systems and puts an end to the transverse variation of the wave packet. They established an equation for laser spot size and presented the computational curves for self-focusing. The outcomes they have obtained showed that the intense laser beams can be

focused down to diameters comparable to the Nd-glass laser wavelength. The effects of laser intensity on the self-focusing parameters were also investigated. Based on their reliable derived equations and introduction of more effective ramped density profile, a much sooner and stronger focusing is observed.

Patil et al. (2009) [73] established the differential equation under WKB and paraxial approximations and analytical solution is obtained for the same. By considering various absorption levels in the medium, the behavior of beam width parameter is studied at various decentered parameter b values. Their results show that the sharp self-focusing occurs on the grounds of absorption. Further they suggested that depending up on the state of being desirable self-focusing in a particular application, the decentered parameter of beams can have an extraordinary deed with particular absorption level in the medium.

Xiong et al. (2010) [74] developed a method to study the self-focusing effect in cold plasma using the power of arbitrary magnetic field. They set the magnetic field in the plane which includes y and z -axis. Their results show that there is a different effect on self-focusing corresponding to different angle and intensity. The larger angle between the y axis and outside magnetic field weakens the self-focusing effect and is strengthened by increasing outside magnetic field.

Singh and Walia (2010) [75] established the differential equation under moment theory approach and analytical solution is obtained for the same. They used the Runge-Kutta method to solve it numerically. The results they have obtained are in agreement with the findings of the simulation (3D PIC) and observed a new stable form of self-channelling propagation. Further they reported that the self-focusing length decreases with increase in intensity of the beam. They also found that due to dynamic balance between two competing nonlinear effects i.e. diffraction and non-linear refraction, periodic self-focusing occurs.

Patil et al. (2010) [76] investigated the focusing of Hermit-cosh-Gaussian (HchG) laser beams in collision-less magneto-plasma by using WKB and paraxial approximations. They presented the dynamics of the combined effects of nonlinearity and spatial diffraction and

highlighted the nature of focusing. They found that the self-focusing/defocusing of HChG beams is dependent on the mode index and decentered parameter.

Kant et al. (2011) [77] analyzed the self-focusing and found that ponderomotive self-focusing becomes stronger when density transition is taken into account. To reduce the oscillation amplitude, plasma density is increased slowly. Further, in the ramped density region, the laser can perceive a narrowing channel at a slow pace due to which the oscillation amplitude of the spot size contracts. Therefore, the laser beam undergoing plasma density ramp is expected to become more focused.

Gill et al. (2011) [78] investigated the characteristics of cosh-Gaussian laser beam propagation in magnetoplasma using variational approach. They derived nonlinear Schrodinger equation in an appropriate way and discussed the necessary phase modulation. They found that the decentered parameter b along with magnetic field play a key role in self-focusing/ defocusing enhancement of the beam.

Kim et al. (2011) [79] investigated the effect of the density ramp structure on the electron energy in laser wake field acceleration. They have reported that with a downward density ramp, the electron energy decreased due to a lag in the acceleration region and to the acceleration field strength being lower than that with a uniform density, but with an upward ramp, the energy increased because of the higher acceleration field and the position of the acceleration region. These effects were studied by using simulations having a 2-dimensional particle-in-cell code and by experiments using a 20TW laser.

Gill et al. (2011) [21] have taken in to account the combined effect of relativistic and ponderomotive nonlinearities to analyze the self-focusing with linear absorption. At various b values with various absorption levels, the self-phase modulation, self-focusing and self-trapping of beam have been studied. They observed that in the absence of decentered parameter, the self-focusing effect becomes weaker for a large value of absorption coefficient. However, an oscillatory self-focusing takes place for a higher value of decentered parameter $b = 1$ and for $b = 2$, self-focusing effect is observed in a sharp manner.

Kant et al. (2012) [22] reported the self-focusing of Hermite-Gaussian beam propagation in plasma under the application of plasma density ramp. They derived the differential equation by using WKB approximation and paraxial approximation. The density ramp causes reduction in the spot size of laser beam close to the axis of propagation. They found that by choosing appropriate and optimized parameters, self-focusing effect is enhanced.

Navare et al. (2012) [80] investigated theoretically the self-focusing of laser in collisional plasma and considered the impact of linear absorption. They used the parabolic equation approach in order to obtain the differential equation through WKB and paraxial approximations. While, considering the collisional nonlinearity and linear absorption, it has been found that the absorption plays a crucial role in self-focusing effect. It destroys the oscillatory character of laser beam during propagation. Further, with increase in initial irradiance, the laser beam bends towards the focusing mode.

Gill et al. (2012) [81] established the differential equation for super-Gaussian beam propagation and analytical solution is obtained for the same. They considered the magnetic field and the condition for the formation of a dark and bright ring. Their work involves the higher order terms of the dielectric function and reported that the inclusion of such terms affects the beam width parameter. Consequently a substantial increase in self-focusing is observed only in case of a dark ring. However, the results contradict for a bright ring.

Habibi and Ghamari (2012) [82] used the density ramp profile to investigate the process of self-focusing in cold quantum plasma (CQP). They established the differential equation and analytical solution is obtained for the same. Their results reveal that the quantum effect significantly adds to self-focusing effect in comparison to classical relativistic effect. However, apart from quantum effects, the ramped density profile gives rise to higher oscillations and enhanced focusing of laser beam in cold quantum plasma.

Abari and Shokri (2012) [83] investigated the process of self-focusing and defocusing in underdense plasma by considering the nonlinear ohmic heating and ponderomotive force effects. They reported that it is the ion temperature which strongly influences the laser spot size. Further,

in the self-focusing regime, the perturbed electrons oscillate continuously in between the initial and a minimum value due to high ion temperature. However, reverse is true for defocusing.

Patil et al. (2013) [84] found that with increase in intensity, there is a faster decrease in initial beam width for cold quantum plasma than classical relativistic case. Further, the beam is weaker at high intensity for classical relativistic plasma than cold quantum case. Moreover, the quantum effect plays an important and a captivating role in making the self-focusing effect stronger.

Patil and Takale (2013) [85] reported that the upward plasma density ramp in weakly relativistic and ponderomotive regime can accelerate the electron to higher energy over a long propagation distance as compared with uniform density relativistic plasma. Further, apart from density profile and intensity parameter, the electronic temperature plays a captivating role in self-focusing of laser and hence gives reasonably interesting results.

Patil et al. (2013) [86] explored the impact of electron plasma temperature, relative density plasma and intensity parameter on the laser beam evolution in plasma. They established the differential equation for beam propagation and analytical solution is obtained for the same. Their results reveal that as relative plasma density grows, the self-focusing of laser beam takes place for earlier values of propagation distance and then becomes stronger. Hence, the optimum self-focusing is achieved.

Gupta et al. (2013) [87] found that the ion temperature causes thermal self-focusing and has a serious influence on the evolution of laser beam in plasma. Further, by modifying the plasma density resulting in the generation of the nonlinearity, their obtained outcomes show a noticeable nonlinearity in laser self-focusing.

Mahajan et al. (2013) [88] reported that the oscillatory self-focusing takes place for different intensity parameter values. They established the differential equation for beam propagation and analytical solution is obtained for the same. As soon as intensity parameter is increased, the distance between the points having a logical sequence at intersecting point of two

beams increases. Again, with increase in intensity parameter, a substantial increase in self-focusing is observed.

Kaur et al. (2013) [89] investigated the interaction between parallel Gaussian electromagnetic beams in relativistic magnetoplasma. They found that in relativistic magnetoplasma, self-focusing occurs at lower values of distance of propagation. It is further observed that for higher values of magnetic field, an earlier self-focusing is observed and the beam shows oscillatory behavior with increasing intensity.

Nanda et al. (2013) [90] laid an emphasis on the decentered parameter sensitivity for relativistic self-focusing. They used the WKB and paraxial approximation to derive the nonlinear differential equation for three mode indices 0, 1 and 2. In their work, the emphasis was laid on the selection of decentered parameter. The results, they have obtained indicate that the proper and appropriate decentered parameter selection is enough important for self-focusing of HchG beam.

Nanda et al. (2013) [91] found that it is the decentered parameter and ramped density profile that results in self-focusing of laser beam. They used the WKB and paraxial approximation to derive the nonlinear differential equation. By considering the ramped density profile and magnetic field for HchG laser beam, it has been found that the presence of density transition and magnetic field enhances the required effect to a larger extent.

Nanda and Kant (2014) [92] investigated the relativistic self-focusing in an enhanced manner under density transition. They used the WKB and paraxial approximation to derive the nonlinear differential equation for three mode indices 0, 1 and 2. For decentered parameter $b = 1.8$ and for $m = 0$ and 1 modes, early and enhanced self-focusing is seen. However, for $b = 1.8$ and for $m = 2$ mode, diffraction is seen. They also observed that decentered parameter and ramp density transition enhances the required self-focusing effect.

Nanda and Kant (2014) [93] studied strongly the process of self-focusing in collisionless magnetoplasma under ramped density profile. They used the WKB and paraxial approximation to derive the nonlinear differential equation by considering ponderomotive nonlinearity. They analyzed the density transition effect and magnetic field on the propagation of cosh-Gaussian

beam. The focusing and defocusing nature of beam has been studied at various optimized parameters. They observed that for decentered parameter $b = 2.12$, sooner and better self-focusing. Further, their results reveal that the optimized laser and plasma parameters are important in making the effect.

Aggarwal et al. (2014) [94] derived the nonlinear partial differential equation which governs the laser spot size by using paraxial approximation and slowly varying approximation. They found that due to the prime importance of self-focusing effect over diffraction effect, the laser beam converges in high plasma density region and diverges in low plasma density region. Further, the required effect is obtained by optimizing wavelength and intensity parameters of beams in rippled density plasma.

Milani et al. (2014) [95] derived the coupled differential equations by using WKB and paraxial approximations. Effects of collision frequency, axis laser intensity distribution and initial laser intensity are analyzed in warm collisional plasma. Their results reveal that firstly, the collision frequency causes self-focusing and secondly, it defocuses the laser. However, as soon as it is increased, the self-focusing length becomes shorter with the result the larger collision frequency prevents the longer beam propagation through the plasma.

Malekshahi et al. (2014) [96] investigated the self-focusing of the high intensity ultra short laser pulse propagating through relativistic magnetized plasma. They have taken in to account the nonlinearity up to third order and external magnetic field and studied the relativistic effect under paraxial approach. Their results reveal that imposing the external magnetic field enhances the capacity of self-focusing. However, the self-focusing property decreases by increasing the angle between the laser field and external magnetic field.

Zare et al. (2015) [97] have considered the density ramped profile to study the propagation of Gaussian x – ray laser beam by using WKB and paraxial approximation in thermal collisionless quantum plasma. A mathematical formulation is obtained by following parabolic approach. They found that increase in plasma density leads to stronger self-focusing effect i. e the beam having less oscillation amplitude and smaller spot size, focuses faster.

Further, it has been found that the laser and plasma parameters are crucial for self-focusing as it is enhanced with optimized laser and plasma parameters.

Habibi and Ghamari (2015) [98] used the higher order paraxial theory (up to r^4) to investigate the focusing of a laser beam in quantum plasma. The eikonal have been taken in to account and extended paraxial theory to investigate the preliminary study of ChG beams. The paraxial theory allows the adjustment in the shape of radial intensity distribution and affects the beam spot size. Further, the inclusion of higher order terms of dielectric function affects the behavior of beam width parameter significantly. By using more effective decentered parameter, better self-focusing is observed for chG beams in comparison to Gaussian laser beams in cold quantum plasma (CQP).

Habibi and Ghamari (2015) [99] studied the propagation of high power laser beam entering in to the high density plasmas by considering ramped density profile and quantum correction in relativistic regime. They followed the higher order paraxial theory and derived the governing equations in cylindrical coordinate system. By utilizing higher order paraxial theory and the sensitivity of decentered parameter b , a significant enhancement in self-focusing is reported. Further, their results reveal that a stronger self-focusing effect is observed in inhomogeneous cold quantum plasma (ICQP) under plasma density ramp.

Aggarwal et al. (2015) [100] investigated the effect of self-focusing in an inhomogeneous magnetized plasma with ponderomotive nonlinearity. They have taken in to account the paraxial approximation and developed desired relation for dielectric constant. They have derived an appropriate expression for the nonlinear differential equation in presence of external magnetic field and linear absorption. They predicted that initially converging beams show oscillatory convergence while as initially diverging beams show oscillatory divergence. Further, the laser beam is more focused at lower intensity in extraordinary as well as in ordinary mode.

Aggarwal et al. (2015) [101] studied the circularly polarized quadruple Gaussian beam propagation in magnetoplasma. They considered the nonlinearity due to relativistic mass increase of electrons which changes the refractive index. They used the WKB approximation for the derivation of nonlinear differential equation and self-trapped condition. On the application of

external magnetic field, the quadruple Gaussian beam can be studied in three different regions especially self-focusing, oscillatory and smooth divergence. They reported that the magnetic field improves the self-focusing effect in extraordinary mode and worsen it in ordinary mode.

Aggarwal et al. (2015) [102] paid an attention to the investigation of beam propagation in cold magnetized plasma in presence of density transition. They used the Maxwell's equations and derived the differential equation by using WKB and paraxial approximation. They found that the laser and plasma parameters are crucial for self-focusing as it is enhanced with such optimized parameters. The strong self-focusing is obtained at optimized intensity $\alpha_0 E_{00}^2 = 0.6$ for extraordinary mode and a comparison have been made in presence and absence of transition based density at $\omega_c / \omega_0 = 0.3$. The plasma density ramp and the magnetic field are found to increase ability of self-focusing in cold plasma.

Varshney et al. (2016) [103] analyzed the relativistic nonlinear propagation of rippled Gaussian beam by following WKB and paraxial-ray approximations for arbitrary magnitude of nonlinearity. At relativistic intensities, the nonlinearity allows the refractive index to have slower radial dependence in the paraxial regime. They found that a small ripple grows rapidly on the axis of the main beam. Further, the nonlinear refractive index has a slower radial dependence in the paraxial regime. It therefore results in extraction of less energy from its vicinity.

Eslami and Nami (2016) [104] investigated the self-focusing characteristics of a laser pulse by considering lateral and axial plasma density variations. They have taken ponderomotive and relativistic effects to derive nonlinear dielectric permittivity of plasma and to develop a complete analytical model to study the phenomenon of self-focusing. With increase in channel width, the self-focusing length increases. Further, they reported that the self-focusing effect is enhanced and shifts towards lower values of distance of propagation due to increase in intensity of the laser beam.

CHAPTER-3

SELF-FOCUSING OF HERMITE-COSH-GAUSSIAN LASER BEAM IN PLASMA UNDER DENSITY TRANSITION

3.1 INTRODUCTION

The process of self-focusing of laser beams in a nonlinear medium is a captivating field which has an excellence both in theoretical and experimental interests [2, 8, 12]. In magnetoplasma using variational approach, it is found that the decentered parameter b along with absorption coefficient play a key role on the self-focusing/ defocusing nature of the beam [78]. However, for a cos-Gaussian beam propagating in a Kerr medium, the RMS beam width broadens, the central parts of the beam give rise to an initial radial compression and have a noticeable redistribution during propagation. The partial collapse of central part of the beam appears while the RMS beam width still increases or remains constant. It is further observed that the cos-Gaussian beam eventually converts in to a cosh-Gaussian type beam with a low and moderate power [27]. In relativistic and ponderomotive regime, it is observed that a large value of absorption level weakens the self-focusing effect in the absence of decentered parameter. However, oscillatory self-focusing takes place for a higher value of decentered parameter, $b = 1$, and all curves are seen as displaying the sharp self-focusing effect for $b = 2$ [21]. Under plasma density transition, the pulse acquires a minimum spot size very close to the axis of propagation. As the laser beam passes through the ramped density region, it detects a low pace narrowing channel. In this case the oscillation amplitude of the spot size contracts and the beam propagating under density transition tends to become more focused. In the absence of density ramp, due to the supremacy of the diffraction effect, the laser pulse is defocused. As the plasma density increases, self-focusing occurs sooner and becomes stronger. Similarly, in the absence of density transition, the beam width parameter does not increase much and after various Rayleigh lengths, it acquires a very lower value and maintains it for a large distance. Consequently, the enhancement in laser beam self-focusing is observed [77].

Nanda *et al.* [92] while studying the relativistic self-focusing of HchG beam in plasma under density transition observed that an appropriate and proper decentered parameter selection and

presence of density transition results to stronger self-focusing. Further, for such beams when propagating in a magnetoplasma with a ramped density profile, the authors concluded that the presence of density transition and magnetic field enhances the self-focusing effect to a larger extent [91]. Consideration of proper and an appropriate decentered parameter selection is very much sensitive to self-focusing [90]. However in studying the self-focusing under density transition by Kant *et al.* [22], the authors found that the effects of density transition and initial intensity of the laser beam are important and have a key role in maintaining the laser plasma interaction as a captivating field of research and hence in strong self-focusing.

Recently, the HchG beam has been studied extensively and it has been found that such beams can be produced by the superposition of two decentered Hermite-Gaussian beams as cosh-Gaussian ones [23]. In this paper, we mainly study the self-focusing of HchG laser beams propagating in underdense plasma under plasma density ramp of the form $n(\xi) = n_0 \tan(\xi/d)$ by a ponderomotive mechanism. Analytical formulas for HchG beams are derived and results are discussed.

3.2 FIELD DISTRIBUTION OF HCHG LASER BEAMS

The field distribution of HchG beams propagating in the plasma medium along z-axis is of the form:

$$E(r, z) = \frac{E_0}{2f(z)} \left[H_m \left(\frac{\sqrt{2r}}{r_0 f(z)} \right) \right] \text{Exp} \left[\frac{b^2}{4} \right] \times \left\{ \text{Exp} \left[- \left(\frac{r}{r_0 f(z)} + \frac{b}{2} \right)^2 \right] + \text{Exp} \left[- \left(\frac{r}{r_0 f(z)} - \frac{b}{2} \right)^2 \right] \right\} \quad (3.1)$$

Where, m represents the mode index for the Hermite polynomial of m^{th} order, r_0 is the spot size of the beam and b is the decentered parameter of the beam, r is the radial coordinate, $E(r, z)$ is the amplitude of HchG beam at $r = z = 0$. $f(z)$ is the dimensionless beam width parameter, which is a measure of both intensity along the axis and waist width of the beam.

3.3 NON-LINEAR DIELECTRIC CONSTANT

We consider propagation of HchG laser beam in a nonlinear medium characterized by dielectric constant given by Sodha *et al.* [20]:

$$\varepsilon = \varepsilon_0 + \phi(EE^*) \quad (3.2)$$

With, $\varepsilon_0 = 1 - \omega_p^2 / \omega^2$, $\omega_p^2 = 4\pi n(\xi)e^2 / m$, $\omega_p^2 = \omega_{p0}^2 \tan(\xi / d)$ and $\omega_{p0}^2 = 4\pi n_0 e^2 / m$, here ' ε_0 ' represents the linear part and $\phi \approx (1/2)\varepsilon_2 A_0^2$ represents the non-linear parts of the dielectric constant respectively. Here, $\varepsilon_2 = 2(\omega_p^2 / \omega^2)\alpha$, ' ω_{p0} ' is the plasma frequency, ' e ' is the electronic charge, ' m ' is the rest mass of the electron, ' ω ' is the frequency of the incidents laser beam and ' n_0 ' is the equilibrium electron density. With, $\alpha = e^2 M / 6m^2 \omega^2 k_B T_0$, here ' M ' is the scatterer mass in the plasma, ' k_b ' is the Boltzmann constant and ' T_0 ' is the equilibrium plasma temperature, ξ is the propagation distance and d is a constant adjustable parameter.

3.4 SELF-FOCUSING

For isotropic, non-conducting and non-absorbing medium with $\mu = 1$, Maxwell's equation are:

$$\vec{\nabla} \times \vec{H} = \frac{1}{c} \frac{\partial \vec{D}}{\partial t} \quad (3.3)$$

$$\vec{\nabla} \times \vec{E} = -\frac{1}{c} \frac{\partial \vec{H}}{\partial t} \quad (3.4)$$

$$\vec{\nabla} \cdot \vec{D} = 0 \quad (3.4a)$$

$$\vec{\nabla} \cdot \vec{B} = 0 \quad (3.4b)$$

Taking curl of equation (3.4),

$$\vec{\nabla} \times \vec{\nabla} \times \vec{E} = -\frac{1}{c} \frac{\partial}{\partial t} (\vec{\nabla} \times \vec{H})$$

Substituting the value of $(\vec{\nabla} \times \vec{H})$ from equation (3.4a) and applying vector identity, $\vec{A} \times \vec{B} \times \vec{C}$, we get

$$\begin{aligned}\vec{\nabla}(\vec{\nabla} \cdot \vec{E}) - \vec{E}(\vec{\nabla} \cdot \vec{\nabla}) &= -\frac{1}{c} \frac{\partial}{\partial t} \left(\frac{1}{c} \frac{\partial \vec{D}}{\partial t} \right) \\ \vec{\nabla}(\vec{\nabla} \cdot \vec{E}) - \nabla^2 \vec{E} &= -\frac{1}{c^2} \frac{\partial^2 \vec{D}}{\partial t^2} \\ -\nabla^2 \vec{E} + \frac{1}{c^2} \frac{\partial^2 \vec{D}}{\partial t^2} + \vec{\nabla}(\vec{\nabla} \cdot \vec{E}) &= 0\end{aligned}\tag{3.5}$$

From equation (3.4a),

$$\vec{\nabla} \cdot \vec{D} = 0$$

$$\vec{\nabla}(\epsilon \vec{E}) = 0$$

Here ' ϵ ' is a variable quantity, thus we have,

$$\epsilon \vec{\nabla} \cdot \vec{E} + \vec{E} \vec{\nabla} \cdot \epsilon = 0$$

$$\vec{\nabla} \cdot \vec{E} = -\frac{\vec{E} \vec{\nabla} \cdot \epsilon}{\epsilon}$$

Thus equation (3.5) becomes,

$$\begin{aligned}-\nabla^2 \vec{E} + \frac{1}{c^2} \frac{\partial^2 \vec{D}}{\partial t^2} + \vec{\nabla} \left(-\frac{\vec{E} \vec{\nabla} \cdot \epsilon}{\epsilon} \right) &= 0 \\ \nabla^2 \vec{E} - \frac{\epsilon}{c^2} \frac{\partial^2 \vec{E}}{\partial t^2} + \vec{\nabla} \left(\frac{\vec{E} \vec{\nabla} \cdot \epsilon}{\epsilon} \right) &= 0\end{aligned}\tag{3.6}$$

For a plane polarized wave with electric field vector along y-axis, propagating in the z-direction, the solution of equation (3.6) is given by,

$$\vec{E} = \hat{j}E_0 \text{Exp}[i(\omega t - kz)] \quad (3.7)$$

where \hat{j} is the unit vector along y-direction.

Differentiating equation (3.7) twice, w. r. t. 't', we get

$$\frac{\partial \vec{E}}{\partial t} = i\omega \hat{j}E_0 \text{Exp}[i(\omega t - kz)]$$

$$\frac{\partial^2 \vec{E}}{\partial t^2} = -\omega^2 \hat{j}E_0 \text{Exp}[i(\omega t - kz)]$$

$$\frac{\partial^2 \vec{E}}{\partial t^2} = -\omega^2 \vec{E} \quad (3.8)$$

Thus equation (3.6) becomes,

$$\nabla^2 \vec{E} - \frac{\varepsilon}{c^2} (-\omega^2 \vec{E}) + \vec{\nabla} \left(\frac{\vec{E} \vec{\nabla} \cdot \varepsilon}{\varepsilon} \right) = 0$$

$$\nabla^2 \vec{E} + \frac{\varepsilon}{c^2} \omega^2 \vec{E} + \vec{\nabla} \left(\frac{\vec{E} \vec{\nabla} \cdot \varepsilon}{\varepsilon} \right) = 0$$

$$\nabla^2 \vec{E} + k^2 \vec{E} + \vec{\nabla} \left(\frac{\vec{E} \vec{\nabla} \cdot \varepsilon}{\varepsilon} \right) = 0 \quad \left(\because k^2 = \varepsilon \frac{\omega^2}{c^2} \right)$$

$$\nabla^2 \vec{E} + k^2 \vec{E} + \left[-\vec{E} \left(\frac{\vec{\nabla} \varepsilon}{\varepsilon} \right)^2 + \vec{E} \left(\frac{\nabla^2 \varepsilon}{\varepsilon} \right) \right] = 0$$

$$\nabla^2 \vec{E} + \left[k^2 - \left(\frac{\vec{\nabla} \varepsilon}{\varepsilon} \right)^2 + \left(\frac{\nabla^2 \varepsilon}{\varepsilon} \right) \right] \vec{E} = 0$$

$$\nabla^2 \vec{E} + \left[k^2 + \vec{\nabla} \left(\frac{\vec{\nabla} \varepsilon}{\varepsilon} \right) \right] \vec{E} = 0$$

$$\nabla^2 \vec{E} + \left[k^2 + \nabla^2 (\ln \varepsilon) \right] \vec{E} = 0$$

$$\nabla^2 \vec{E} + k^2 \left[1 + \frac{1}{k^2} \nabla^2 (\ln \varepsilon) \right] \vec{E} = 0 \quad (3.9)$$

If $(1/k^2) \nabla^2 (\ln \varepsilon) \ll 1$, then,

$$\nabla^2 \vec{E} + k^2 \vec{E} = 0$$

$$\text{Or, } \nabla^2 \vec{E} + \frac{\omega^2}{c^2} \varepsilon \vec{E} = 0$$

In cylindrical co-ordinate system, we can write this equation as

$$\frac{\partial^2 \vec{E}}{\partial z^2} + \frac{\partial^2 \vec{E}}{\partial r^2} + \frac{1}{r} \frac{\partial \vec{E}}{\partial r} + \varepsilon \frac{\omega^2}{c^2} \vec{E} = 0 \quad (3.10)$$

For slowly converging or diverging cylindrically symmetric beam, the solution of equation (3.10) is of the following form,

$$\vec{E} = A(r, z) \text{Exp}[i(\omega t - kz)] \quad (3.11)$$

$$\text{With } k^2 = \varepsilon_0 \omega^2 / c^2 = \omega^2 / c^2 \left(1 - \omega_{p0}^2 \tan(\xi / d) / \omega^2 \right)$$

Differentiating equation (3.11) twice w. r. t. 'r' and 'z', we get

$$\frac{\partial \vec{E}}{\partial r} = \text{Exp}[i(\omega t - kz)] \frac{\partial A(r, z)}{\partial r}$$

$$\frac{\partial^2 \vec{E}}{\partial r^2} = \text{Exp}[i(\omega t - kz)] \frac{\partial^2 A(r, z)}{\partial r^2}$$

And

$$\begin{aligned}
\frac{\partial \vec{E}}{\partial z} &= \text{Exp}[i(\omega t - kz)] \left[-\frac{i\omega A}{c} \sqrt{1 - \frac{\omega_{p0}^2}{\omega^2} \tan(z/dR_d)} + \left(\frac{i\omega}{2cdR_d} \right) \frac{\omega_{p0}^2}{\omega^2} \frac{zA \text{Sec}^2(z/dR_d)}{\sqrt{1 - \frac{\omega_{p0}^2}{\omega^2} \tan(z/dR_d)}} + \frac{\partial A}{\partial z} \right] \\
\frac{\partial^2 \vec{E}}{\partial z^2} &= \text{Exp}[i(\omega t - kz)] \left[\frac{\partial^2 A(r, z)}{\partial z^2} + \left(\frac{i\omega}{c} \right) \frac{\partial A(r, z)}{\partial z} \left(\frac{\omega_{p0}^2 z \text{Sec}^2(z/dR_d)}{\omega^2 dR_d \sqrt{1 - \frac{\omega_{p0}^2}{\omega^2} \tan(z/dR_d)}} \right) \right. \\
&\quad \left. - 2 \sqrt{1 - \frac{\omega_{p0}^2}{\omega^2} \tan(z/dR_d)} \right] \\
&+ \frac{\omega A}{c} \text{Exp}[i(\omega t - kz)] \left[\frac{i\omega_{p0}^2 z \text{Sec}^2(z/dR_d)}{\omega^2 dR_d \sqrt{1 - \frac{\omega_{p0}^2}{\omega^2} \tan(z/dR_d)}} + \frac{\omega z \omega_{p0}^2 z \text{Sec}^2(z/dR_d)}{c\omega^2 dR_d} \right] \\
&+ \frac{\omega}{c} \text{Exp}[i(\omega t - kz)] \frac{iA \omega_{p0}^2 z \text{Sec}^2(z/dR_d)}{\omega^2 d^2 R_d^2 \sqrt{1 - \frac{\omega_{p0}^2}{\omega^2} \tan(z/dR_d)}} \left[\tan(z/dR_d) + \frac{\omega_{p0}^2 \text{Sec}^2(z/dR_d)}{4\omega^2 \left(1 - \frac{\omega_{p0}^2}{\omega^2} \tan(z/dR_d) \right)} \right] \\
&- \frac{\omega^2 A}{c^2} \text{Exp}[i(\omega t - kz)] \left[\frac{\omega_{p0}^4 z^2 \text{Sec}^4(z/dR_d)}{4\omega^4 d^2 R_d^2 \left(1 - \frac{\omega_{p0}^2}{\omega^2} \tan(z/dR_d) \right)} + \left(1 - \frac{\omega_{p0}^2}{\omega^2} \tan(z/dR_d) \right) \right]
\end{aligned}$$

Substituting these values in equation (3.10), and neglecting $\partial^2 A / \partial z^2$ we get

$$\begin{aligned}
& \frac{i\omega}{c} \left(2\sqrt{1 - \frac{\omega_{p0}^2}{\omega^2} \tan(z/dR_d)} - \frac{\frac{\omega_{p0}^2}{\omega^2} z \sec^2(z/dR_d)}{dR_d \sqrt{1 - \frac{\omega_{p0}^2}{\omega^2} \tan(z/dR_d)}} \right) \left(\frac{\partial A}{\partial z} \right) - \frac{\frac{\omega_{p0}^2}{\omega^2} A \sec^2(z/dR_d)}{dR_d \sqrt{1 - \frac{\omega_{p0}^2}{\omega^2} \tan(z/dR_d)}} \\
& - \frac{\frac{\omega_{p0}^2}{\omega^2} Az \sec^2(z/dR_d)}{d^2 R_d^2 \sqrt{1 - \frac{\omega_{p0}^2}{\omega^2} \tan(z/dR_d)}} \left(\tan(z/dR_d) + \frac{\frac{\omega_{p0}^2}{\omega^2} \sec^2(z/dR_d)}{4 \left(1 - \frac{\omega_{p0}^2}{\omega^2} \tan(z/dR_d) \right)} \right) \\
& = \frac{\omega^2}{c^2} \left(\frac{\frac{\omega_{p0}^2}{\omega^2} Az \sec^2(z/dR_d)}{dR_d} - \frac{\left(\frac{\omega_{p0}^2}{\omega^2} \right)^2 Az^2 \sec^4(z/dR_d)}{4d^2 R_d^2 \left(1 - \frac{\omega_{p0}^2}{\omega^2} \tan(z/dR_d) \right)} \right) \left(\frac{\partial^2 A}{\partial r^2} + \frac{1}{r} \frac{\partial A}{\partial r} + \frac{\omega^2}{c^2} \Phi(AA^*) A \right)
\end{aligned}
\tag{3.12}$$

To solve equation (3.12), we express

$$A(r, z) = A_0(r, z) \text{Exp}[-ikS(r, z)] \tag{3.13}$$

Where, k has been defined above and A_0 and S are the real functions of ' r ' and ' z '.

Differentiating equation (3.13) twice, w. r. t. ' r ', we get

$$\begin{aligned}
\frac{\partial A(r, z)}{\partial r} &= \text{Exp}[-ikS(r, z)] \left[\frac{\partial A_0}{\partial r} - \frac{i\omega A_0}{c} \sqrt{1 - \frac{\omega_{p0}^2}{\omega^2} \tan(z/dR_d)} \left(\frac{\partial S(r, z)}{\partial r} \right) \right] \\
\frac{\partial^2 A(r, z)}{\partial r^2} &= \text{Exp}[-ikS(r, z)] \left[\frac{\partial^2 A_0}{\partial r^2} - \frac{2i\omega}{c} \sqrt{1 - \frac{\omega_{p0}^2}{\omega^2} \tan(z/dR_d)} \left(\frac{\partial S}{\partial r} \right) \left(\frac{\partial A_0}{\partial r} \right) \right] - \\
& \frac{\omega A_0}{c} \sqrt{1 - \frac{\omega_{p0}^2}{\omega^2} \tan(z/dR_d)} \left[i \left(\frac{\partial^2 S}{\partial r^2} \right) + \frac{\omega}{c} \sqrt{1 - \frac{\omega_{p0}^2}{\omega^2} \tan(z/dR_d)} \left(\frac{\partial S}{\partial r} \right)^2 \right] \text{Exp}[-ikS(r, z)]
\end{aligned}$$

Now differentiating equation (3.13) w. r. t. ' z ',

$$\frac{\partial A(r, z)}{\partial z} = \text{Exp}[-ikS(r, z)] \left[\frac{\partial A_0}{\partial z} - \frac{i\omega A_0}{c} \left\{ \frac{\sqrt{1 - \frac{\omega_{p0}^2}{\omega^2} \tan(z/dR_d)} \left(\frac{\partial S}{\partial z} \right) - S(r, z) \omega_{p0}^2 \frac{\text{Sec}^2(z/dR_d)}{2d\omega^2 R_d \sqrt{1 - \frac{\omega_{p0}^2}{\omega^2} \tan(z/dR_d)}}}{\right.} \right]$$

Thus equation (3.12) becomes,

$$\begin{aligned} & \frac{i\omega}{c} \left(\frac{z\omega_{p0}^2 \text{Sec}^2(z/dR_d)}{d\omega^2 R_d \sqrt{1 - \frac{\omega_{p0}^2}{\omega^2} \tan(z/dR_d)}} - 2\sqrt{1 - \frac{\omega_{p0}^2}{\omega^2} \tan(z/dR_d)} \right) \frac{\partial A_0}{\partial z} + \frac{\partial^2 A_0}{\partial r^2} + \frac{1}{r} \frac{\partial A_0}{\partial r} + \\ & \frac{\omega^2 A_0}{c^2} \sqrt{1 - \frac{\omega_{p0}^2}{\omega^2} \tan(z/dR_d)} \left[\frac{z\omega_{p0}^2 \text{Sec}^2(z/dR_d)}{d\omega^2 R_d \left(1 - \frac{\omega_{p0}^2}{\omega^2} \tan(z/dR_d)\right)} - \frac{S\omega_{p0}^2 \text{Sec}^2(z/dR_d)}{2d\omega^2 R_d \left(1 - \frac{\omega_{p0}^2}{\omega^2} \tan(z/dR_d)\right)} \right] \\ & + \frac{i\omega A_0 \omega_{p0}^2 \text{Sec}^2(z/dR_d)}{cd\omega^2 R_d \sqrt{1 - \frac{\omega_{p0}^2}{\omega^2} \tan(z/dR_d)}} \left[1 + \frac{z}{dR_d} \left(\tan(z/dR_d) + \frac{\omega_{p0}^2 \text{Sec}^2(z/dR_d)}{4 \left(1 - \frac{\omega_{p0}^2}{\omega^2} \tan(z/dR_d)\right)} \right) \right] \\ & = \frac{\omega^2 A_0}{c^2} \left(\frac{z^2 \omega_{p0}^4 \text{Sec}^4(z/dR_d)}{4d^2 \omega^4 R_d^2 \left(1 - \frac{\omega_{p0}^2}{\omega^2} \tan(z/dR_d)\right)} - \frac{\omega_{p0}^2 z \text{Sec}^2(z/dR_d)}{dR_d} + \left(1 - \frac{\omega_{p0}^2}{\omega^2} \tan(z/dR_d)\right) \left(\frac{\partial S}{\partial r} \right)^2 \right) \\ & + \frac{i\omega}{c} \sqrt{1 - \frac{\omega_{p0}^2}{\omega^2} \tan(z/dR_d)} \left(2 \frac{\partial S}{\partial r} \frac{\partial A_0}{\partial r} + A_0 \frac{\partial^2 S}{\partial r^2} + A_0 \frac{\partial S}{\partial r} \right) - \frac{\omega^2 A_0}{c^2} \phi(A_0^2) \end{aligned} \quad (3.14)$$

Comparing real and imaginary parts of equation (3.14), we get

Real part equation is

$$\begin{aligned} \frac{c^2}{\omega^2 A_0} \left(\frac{\partial^2 A_0}{\partial r^2} + \frac{1}{r} \frac{\partial A_0}{\partial r} \right) + \Phi(A_0^2) = & \left(2 \left(1 - \frac{\omega_{p0}^2}{\omega^2} \text{Tan}(z/dR_d) \right) - \frac{\omega_{p0}^2}{\omega^2} \frac{z \text{Sec}^2(z/dR_d)}{dR_d} \right) \frac{\partial S}{\partial z} \\ & + \left(1 - \frac{\omega_{p0}^2}{\omega^2} \text{Tan}(z/dR_d) \right) \left(\frac{\partial S}{\partial r} \right)^2 - \frac{\omega_{p0}^2}{\omega^2} \frac{\text{Sec}^2(z/dR_d)}{dR_d} \left(S + z - \frac{\omega_{p0}^2}{\omega^2} \frac{z \text{Sec}^2(z/dR_d)(S - z/2)}{2dR_d \left(1 - \frac{\omega_{p0}^2}{\omega^2} \text{Tan}(z/dR_d) \right)} \right) \end{aligned} \quad (3.15)$$

Imaginary part equation is

$$\begin{aligned} & \left(1 - \frac{\omega_{p0}^2}{\omega^2} \frac{z \text{Sec}^2(z/dR_d)}{2dR_d \left(1 - \frac{\omega_{p0}^2}{\omega^2} \text{Tan}(z/dR_d) \right)} \right) \frac{\partial A_0^2}{\partial z} + \frac{\partial S}{\partial r} \frac{\partial A_0^2}{\partial r} + \left(\frac{\partial^2 S}{\partial r^2} + \frac{1}{r} \frac{\partial S}{\partial r} \right) A_0^2 \\ & - \left(\frac{\omega_{p0}^2}{\omega^2} \frac{\text{Sec}^2(z/dR_d)}{dR_d \sqrt{1 - \frac{\omega_{p0}^2}{\omega^2} \text{Tan}(z/dR_d)}} + \frac{\omega_{p0}^2}{\omega^2} \frac{z \text{Sec}^2(z/dR_d) \text{Tan}(z/dR_d)}{d^2 R_d^2 \sqrt{1 - \frac{\omega_{p0}^2}{\omega^2} \text{Tan}(z/dR_d)}} \right) A_0^2 \\ & - \left(\frac{\omega_{p0}^2}{\omega^2} \right)^2 \left(\frac{z \text{Sec}^4(z/dR_d)}{4d^2 R_d^2 \left(1 - \frac{\omega_{p0}^2}{\omega^2} \text{Tan}(z/dR_d) \right)} \right) A_0^2 = 0 \end{aligned} \quad (3.16)$$

For initially Hermite-cosh-Gaussian beam, the solution of equation (3.15) and (3.16) are of the form

$$A_0^2 = \frac{E_0^2}{4f^2(z)} \left[H_m \left(\frac{\sqrt{2}r}{r_0 f(z)} \right) \right]^2 \text{Exp} \left[\frac{b^2}{2} \right] \\ \left\{ \text{Exp} \left[-2 \left(\frac{r}{r_0 f(z)} + \frac{b}{2} \right) \right] + \text{Exp} \left[-2 \left(\frac{r}{r_0 f(z)} - \frac{b}{2} \right) \right] + 2 \text{Exp} \left[- \left(\frac{2r^2}{r_0^2 f^2(z)} + \frac{b^2}{2} \right) \right] \right\} \quad (3.17)$$

And

$$S(r, z) = \frac{r^2}{2} \beta(z) + \varphi(z) \quad (3.18)$$

with, $\beta(z) = (1/f(z)) \partial f / \partial z$. where ' $\varphi(z)$ ' is an arbitrary function of ' z ' .

$$\text{For, } m = 0, \text{ mode (chG beam) } \left[H_m \left(\frac{\sqrt{2}r}{r_0 f(z)} \right) \right]^2 = 1$$

$$\therefore A_0^2 = \frac{E_0^2}{4f^2(z)} \text{Exp} \left[\frac{b^2}{2} \right] \\ \left\{ \text{Exp} \left[-2 \left(\frac{r}{r_0 f(z)} + \frac{b}{2} \right) \right]^2 + \text{Exp} \left[-2 \left(\frac{r}{r_0 f(z)} - \frac{b}{2} \right) \right]^2 + 2 \text{Exp} \left[- \left(\frac{2r^2}{r_0^2 f^2(z)} + \frac{b^2}{2} \right) \right] \right\} \quad (3.19)$$

Differentiating equation (3.18) w. r. t. ' z ' and ' r ' respectively,

$$\frac{\partial S(r, z)}{\partial z} = \frac{r^2}{2} \frac{\partial \beta}{\partial z} + \frac{\partial \varphi}{\partial z}$$

$$\frac{\partial S(r, z)}{\partial z} = \frac{r^2}{2f(z)} \frac{\partial^2 \beta}{\partial z^2} - \frac{r^2}{2f^2(z)} \left(\frac{\partial f(z)}{\partial z} \right)^2 + \frac{\partial \varphi}{\partial z}$$

$$\frac{\partial S(r, z)}{\partial r} = 2r \frac{\beta}{2} = r\beta = \frac{r}{f(z)} \frac{\partial f(z)}{\partial z}$$

Differentiating equation (3.19) twice w. r. t. 'r', we get

$$\frac{\partial A_0}{\partial r} = \frac{E_0}{2f(z)} \left\{ \left(\frac{2rb^2}{r_0^2 f^2(z)} \right) - \frac{4r}{r_0^2 f^2(z)} - \left(\frac{4r^3 b^2}{r_0^4 f^4(z)} \right) + \frac{4r^3}{r_0^4 f^4(z)} \right\}$$

$$\frac{\partial^2 A_0}{\partial r^2} = \frac{E_0}{2f(z)} \left\{ \left(\frac{2rb^3}{r_0^3 f^3(z)} \right) - \frac{2r^2 b^2}{r_0^4 f^4(z)} - \left(\frac{4r^3 b}{r_0^5 f^5(z)} \right) - \left(\frac{12rb}{r_0^3 f^3(z)} \right) - \left(\frac{4}{r_0^2 f^2(z)} \right) \right\}$$

$$\left. \begin{aligned} & - \frac{4r^2}{r_0^4 f^4(z)} - \left(\frac{6r^3 b^3}{r_0^5 f^5(z)} \right) \end{aligned} \right\}$$

Substituting the values of $\partial S(r,z)/\partial z$, $\partial S(r,z)/\partial r$, $\partial A_0/\partial r$, $\partial^2 A_0/\partial r^2$ and A_0^2 in equation (3.15) and solving, we get

$$\begin{aligned} & \frac{c^2 E_0}{2\omega^2 A_0 f(z)} \left(\frac{2rb^3}{r_0^3 f^3(z)} - \frac{2r^2 b^2}{r_0^4 f^4(z)} - \frac{4r^3 b}{r_0^5 f^5(z)} - \frac{12rb}{r_0^3 f^3(z)} - \frac{6r^3 b^3}{r_0^5 f^5(z)} + \frac{2b^2}{r_0^2 f^2(z)} - \frac{4r^2}{r_0^4 f^4(z)} \right) \\ & - \frac{E_0^2 r^2}{2r_0^4 f^4(z)} \left(\frac{\alpha \omega_{p0}^2}{\omega^2} \tan(z/dR_d) \right) = \left(1 - \frac{\omega_{p0}^2}{\omega^2} \tan(z/dR_d) \right) r^2 \beta^2 + \varphi(z) + z \\ & + \left(2 - \frac{2\omega_{p0}^2}{\omega^2} \tan(z/dR_d) - \frac{z\omega_{p0}^2 \text{Sec}^2(z/dR_d)}{d\omega^2 R_d} \right) \left(\frac{r^2 \partial \beta}{2\partial z} + \frac{\partial \varphi}{\partial z} \right) + \frac{r^2 \beta z \omega_{p0}^4 \text{Sec}^4(z/dR_d)}{4d^2 \omega^4 R_d^2 \left(1 - \frac{\omega_{p0}^2}{\omega^2} \tan(z/dR_d) \right)} \\ & - \frac{r^2 \beta \omega_{p0}^2 \text{Sec}^2(z/dR_d)}{2d\omega^2 R_d} - \frac{\omega_{p0}^2 z \text{Sec}^2(z/dR_d) \varphi(z)}{2d\omega^2 R_d \left(1 - \frac{\omega_{p0}^2}{\omega^2} \tan(z/dR_d) \right)} \\ & + \frac{\omega_{p0}^2 z^2 \text{Sec}^2(z/dR_d) \varphi(z)}{4d\omega^2 R_d \left(1 - \frac{\omega_{p0}^2}{\omega^2} \tan(z/dR_d) \right)} \end{aligned} \quad (3.20)$$

Now, equating coefficients of r^2 on both sides of Eq. (3.20), one obtains

$$\begin{aligned}
& \frac{6c^2 b^2}{(2-b^2)\omega^2 r_0^2 f(z)} + \frac{\alpha E_0^2 \omega_{p0}^2}{2r_0^2 f^3(z)\omega^2} \tan(z/dR_d) = \left(\frac{z\omega_{p0}^2 \text{Sec}^2(z/dR_d)}{2d\omega^2 R_d} + \frac{\omega_{p0}^2}{\omega^2} \tan(z/dR_d) - 1 \right) \frac{\partial^2 f}{\partial z^2} \\
& - \frac{1}{f(z)} \left(\frac{z\omega_{p0}^2 \text{Sec}^2(z/dR_d)}{2d\omega^2 R_d} \right) \left(\frac{\partial f}{\partial z} \right)^2 + \frac{\omega_{p0}^2 \text{Sec}^2(z/dR_d)}{2d\omega^2 R_d} \left[1 - \frac{z\omega_{p0}^2 \text{Sec}^2(z/dR_d)}{2d\omega^2 R_d \left(1 - \frac{\omega_{p0}^2}{\omega^2} \tan(z/dR_d) \right)} \right] \frac{\partial f}{\partial z}
\end{aligned} \tag{3.21}$$

Since, $\xi = z/R_d$, $z = \xi R_d$ and $z/dR_d = \xi/d$. Therefore, we can write as:

$$\frac{\partial f}{\partial z} = \frac{\partial f}{\partial \xi} \times \frac{\partial \xi}{\partial z} = \frac{1}{R_d} \frac{\partial f}{\partial \xi} \quad \text{and} \quad \frac{\partial^2 f}{\partial z^2} = \frac{1}{R_d^2} \frac{\partial^2 f}{\partial \xi^2}$$

Substituting the above values in Eq. (3.21), we get

$$\begin{aligned}
& \left(1 - \frac{\omega_{p0}^2}{\omega^2} \text{Tan}(\xi/d) \right) \left(\frac{6b^2}{(2-b^2)f} \right) + \frac{\alpha E_0^2}{2} \left(\frac{r_0 \omega}{c} \right)^2 \left(\frac{\omega_{p0}^2}{\omega^2} \right) \left(1 - \frac{\omega_{p0}^2}{\omega^2} \text{Tan}(\xi/d) \right) \frac{\text{Tan}(\xi/d)}{f^3} \\
& = \left[\left(\frac{\omega_{p0}^2}{\omega^2} \right) \text{Tan}(\xi/d) + \left(\frac{\omega_{p0}^2}{\omega^2} \right) \frac{\xi \text{Sec}^2(\xi/d)}{2d} - 1 \right] \frac{\partial^2 f}{\partial \xi^2} - \left[\left(\frac{\omega_{p0}^2}{\omega^2} \right) \frac{\xi \text{Sec}^2(\xi/d)}{2d} \right] \frac{1}{f} \left(\frac{\partial f}{\partial \xi} \right)^2 \\
& + \left(\frac{\omega_{p0}^2}{\omega^2} \right) \frac{\text{Sec}^2(\xi/d)}{2d} \left[1 - \left(\frac{\omega_{p0}^2}{\omega^2} \right) \frac{\xi \text{Sec}^2(\xi/d)}{2d \left(1 - \left(\frac{\omega_{p0}^2}{\omega^2} \right) \text{Tan}(\xi/d) \right)} \right]
\end{aligned} \tag{3.22}$$

Equations (3.22) is the required expression for beam width parameter f .

3.5 RESULTS AND DISCUSSION

For an initially plane wave front of the beam, we follow the boundary condition $f = 1$ and $\partial f / \partial \xi = 0$ at $\xi = 0$. For the analysis done above (Eq. 3.22), the following parameters are chosen for the purpose of numerical calculations: $\omega = 3 \times 10^{14} \text{ rad/sec}$, $r_0 = 3 \times 10^{-4} \text{ cm}$ and $n_0 = 9.983 \times 10^{17} \text{ cm}^{-3}$ [90]. Figures 3.1 (a) and 3.1 (b) show the dependence of f on ξ with upward density transition for different values of ω_{p0} / ω . The decentered parameter is fixed at $b = 0$ and 1 respectively. From these figures, it is clear that with increase in the values of relative plasma density, the beam width parameter decreases sharply. The plots reveal that due to supremacy of nonlinear term, the laser beam gets more focused. This is due to the fact that in the low plasma density region, the electrons are forced to move away from the region having high intensity by a ponderomotive mechanism. The nonlinearity in the plasma comes because of mass variation of electron, which is also due to high intensity of the laser beam. Figures 3.2 (a) and 3.2 (b) represent the dependence of f on ξ for various decentered parameter values. Keeping ω_{p0} / ω fixed at 0.02 in figure 3.2 (a) and at 0.03 in figure 3.2 (b) respectively. From these figures it is clear that on increasing decentered parameter b , the beam width parameter f decreases on a large scale. Hence self-focusing occurs sooner and becomes further strong. Thus, it is obvious from the figures that the decentered parameter affects the behavior of beam width parameter to greater extent. Moreover, the appropriate selection and sensitivity of decentered parameter is very important in deciding the focusing of laser beam.

Figure 3.3 represents the dependence of f on ξ for various decentered parameter values. Keeping ω_{p0} / ω fixed at 0.04 and the other parameters are $d = 5$ and decentered parameter $b = 0$ (Red curve), $b = 1$ (Black curve). The figure 3.3 reveals that as we increase the decentered parameter, the beam width parameter decreases greatly. It is because of the fact that the decentered parameter is sensitive to self-focusing. Hence, one can say that the laser beam gives a self-focusing effect for $b \leq 1$. It is further observed that as the plasma density increases self-focusing becomes much stronger. Combining the results of this chapter with the previous studies on Gaussian beams [20, 25], we see that HchG beams give freedom to mode index (m) and

decentered parameter (b) in changing the self-focusing nature more accurately. However, in the absence of plasma density ramp, the beam-width parameter decreases on a large scale because of nonlinear effects. As the diffraction effects become prevalent, the beam-width parameter increases and after acquiring a very lower value, the laser beam starts to diverge due to nonlinearity saturation. To surmount the defocusing, introduction of plasma density transition is necessary and it is obvious that by applying such a transition, the self-focusing effect is enhanced and the laser is more focused i. e. self-focusing becomes much stronger. Hence, the upward plasma density ramp or density transition has a key role in laser focusing enhancement.

3.6 CONCLUSION

In the present investigation, we have studied the self-focusing of Hermite-cosh-Gaussian (HchG) laser beam in plasma by considering plasma density ramp in a parabolic medium under paraxial approximation. The field distribution of the laser beam is expressed in terms of beam width parameter and decentered parameter. The differential equation for the beam width parameter is derived by using parabolic wave equation and paraxial approximation. To keep away the laser from defocusing, upward density ramp or transition based density is considered and hence, the beam is focused to a small spot size. Such a density transition reduces the defocusing effect and maintains the focal spot size up to several Rayleigh lengths. To discuss the self-focusing nature, the behavior of beam width parameter with the dimensionless distance of propagation for various decentered parameter values has been examined by numerical calculations. Our simulation results show that as the plasma density and decentered parameter increases, the self-focusing effect occurs sooner and becomes stronger. However, sharp self-focusing of such beams occurs for $b \leq 1$. Hence, by introducing such a density profile, a much stronger self-focusing is observed which can be used for various interesting applications.

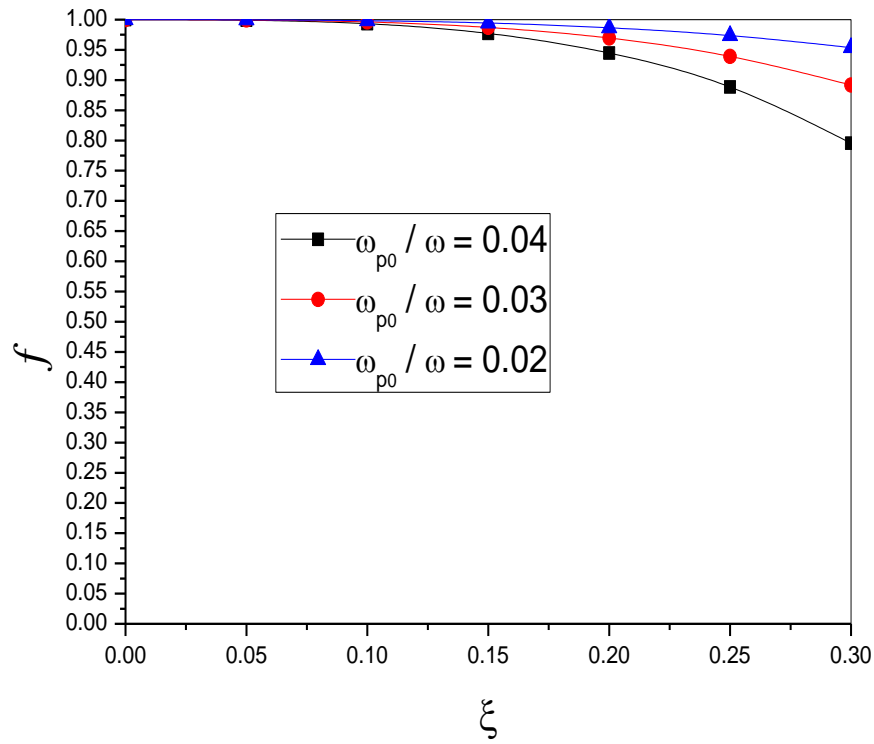


Figure 3.1 (a): Dependence of f on ξ for various values of ω_{p0}/ω . The other parameters are $b = 0$ and $d = 5$.

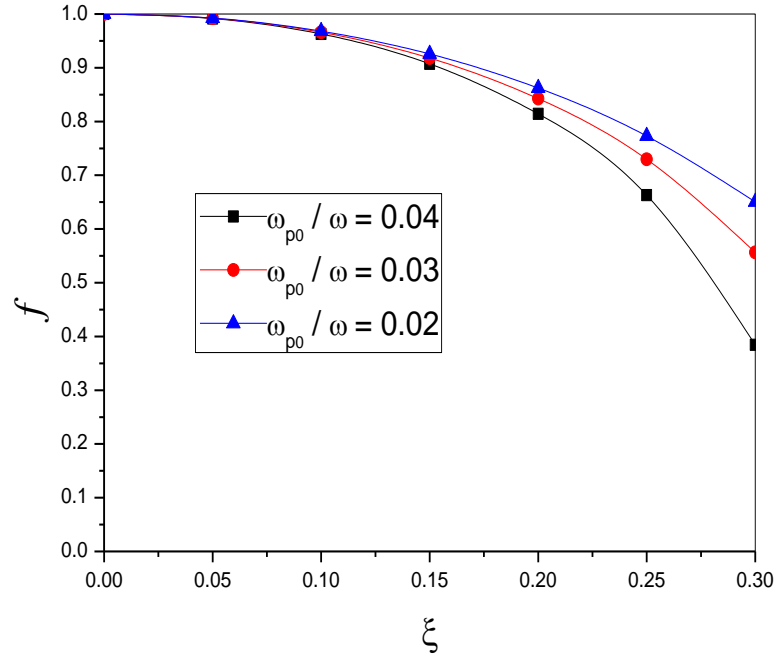


Figure 3.1 (b): Dependence of f on ξ for various values of ω_{p0}/ω . The other parameters are $b = 1$ and $d = 5$.

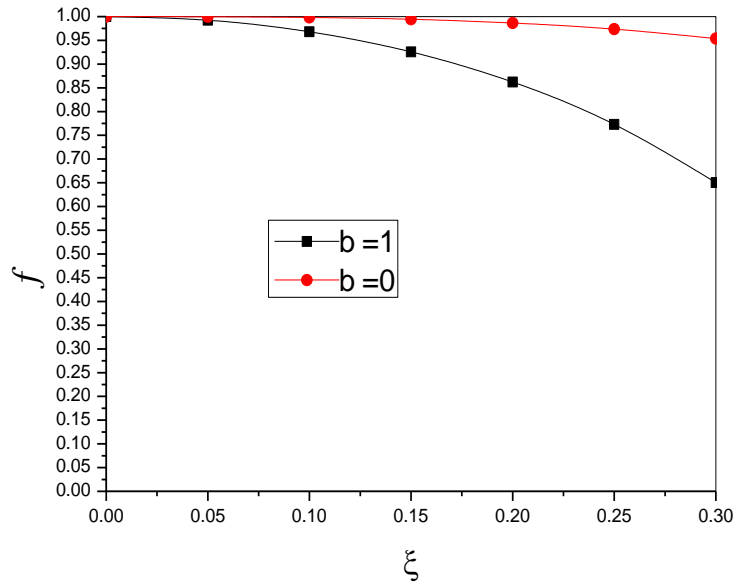


Figure 3.2 (a): Dependence of f on ξ for various values of b . The other parameters are $\omega_{p0}/\omega = 0.02$ and $d = 5$.

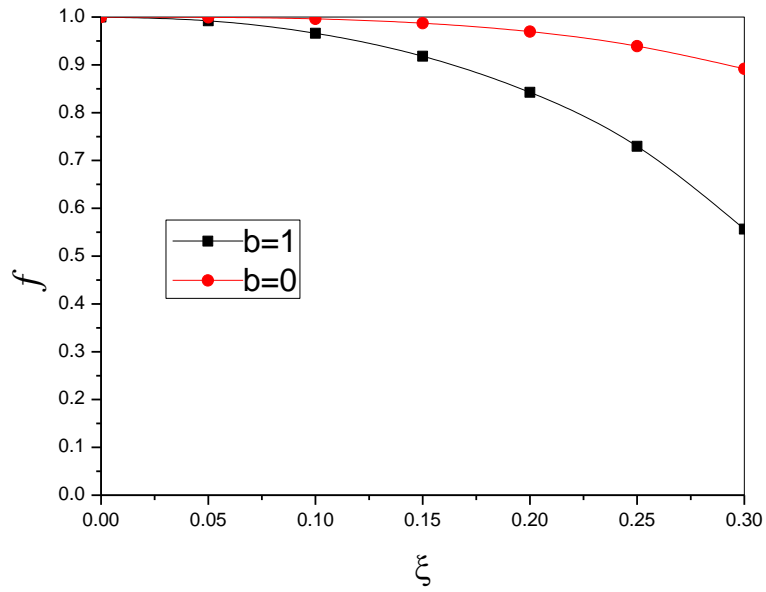


Figure 3.2 (b): Dependence of f on ξ for various values of b . The other parameters are $\omega_{p0}/\omega = 0.03$ and $d = 5$.

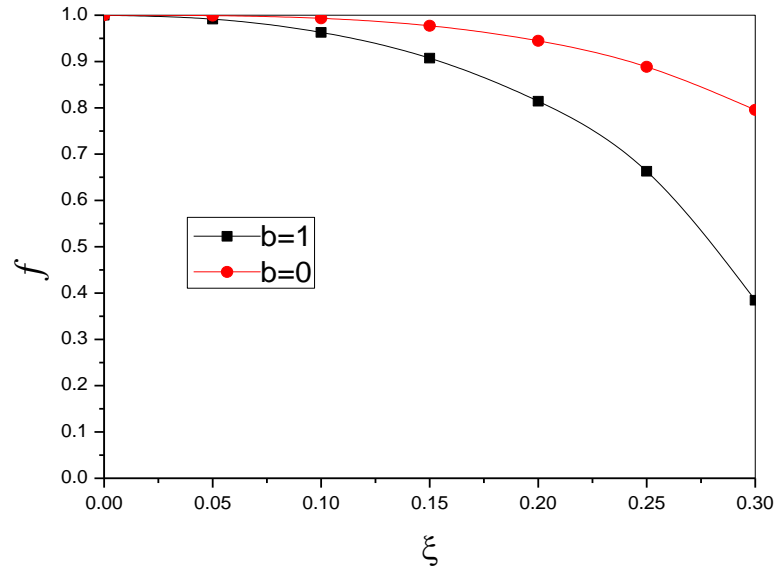


Figure 3.3: Dependence of f on ξ for various values of b . The other parameters are $\omega_{p0}/\omega = 0.04$ and $d = 5$.

CHAPTER-4

DENSITY TRANSITION BASED SELF-FOCUSING OF COSH GAUSSIAN LASER BEAM IN PLASMA WITH LINEAR ABSORPTION

4.1 INTRODUCTION

The interaction of intense laser beams with plasmas has been an important field of research due to various applications like laser electron acceleration [9-11], inertial confinement fusion [13-15] and ionospheric modification [16-19] etc. These applications require large interaction region up to several Rayleigh lengths without loss of energy. When a high power laser beam interacts with the plasma, it provides an oscillatory velocity to the electron so that the dielectric constant gets modified and leads to relativistic self-focusing [105]. The real part of dielectric constant having saturating nonlinearity characterizes the steady- state focusing or defocusing in a medium and the imaginary part being determined by multi photon absorption under paraxial approximation [58]. Takale *et al.* [71] analyzed the self-focusing and defocusing of first six TEM_{op} Hermite-Gaussian laser beams in collision-less plasma and found that modes having odd p-values defocus and those having even p-values are capable of sustaining oscillations as well as are able to have a defocusing character during propagation in collision-less plasma. However, it has been observed that a plasma density ramp of suitable length can reduce these oscillations [64].

The propagation of HchG beams in n-InSb has been studied for various mode indices viz 0, 1 and 2 and incorporates the desirability of process of self-focusing in a particular application by taking an advantage of beams having decentered parameter [24]. The relativistic self-focusing of cosh beams illustrates that oscillatory self-focusing takes place for $b = 0, 1$ and sharp self-focusing effect for $b = 2$ [106]. Nanda *et al.* [92] have observed that decentered parameter and ramp density profile results in self-focusing of laser beam. However, by considering the magnetic field and plasma density ramp for Hermite-cosh Gaussian laser beam, it has been found that the presence of density transition and magnetic field enhance the self-focusing effect to a greater extent [91]. The proper and an appropriate decentered parameter selection is very much sensitive [90]. However, Kant *et al.* [22] have observed the effect of density transition and initial intensity of the laser beam on self-focusing of laser beam. Again, the parameters like density profile, intensity parameter, and decentered parameter play a crucial role in the enhancement of laser

beam focusing significantly. Further, the upward plasma density ramp in weakly relativistic and ponderomotive regime can accelerate the electron to higher energy over a long propagation distance as compared with uniform density relativistic plasma [85]. The oscillatory self-focusing takes place for different values of intensity parameter and with increase in intensity parameter, the distance between two consecutive points of intersection of two beams increases [88]. The laser beam is compressed and amplified in an enhanced manner by the combined effect of magnetic field, relativistic nonlinearity and negative initial chirp [107]. It is to be noted that strong self-focusing is obtained by optimizing wavelength and intensity parameters of beams [94]. In the investigation of self-focusing and frequency broadening of laser pulse in water medium, the laser beam initially undergoes self-focusing due to Kerr nonlinearity and then nonlinear refraction takes place which causes the laser beam to defocus [108]. Also, it has been found that with increase of power density and control parameters lead to trapping of particle in the potential and hence strong focusing [109]. For a short laser pulse undergoing self-focusing in plasma with density ramp, the pulse acquires a very low spot size and the focused pulse then diffracts and focuses in a regular and repeated manner. In this case the oscillation amplitude of the spot size contracts and results in increasing frequency. Hence, the laser propagating in plasma under plasma density ramp may likely become more focused. Further, due to the supremacy of diffraction effect and in absence of density transition, it gets defocused. As the plasma density increases, self-focusing effect becomes stronger [77]. Furthermore, the quantum effect plays a key role in laser-plasma interaction and significantly adds to self-focusing in comparison to classical relativistic case [84]. However, in addition to quantum effects, ramped density profile causes larger and higher oscillations and consequently better focusing in cold quantum plasma (CQP) [82].

In the present communication, we have studied the self-focusing of cosh-Gaussian beam in plasma by taking in to account the plasma density transition effect and linear absorption through parabolic equation approach. The second order differential equation that describes the nature of self-focusing in plasma is obtained by following paraxial approximation. The results are presented graphically and are discussed. Finally, a conclusion is drawn in the last section of this chapter.

4.2 FIELD DISTRIBUTION OF COSH – GAUSSIAN BEAMS

The field distribution of cosh-Gaussian laser beam at $z = 0$ is characterized by [110-112]

$$E(r, 0) = E_0 \exp\left(-\frac{r^2}{r_0^2}\right) \cosh(\Omega_0 r) \quad (4.1)$$

Where, r_0 is the waist width, r is the radial coordinate, E_0 is the amplitude of the electric field at centre position and Ω_0 is called the cosh factor. On the other hand Eq. (4.1) can be expressed as follows:

$$E(r, 0) = \frac{E_0}{2} \exp\left(\frac{b^2}{4}\right) \left\{ \exp\left[-\left(\frac{r+b}{r_0}\right)^2\right] + \exp\left[-\left(\frac{r-b}{r_0}\right)^2\right] \right\} \quad (4.2)$$

Where, $b = r_0 \Omega_0$ is called the decentered parameter.

Now, corresponding to absorption alone, the concentration of energy of the laser beam decreases by a factor of $\exp(-2 \int k_i dz)$ which weakens the nonlinearity effect. Therefore, in accordance with Eq. (4.2), we can construct the following ansatz for the field distribution along the z -axis.

$$E(r, 0) = \frac{E_0}{2f} \exp\left(\frac{b^2}{4}\right) \exp(-2k_i z) \left\{ \exp\left[-\left(\frac{r+b}{r_0 f}\right)^2\right] + \exp\left[-\left(\frac{r-b}{r_0 f}\right)^2\right] \right\} \quad (4.3)$$

Where k_i is the absorption coefficient and $f = f(r, z)$ is the dimensionless beam-width parameter.

4.3 NONLINEAR DIELECTRIC CONSTANT

The cosh-Gaussian beam propagation in plasma is being characterized by a dielectric constant in the following form

$$\varepsilon = \varepsilon_0 + \phi(EE^*) \quad (4.4)$$

With, $\varepsilon_0 = 1 - \omega_p^2 / \omega^2$, $\omega_p^2 = 4\pi n(\xi)e^2 / m$, $\omega_p^2 = \omega_{p0}^2 \tan(\xi / d)$ and $\omega_{p0}^2 = 4\pi n_0 e^2 / m$, here ' ε_0 ' represents the linear part and ϕ represents the non-linear parts of the dielectric constant respectively. Here, ' ω_{p0} ' the plasma frequency, ' e ' the electronic charge, ' m ' the rest mass of the electron, ' ω ' the frequency of the incident laser beam and ' n_0 ' the equilibrium electron density, ξ the normalized propagation distance and d is a dimensionless adjustable parameter.

4.4 SELF-FOCUSING EQUATIONS

The wave equation that describes the laser beam propagation in plasma may be written as

$$\nabla^2 \vec{E} - \frac{\varepsilon}{c^2} (-\omega^2 \vec{E}) + \vec{\nabla} \left(\frac{\vec{E} \vec{\nabla} \cdot \varepsilon}{\varepsilon} \right) = 0 \quad (4.5)$$

The last term of Eq. (4.5) on left hand side is neglected under the condition $k^{-2} \nabla^2 (\ln \varepsilon) \ll 1$, where 'k' represents the wave number the laser beam. Thus,

$$\nabla^2 \vec{E} + \frac{\omega^2}{c^2} \varepsilon \vec{E} = 0$$

This equation is solved by employing WKB approximation. In cylindrical co-ordinate system, we can write this equation as

$$\frac{\partial^2 \vec{E}}{\partial z^2} + \frac{\partial^2 \vec{E}}{\partial r^2} + \frac{1}{r} \frac{\partial \vec{E}}{\partial r} + \varepsilon \frac{\omega^2}{c^2} \vec{E} = 0 \quad (4.6)$$

For slowly converging or diverging cylindrically symmetric beam, the solution of equation (4.6) is of the following form,

$$\vec{E} = A(r, z) \text{Exp}[i(\omega t - kz)] \quad (4.7)$$

With $k^2 = \varepsilon_0 \omega^2 / c^2 = \omega^2 / c^2 \left(1 - \omega_{p0}^2 \tan(\xi / d) / \omega^2 \right)$

Differentiating equation (4.7) twice w. r. t. 'r' and 'z', we get

$$\frac{\partial \vec{E}}{\partial r} = \text{Exp}[i(\omega t - kz)] \frac{\partial A(r, z)}{\partial r}$$

$$\frac{\partial^2 \vec{E}}{\partial r^2} = \text{Exp}[i(\omega t - kz)] \frac{\partial^2 A(r, z)}{\partial r^2}$$

And

$$\frac{\partial \vec{E}}{\partial z} = \text{Exp}[i(\omega t - kz)] \left[\frac{\partial A}{\partial z} - \frac{i\omega A}{c} \sqrt{1 - \frac{\omega_{p0}^2}{\omega^2} \tan(z / dR_d)} + \left(\frac{i\omega}{2cdR_d} \right) \frac{\omega_{p0}^2}{\omega^2} \frac{zA \text{Sec}^2(z / dR_d)}{\sqrt{1 - \frac{\omega_{p0}^2}{\omega^2} \tan(z / dR_d)}} \right]$$

$$\begin{aligned}
\frac{\partial^2 \bar{E}}{\partial z^2} = & \text{Exp}[i(\omega t - kz)] \left[\frac{\partial^2 A(r, z)}{\partial z^2} + \left(\frac{i\omega}{c} \right) \frac{\partial A(r, z)}{\partial z} \left(\frac{\omega^2 dR_d \sqrt{1 - \frac{\omega_{p0}^2}{\omega^2} \tan(z/dR_d)}}{-2\sqrt{1 - \frac{\omega_{p0}^2}{\omega^2} \tan(z/dR_d)}} \right) \right] \\
+ \frac{\omega A}{c} \text{Exp}[i(\omega t - kz)] & \left[\frac{i\omega_{p0}^2 z \text{Sec}^2(z/dR_d)}{\omega^2 dR_d \sqrt{1 - \frac{\omega_{p0}^2}{\omega^2} \tan(z/dR_d)}} + \frac{\omega z \omega_{p0}^2 z \text{Sec}^2(z/dR_d)}{c \omega^2 dR_d} \right] \\
+ \frac{\omega}{c} \text{Exp}[i(\omega t - kz)] & \frac{iA \omega_{p0}^2 z \text{Sec}^2(z/dR_d)}{\omega^2 d^2 R_d^2 \sqrt{1 - \frac{\omega_{p0}^2}{\omega^2} \tan(z/dR_d)}} \left[\tan(z/dR_d) + \frac{\omega_{p0}^2 \text{Sec}^2(z/dR_d)}{4\omega^2 \left(1 - \frac{\omega_{p0}^2}{\omega^2} \tan(z/dR_d) \right)} \right] \\
- \frac{\omega^2 A}{c^2} \text{Exp}[i(\omega t - kz)] & \left[\frac{\omega_{p0}^4 z^2 \text{Sec}^4(z/dR_d)}{4\omega^4 d^2 R_d^2 \left(1 - \frac{\omega_{p0}^2}{\omega^2} \tan(z/dR_d) \right)} + \left(1 - \frac{\omega_{p0}^2}{\omega^2} \tan(z/dR_d) \right) \right]
\end{aligned}$$

Substituting these values in equation (4.6), and neglecting $\partial^2 A / \partial z^2$ we get

$$\begin{aligned}
\frac{i\omega}{c} & \left(2\sqrt{1 - \frac{\omega_{p0}^2}{\omega^2} \tan(z/dR_d)} - \frac{\frac{\omega_{p0}^2}{\omega^2} z \text{Sec}^2(z/dR_d)}{dR_d \sqrt{1 - \frac{\omega_{p0}^2}{\omega^2} \tan(z/dR_d)}} \right) \left(\frac{\partial A}{\partial z} \right) - \frac{\frac{\omega_{p0}^2}{\omega^2} A \text{Sec}^2(z/dR_d)}{dR_d \sqrt{1 - \frac{\omega_{p0}^2}{\omega^2} \tan(z/dR_d)}} \\
- \frac{\frac{\omega_{p0}^2}{\omega^2} A z \text{Sec}^2(z/dR_d)}{d^2 R_d^2 \sqrt{1 - \frac{\omega_{p0}^2}{\omega^2} \tan(z/dR_d)}} & \left(\tan(z/dR_d) + \frac{\frac{\omega_{p0}^2}{\omega^2} \text{Sec}^2(z/dR_d)}{4 \left(1 - \frac{\omega_{p0}^2}{\omega^2} \tan(z/dR_d) \right)} \right) \\
= \frac{\omega^2}{c^2} & \left(\frac{\frac{\omega_{p0}^2}{\omega^2} A z \text{Sec}^2(z/dR_d)}{dR_d} - \frac{\left(\frac{\omega_{p0}^2}{\omega^2} \right)^2 A z^2 \text{Sec}^4(z/dR_d)}{4d^2 R_d^2 \left(1 - \frac{\omega_{p0}^2}{\omega^2} \tan(z/dR_d) \right)} \right)
\end{aligned}$$

$$+\frac{\partial^2 A}{\partial r^2} + \frac{1}{r} \frac{\partial A}{\partial r} + \frac{\omega^2}{c^2} \Phi(AA^*)A \quad (4.8)$$

To solve equation (4.8), we express

$$A(r, z) = A_0(r, z) \text{Exp}[-ikS(r, z)] \quad (4.9)$$

Where, k has been defined above and A_0 and S depend on ' r ' and ' z '.

Differentiating equation (4.9) twice, w. r. t. ' r ', we get

$$\begin{aligned} \frac{\partial A(r, z)}{\partial r} &= \text{Exp}[-ikS(r, z)] \left[\frac{\partial A_0}{\partial r} - \frac{i\omega A_0}{c} \sqrt{1 - \frac{\omega_{p0}^2}{\omega^2} \tan(z/dR_d)} \left(\frac{\partial S(r, z)}{\partial r} \right) \right] \\ \frac{\partial^2 A(r, z)}{\partial r^2} &= \text{Exp}[-ikS(r, z)] \left[\frac{\partial^2 A_0}{\partial r^2} - \frac{2i\omega}{c} \sqrt{1 - \frac{\omega_{p0}^2}{\omega^2} \tan(z/dR_d)} \left(\frac{\partial S}{\partial r} \right) \left(\frac{\partial A_0}{\partial r} \right) - \right. \\ &\quad \left. \frac{\omega A_0}{c} \sqrt{1 - \frac{\omega_{p0}^2}{\omega^2} \tan(z/dR_d)} \left[i \left(\frac{\partial^2 S}{\partial r^2} \right) + \frac{\omega}{c} \sqrt{1 - \frac{\omega_{p0}^2}{\omega^2} \tan(z/dR_d)} \left(\frac{\partial S}{\partial r} \right)^2 \right] \text{Exp}[-ikS(r, z)] \right] \end{aligned}$$

Now differentiating equation (4.9) w. r. t. ' z ',

$$\frac{\partial A(r, z)}{\partial z} = \text{Exp}[-ikS(r, z)] \left[\frac{\partial A_0}{\partial z} - \frac{i\omega A_0}{c} \left\{ \sqrt{1 - \frac{\omega_{p0}^2}{\omega^2} \tan(z/dR_d)} \left(\frac{\partial S}{\partial z} \right) - \frac{S(r, z)\omega_{p0}^2}{2d\omega^2 R_d} \frac{\text{Sec}^2(z/dR_d)}{\sqrt{1 - \frac{\omega_{p0}^2}{\omega^2} \tan(z/dR_d)}} \right\} \right]$$

Thus equation (4.8) becomes,

$$\begin{aligned}
& \frac{i\omega}{c} \left(\frac{z\omega_{p0}^2 \text{Sec}^2(z/dR_d)}{d\omega^2 R_d \sqrt{1 - \frac{\omega_{p0}^2}{\omega^2} \tan(z/dR_d)}} - 2\sqrt{1 - \frac{\omega_{p0}^2}{\omega^2} \tan(z/dR_d)} \right) \frac{\partial A_0}{\partial z} + \frac{\partial^2 A_0}{\partial r^2} + \frac{1}{r} \frac{\partial A_0}{\partial r} + \\
& \frac{\omega^2 A_0}{c^2} \sqrt{1 - \frac{\omega_{p0}^2}{\omega^2} \tan(z/dR_d)} \left[\frac{z\omega_{p0}^2 \text{Sec}^2(z/dR_d)}{d\omega^2 R_d \left(1 - \frac{\omega_{p0}^2}{\omega^2} \tan(z/dR_d)\right)} - \frac{S\omega_{p0}^2 \text{Sec}^2(z/dR_d)}{2d\omega^2 R_d \left(1 - \frac{\omega_{p0}^2}{\omega^2} \tan(z/dR_d)\right)} \right. \\
& \quad \left. + \frac{\partial S}{\partial z} - 2 \right] \\
& + \frac{i\omega A_0 \omega_{p0}^2 \text{Sec}^2(z/dR_d)}{cd\omega^2 R_d \sqrt{1 - \frac{\omega_{p0}^2}{\omega^2} \tan(z/dR_d)}} \left[1 + \frac{z}{dR_d} \left(\tan(z/dR_d) + \frac{\omega_{p0}^2 \text{Sec}^2(z/dR_d)}{4 \left(1 - \frac{\omega_{p0}^2}{\omega^2} \tan(z/dR_d)\right)} \right) \right] \\
& = \frac{\omega^2 A_0}{c^2} \left(\frac{z^2 \omega_{p0}^4 \text{Sec}^4(z/dR_d)}{4d^2 \omega^4 R_d^2 \left(1 - \frac{\omega_{p0}^2}{\omega^2} \tan(z/dR_d)\right)} - \frac{\omega_{p0}^2 z \text{Sec}^2(z/dR_d)}{dR_d} + \left(1 - \frac{\omega_{p0}^2}{\omega^2} \tan(z/dR_d)\right) \left(\frac{\partial s}{\partial r}\right)^2 \right) \\
& + \frac{i\omega}{c} \sqrt{\left(1 - \frac{\omega_{p0}^2}{\omega^2} \tan(z/dR_d)\right)} \left(2 \frac{\partial S}{\partial r} \frac{\partial A_0}{\partial r} + A_0 \frac{\partial^2 S}{\partial r^2} + A_0 \frac{\partial S}{\partial r} \right) - \frac{\omega^2 A_0}{c^2} \phi(A_0^2) \tag{4.10}
\end{aligned}$$

Comparing real and imaginary parts of equation (4.10), we get

Real part equation is

$$\begin{aligned}
& \frac{1}{\omega^2 c^2} \left[\omega^2 - \omega_{p0}^2 \tan(z/dR_d) - \frac{\omega_{p0}^2 z \sec^2(z/dR_d)}{2dR_d} \right] \left(\frac{\partial s}{\partial z} \right) + \frac{1}{\omega^2 c^2} \left[\omega^2 - \omega_{p0}^2 \tan(z/dR_d) \right] \left(\frac{\partial s}{\partial r} \right)^2 + \\
& \frac{\omega_{p0}^2 \sec^2(z/dR_d)}{4\omega^2 c^2 d^2 R_d^2 \left(\omega^2 - \omega_{p0}^2 \tan(z/dR_d) \right)} \left[\omega_{p0}^2 z(z+s) \sec^2(z/dR_d) - 2dR_d(s+2z) \left(\omega^2 - \omega_{p0}^2 \tan(z/dR_d) \right) \right]
\end{aligned}$$

$$= \frac{1}{\omega^2 A_0} \left[\frac{\partial^2 A_0}{\partial r^2} + \frac{1}{r} \frac{\partial A_0}{\partial r} \right] + \frac{\Phi(A_0^2)}{c^2} \quad (4.11)$$

Imaginary part equation is

$$\begin{aligned} & \left(1 - \frac{\omega_{p0}^2}{\omega^2} \frac{z \text{Sec}^2(z/dR_d)}{2dR_d \left(1 - \frac{\omega_{p0}^2}{\omega^2} \text{Tan}(z/dR_d) \right)} \right) \frac{\partial A_0^2}{\partial z} + \frac{\partial S}{\partial r} \frac{\partial A_0^2}{\partial r} + \left(\frac{\partial^2 S}{\partial r^2} + \frac{1}{r} \frac{\partial S}{\partial r} \right) A_0^2 \\ & - \left(\frac{\omega_{p0}^2}{\omega^2} \frac{\text{Sec}^2(z/dR_d)}{dR_d \sqrt{1 - \frac{\omega_{p0}^2}{\omega^2} \text{Tan}(z/dR_d)}} + \frac{\omega_{p0}^2}{\omega^2} \frac{z \text{Sec}^2(z/dR_d) \text{Tan}(z/dR_d)}{d^2 R_d^2 \sqrt{1 - \frac{\omega_{p0}^2}{\omega^2} \text{Tan}(z/dR_d)}} \right) A_0^2 \\ & - \left(\frac{\omega_{p0}^2}{\omega^2} \right)^2 \left(\frac{z \text{Sec}^4(z/dR_d)}{4d^2 R_d^2 \left(1 - \frac{\omega_{p0}^2}{\omega^2} \text{Tan}(z/dR_d) \right)} \right) A_0^2 = 0 \end{aligned} \quad (4.12)$$

For cosh-Gaussian beam, the solution of equation (4.11) and (4.12) are of the form

$$\begin{aligned} A_0^2 &= \frac{E_0^2}{4f^2(z)} \text{Exp} \left[\frac{b^2}{2} \right] \text{Exp}[-k_i z] \\ & \left\{ \text{Exp} \left[-2 \left(\frac{r}{r_0 f(z)} + \frac{b}{2} \right) \right] + \text{Exp} \left[-2 \left(\frac{r}{r_0 f(z)} - \frac{b}{2} \right) \right] + 2 \text{Exp} \left[- \left(\frac{2r^2}{r_0^2 f^2(z)} + \frac{b^2}{2} \right) \right] \right\} \end{aligned} \quad (4.13)$$

And

$$S(r, z) = \frac{r^2}{2} \beta(z) + \varphi(z) \quad (4.14)$$

The eikonal $S(r, z)$ determines the convergence or divergence of the beam.

with, $\beta(z) = (1/f(z)) \partial f / \partial z$ is regarded as the wavefront curvature, ' $\varphi(z)$ ' is an arbitrary function of ' z ' and is called phase factor. Also,

$$\Phi(A_0^2) = \frac{1}{2} \varepsilon_2 A_0^2 \quad (4.15)$$

Where ε_2 is the nonlinear coefficient.

Differentiating equation (4.14) w. r. t. 'z' and 'r' respectively,

$$\begin{aligned} \frac{\partial S(r, z)}{\partial z} &= \frac{r^2}{2} \frac{\partial \beta}{\partial z} + \frac{\partial \varphi}{\partial z} \\ \frac{\partial S(r, z)}{\partial z} &= \frac{r^2}{2f(z)} \frac{\partial^2 \beta}{\partial z^2} - \frac{r^2}{2f^2(z)} \left(\frac{\partial f(z)}{\partial z} \right)^2 + \frac{\partial \varphi}{\partial z} \\ \frac{\partial S(r, z)}{\partial r} &= 2r \frac{\beta}{2} = r\beta = \frac{r}{f(z)} \frac{\partial f(z)}{\partial z} \end{aligned}$$

Now, using paraxial approximation and differentiating equation (4.13) twice w. r. t. 'r', we get

$$\begin{aligned} \frac{\partial A_0}{\partial r} &= \frac{r^2 b E_0}{2r_0^3 f^4(z)} \text{Exp} \left[\frac{b^2}{4} - 2k_i z \right] \\ \frac{\partial^2 A_0}{\partial r^2} &= -\frac{r^2 E_0}{r_0^4 f^5(z)} \text{Exp} \left[\frac{b^2}{4} - 2k_i z \right] \left(5 + \frac{3}{2} b^2 \right) \end{aligned}$$

Substituting the values of $\partial S(r, z)/\partial z$, $\partial S(r, z)/\partial r$, $\partial A_0/\partial r$, $\partial^2 A_0/\partial r^2$ and A_0^2 in equation (4.11) and solving, we get

$$\begin{aligned} &\frac{1}{\omega^2} \left[-\frac{r^2}{r_0^4 f^4(z)} \left(5 + \frac{3}{2} b^2 \right) - \frac{r^2 b^2}{4r_0^4 f^4(z)} \left(5 + \frac{3}{2} b^2 \right) \right] - \frac{r^2 E_0 \varepsilon_2}{c^2 r_0^2 f^4(z)} \text{Exp} \left[\frac{b^2}{2} - k_i \xi k r_0^2 \right] \\ &= \frac{1}{\omega^2 c^2} \left[\omega^2 - \omega_{p0}^2 \tan(\xi/d) - \frac{\omega_{p0}^2 \xi \text{Sec}^2(\xi/d)}{d} \right] \left[\frac{r^2}{2r_0^4 k^2 f} \left\{ \frac{\partial^2 f}{\partial \xi^2} - \frac{1}{f} \left(\frac{\partial f}{\partial \xi} \right)^2 \right\} + \frac{\partial \varphi}{\partial z} \right] \\ &+ \frac{\omega_{p0}^2 (S + \xi k r_0^2) \text{Sec}^2(\xi/d)}{4\omega^2 c^2 d^2 k r_0^2 (\omega^2 - \omega_{p0}^2 \tan(\xi/d))} \left[\omega_{p0}^2 \xi \text{Sec}^2(\xi/d) - 2d(\omega^2 - \omega_{p0}^2 \tan(\xi/d)) \right] \\ &+ \frac{r^2}{\omega^2 c^2 r_0^4 k^2 f^2} (\omega^2 - \omega_{p0}^2 \tan(\xi/d)) \left(\frac{\partial f}{\partial \xi} \right)^2 \quad (4.16) \end{aligned}$$

Now, equating coefficients of r^2 on both sides of Eq. (4.16) and adopting the procedure of Akhmanov *et al.* [113] and Sodha *et al.* [20], the differential equation for the cosh-Gaussian propagation with linear absorption is written as:

$$\begin{aligned} & \left[1 - \frac{\omega_{p0}^2}{\omega^2} \tan(\xi/d) - \frac{\omega_{p0}^2}{\omega^2} \left(\frac{\xi}{d} \right) \sec^2(\xi/d) \right] \frac{\partial^2 f}{\partial \xi^2} + \left[1 - \frac{\omega_{p0}^2}{\omega^2} \tan(\xi/d) + \frac{\omega_{p0}^2}{\omega^2} \left(\frac{\xi}{d} \right) \sec^2(\xi/d) \right] \frac{1}{f} \left(\frac{\partial f}{\partial \xi} \right)^2 \\ & = \frac{2}{f^3} \left(1 - \frac{\omega_{p0}^2}{\omega^2} \tan(\xi/d) \right) \left[\left(5 + \frac{3b^2}{2} \right) \left(1 + \frac{b^2}{4} \right) - \left(\frac{r_0 \omega}{c} \right)^2 \varepsilon_2 E_0^2 \exp\left(\frac{b^2}{2} - k'_i \xi \right) \right] \end{aligned} \quad (4.17)$$

Where, $k'_i = k_i r_0 \left(\frac{r_0 \omega}{c} \right) \sqrt{1 - \frac{\omega_{p0}^2}{\omega^2} \tan(\xi/d)}$ is the normalized absorption coefficient.

Equation (4.17) is the required equation for the beam width parameter and can be solved with f depending on ξ for various k'_i levels.

4.5 RESULTS AND DISCUSSION

Eq. (4.17) is the second order nonlinear differential equation governing beam width parameter of beam in plasma with density ramp and linear absorption. The self-focusing (convergence) or defocusing (divergence) of the laser beam is estimated by the relative magnitude of nonlinear and diffraction terms of Eq. (4.17). The numerical solution of this equation is possible by using Runge–Kutta method with the set of following parameters for the purpose of numerical calculation [73]:

$\omega = 1.778 \times 10^{14} \text{ rad/sec}$, $r_0 = 253 \mu\text{m}$, $n_0 = 10^{17} \text{ cm}^{-3}$ and the value of intensity is $I_0 = 10^{19} \text{ W/cm}^2$. Fig. 4.1 shows the dependence of beam-width parameter f with propagation distance ξ for decentered parameter $b = 0$ with $\omega_{p0}/\omega = 0.2, 0.3, 0.4, 0.5$ for different absorption levels $k'_i = 0.5, 0.6, 0.7, 0.8$. These curves illustrate that beam-width parameter first decreases, attains a minimum value and then increases, with the result sharp self-focusing occurs up to $\omega_{p0}/\omega = 0.5$, $k'_i = 0.8$ and then defocusing takes place as absorption weakens self-focusing effect. In fig. 4.2, the dependence of f on ξ for $b = 1$ is shown. It is clear from the figure that sharp self-focusing is observed for $\omega_{p0}/\omega = 0.5$, $k'_i = 1.3$. So, with further increase in absorption level, the laser beam is further enhanced. This is because, the parameters like decentered

parameter, plasma density ramp and absorption coefficient are such that they change the self-focusing / defocusing nature of the beam in a significant manner. Figure 4.3 shows the dependence of f on ξ for various combinations of ω_{p0}/ω and k'_i . Beam width parameter attains a minimum value at $\omega_{p0}/\omega=0.2$ with $k'_i = 2$ and $\omega_{p0}/\omega=0.3$ with $k'_i = 3$ for decentered parameter $b = 2$ which leads to strong self-focusing in plasma. Thereafter as soon as values of ω_{p0}/ω and k'_i are increased, defocusing of laser beam takes place. But, the self-focusing length increases with absorption level. However, in fig. 4.4, the dependence of f on ξ is shown for decentered parameter $b = 0, 1, 2$ and keeping ω_{p0}/ω and absorption coefficient k'_i constant at 0.2 and 2 respectively. It is clear from Fig. 4.4 that sharp self-focusing occurs for $b = 2$ and for $b = 0$ and 1, f first decreases and then increases very slowly for lower values of “b”. Our results support the results obtained with different approach by Gill *et al.* [21] Figure 4.5 shows the dependence of f on ξ for $\omega_{p0}/\omega=0.5$ and $b = 1$ with different values of absorption level k'_i . It is important to notice here that early and strong self-focusing occurs for $k'_i < 2$. After $k'_i \geq 2$, the beam width parameter decreases slowly and defocusing takes place.

However, Patil *et al.* [73] have reported the self-focusing of cosh beams in a parabolic medium at various values of linear absorption (k'_i) and decentered parameter (b) and concluded that for $b=0$, the self-focusing occurs only up to $k'_i < 2$. But, firstly f decreases and secondly it increases slowly for $k'_i \geq 2$ corresponding to $\xi = 0.3$. However, for decentered parameter $b = 1$, the self-focusing occurs only up to $k'_i < 3$ corresponding to $\xi = 0.2$. Finally for decentered parameter $b = 2$, the beam width parameter attains a minimum value at $\xi = 0.06$ showing that the self-focusing length increases with absorption level. Further, in the work of Navare *et al.* [80], while considering the collisional nonlinearity, they found that the absorption plays a vital role in the self-focusing effect and destroys the oscillatory self-focusing character of laser beam during propagation. Hence, in comparison to ref. [73] and ref. [80], by applying the density ramp and taking in to account the effect of linear absorption, we observe that self-focusing occurs even at $\xi = 0.02$. Further, we found that study of cosh beams can be analyzed in a medium like plasma, but the important thing is that the decentered parameter, absorption coefficient and plasma density

ramp are found to behave in such a way that they change the self-focusing / defocusing nature of the laser beam in a significant manner.

4.6 CONCLUSION

This communication provides us an analysis of the evolution of cosh beams in plasma with density ramp and linear absorption using paraxial approximation. The effect of density transition on self-focusing has been studied at various values of absorption levels and decentered parameter. By choosing appropriate and optimized parameters, the combined effect of density ramp, decentered parameter and linear absorption on beam width parameter variation has been investigated and hence plotted. The results show that self-focusing occurs earlier and then defocusing takes place. However, it would be quite interesting to compare the investigated results for non-paraxial region of the beam, which so far has not been studied as per the literature available at present.

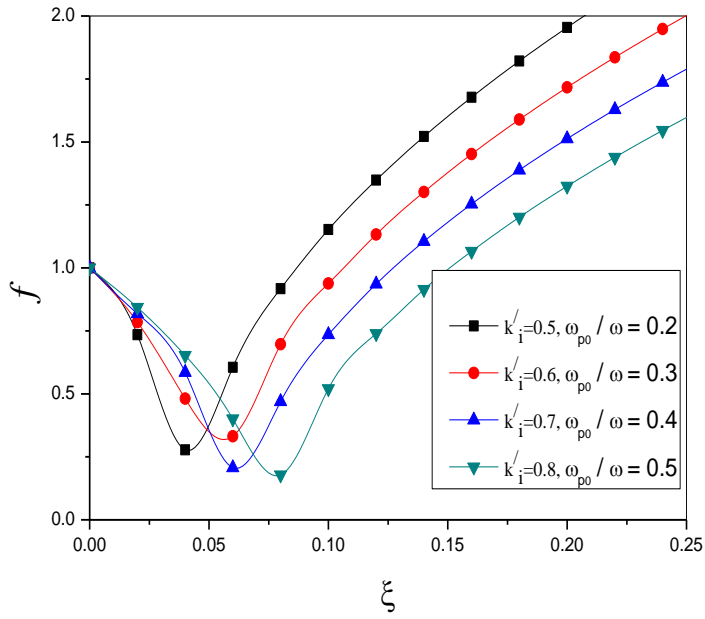


Figure 4.1: Dependence of f on ξ for various values of k'_i and ω_{p0}/ω at $b = 0$.

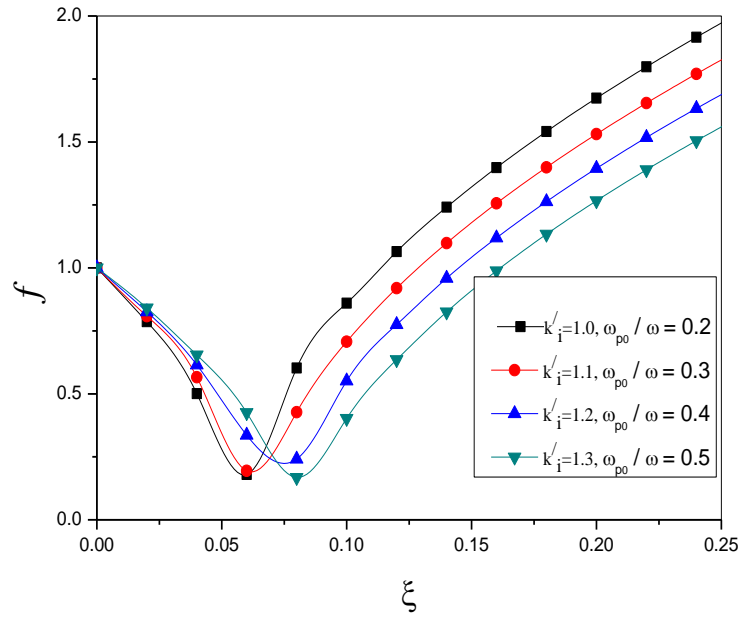


Figure 4.2: Dependence of f on ξ for various values of k_i' and ω_{ρ_0}/ω at $b = 1$

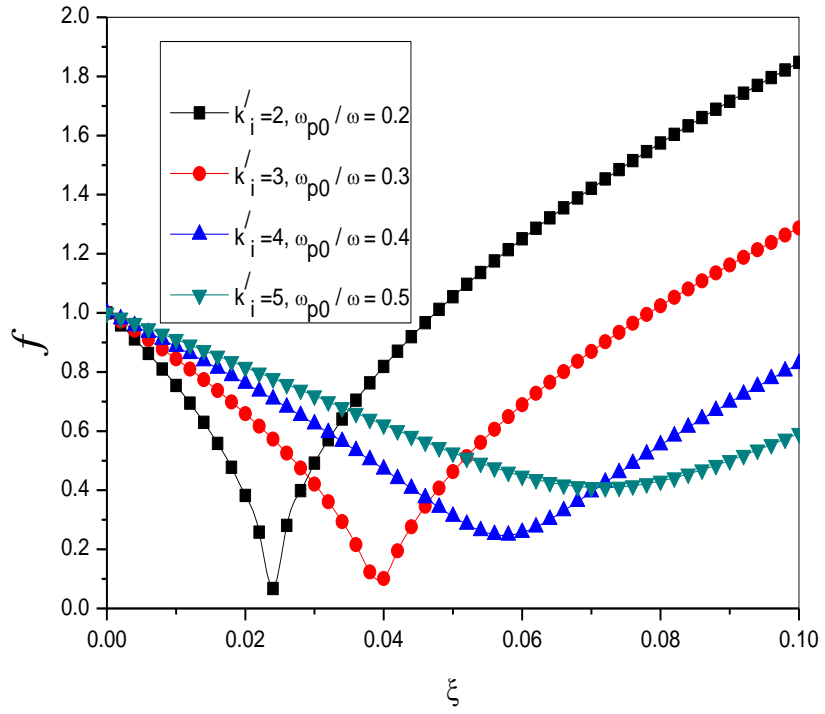


Figure 4.3: Dependence of f on ξ for various values of k_i' and ω_{p0}/ω at $b = 2$.

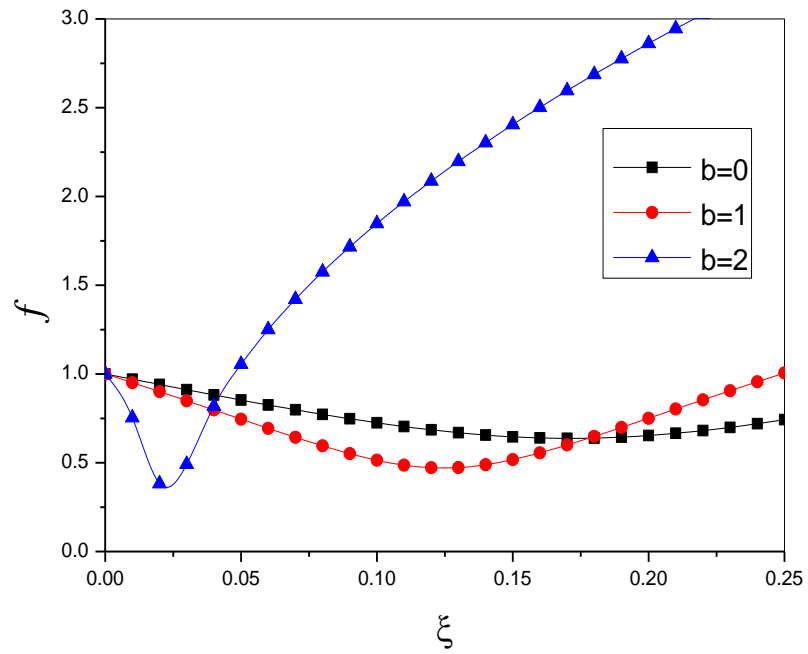


Figure 4.4: Dependence of f on ξ for $\omega_{p0}/\omega=0.2$, $k'_i=2$ and for various decentered parameter (b) values.

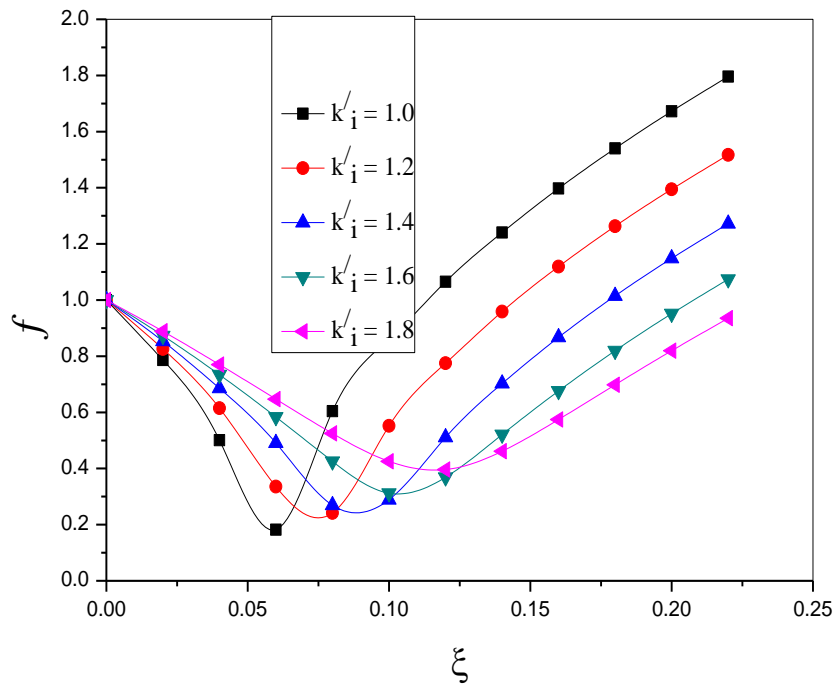


Figure 4.5: Dependence of f on ξ for $\omega_{p0}/\omega = 0.5$, $b = 1$ and for various values of k_i

CHAPTER-5

INVESTIGATION OF RELATIVISTIC SELF-FOCUSING OF HERMITE-COSINE- GAUSSIAN LASER BEAM IN COLLISIONLESS PLASMA

5.1 INTRODUCTION

The interaction of high power laser beams with plasmas occupies a unique place in the field of research due to wide-ranging applications in laser-driven fusion, laser-driven charged particle accelerators, x-ray lasers etc. [8, 115, 4]. For such applications, it is necessary that the laser beam is highly powerful, intense and propagates for extended distances without divergence, resulting in various nonlinear phenomena like self-focusing etc. Therefore, it is important to study such phenomena numerically and analytically. Since the first investigation on self-trapping of optical beams was reported by Askaryan [1] and later the self-focusing was examined by a number of authors [116, 43, 117]. The self-focusing, self-trapping and filamentation of laser has been theoretically investigated by Akhmanov *et al.* [113] and then developed by Sodha *et al.* [114]. The study of quadruple Gaussian beam in inhomogeneous magnetized plasma with ponderomotive nonlinearity and linear absorption confirms that converging beam shows oscillatory convergence whereas diverging beam shows oscillatory divergence. Further, the beam is more focused at lower intensity under the influence of linear absorption and magnetic field [100]. Kant and Wani [118] reported that the density transition, decentered parameter and linear absorption coefficient act in such a way that they change the self-focusing / defocusing nature of the beam in a significant manner. The absorption weakens the self-focusing effect and density transition sets sooner, early and stronger self-focusing of cosh-Gaussian beam in plasma. The propagation of circularly polarized quadruple Gaussian laser beam can be studied in three different regimes viz steady divergence, oscillatory divergence and self-focusing regime by taking in to account the effect of magnetic field. The magnetic field improves self-focusing for extraordinary mode but, weakens the effect for ordinary mode [101]. An intense laser beam undergoes self-focusing due to the relativistic mass and ponderomotive effects. It then diffracts and focuses more and more during propagation. In order to have sooner and better focusing, the relative plasma density is to be increased. This is because the parameters like density profile and intensity parameter play a vital role for self-focusing [22].

In thermal collisionless quantum plasma, the diffraction effect becomes predominant giving rise to increase in beam width and thus, showing an oscillatory behaviour of beam width parameter. Further, with the increase in plasma density as a ramp slope, the laser beam focuses quickly with lower oscillation amplitude, leads to smaller spot size of laser beam with more oscillations. The laser self-focusing is enhanced more in thermal quantum plasma than in classical regime [97]. However, the magnetic field and plasma density ramp play an important role in the enhancement of self-focusing. This is due to the combined role of magnetic field and density ramp that can reduce the spot size of the beam efficiently close to the axis of propagation [91]. The self-focusing decreases by increasing laser wavelength, ripple wave number and intensity. It is because of the direct dependence of self-focusing on decentered parameter b [94]. Therefore, the phenomenon of self-focusing is obtained by optimizing wavelength and intensity parameters. Moreover, the decentered parameter and ramp density profile are sensitive to the self-focusing of laser beam. It is the density ramp that shrinks the spot size of laser beam as it gets penetrated deeper in to the plasma. Due to which the laser becomes more focussed and can propagate over a long distance without divergence [92]. Further, the proper selection of decentered parameter is important for stronger self-focusing [90]. Gill *et al.* [81] used the condition for the formation of a dark and bright ring to study the focusing / defocusing of super-Gaussian laser beam in plasma with transverse magnetic field. They included higher order terms of the dielectric function and reported that the inclusion of such terms affects the beam width parameter variation and consequently substantial increase in self-focusing is observed. This is possible only in case of the dark ring. However, the results contradict in case of a bright ring. Under the ponderomotive self-focusing, the pulse acquires a minimum spot size due to the role of plasma density ramp. It then diffracts and gets focused in a periodic manner because of the fact that channel size and spot size do not match together. In such a case the oscillation amplitude of the spot size decreases, while its frequency increases. Further, as the plasma density increases under plasma density ramp, the beam gets more focused. However, in the absence density ramp and due to supremacy of the diffraction effect, it gets defocused [77]. The quantum effect gives more self-focusing in comparison to that of classical relativistic case. This is due to the fact that the beam is weaker at high intensity for classical relativistic case than cold quantum case [84].

The initial beam profile of HcosG beam remains invariant during propagation. However, in uniaxial crystals, the initial symmetry and linear polarization of HcosG beam cannot be kept intact. In addition the distribution of field of HcosG beam is closely related to the decentered parameter. In this paper, the relativistic self-focusing of HcosG beam in collisionless plasma is investigated. Using WKB and paraxial approximations through the parabolic equation, a mathematical formulation for the beam width parameter in collisionless plasma is obtained from the wave equation. The evolution of beam width parameter with the propagation distance is presented. It is hereby noticed that the laser self-focusing increases more than predicted by Aggarwal *et al.* [101]. Moreover, the effect of parameters like decentered parameter, laser intensity and initial plasma density is investigated. We previously studied the self-focusing of HchG beam in plasma under density transition [119] and found that self-focusing occurs under the influence of density ramp and decentered parameter. However, in the present communication, the authors lay emphasis on relativistic self-focusing of HcosG laser beam propagating in underdense plasma which was not done earlier for such a beam as per the literature available at present. The importance of the present work lies in the fact that an increase in self-focusing length leads to decrease in the minimum spot size of the beam and hence modulates the phenomenon of self-focusing. The computational results in context of plasma density, decentered parameter and laser intensity are discussed and finally a brief conclusion is given in the last section of this chapter. Above all in the present analysis the decentered parameter and laser intensity has good impact on the propagation of HcosG beam in plasma.

5.2 FIELD DISTRIBUTION OF HERMITE – COSINE – GAUSSIAN (HCOSG) BEAM

Consider the HcosG laser beam propagating in collisionless plasma along z-axis having field distribution of the form

$$E(x, y, z) = \frac{E_0}{\sqrt{f_1(z)f_2(z)}} H_m \left(\frac{\sqrt{2}x}{r_0 f_1(z)} \right) H_n \left(\frac{\sqrt{2}y}{r_0 f_2(z)} \right) \exp \left[- \left(\frac{x^2}{r_0^2 f_1^2(z)} + \frac{y^2}{r_0^2 f_2^2(z)} \right) \right] \times \cos \left(\frac{\Omega_0 x}{f_1(z)} \right) \cos \left(\frac{\Omega_0 y}{f_2(z)} \right) \quad (5.1)$$

where H_m and H_n are the m^{th} and n^{th} order Hermite polynomial respectively, E_0 is the constant

amplitude of the electric field, r_0 is the waist width, Ω_0 is the parameter associated with the cosine function, $f_1(z)$ and $f_2(z)$ are the beam width parameters in x and y directions respectively.

5.3 NONLINEAR DIELECTRIC CONSTANT

Consider the propagation of HcosG laser beam in plasma characterized by dielectric constant of the fo

$$\varepsilon = \varepsilon_0 + \phi(EE^*) \quad (5.2)$$

with $\varepsilon_0 = 1 - \omega_p^2 / \omega^2$, $\omega_p^2 = 4\pi n_0 e^2 / m$, $m = m_0 \gamma$. Where, $\gamma = 1 / \sqrt{1 - v^2 / c^2}$, m_0 and e are the rest mass and charge on the electron. Therefore, $\omega_p^2 = \omega_{p0}^2 / \gamma$, $\omega_{p0}^2 = 4\pi n_0 e^2 / m_0$, ϕ represents the nonlinear part of the dielectric constant, ω is the angular frequency of laser beam, ω_p is plasma frequency, n_0 is the equilibrium electron density, R_d is the diffraction length and ξ is the normalized propagation distance.

The nonlinear dielectric constant for collisionless plasma can be expressed as [114]

$$\phi(EE^*) = \frac{\omega_{p0}^2}{\gamma \omega^2} \left[1 - \exp\left(-\frac{3m_0 \gamma}{4M} \alpha EE^*\right) \right] \quad (5.3)$$

Where $\alpha = e^2 M / 6m_0^2 \gamma^2 \omega^2 k_B T$ and M is the mass of scatterer, T is the plasma temperature and k_B is the Boltzmann constant.

5.4 SELF-FOCUSING EQUATIONS

The wave equation describing the laser beam propagation may be written as

$$\nabla^2 \vec{E} - \frac{\varepsilon}{c^2} (-\omega^2 \vec{E}) + \vec{\nabla} \left(\frac{\vec{E} \vec{\nabla} \cdot \varepsilon}{\varepsilon} \right) = 0 \quad (5.4)$$

The last term of equation (5.4) on left hand side is neglected under the condition that $k^{-2} \nabla^2 (\ln \varepsilon) \ll 1$, where 'k' represents the wave number the laser beam. Thus,

$$\nabla^2 \vec{E} + \frac{\omega^2}{c^2} \varepsilon \vec{E} = 0 \quad (5.5)$$

In Cartesian co-ordinate system, we can write this equation as

$$\frac{\partial^2 \vec{E}}{\partial x^2} + \frac{\partial^2 \vec{E}}{\partial y^2} + \frac{\partial^2 \vec{E}}{\partial z^2} + \varepsilon \frac{\omega^2}{c^2} \vec{E} = 0 \quad (5.6)$$

The solution of equation (5.6) is of the following form,

$$\vec{E} = A(x, y, z) \text{Exp}[i(\omega t - kz)] \quad (5.7)$$

With $k^2 = \varepsilon_0 \omega^2 / c^2$.

Differentiating equation (3.11) twice w. r. t. 'x, y and z respectively , we get

$$\frac{\partial \vec{E}}{\partial x} = \text{Exp}[i(\omega t - kz)] \frac{\partial A}{\partial x}$$

$$\frac{\partial^2 \vec{E}}{\partial x^2} = \text{Exp}[i(\omega t - kz)] \frac{\partial^2 A}{\partial x^2}$$

$$\frac{\partial \vec{E}}{\partial y} = \text{Exp}[i(\omega t - kz)] \frac{\partial A}{\partial y}$$

$$\frac{\partial^2 \vec{E}}{\partial y^2} = \text{Exp}[i(\omega t - kz)] \frac{\partial^2 A}{\partial y^2}$$

Similarly,

$$\frac{\partial^2 \vec{E}}{\partial z^2} = \text{Exp}[i(\omega t - kz)] \left[\frac{\partial^2 A}{\partial z^2} - 2ik \frac{\partial A}{\partial z} - k^2 A \right]$$

Neglecting, $\frac{\partial^2 A}{\partial z^2}$, we get

$$\frac{\partial^2 \vec{E}}{\partial z^2} = -\text{Exp}[i(\omega t - kz)] \left[2ik \frac{\partial A}{\partial z} + k^2 A \right]$$

Therefore, using the above values, Eq. (5.6), under Wentzel-Kramers-Brillouin (WKB) approximation becomes as:

$$2ik \frac{\partial A}{\partial z} = \frac{\partial^2 A}{\partial x^2} + \frac{\partial^2 A}{\partial y^2} + \frac{k^2}{\varepsilon_0} \Phi(AA^*)A = 0 \quad (5.8)$$

To solve equation (5.8) we express A as

$$A(x, y, z) = A_{mm}(x, y, z) \exp[-ikS(x, y, z)] \quad (5.9)$$

Where, $k = (\omega/c)\epsilon_0^{1/2}$ and A_{mn} and S depend on x , y and z . Differentiating Eq. (5.9) w. r. t.

' x , y and z , we get

$$\frac{\partial \bar{A}}{\partial x} = \text{Exp}[-iKS(x, y, z)] \left[\frac{\partial A_{mn}}{\partial x} - ikA_{mn} \frac{\partial S}{\partial x} \right]$$

$$\frac{\partial^2 \bar{A}}{\partial x^2} = \text{Exp}[-iKS(x, y, z)] \left[\frac{\partial^2 A_{mn}}{\partial x^2} - ikA_{mn} \frac{\partial^2 S}{\partial x^2} - 2ik \frac{\partial S}{\partial x} \frac{\partial A_{mn}}{\partial x} - k^2 A_{mn} \left(\frac{\partial S}{\partial x} \right)^2 \right]$$

Similarly,

$$\frac{\partial^2 \bar{A}}{\partial y^2} = \text{Exp}[-iKS(x, y, z)] \left[\frac{\partial^2 A_{mn}}{\partial y^2} - ikA_{mn} \frac{\partial^2 S}{\partial y^2} - 2ik \frac{\partial S}{\partial y} \frac{\partial A_{mn}}{\partial y} - k^2 A_{mn} \left(\frac{\partial S}{\partial y} \right)^2 \right]$$

$$\frac{\partial \bar{A}}{\partial z} = \text{Exp}[-iKS(x, y, z)] \left[\frac{\partial A_{mn}}{\partial z} - ikA_{mn} \frac{\partial S}{\partial z} \right]$$

Substituting the above values in Eq. (5.8), we get

$$\begin{aligned} 2ik \left[\frac{\partial A_{mn}}{\partial z} - ikA_{mn} \frac{\partial S}{\partial z} \right] &= \frac{\partial^2 A_{mn}}{\partial x^2} + \frac{\partial^2 A_{mn}}{\partial y^2} - ikA_{mn} \left(\frac{\partial^2 S}{\partial x^2} + \frac{\partial^2 S}{\partial y^2} \right) - 2ik \left(\frac{\partial S}{\partial x} \frac{\partial A_{mn}}{\partial x} + \frac{\partial S}{\partial y} \frac{\partial A_{mn}}{\partial y} \right) \\ - k^2 A_{mn} \left[\left(\frac{\partial S}{\partial x} \right)^2 + \left(\frac{\partial S}{\partial y} \right)^2 \right] &+ \frac{k^2 \phi(A_{mn}^2) A_{mn}}{\epsilon_0} \end{aligned} \quad (5.10)$$

Now, equating real and imaginary parts on both sides of Eq. (5.10), we get

Real part equation is

$$2 \left(\frac{\partial S}{\partial z} \right) + \left(\frac{\partial S}{\partial x} \right)^2 + \left(\frac{\partial S}{\partial y} \right)^2 = \frac{1}{k^2 A_{mn}} \left(\frac{\partial^2 A_{mn}}{\partial x^2} + \frac{\partial^2 A_{mn}}{\partial y^2} \right) + \frac{\phi(A_{mn}^2)}{\epsilon_0} \quad (5.11)$$

Imaginary part equation is

$$\frac{\partial A_{mn}^2}{\partial z} + \frac{\partial S}{\partial x} \frac{\partial A_{mn}^2}{\partial x} + \frac{\partial S}{\partial y} \frac{\partial A_{mn}^2}{\partial y} + A_{mn}^2 \left(\frac{\partial^2 S}{\partial x^2} + \frac{\partial^2 S}{\partial y^2} \right) = 0 \quad (5.12)$$

The solutions of equations (5.11) and (5.12) can be written as:

$$A_{mn}^2 = \frac{E_0^2}{f_1(z)f_2(z)} H_m\left(\frac{\sqrt{2}x}{r_0 f_1(z)}\right) H_n\left(\frac{\sqrt{2}y}{r_0 f_2(z)}\right) \exp\left[-\left(\frac{x^2}{r_0^2 f_1^2(z)} + \frac{y^2}{r_0^2 f_2^2(z)}\right)\right] \times \cos\left(\frac{\Omega_0 x}{f_1(z)}\right) \cos\left(\frac{\Omega_0 y}{f_2(z)}\right) \quad (5.13)$$

And

$$S = \frac{x^2}{2} \beta_1(z) + \frac{y^2}{2} \beta_2(z) + \varphi(z) \quad (5.14)$$

Where, $\beta_1(z) = (1/f_1(z))(\partial f_1/\partial z)$ and $\beta_2(z) = (1/f_2(z))(\partial f_2/\partial z)$ represent the curvature of the wavefront in x and y directions respectively. Now, considering the mode for which, $m = 0$ and $n = 0$, we have, $H_0(\sqrt{2}x/(r_0 f_1(z))) = 1$ and $H_0(\sqrt{2}y/(r_0 f_2(z))) = 1$. Further, employing the paraxial approximation and differentiating Eq. (5.13) and (5.14), we get

$$\frac{\partial A_{mn}}{\partial x} = \frac{-E_0}{\sqrt{f_1 f_2}} \sqrt{\cos\left(\frac{\Omega_0 y}{f_2}\right)} \text{Exp}\left[-\frac{1}{2r_0^2}\left(\frac{x^2}{f_1^2} + \frac{y^2}{f_2^2}\right)\right] \left[\frac{\Omega_0}{2f_1} \frac{\sin\left(\frac{\Omega_0 x}{f_1}\right)}{\sqrt{\cos\left(\frac{\Omega_0 x}{f_1}\right)}} + \frac{x \sqrt{\cos\left(\frac{\Omega_0 x}{f_1}\right)}}{r_0^2 f_1^2} \right]$$

$$\frac{\partial^2 A_{mn}}{\partial x^2} = A_{mn} \left[\frac{\Omega_0 x}{r_0^2 f_1^3} \tan\left(\frac{\Omega_0 x}{f_1}\right) - \frac{\Omega_0^2}{4f_1^2} \tan^2\left(\frac{\Omega_0 x}{f_1}\right) + \frac{x^2}{r_0^4 f_1^4} - \frac{\Omega_0^2}{2f_1^2} - \frac{1}{r_0^2 f_1^2} \right]$$

$$\text{Similarly, } \frac{\partial^2 A_{mn}}{\partial y^2} = A_{mn} \left[\frac{\Omega_0 y}{r_0^2 f_2^3} \tan\left(\frac{\Omega_0 y}{f_2}\right) - \frac{\Omega_0^2}{4f_2^2} \tan^2\left(\frac{\Omega_0 y}{f_2}\right) + \frac{y^2}{r_0^4 f_2^4} - \frac{\Omega_0^2}{2f_2^2} - \frac{1}{r_0^2 f_2^2} \right]$$

$$\text{And } \frac{\partial S}{\partial x} = x\beta_1, \frac{\partial S}{\partial y} = y\beta_2 \text{ and } \frac{\partial S}{\partial z} = \frac{x^2}{2} \frac{\partial \beta_1}{\partial z} + \frac{y^2}{2} \frac{\partial \beta_2}{\partial z} + \frac{\partial \varphi}{\partial z}$$

Therefore, using the above values in Eq. (5.11), we get

$$x^2 \left(\frac{1}{f_1} \frac{\partial^2 f_1}{\partial z^2} \right) + y^2 \left(\frac{1}{f_2} \frac{\partial^2 f_2}{\partial z^2} \right) + 2 \frac{\partial \varphi}{\partial z} = \frac{1}{k^2} \left[\frac{\Omega_0 x}{r_0^2 f_1^3} \tan\left(\frac{\Omega_0 x}{f_1}\right) - \frac{\Omega_0^2}{4f_1^2} \tan^2\left(\frac{\Omega_0 x}{f_1}\right) + \frac{x^2}{r_0^4 f_1^4} \right]$$

$$\begin{aligned}
&= \frac{1}{k^2} \left[-\frac{\Omega_0^2}{2f_1^2} - \frac{1}{r_0^2 f_1^2} + \frac{\Omega_0 y}{r_0^2 f_2^3} \tan\left(\frac{\Omega_0 y}{f_2}\right) - \frac{\Omega_0^2}{4f_2^2} \tan^2\left(\frac{\Omega_0 y}{f_2}\right) + \frac{y^2}{r_0^4 f_2^4} - \frac{\Omega_0^2}{2f_2^2} - \frac{1}{r_0^2 f_2^2} \right] \\
&- \frac{E_0^2 \Phi'(A_{mn}^2)}{\varepsilon_0 r_0^2 f_1 f_2} \left(1 + \frac{r_0^2 \Omega_0^2}{2} \right) \left(\frac{x^2}{f_1^2} + \frac{y^2}{f_2^2} \right)
\end{aligned} \tag{5.15}$$

Now, equating the coefficients of x^2 and y^2 on both sides of Eq. (5.15) and using $\xi = z/R_d$,

where, $R_d = kr_0^2$ we get

$$\frac{\partial^2 f_1}{\partial \xi^2} = \frac{1}{f_1^3} - \frac{E_0^2 R_d^2 \Phi'(A_{mn}^2)}{\varepsilon_0 r_0^2 f_1^2 f_2} \left(1 + \frac{r_0^2 \Omega_0^2}{2} \right) \tag{5.16}$$

Similarly,

$$\frac{\partial^2 f_2}{\partial \xi^2} = \frac{1}{f_2^3} - \frac{E_0^2 R_d^2 \Phi'(A_{mn}^2)}{\varepsilon_0 r_0^2 f_2^2 f_1} \left(1 + \frac{r_0^2 \Omega_0^2}{2} \right) \tag{5.17}$$

Where, $\Phi'(A_{mn}^2) = \left(\frac{\omega_{p0}}{\omega} \right)^2 \left(\frac{3m_0 \alpha}{4M} \right) \exp \left[- \left(\frac{3}{4} \right) \left(\frac{m_0 \gamma}{M} \right) \left(\frac{\alpha E_0^2}{f_1 f_2} \right) \right]$

After simplifying the equations (5.16) and (5.17), we obtain the expressions for beam width parameters f_1 and f_2 as:

$$\frac{\partial^2 f_1(z)}{\partial \xi^2} = \frac{1}{f_1^3} - \left(\frac{3}{4} \right) \left(\frac{m_0}{M} \right) (\alpha E_0^2) \left(\frac{\omega_{p0}}{\omega} \right)^2 \left(\frac{r_0 \omega}{c} \right)^2 \frac{(1+b^2/2)}{f_1^2 f_2} \exp \left[- \left(\frac{3}{4} \right) \left(\frac{m_0 \gamma}{M} \right) \left(\frac{\alpha E_0^2}{f_1 f_2} \right) \right] \tag{5.18}$$

And

$$\frac{\partial^2 f_2(z)}{\partial \xi^2} = \frac{1}{f_2^3} - \left(\frac{3}{4} \right) \left(\frac{m_0}{M} \right) (\alpha E_0^2) \left(\frac{\omega_{p0}}{\omega} \right)^2 \left(\frac{r_0 \omega}{c} \right)^2 \frac{(1+b^2/2)}{f_2^2 f_1} \exp \left[- \left(\frac{3}{4} \right) \left(\frac{m_0 \gamma}{M} \right) \left(\frac{\alpha E_0^2}{f_1 f_2} \right) \right] \tag{5.19}$$

where $b = r_0 \Omega_0$ is called decentered parameter and ξ is the dimensionless distance of propagation.

Equations (5.18) and (5.19) are the required expressions for beam width parameters f_1 and f_2 respectively.

5.5 SELF-TRAPPED CONDITION

For initially plane wavefront, $(\partial f_1 / \partial \xi)_{\xi=0} = 0$, $(f_1)_{\xi=0} = 1$ and $(\partial f_2 / \partial \xi)_{\xi=0} = 0$, $(f_2)_{\xi=0} = 1$, the conditions $\partial^2 f_1 / \partial \xi^2 = 0$ and $\partial^2 f_2 / \partial \xi^2 = 0$ lead to the propagation of laser beam in self-

trapped mode. Substituting for $\partial^2 f_1 / \partial \xi^2 = 0$ and $\partial^2 f_2 / \partial \xi^2 = 0$ in Eq. (5.18) and Eq. (5.19) respectively, we obtain a relation for dimensionless initial beam width $\rho_0 (= r_0 \omega / c)$ and is given as follows:

$$\rho_0 = \left\{ \frac{\exp \left[\left(\frac{3}{4} \right) \left(\frac{m_0 \gamma}{M} \right) (\alpha E_0^2) \right]}{\left(\frac{3}{4} \right) \left(\frac{m_0}{M} \right) (\alpha E_0^2) (1 + b^2 / 2)} \right\}^{1/2} \quad (5.20)$$

To explain the results for HcosG beam propagation in relativistic plasma, we numerically analyze the dependence of initial beam width ρ_0 as a function of αE_0^2 for the plasma under self-trapped condition. The results are depicted in Fig. 5.1. It is found that decrease in ρ_0 is observed with increase in αE_0^2 for relativistic plasma at different values of decentered parameter.

5.6 RESULTS AND DISCUSSION

We conduct the numerical analysis and computational simulations for solving the beam width parameter equations. The various parameters chosen for the purpose of numerical calculations are: $\omega = 10^{14} \text{ rad/sec}$, $\omega_{p0} = 1.87 \times 10^{14} \text{ rad/sec}$, $r_0 = 5 \times 10^{-3} \text{ cm}$ and

$$n_0 = 9.98 \times 10^{17} \text{ cm}^{-3} [71].$$

The relativistic nonlinear effect emerging from the relativistic mass correction that depends on factor αE_0^2 and relative plasma density ω_{p0} / ω . The diffractive divergence of the beam is due to the diffraction term while as self-focusing is due to nonlinear term. Fig. 5.2 shows the dependence f on ξ for various values of $b = 0, 0.5$ & 1 with $\omega_{p0} / \omega = 0.4$ and $\alpha E_0^2 = 1.5$. It is clear from fig. 5.2 that strong self-focusing occurs at $\xi = 2.65$ for $b = 1$ and at $\xi = 3.1$ for $b = 0.5$. Decentered parameter is an important parameter that is to be optimized for stronger self-focusing at smaller distance. This is because of the fact that the decentered parameter changes the nature of self-focusing of the beam significantly. Fig. 5.3, illustrates the behaviour of f with ξ for $\alpha E_0^2 = 1, 1.25$ & 1.50 . It is obvious from the figure that sharp self-focusing is observed at $\xi = 3.1$. It is seen from fig. 5.3 that as we increase the values of αE_0^2 , self-focusing occurs earlier and

becomes stronger. This is because of the supremacy of self-focusing term over the diffraction term because of the relativistic nonlinearity.

Fig. 5.4 shows the dependence f on ξ for various values $b = 0, 1 \& 2$ with $\omega_{p0} / \omega = 0.6$ and $\alpha E_0^2 = 2$. It has been predicted that by increasing the values b , f decreases greatly up to $\xi = 2.35$, thereby showing that the self-focusing of laser beam is enhanced further. Further, it can be seen that for a high intensity laser, the self-focusing occurs at lower values of b . Therefore, the decentered parameter is sensitive for the self-focusing of HcosG laser beam and thus, supports the results predicted by Nanda *et al.* [90]. Moreover, the beam converges more rapidly and focuses up to smaller spot size. The beam width parameter decreases monotonically with intensity, decentered parameter and plasma density. Finally, to throw light upon the nature of self-focusing of HcosG laser beam in collisionless plasma, in Fig. 5.5, we observe the stronger and earlier self-focusing (corresponding to $\xi = 0.25$) of laser beam as a result of increase in plasma density. This is due to the fact that when the plasma density is increased at relativistic intensities, the beam having more relativistic electrons travels with the laser pulse. With the result, a higher current and consequently a high magnetic field is generated, which leads to further enhancement of self-focusing.

5.7 CONCLUSION

We have investigated the self-focusing of HcosG laser beam in collisionless plasma by taking into account the relativistic nonlinearity, using WKB and paraxial approximation. The equation of beam width parameter and self-trapped mode has been derived under the weak relativistic ponderomotive nonlinearity. Depending on the values of decentered parameter, laser intensity and plasma density, the variation of dimensionless beam width parameter as a function of normalized propagation distance is seen and discussed. We have found that the laser beam focuses faster and earlier with smaller spot size. The spot size can be controlled by optimizing laser plasma parameters. Thus, one may conclude that the decentered parameter and laser intensity has a significant role in improving self-focusing of HcosG laser beam in plasma. It is expected that the results of present analysis may be useful in laser driven fusion.

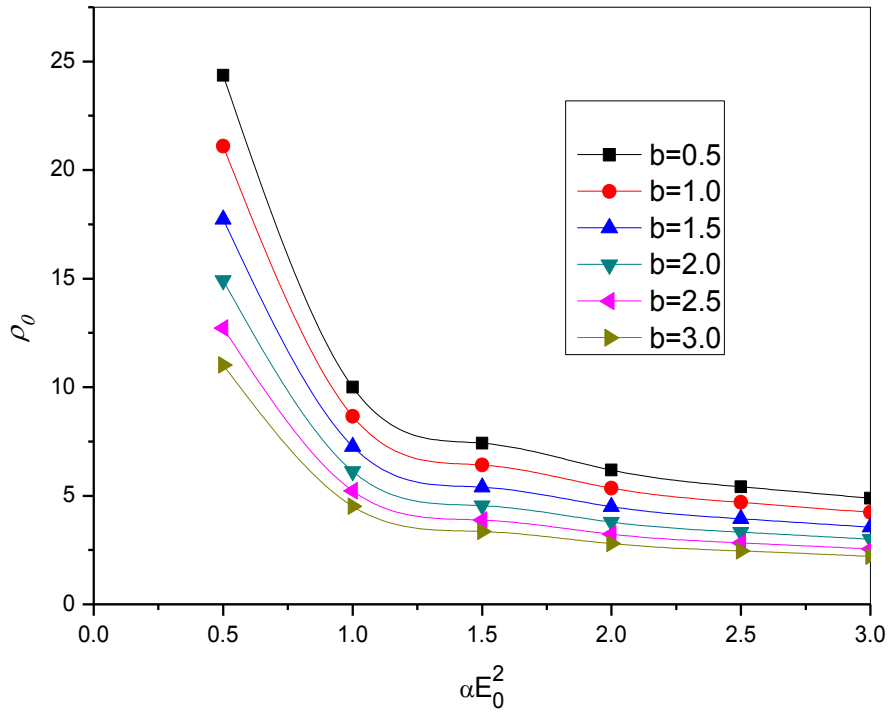


Figure 5.1: Dependence of $\rho_0(r_0\omega_{p0}/c)$ on αE_0^2 for $m_0/M = 0.02$ and $\gamma = 1.25$

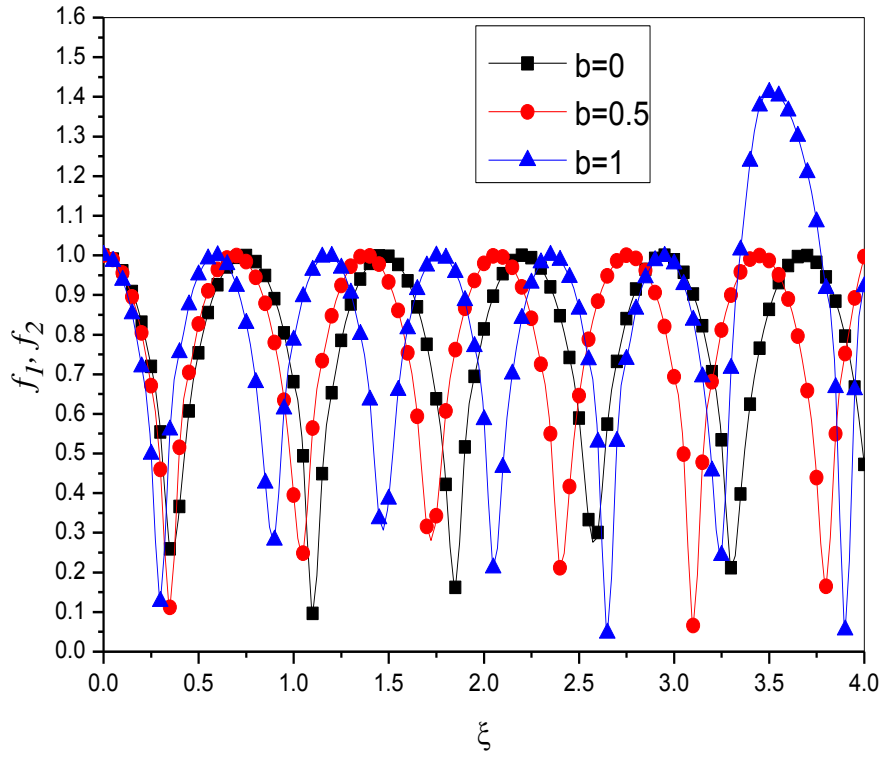


Figure 5.2: Dependence of f_1 and f_2 on ξ for various values of b . The other parameters are $\omega_{p0}/\omega = 0.6$, $\alpha E_0^2 = 1.5$, $m_0/M = 0.02$, $r_0\omega/c = 50$, $\gamma = 1.25$

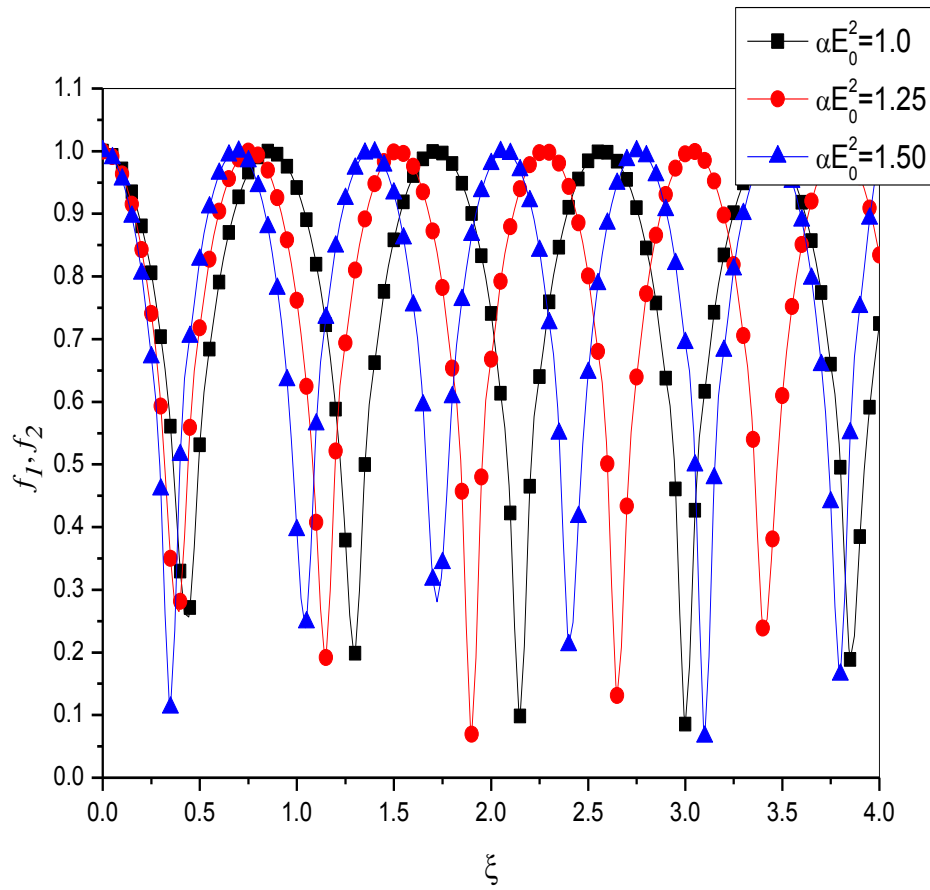


Figure 5.3: Dependence of f_1 and f_2 on ξ for various values of αE_0^2 . The other parameters are $\omega_{p0}/\omega = 0.4$, $b = 0.5$, $m_0/M = 0.02$, $r_0\omega/c = 50$, $\gamma = 1.25$

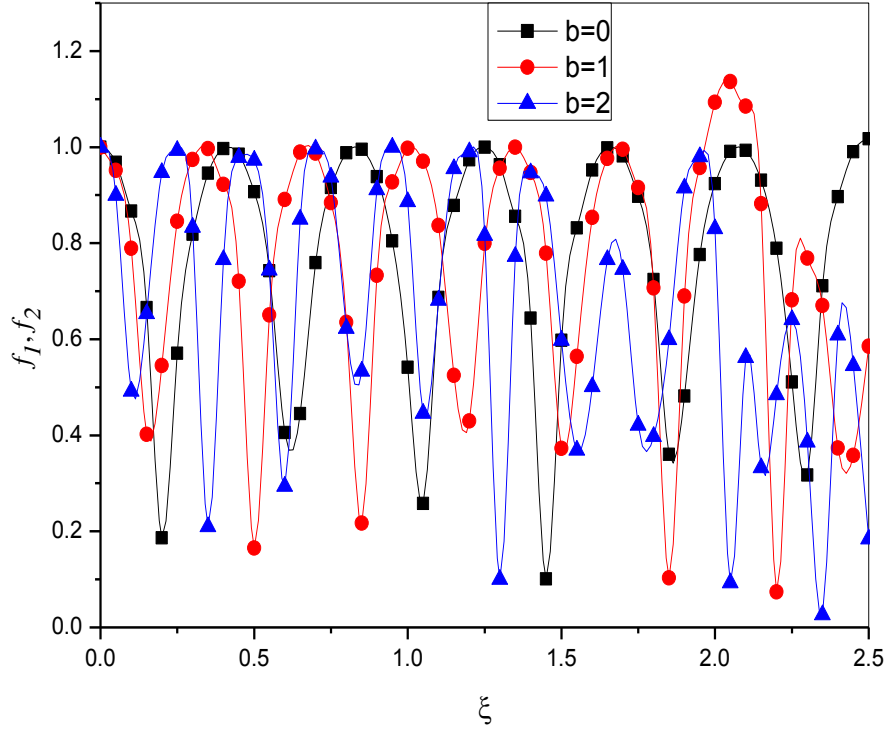


Figure 5.4: Dependence of f_1 and f_2 on ξ for various values of b . The other parameters are $\omega_{p0} / \omega = 0.6$, $\alpha E_0^2 = 2$, $m_0 / M = 0.02$, $r_0 \omega / c = 50$, $\gamma = 1.40$

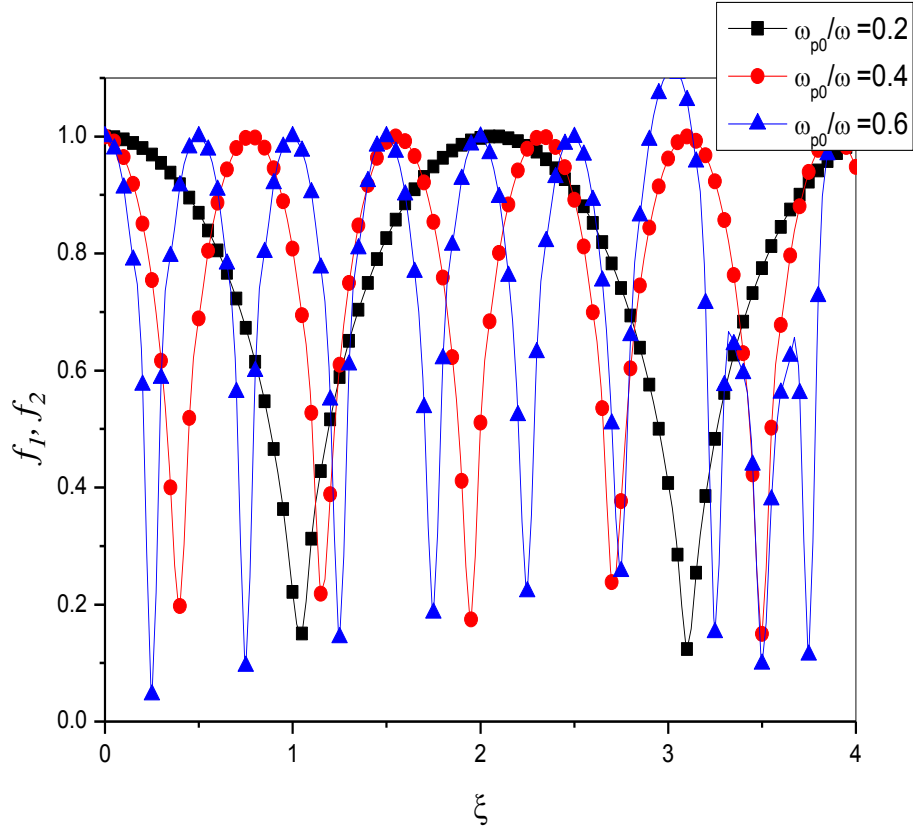


Figure 5.5: Dependence f_1 and f_2 on ξ for various values of ω_{p0}/ω . The other parameters are $\alpha E_0^2 = 1.2$, $m_0/M = 0.02$, $r_0\omega/c = 50$, $\gamma = 1.25$ and $b = 0.5$

CHAPTER-6

NONLINEAR PROPAGATION OF GAUSSIAN LASER BEAM IN AN INHOMOGENEOUS PLASMA UNDER PLASMA DENSITY RAMP

6.1 INTRODUCTION

The theoretical and experimental study of interaction of high intensity laser beams with plasmas is a fascinating field of research which gives rise to various important applications such as plasma based accelerators [5], inertial confinement fusion [6, 7], ionospheric modification [17, 18] etc. For the success of these applications, the laser beam propagates over distances greater than several Rayleigh lengths [64, 120, 65]. Self-focusing is a nonlinear phenomenon which is induced due to change in the refractive of the medium. It can be relativistic [121] as well as ponderomotive [42]. The former is due to relativistic mass variation of electrons and the later is due to plasma density variations produced by ponderomotive forces. The phenomenon of self-focusing has been studied by many authors [122, 35, 92, 71, 91, 22] and found that optimized parameters are important for self-focusing. Gupta *et al.* [87] found that the ion temperature causes thermal self-focusing and has a serious influence on the evolution of laser beam in plasma. However, optimum self-focusing is achieved by taking in to account the combined effect of relativistic and ponderomotive self-focusing [86].

Jafari Milani *et al.* [95] investigated the ponderomotive self-focusing of Gaussian laser beam and reported that the collision frequency at first causes self-focusing and then defocusing of laser beam takes place in warm collisional plasma. But, as collision frequency is increased, the self-focusing length becomes shorter with the result larger collision frequency prevents the longer propagation of laser beam through plasma. The higher order axial electron temperature decreases the influence of collisional nonlinearity. It changes the electron density distribution and increases the dielectric constant therefore, leads to fast divergence of the laser beam [123]. However, following higher order paraxial theory with ramped density profile enhances the focusing [99]. Again, Patil *et al.* [85] have found that the upward plasma density ramp tends to enhance the self-focusing significantly and the beam gets more focused while traversing several Rayleigh lengths as compared with uniform density relativistic plasma. Kant and Wani [181] reported that the decentered parameter and linear absorption change the self-focusing / defocusing nature of the

beam. The absorption weakens the self-focusing effect and the density transition sets sooner and an earlier self-focusing.

In this paper, our purpose is to analyze the impact of upward plasma density ramp on nonlinear Gaussian propagation in an inhomogeneous plasma. The plasma density ramp profile chosen is of the form $n(\xi) = n_0 \tan(\xi/d)$. The non-linear dielectric constant of plasma is presented in ponderomotive regime. The equations governing the laser beam evolution are derived. The computational results in the context of plasma density, laser intensity and initial beam width are discussed and finally a brief conclusion is added. The importance of the present work lies in the fact that the upward plasma density ramp enhances the self-focusing to a greater extent in inhomogeneous plasma.

6.2 NONLINEAR DIELECTRIC CONSTANT

The nonlinear dielectric function ε for an isotropic inhomogeneous medium can be expressed as

$$\varepsilon = \varepsilon_r(z, EE^*) - i\varepsilon_i(z, EE^*), \quad (6.1)$$

where, ε_r and ε_i are the functions of z and the irradiance EE^* . Further, ε_r can be expressed as:

$$\varepsilon_r(z, EE^*) = \varepsilon_0(z) + \varepsilon_s \mu(z) \frac{\varepsilon_2 EE^*}{1 + \varepsilon_2 EE^*}, \quad (6.2)$$

where, ε_0 and μ are functions of z . The function $\mu(z)$ is identified with the plasma frequency.

In this case $\varepsilon_0(z) = 1 - (\omega_{p0}^2 / \omega^2) \mu(z)$, $\varepsilon_s = \omega_{p0}^2 / \omega^2$, $\varepsilon_i(z) = \mu(z) \varepsilon_i(0)$ with, $\mu(z) = \omega_p^2 / \omega_{p0}^2 = \tan(\xi/d)$, $\omega_p^2 = \omega_{p0}^2 \tan(\xi/d)$ and $\omega_{p0}^2 = 4\pi n_0 e^2 / m$. Where, ω_{p0} is the plasma frequency, ω is the angular frequency of incident laser beam, ε_i is the characteristic of absorption in the medium, $\mu(z)$ is characteristic of the density of dipoles, m , e and n_0 are the electron's rest mass, charge on the electron and equilibrium electron density respectively, ξ is the propagation distance and d is a dimensionless parameter. In case of Gaussian beam $\varepsilon_r(z)$ can be expanded as:

$$\varepsilon_r(z) = \varepsilon_{r0}(z) - r^2 \varepsilon_{r2}(z). \quad (6.3)$$

6.3 SELF-FOCUSING EQUATIONS

Consider the Gaussian laser beam propagating along the z -direction with electric vector \vec{E} satisfies the scalar wave equation of the form

$$\frac{\partial^2 E}{\partial z^2} + \left\{ \frac{\partial^2}{\partial r^2} + \frac{1}{r} \frac{\partial}{\partial r} \right\} E + \frac{\omega^2}{c^2} \varepsilon(r, z) E = 0, \quad (6.4)$$

where, c is the speed of light in vacuum. Eq. (6.4) can be solved in the paraxial approximation by adopting the analysis of Akhmanov *et al.* [113] and Sodha *et al.* [20, 114]. The solution of equation (6.4) is of the form

$$E(r, z) = A(r, z) \exp \left[- \int_0^z ik(z) dz \right], \quad (6.5)$$

where, $A(r, z)$ is the slowly varying envelope of the beam and k is the wave propagation constant which is given by $k^2(z) = (\omega^2 / c^2) \varepsilon_{r,0}(z)$.

Differentiating equation (6.5) twice w. r. t. ' r ' and ' z ' and neglecting $(\partial^2 A / \partial z^2)$, we get

$$\frac{\partial \vec{E}}{\partial r} = \text{Exp} \left[- \int_0^z ik(z) dz \right] \frac{\partial A(r, z)}{\partial r}$$

$$\frac{\partial^2 \vec{E}}{\partial r^2} = \text{Exp} \left[- \int_0^z ik(z) dz \right] \frac{\partial^2 A(r, z)}{\partial r^2}$$

And

$$\frac{\partial \vec{E}}{\partial z} = \text{Exp} \left[- \int_0^z ik(z) dz \right] \left[\frac{\partial A(r, z)}{\partial z} - iA(r, z)k(z) \right]$$

$$\frac{\partial^2 \vec{E}}{\partial z^2} = \text{Exp} \left[- \int_0^z ik(z) dz \right] \left[-2ik(z) \frac{\partial A(r, z)}{\partial z} - iA(r, z) \frac{\partial k(z)}{\partial z} - k^2(z)A(r, z) \right]$$

Substituting the above values in Eq. (6.4), under WKB approximation, one obtains

$$-2ik \frac{\partial A}{\partial z} - iA \frac{\partial k}{\partial z} - k^2 A + \frac{\partial^2 A}{\partial r^2} + \frac{1}{r} \frac{\partial A}{\partial r} + \frac{\omega^2}{c^2} \varepsilon(r, z) A = 0, \quad (6.6)$$

To solve Eq. (6.6) in the paraxial approximation, the complex amplitude $A(r, z) = A_0(r, z)\exp[-ik(z)S(r, z)]$ is considered. Here, A_0 and S depend on r and z .

Therefore, from Eq. (6.6), we get

$$-2k^2 A_0 \frac{\partial S}{\partial z} - 2k A_0 S \frac{\partial k}{\partial z} - k^2 A_0 + \frac{\partial^2 A_0}{\partial r^2} - k^2 A_0 \left(\frac{\partial S}{\partial r} \right)^2 + \frac{1}{r} \frac{\partial A_0}{\partial r} + \frac{\omega^2 A_0}{c^2} (\varepsilon_{r0}(z) - r^2 \varepsilon_{r2}(z)) - \left(2k \frac{\partial A_0}{\partial z} + A_0 \frac{\partial k}{\partial z} + k A_0 \frac{\partial^2 S}{\partial r^2} + 2k \frac{\partial S}{\partial r} \frac{\partial A_0}{\partial r} + \frac{k A_0}{r} \frac{\partial S}{\partial r} + \frac{\omega^2 \varepsilon_i(0) A_0}{c^2} \tan(z/dR_d) \right) = 0 \quad (6.7)$$

Now, equating real and imaginary parts of Eq. (6.7), we get

Real part equation is

$$2 \frac{\partial S}{\partial z} + \left(\frac{\partial S}{\partial r} \right)^2 + \left(\frac{2S}{k} \right) \frac{\partial k}{\partial z} = \frac{1}{k^2 A_0} \left(\frac{\partial^2 A_0}{\partial r^2} + \frac{1}{r} \frac{\partial A_0}{\partial r} \right) - \frac{r^2 \varepsilon_{r2}(z)}{\varepsilon_{r0}(z)}, \quad (6.8)$$

Imaginary part equation is

$$\frac{\partial A_0^2}{\partial z} + A_0^2 \left(\frac{\partial^2 S}{\partial r^2} + \frac{1}{r} \frac{\partial S}{\partial r} \right) + \frac{\partial A_0^2}{\partial r} \frac{\partial S}{\partial r} = A_0^2 \left(\frac{-\tan(z/dR_d) k \varepsilon_i(0)}{\varepsilon_{r0}(z)} - \frac{1}{k} \frac{\partial k}{\partial z} \right). \quad (6.9)$$

The solution of Eq. (6.9) can be written as

$$A_0^2(r, z) = \left(\frac{E_0^2(z)}{f^2(z)} \right) \mathfrak{S} \left(\frac{r}{r_0 f(z)} \right), \quad (6.10)$$

where, \mathfrak{S} is any arbitrary parameter and $E_0^2(z)$ is the axial irradiance. For an initially Gaussian

beam at $z = 0$, $EE^* = A_0^2 = E_{00}^2 \exp(-r^2/r_0^2)$ and the eikonal $S(r, z) = (r^2/2)\beta(z) + \phi(z)$,

where, $\beta(z) = (1/f(z))(\partial f/\partial z)$ represents the curvature of the wavefront. Substituting for A_0^2

and using the above values in Eq. (6.8), we get

$$r^2 \left[\frac{1}{r_0^4 k^2 f} \frac{\partial^2 f}{\partial \xi^2} + \frac{1}{2k^2 f r_0^4 \varepsilon_{r0}} \left(\frac{\partial f}{\partial \xi} \right) \left(\frac{\partial \varepsilon_{r0}}{\partial \xi} \right) \right] + 2 \frac{\partial \phi}{\partial z} + \frac{\phi(z)}{k r_0^2 \varepsilon_{r0}} \left(\frac{\partial \varepsilon_{r0}}{\partial \xi} \right) = - \frac{2c^2}{\omega^2 r_0^2 \varepsilon_{r0} f^2} + r^2 \left[\frac{c^2}{\omega^2 r_0^4 \varepsilon_{r0} f^4} - \frac{\varepsilon_{r2}(z)}{\varepsilon_{r0}} \right]. \quad (6.11)$$

Now, equating the coefficients of r^2 on both sides of Eq. (6.11), we get

the resulting equation. One obtains

$$\frac{\partial^2 f}{\partial \xi^2} = -\frac{\rho^2}{f} \left[\varepsilon'_{r_2} - \frac{1}{\rho^2 f^2} \right] - \frac{1}{2\varepsilon_{r_0}} \left(\frac{\partial f}{\partial \xi} \right) \left(\frac{\partial \varepsilon_{r_0}}{\partial \xi} \right), \quad (6.12)$$

where, $\varepsilon'_{r_2} = r_0^2 f^2 \varepsilon_{r_2} (E_0^2 / f^2)$, $\rho_0 = r_0 \omega / c$ is the equilibrium beam radius, $\xi = z / R_d$ is the propagation distance, $R_d = k r_0^2$ represents the diffraction length. Thus, with the dependence of ε'_{r_2} on f and ξ , Eq. (6.12) can be solved for f as a function of ξ . Further, expanding $A_0^2(r, z)$ from Eq. (6.10) in a series of r^2 and retaining terms up to r^2 (in the paraxial approximation). We have

$$EE^* = \frac{E_0^2}{f^2} \left(1 - \frac{r^2}{r_0^2 f^2} \right), \quad (6.13)$$

Using Eq. (6.13) in Eq. (6.2) one obtains

$$\varepsilon_{r_0} = \varepsilon_0(z) + \varepsilon_s \tan(z / d R_d) \frac{(\varepsilon_2 E_0^2 / f^2)}{1 + (\varepsilon_2 E_0^2 / f^2)} \quad (6.14)$$

and

$$\varepsilon'_{r_2} = \frac{\varepsilon_s \varepsilon_2 E_0^2 \tan(z / d R_d)}{1 + \varepsilon_2 E_0^2 / f^2}. \quad (6.15)$$

Using Eq. (6.14) and (6.15) in Eq. (6.12), we get

$$\frac{\partial^2 f}{\partial \xi^2} = -\frac{\rho^2}{f} \left[\frac{\varepsilon_s \varepsilon_2 E_0^2 \tan(\xi / d)}{1 + \varepsilon_2 E_0^2 / f^2} - \frac{1}{\rho^2 f^2} \right] + \left[\frac{1}{1 - \varepsilon_s \tan(\xi / d) + \frac{\varepsilon_s \varepsilon_2 E_0^2 \tan(\xi / d)}{f^2 + \varepsilon_2 E_0^2}} \right] \times$$

$$\left[\frac{f^2 \text{Sec}^2(\xi / d)}{2d} + \frac{\varepsilon_2 E_0^2 f \tan(\xi / d)}{f^2 + \varepsilon_2 E_0^2} \right] \left(\frac{\partial f}{\partial \xi} \right) \frac{\varepsilon_s}{f^2 + \varepsilon_2 E_0^2} \left(\frac{\partial f}{\partial \xi} \right). \quad (6.16)$$

Equation (6.16) is the required equation for the beam width parameter f , which could be solved by applying the initial condition at $\xi = 0$, $f = 1$, $(\partial f / \partial \xi) = 0$ and $(\partial^2 f / \partial \xi^2) = 0$

6.4 RESULTS AND DISCUSSION

In the present communication, we have seen the effect of ramped density profile on the propagation of Gaussian laser beam in inhomogeneous plasma. We have solved Eq. (6.16) numerically and the various parameters taken for numerical calculation are: $\omega = 1.778 \times 10^{14} \text{ rad/sec}$, $r_0 = 20 \mu\text{m}$ and $\lambda = 1.06 \mu\text{m}$ [101]. The value of intensity of laser beam is $I_0 = 1.21 \times 10^{18} \text{ W/cm}^2$. Fig. 6.1 represents the dependence f on ξ for various values of ω_{p0}/ω . The other parameters are $d = 10$, $\varepsilon_2 E_0^2 = 10$, $\rho^{-2} = 0.04$. It is observed that by increasing the values of ω_{p0}/ω , f decreases strongly with ξ and reaches its minimum at $\omega_{p0}/\omega = 0.8$. The laser beam then undergoes oscillatory behavior and the frequency of oscillation increases, while amplitude decreases gradually close to the propagation axis. Therefore, the plasma dielectric constant decreases rapidly as initial electron density depends on ξ with the result, self-focusing is observed at large ξ values. The results of present analysis can be compared with those of Kaur *et al.* [109]. Wherein, the introduction of two scale length leads the laser beam to oscillate periodically for a long propagation distance with constant amplitude. Fig. 6.2 illustrates the behavior of f with ξ for various values of $\varepsilon_2 E_0^2$. The other parameters are $\omega_{p0}/\omega = 0.4$, $d = 15$, $\rho^{-2} = 0.08$. From figure 6.2 it is clear that while propagating the laser beam through the plasma, the diffraction of beam starts earlier with increase in $\varepsilon_2 E_0^2$ and hence controls the behavior of beam width parameter. Due to increase in the value of intensity, highly energetic electrons will continue to move forward without loss of energy. Further, the beam width parameter is a function of laser spot size and depends on intensity of laser beam. Therefore, the intensity rise results in the reduction of spot size of laser beam with the result, self-focusing of laser beam slows down and becomes stronger. Figure 6.3 shows the dependence of f on ξ for different ρ^{-2} values. The plasma density is fixed at $\omega_{p0}/\omega = 0.8$ and the other parameters are same as taken in figure 6.1. From figure 6.3, it is clear that the oscillatory character of the beam width parameter is observed for a chosen set of parameters. Remarkably, the amplitude of oscillations decreases gradually with the distance of propagation on account of

effect of nonlinearity. Further, with increase in the values of $1/\rho^{-2}$, the beam width parameter first increases, attains a maximum and then decreases thereby, exhibits oscillatory character. Therefore, the behavior of beam width parameter is highly affected by the beam radius under density transition. Again, Navare *et al.* [80] concluded that by taking in to account the collisional nonlinearity and linear absorption, the oscillatory behavior of beam width parameter weakens with the distance of propagation. The self-focusing of laser beam takes place only for a short propagation distance and the beam then defocuses. However, in the present work, introduction of density ramp leads the beam width parameter to decrease with a higher rate. Consequently, the self-focusing of laser beam is enhanced to a greater extent by exploiting the density transition in an inhomogeneous plasma. Above all, the density transition plays a vital role in laser plasma interaction and is important for the injection of plasma electrons to acceleration stage.

6.5 CONCLUSION

In the present investigation, we have investigated the Gaussian beam propagation in inhomogeneous plasma under plasma density ramp. The differential equation for beam width parameter is established under paraxial approximation. The effect of plasma density, laser intensity and initial beam width on self-focusing has been discussed. By optimizing laser and plasma parameters, the effect of density transition on the behavior of beam width parameter with the propagation distance has been analyzed and plotted. The results reveal that the amplitude of oscillation decreases considerably with the distance. The oscillatory behavior of beam width parameter becomes slow with increase in relative plasma density and intensity of laser beam. The saturation behavior of the beam width parameter shows that the laser beam evolves differently when propagates through underdense plasma. Further, after initial laser focusing, the relativistic mass effect is more declared in high plasma density region. Therefore, the plasma density ramp enhances the self-focusing effect to a greater extent. The outcomes obtained in the present analysis may be useful in understanding the physics of plasma based accelerators.

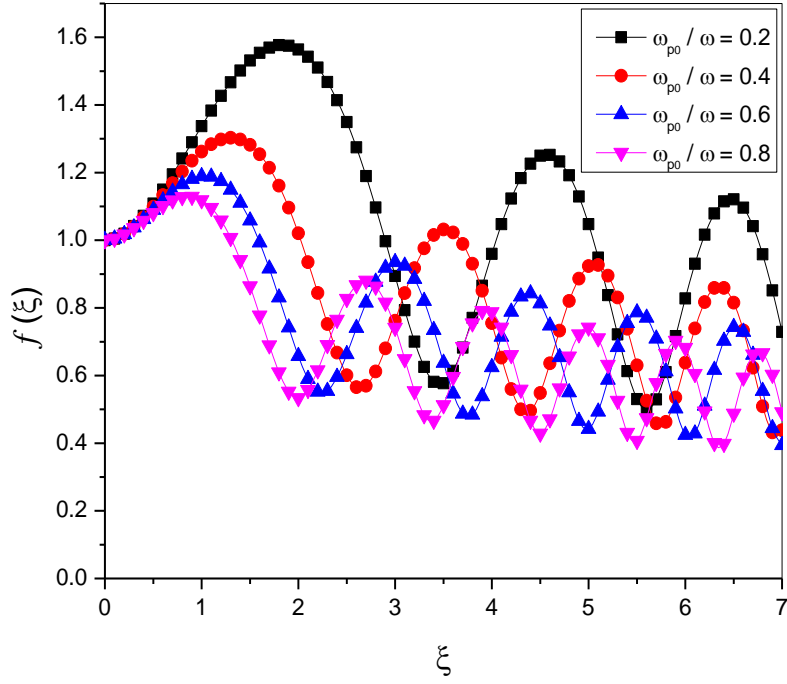


Figure 6.1: Dependence f on ξ for various values of ω_{p0}/ω . The other parameters are $d = 10$, $\varepsilon_2 E_0^2 = 10$, $\rho^{-2} = 0.04$.

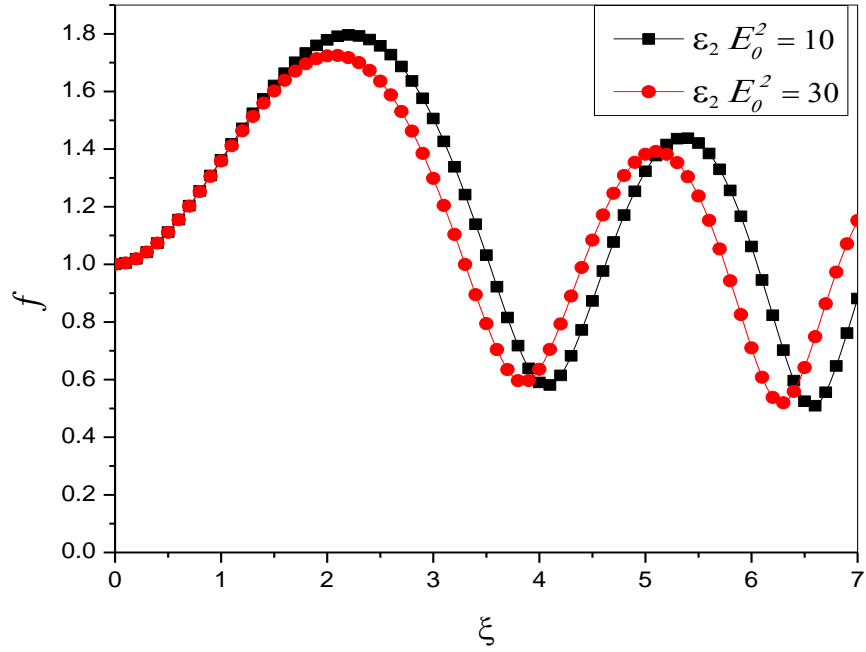


Figure 6.2: Dependence f on ξ for various values of $\epsilon_2 E_0^2$. The other parameters are $\omega_{p0}/\omega = 0.4$, $d = 15$, $\rho^{-2} = 0.08$

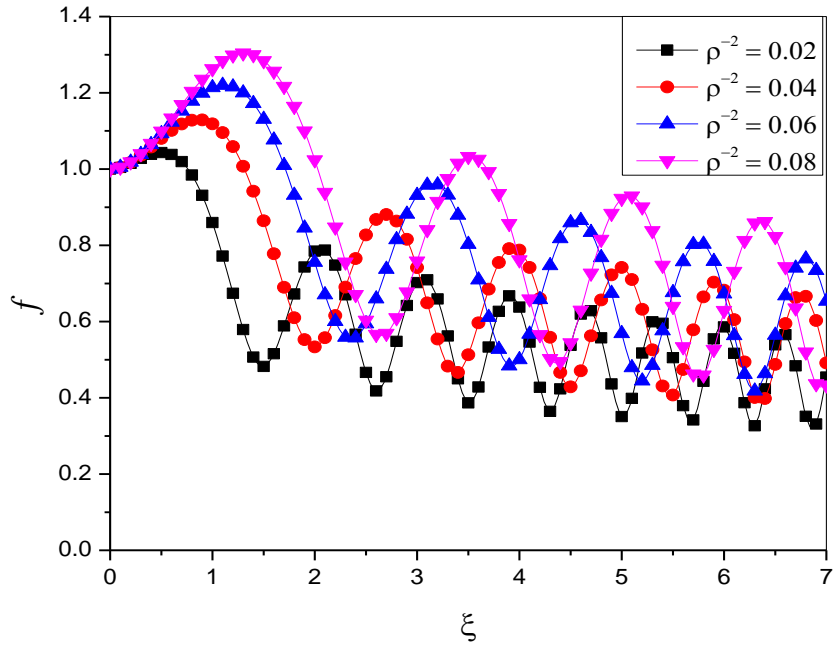


Figure 6.3: Dependence f on ξ for various values of ρ^{-2} . The other parameters are $\varepsilon_2 E_0^2 = 10$, $\omega_{p0} / \omega = 0.8$, $d = 10$

CHAPTER-7

SELF-FOCUSING / DEFOCUSING OF CHIRPED GAUSSIAN LASER BEAM IN COLLISIONAL PLASMA WITH LINEAR ABSORPTION

7.1 INTRODUCTION

The interaction of high power laser beams with plasmas has known to be an important and captivating field of research because of its applications in charged particle accelerators, x-ray lasers etc. [8, 115, 4]. In all these applications, it is necessary to know the characteristics of a high power beam that propagates over extended distances with no loss of energy. When such a beam interacts with the plasma, various nonlinear phenomena's (self-focusing, harmonic generation, electron acceleration in vacuum etc.) are likely to occur. Among, these phenomena's self-focusing is very important nonlinear phenomenon in which the wave front of laser acquires a curvature and laser tends to focus. In general, there are two types of self-focusing viz., relativistic self-focusing [121] and ponderomotive self-focusing [42] and many papers have been published in achieving the self-focusing of laser beams in plasmas [28, 113, 77, 64, 85]. The self-focusing decreases with rising intensity of the beam due to supremacy of diffraction effect at higher intensity [84]. Gill *et al.* [81] used the higher order paraxial theory to study the relativistic self-focusing of super Gaussian laser beam in plasma and reported that the inclusion of higher order terms of dielectric function affects the behavior of beam width parameter significantly and the magnetic field improves the self-focusing of laser beam in plasma [101, 124]. Recently, Habibi and Ghamari [98] have extended the same theory for cosh-Gaussian beam in quantum plasma. By using more effective decentered parameter, better self-focusing is observed for cosh-Gaussian beams in comparison to Gaussian beams in quantum plasma.

The density transition is considered to be important in laser and plasma interactions, particularly for the self-focusing in plasma medium. Increase in initial density and ramp slope lowers the minimum spot size of the laser beam. These parameters play a key role and are crucial for self-focusing as it is enhanced with optimized laser and plasma parameters [22, 92, 97, 102, 91]. Kant and Wani [118] studied the self-focusing under density transition with linear absorption. Due to absorption, the self-focusing effect weakens and density transition sets sooner and an earlier self-

focusing. Gupta *et al.* [87] considered the relativistic ponderomotive nonlinearity and their results have shown that the ion temperature causes thermal self-focusing and has a serious influence on laser beam evolution in collisional plasma. Taking in to account the higher order axial electron temperature, it has been reported that it decreases the influence of collisional nonlinearity. It further changes the electron density distribution and increases the dielectric constant, with the result, it leads to fast divergence of the beam [123]. The chirp was used to study the electron acceleration in vacuum. It increases the electron energy and hence momentum so that the electron escapes from the laser beam. The value of chirp parameter decreases with laser intensity and initial electron energy. It further, increases the amplitude of wake wave that has been generated in the plasma by an electromagnetic beam [125, 126]. Ghotra and Kant [127] used the chirped laser pulse to study the electron acceleration in vacuum in presence of azimuthal magnetic field. The chirp increases the duration of interaction of laser beam with electron and strengths the resonance for longer duration. Further, the magnetic field improves the electron acceleration to high energy of the order of GeV.

In the present communication, we analyzed the effect of chirp on the self-focusing / defocusing of Gaussian beam propagating in collisional plasma with linear absorption. Effects of chirp parameter, collision frequency and other laser plasma parameters are seen on the self-focusing / defocusing in plasma. Although, without chirp, the laser beam shows self-focusing but, as the propagation distance increases, it starts to experience defocusing. To reduce this defocusing, the effect of chirp is considered. The chirp parameter minimizes the defocusing and increases the ability of self-focusing. Further, the amplitude of oscillations decreases with the propagation distance so that sooner and stronger self-focusing is achieved. This paper is constituted as follows: in section 7.2 the nonlinear dielectric constant and the equation that governs the behavior of beam width parameter with the propagation distance is presented. Section 7.3 is devoted to results and discussions. Finally, the conclusion is considered in last section 7.4.

7.2 SELF FOCUSING OF CHIRPED GAUSSIAN LASER BEAM

Consider the propagation of a Gaussian beam in plasma along the z - axis. Its initial intensity distribution is given by

$$EE^* = E_0^2 \exp\left(-\frac{r^2}{r_0^2}\right), \quad (7.1)$$

where, \vec{E} is the electric vector and r_0 is the waist width of the beam. The wave equation that governs the laser beam propagation may be written as

$$\nabla^2 \vec{E} + \left(\frac{\omega^2}{c^2}\right) \varepsilon \vec{E} + \nabla \left(\frac{\vec{E} \cdot \nabla \varepsilon}{\varepsilon}\right) = 0. \quad (7.2)$$

The last term on the left hand side of above equation (7.2) is neglected under the condition $k^{-2} \nabla^2 (\ln \varepsilon) \ll 1$, where, k represents the wave number of the laser beam. Thus,

$$\nabla^2 \vec{E} + \frac{\omega^2}{c^2} (\varepsilon \cdot \vec{E}) = 0.$$

Or, in cylindrical co-ordinate system, we can write this equation as

$$\frac{\partial^2 \vec{E}}{\partial z^2} + \frac{\partial^2 \vec{E}}{\partial r^2} + \frac{1}{r} \frac{\partial \vec{E}}{\partial r} + \varepsilon \frac{\omega^2}{c^2} \vec{E} = 0 \quad (7.3)$$

The effective dielectric constant of the plasma can be expressed as

$$\varepsilon = \varepsilon_0 + \phi(EE^*) - i\varepsilon_i, \quad (7.4)$$

where, $\varepsilon_0 = 1 - \omega_p^2 / \omega^2$ is a linear part and ϕ is a nonlinear part of dielectric constant, $\varepsilon_i = (\omega_p^2 / \omega^2)(\nu / \omega)$ takes care of linear absorption ($\varepsilon_i \ll \varepsilon_0$), ν is the collision frequency, $\omega = \omega_0(1 + b(\omega_0 t - \omega_0 z / c))$ is the angular frequency of chirped Gaussian laser beam, ω_0 is the angular frequency of incident laser beam, b is the chirp parameter, c is the velocity of light, ω_p is the plasma frequency given by $\omega_p^2 = 4\pi n_0 e^2 / m$, where, m is the rest mass of electron, e is the charge of electron and n_0 is the equilibrium electron density. Following [114], $\phi(EE^*)$ can be expressed as:

$$\phi(EE^*) = \frac{\omega_p^2}{\omega^2} \left[1 - \left(1 + \frac{\alpha}{2} EE^* \right)^{(s_0/2)-1} \right], \quad (7.5)$$

where, s_0 is a parameter characterizing the nature of collisions, $\alpha = e^2 M / 6m^2 \omega^2 k_B T$, M is the mass of scatterer in the plasma, T is the equilibrium plasma temperature and k_B is the Boltzmann constant. Now, the solution of equation (7.3) is of the following form,

$$\vec{E} = A(r, z, t) \text{Exp}[i(\omega t - kz)] \quad (7.6)$$

With $k^2 = \varepsilon_0 \omega^2 / c^2 = \omega_0^2 / c^2 (1 + b(\omega_0 t - \omega_0 z / c))^2 [1 - (\omega_p^2 / \omega_0^2)(1 + b(\omega_0 t - \omega_0 z / c))^{-2}]$, where, $A(r, z)$ is the complex amplitude. Differentiating equation (7.6) twice w. r. t. 'r' and 'z', we get

$$\frac{\partial \vec{E}}{\partial r} = \text{Exp}[i(\omega t - kz)] \frac{\partial A(r, z, t)}{\partial r}$$

$$\frac{\partial^2 \vec{E}}{\partial r^2} = \text{Exp}[i(\omega t - kz)] \frac{\partial^2 A(r, z, t)}{\partial r^2}$$

And

$$\frac{\partial \vec{E}}{\partial z} = \text{Exp}[i(\omega t - kz)] \left[\frac{\partial A}{\partial z} + \frac{iAz b \omega_p^2}{c^2} \left(1 + b\omega_0 t - \frac{b\omega_0 z}{c}\right)^{-2} \left\{ 1 - \frac{\omega_p^2}{\omega_0^2} \left(1 + b\omega_0 t - \frac{b\omega_0 z}{c}\right)^{-2} \right\}^{-1/2} \right]$$

$$- \frac{iA\omega_0}{c} \text{Exp}[i(\omega t - kz)] \left[b\omega_0 t + \left(1 + b\omega_0 t - \frac{2b\omega_0 z}{c}\right) \left\{ 1 - \frac{\omega_p^2}{\omega_0^2} \left(1 + b\omega_0 t - \frac{b\omega_0 z}{c}\right)^{-2} \right\}^{1/2} \right]$$

$$\frac{\partial^2 \vec{E}}{\partial z^2} = \frac{2iAb\omega_0^2}{c^2} \text{Exp}[i(\omega t - kz)] \left\{ 1 - \frac{\omega_p^2}{\omega_0^2} \left(1 + b\omega_0 t - \frac{b\omega_0 z}{c}\right)^{-2} \right\}^{1/2} + \frac{iAb\omega_0^2}{c^2} \frac{\omega_p^2}{\omega_0^2} \text{Exp}[i(\omega t - kz)] \times$$

$$\left[\left(1 + b\omega_0 t - \frac{b\omega_0 z}{c}\right)^{-2} \left\{ 1 - \frac{\omega_p^2}{\omega_0^2} \left(1 + b\omega_0 t - \frac{b\omega_0 z}{c}\right)^{-2} \right\}^{-1/2} \right] \left[\begin{array}{l} 2 + \frac{b\omega_0 z}{c} \left(1 + b\omega_0 t - \frac{b\omega_0 z}{c}\right)^{-1} \\ + \frac{b\omega_0 z}{c} \frac{\omega_p^2}{\omega_0^2} \left(1 + b\omega_0 t - \frac{b\omega_0 z}{c}\right)^{-3} \times \\ \left\{ 1 - \frac{\omega_p^2}{\omega_0^2} \left(1 + b\omega_0 t - \frac{b\omega_0 z}{c}\right)^{-2} \right\}^{-1} \end{array} \right]$$

$$\begin{aligned}
& -\frac{2ib\omega_0}{c} \frac{\partial A}{\partial z} \text{Exp}[i(\omega t - kz)] \left[\omega_0 t + \frac{z\omega_p^2}{c\omega_0^2} \left(1 + b\omega_0 t - \frac{b\omega_0 z}{c}\right)^{-2} \left\{ 1 - \frac{\omega_p^2}{\omega_0^2} \left(1 + b\omega_0 t - \frac{b\omega_0 z}{c}\right)^{-2} \right\}^{-1/2} \right] \\
& -\frac{2i\omega_0}{c} \frac{\partial A}{\partial z} \text{Exp}[i(\omega t - kz)] \left(1 + b\omega_0 t - \frac{2b\omega_0 z}{c}\right) \left\{ 1 - \frac{\omega_p^2}{\omega_0^2} \left(1 + b\omega_0 t - \frac{b\omega_0 z}{c}\right)^{-2} \right\}^{1/2} \\
& -A \text{Exp}[i(\omega t - kz)] \left[\frac{b^2\omega_0^4 t^2}{c^2} + \left\{ 1 - \frac{\omega_p^2}{\omega_0^2} \left(1 + b\omega_0 t - \frac{b\omega_0 z}{c}\right)^{-2} \right\} \left\{ \frac{\omega_p^2}{\omega_0^2} \left(1 + b\omega_0 t - \frac{b\omega_0 z}{c}\right)^{-2} \right\}^2 \right. \\
& \quad \left. - \frac{b\omega_0^2 z}{c^2} \right] \\
& -\frac{Ab^2\omega_0^4 z^2}{c^4} \frac{\omega_p^4}{\omega_0^4} \text{Exp}[i(\omega t - kz)] \left(1 + b\omega_0 t - \frac{b\omega_0 z}{c}\right)^{-4} \left\{ 1 - \frac{\omega_p^2}{\omega_0^2} \left(1 + b\omega_0 t - \frac{b\omega_0 z}{c}\right)^{-2} \right\}^{-1} \\
& -\frac{2Ab\omega_0^2 t}{c} \text{Exp}[i(\omega t - kz)] \left\{ 1 - \frac{\omega_p^2}{\omega_0^2} \left(1 + b\omega_0 t - \frac{b\omega_0 z}{c}\right)^{-2} \right\}^{1/2} \left\{ \frac{\omega_p^2}{\omega_0^2} \left(1 + b\omega_0 t - \frac{b\omega_0 z}{c}\right) - \frac{b\omega_0^2 z}{c^2} \right\} \\
& +\frac{2Abz\omega_0^2}{c^2} \frac{\omega_p^2}{\omega_0^2} \text{Exp}[i(\omega t - kz)] \left(1 + b\omega_0 t - \frac{b\omega_0 z}{c}\right)^{-2} \left\{ \frac{\omega_p^2}{\omega_0^2} \left(1 + b\omega_0 t - \frac{b\omega_0 z}{c}\right) - \frac{b\omega_0^2 z}{c^2} \right\} \\
& +\frac{2Ab^2 tz\omega_0^4}{c^3} \frac{\omega_p^2}{\omega_0^2} \text{Exp}[i(\omega t - kz)] \left(1 + b\omega_0 t - \frac{b\omega_0 z}{c}\right)^{-2} \left\{ 1 - \frac{\omega_p^2}{\omega_0^2} \left(1 + b\omega_0 t - \frac{b\omega_0 z}{c}\right)^{-2} \right\}^{-1/2}
\end{aligned}$$

Now, substituting the above values in Eq. (7.3) and employing the WKB approximation, we get

$$-2ik \frac{\partial A}{\partial z} \left[b\tau(1+b\tau)\sqrt{\varepsilon_0} + (1+b\tau)^2 \varepsilon_0 + \frac{bzk(\sqrt{\varepsilon_0}-1)}{\sqrt{\varepsilon_0}} \right] + \left(\frac{\partial^2 A}{\partial r^2} + \frac{1}{r} \frac{\partial A}{\partial r} \right) (1+b\tau)^2 \varepsilon_0 +$$

$$k^2(1+b\tau)^2 [\varepsilon_0 + \phi(EE^*) - i\varepsilon_i] A + ik^2 A \left(2b\sqrt{\varepsilon_0} + \frac{b^2 kz(1-\varepsilon_0)(1+b\tau)^{-2}}{\varepsilon_0} \right) -$$

$$A \left[b\tau + \frac{\varepsilon_0}{k} \frac{\omega_p^2}{\omega_0^2} (1+b\tau)^2 + \frac{bzk(\varepsilon_0 - \sqrt{\varepsilon_0})}{(1+b\tau)\varepsilon_0^{3/2}} \right]^2 = 0. \quad (7.7)$$

To solve Eq. (7.7), we express A as

$$A = A_0(r, z) \exp(-ikS), \quad (7.8)$$

where, A_0 and S depend on r and z . Now, differentiating Eq. (7.8) twice w. r. t r and z , we get

$$\begin{aligned} \frac{\partial A}{\partial r} &= \text{Exp}[-ikS] \left[\frac{\partial A_0}{\partial r} - \frac{i\omega_0 A_0}{c} \left(1 + b\omega_0 t - \frac{b\omega_0 z}{c}\right) \left\{ 1 - \frac{\omega_p^2}{\omega_0^2} \left(1 + b\omega_0 t - \frac{b\omega_0 z}{c}\right)^{-2} \right\}^{1/2} \left(\frac{\partial S}{\partial r}\right) \right] \\ \frac{\partial^2 A}{\partial r^2} &= \text{Exp}[-ikS] \left[\frac{\partial^2 A_0}{\partial r^2} - \frac{\omega_0^2 A_0}{c^2} \left(1 + b\omega_0 t - \frac{b\omega_0 z}{c}\right)^2 \left\{ 1 - \frac{\omega_p^2}{\omega_0^2} \left(1 + b\omega_0 t - \frac{b\omega_0 z}{c}\right)^{-2} \right\} \left(\frac{\partial S}{\partial r}\right)^2 \right] \\ &\quad - \frac{i\omega_0}{c} \text{Exp}[-ikS] \left[\left(1 + b\omega_0 t - \frac{b\omega_0 z}{c}\right) \left\{ 1 - \frac{\omega_p^2}{\omega_0^2} \left(1 + b\omega_0 t - \frac{b\omega_0 z}{c}\right)^{-2} \right\}^{1/2} \left(\frac{\partial S}{\partial r}\right)^2 \right] \times \\ &\quad \left[A_0 \frac{\partial^2 S}{\partial r^2} + 2 \frac{\partial S}{\partial r} \frac{\partial A_0}{\partial r} \right] \\ \frac{\partial A}{\partial z} &= \text{Exp}[-ikS] \left[\frac{\partial A_0}{\partial z} + \frac{i\omega_0 A_0}{c} \left\{ \frac{bS\omega_0}{c} + \left(1 + b\omega_0 t - \frac{b\omega_0 z}{c}\right) \frac{\partial S}{\partial z} \right\} \left\{ 1 - \frac{\omega_p^2}{\omega_0^2} \left(1 + b\omega_0 t - \frac{b\omega_0 z}{c}\right)^{-2} \right\}^{1/2} \right] \\ &\quad + \frac{ibS\omega_0^2}{c^2} \frac{\omega_p^2}{\omega_0^2} \text{Exp}[-ikS] \left(1 + b\omega_0 t - \frac{b\omega_0 z}{c}\right)^{-2} \left[1 - \frac{\omega_p^2}{\omega_0^2} \left(1 + b\omega_0 t - \frac{b\omega_0 z}{c}\right)^{-2} \right]^{-1/2}, \end{aligned}$$

Substituting Eq. (7.8) and all the above values in Eq. (7.7) and after separating real and imaginary parts, one can obtain

Real part equation is

$$\begin{aligned} \frac{\varepsilon_0}{k^2} \left(\frac{\partial^2 A_0}{\partial r^2} + \frac{1}{r} \frac{\partial A_0}{\partial r} \right) - A_0 \left[1 - \frac{\omega_p^2}{\omega_0^2} (1 + b\tau) \right] \left(\frac{\partial S}{\partial r} \right)^2 - A_0 (1 - \varepsilon_0) \left[1 - \left(1 + \frac{\alpha}{2} EE^* \right)^{(s_0/2)-1} \right] + \\ \frac{2A_0 bS}{(1 + b\tau)} \left[\frac{\{k + (1 + b\tau)\sqrt{\varepsilon_0} - (1 + b\tau)\varepsilon_0^{3/2}\}}{(1 + b\tau)\sqrt{\varepsilon_0}} + b \left(\tau + \frac{zk}{(1 + b\tau)\sqrt{\varepsilon_0}} \right) \left(\frac{k}{(1 + b\tau)^2 \varepsilon_0} + \frac{1 - \varepsilon_0}{\sqrt{(1 + b\tau)^2 + \varepsilon_0 - 1}} \right) \right] \end{aligned}$$

$$\begin{aligned}
& -A_0 \left[\frac{b^2 \tau^2}{(1+b\tau)^2} - \frac{\omega_p^6 \varepsilon_0}{\omega_0^6 k^2} + \frac{b^2 z^2 k^2 (3\sqrt{\varepsilon_0} - \varepsilon_0^{3/2} - 2)}{(1+b\tau)^4 \varepsilon_0^{3/2}} + \frac{2b^2 z \tau k (\sqrt{\varepsilon_0} - 1)}{(1+b\tau)^3 \varepsilon_0} + \frac{2b\varepsilon_0 \omega_p^2}{k \omega_0^2} \left(\tau + \frac{zk}{(1+b\tau)\sqrt{\varepsilon_0}} \right) + \right. \\
& \left. \frac{(1+b\tau)\varepsilon_0}{k^2} \left(\frac{\omega_p^4}{\omega_0^4} (1+b\tau) - \frac{2bz\omega_p^2}{\omega_0^2} - \frac{k^2}{(1+b\tau)\varepsilon_0} \right) + \frac{b^2 z^2 (1-\varepsilon_0)^2}{(1+b\tau)^2 \varepsilon_0} \right] \\
& + 2A_0 \frac{\partial S}{\partial z} \left[\varepsilon_0 + \frac{b\tau\sqrt{\varepsilon_0}}{1+b\tau} - \frac{bz(1-\varepsilon_0)(1-\varepsilon_0^3)}{(1+b\tau)\varepsilon_0^3} - \frac{bzk(1-\sqrt{\varepsilon_0})}{(1+b\tau)^2 \sqrt{\varepsilon_0}} \right] - \frac{2A_0 b^2 S z k^2 (2-\varepsilon_0)^2}{(1+b\tau)^4 \varepsilon_0^2} = 0
\end{aligned} \tag{7.9}$$

Imaginary part equation is

$$\begin{aligned}
& A_0^2 \left(\frac{\partial^2 S}{\partial r^2} + \frac{1}{r} \frac{\partial S}{\partial r} \right) + \frac{\partial S}{\partial r} \frac{\partial A_0^2}{\partial r} + \frac{\partial A_0^2}{\partial z} \left[1 + \frac{b\tau}{(1+b\tau)\sqrt{\varepsilon_0}} + \frac{bzk(1-\sqrt{\varepsilon_0})}{(1+b\tau)^2 \varepsilon_0} - \frac{bz(1-\varepsilon_0)}{k(1+b\tau)^2 \sqrt{\varepsilon_0}} \right] \\
& - \frac{bkA_0^2}{\varepsilon_0^{3/2} (1+b\tau)^2} \left[2 + \frac{bz(1-\varepsilon_0)}{(1+b\tau)\varepsilon_0} \right] - \frac{kA_0^2 \varepsilon_i}{\varepsilon_0} = 0.
\end{aligned} \tag{7.10}$$

Where, τ is the dimensionless retarded time. Following Akhmanov et al. [113] and Sodha et al. [20, 114], we can write as follows

$$A_0^2 = \frac{E_0^2}{f^2} \exp \left[-\frac{r^2}{r_0^2 f^2} \right] \exp(-2k_i z), \tag{7.11}$$

$$S = \frac{r^2}{2} \beta(z) + \varphi(z), \tag{7.12}$$

where, $k_i = k\varepsilon_i / 2\varepsilon_0$ is the absorption coefficient with $k = \omega\varepsilon_0^{1/2} / c$ and $\beta(z) = (1/f)(\partial f / \partial z)$, β^{-1} is interrupted as curvature radius and $f(z)$ represents the beam width parameter. Now, using paraxial approximation and substituting Eq. (7.11) and Eq. (7.12) in Eq. (7.9) and then equate the coefficients of r^2 on both sides of the emerging equation, the differential equation for $f(z)$ is obtained as:

$$\begin{aligned}
& \frac{\partial^2 f}{\partial \xi^2} \left[1 + \frac{b\tau}{(1+b\tau)\sqrt{\varepsilon_0}} + \frac{b\xi\rho_0^2}{\varepsilon_0^{7/2}} (\varepsilon_0^{7/2} - \varepsilon_0^4 - \varepsilon_0 - 1) \right] + \frac{b\rho_0^2}{\varepsilon_0} \left(\frac{\partial f}{\partial \xi} \right) \times \\
& \left[\frac{\sqrt{\varepsilon_0}(1+b\tau) + b\tau}{1+b\tau} + (\sqrt{\varepsilon_0} + b\tau)(1 - \varepsilon_0) + b\xi\rho_0^2 (4\varepsilon_0 - \varepsilon_0^{3/2}(1+b\tau) + (2+b\tau)\sqrt{\varepsilon_0} - \varepsilon_0^2 - 4) \right] \\
& - \frac{1}{f} \left(\frac{\partial f}{\partial \xi} \right)^2 \left[\frac{1}{\varepsilon_0} + (1+b\tau) \left(1 - \frac{\omega_p^2}{\omega_0^2 \varepsilon_0} \right) + \frac{b\xi\rho_0^2}{\varepsilon_0^{7/2}} (\varepsilon_0^{7/2} - \varepsilon_0^4 (1+b\tau)^2 - \varepsilon_0 - 1) \right] \\
& - \frac{\omega_p^2 \alpha E_0^2 \rho_0^2}{2\omega_0^2 f^3} \left(\frac{s_0}{2} - 1 \right) \exp(-2k'_i \xi) \left(1 + \frac{\alpha E_0^2}{2f^2} \right)^{(s_0/2)-1} - \frac{1}{f^3} = 0, \tag{7.13}
\end{aligned}$$

where, $\xi = z/R_d$ is propagation distance, $R_d = kr_0^2$ represents diffraction length, $\rho_0 = r_0\omega_0/c$ represents equilibrium beam radius, k'_i is the normalized absorption coefficient. Eq. (7.13) represents the spot size variation of laser beam with the propagation distance.

7.3 RESULTS AND DISCUSSION

Eq. (7.13) is the second order differential equation that governs the behavior of $f(z)$ of chirped Gaussian beam in collisional plasma with linear absorption. We have solved Eq. (7.13) numerically by applying the initial condition at $\xi = 0$, $f = 1$, $(\partial f / \partial \xi) = 0$ and $(\partial^2 f / \partial \xi^2) = 0$ with the following set of typical parameters[125]; $\omega_0 = 1.778 \times 10^{14} \text{ rad/sec}$, laser beam radius $20 \mu\text{m}$ and equilibrium plasma density $n_0 = 4 \times 10^{19} \text{ cm}^{-3}$. By optimizing suitable laser and plasma parameters, we have investigated the self-focusing / defocusing of chirped Gaussian beam in collisional plasma.

Figure 7.1 shows the dependence of f on ξ for various values of ν/ω_0 . The other parameters are: $\omega_p/\omega_0 = 0.4$, $\alpha E_0^2 = 0.4$ and $b = 0$. It is observed that while, neglecting the effect of chirp, the laser beam shows defocusing character. The defocusing of laser beam increases with increase in the values of ν/ω_0 . It is due to the fact that the absorption (corresponding to collision frequency term ν/ω_0) becomes significant and the laser beam shows fast divergence. The

amplitude of oscillations of beam width parameter becomes too large, there by the beam width parameter diverges continuously. In other words, the beam width parameter increases on account of collision frequency and steady divergence occurs due to strong energy attenuation. So, one can say that the laser beam becomes more defocused due to diffraction and absorption effects at higher oscillation frequencies. The outcomes so obtained in this analysis can be compared with those of Navare *et al.* [80], wherein increase in collision frequency is subjected to increase in oscillation amplitude of beam width parameter. Moreover, for higher values of ν/ω_0 , the absorption is more significant and overcomes the self-focusing effect. Again, Jafari Milani *et al.* [95] investigated the ponderomotive self-focusing in warm collisional plasma and reported that firstly self-focusing is caused by collision frequency and secondly it defocuses the laser beam for longer propagation.

Now, in order to account for the defocusing, the effect of chirp is considered. For investigating the effect of chirp parameter (b) on the laser beam propagation in collisional plasma, various values of b are considered. Figure 7.2 (a) illustrates the behavior of f with ξ for various values of chirp parameter b and the other parameters are same as taken in figure 7.1. It is observed from figure 7.2 (a) that in the absence of collision frequency, the beam width parameter initially decreases and then increases showing that the laser beam gets defocused. However, this defocusing can be minimized by increasing the chirp parameter. As soon as the chirp parameter is increased, the amplitude of oscillations of the beam decreases with the distance of propagation. Further, with its passage in the plasma, the angular frequency increases with the result, the dielectric constant of the plasma decreases. The decrease in dielectric constant reduces the spot size amplitude of laser beam close to the axis of propagation. Consequently, $f(z)$ attains a minimum value for further distance of propagation. The effect of negative chirp on the self-focusing or defocusing is shown in the figure 7.2 (b) which represents the variation of f with ξ for various values of negative chirp. From the figure 7.2 (b), it is clear that on increasing the values of negative chirp, the self-focusing at first is strengthened and after attaining a critical value, it gets defocused. This is because the frequency of a linear and negative chirped laser beam changes during the propagation in the plasma. Therefore, the spot size of laser beam depends on ξ and at propagation distances much greater than the Rayleigh length the temporal shape of the

chirped laser beam will be changed. Therefore, the defocusing of laser beam is weakened and there by the self-focusing effect is strengthened by using chirp. Hence, the chirp parameter is important for minimizing the defocusing and increasing the ability of self-focusing in collisional plasma

Figure 7.3 presents the dependence of beam f on ξ for various values of ω_p / ω_0 . The other parameters are: $\nu / \omega_0 = 0.002$, $\alpha E_0^2 = 0.4$ and $b = 0.002$. It is evident from figure 7.3 that with increase in ω_p / ω_0 , the nonlinearity of plasma medium increases, with the result, the amplitude of oscillations decreases further close to the propagation axis. Consequently, f_{\min} shifts towards lower value of $\xi = 0.4$. Therefore, the beam self-focusing occurs earlier and thus supports the results [80, 86]. Figure 7.4 illustrates the behavior f with distance ξ for various values of αE_0^2 . The relative plasma density is fixed at $\omega_p / \omega_0 = 0.4$ and the other parameters are same as taken in figure 7.3. The curves demonstrate that with increase in αE_0^2 of the beam, the spot size and hence the self-focusing length decreases. Again, increase in laser intensity results in increasing the nonlinearity which is responsible for the self-focusing of laser beam in plasma. Consequently, the laser beam bends more towards the focusing mode for higher values of intensity of laser beam. Furthermore, at higher intensity and for higher plasma density, a beam having more electrons travels with the laser beam and generates a higher current. Consequently, a higher quasi-stationary magnetic field is generated, which reduces the focusing length and hence adds to self-focusing.

Again, taking in to account the laser intensities (10^{20}W/cm^2) closer the realistic values, the changing behavior of f with ξ is shown in figure 7. 5. The other parameters are: $b = 0.002$, $\nu / \omega_0 = 0.002$ and $\omega_p / \omega_0 = 0.6$. From the figure 7.5, it is observed that at higher intensities, the oscillating behavior of beam width parameter is destroyed during propagation in plasma and the laser beam undergoes defocusing. In other words, the self-focusing of laser beam disappears with very high intensity and ponderomotive defocusing occurs. This is because of the supremacy of the diffraction effect at high intensity. Further, the frequency of a chirped laser beam changes during the propagation in plasma. As the beam waist depends on ξ and at larger propagation distances, the temporal shape of the chirped laser beam will be changed. However, for shorter

propagation distance less than the Rayleigh length, the change in laser pulse shape is not considerable.

7.4 CONCLUSION

In the present communication, we have investigated the self-focusing / defocusing of chirped Gaussian beam in collisional plasma with linear absorption. We derived the required differential equation for $f(z)$ by using the WKB and paraxial ray approximations and investigated the impression of optimized parameters on the self-focusing / defocusing in collisional plasma. From the results, one can conclude that the chirp parameter is important for the self-focusing / defocusing and maintains the necessary importance of laser-plasma interaction. The laser beam is defocused due to strong diffraction and absorption effects at higher oscillation frequencies. It is further, revealed that initially the amplitude of beam width parameter is too large and continuously diverges in the collisional plasma. The chirp parameter minimizes the divergence and consequently, sooner and an earlier self-focusing is observed. Thus, apart from electron acceleration, the chirp can also be used to analyze the self-focusing / defocusing of laser beam in plasma. The results of present research may be useful in laser – driven fusion and laser plasma based accelerators.

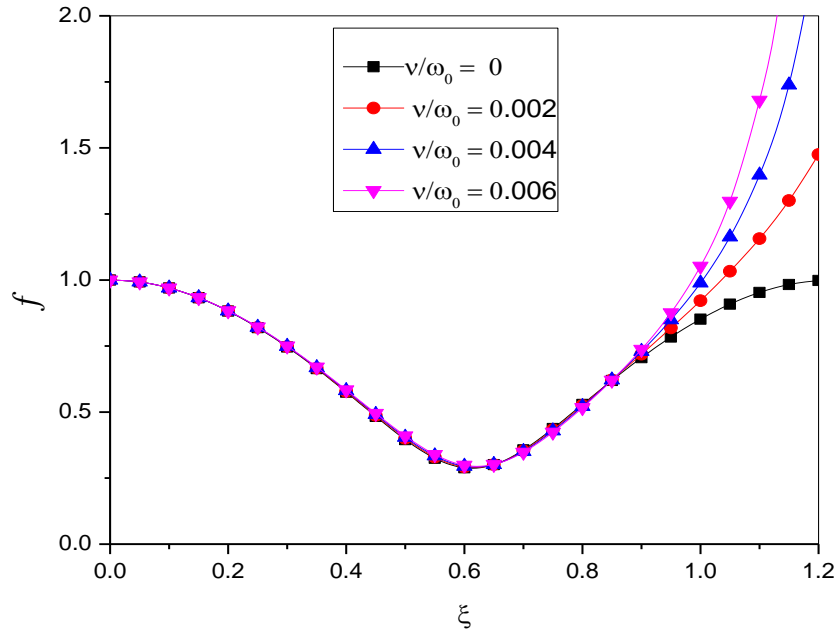


Figure 7.1: Dependence of f on ξ for various values of ν/ω_0 . The other parameters are: $\omega_p/\omega_0=0.4$, $\alpha E_0^2=0.4$ and $b=0$

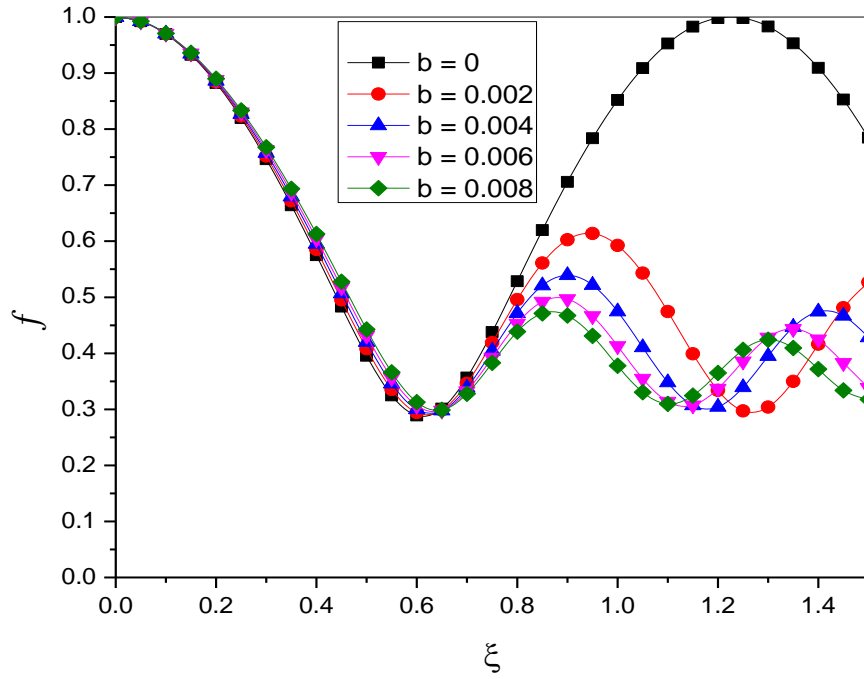


Figure 7.2 (a): Dependence of f on ξ for various values of b . The other parameters are: $\omega_p / \omega_0 = 0.4$, $\alpha E_0^2 = 0.4$ and $\nu / \omega_0 = 0$

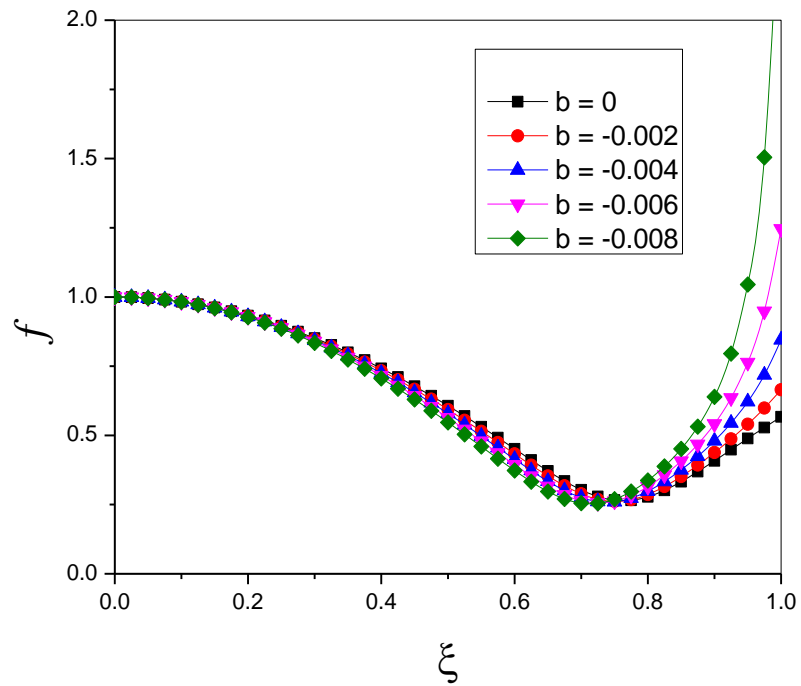


Figure 7.2 (b): Dependence of f on ξ for various values of negative chirp. The other parameters are same as taken in the figure 7.2 (a).

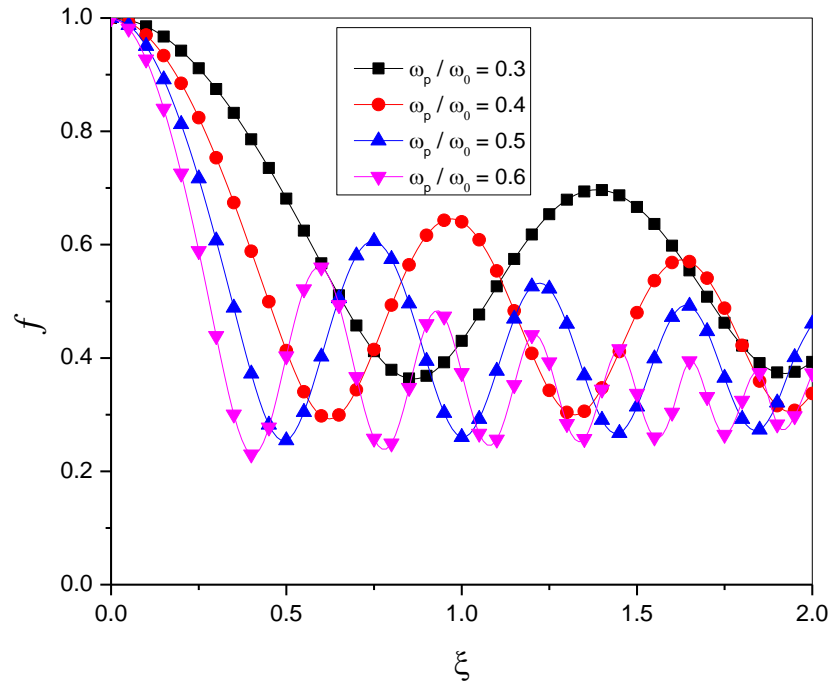


Figure 7.3: Dependence of f on ξ for various values of ω_p / ω_0 . The other parameters are: $\nu / \omega_0 = 0.002$, $\alpha E_0^2 = 0.4$ and $b = 0.002$

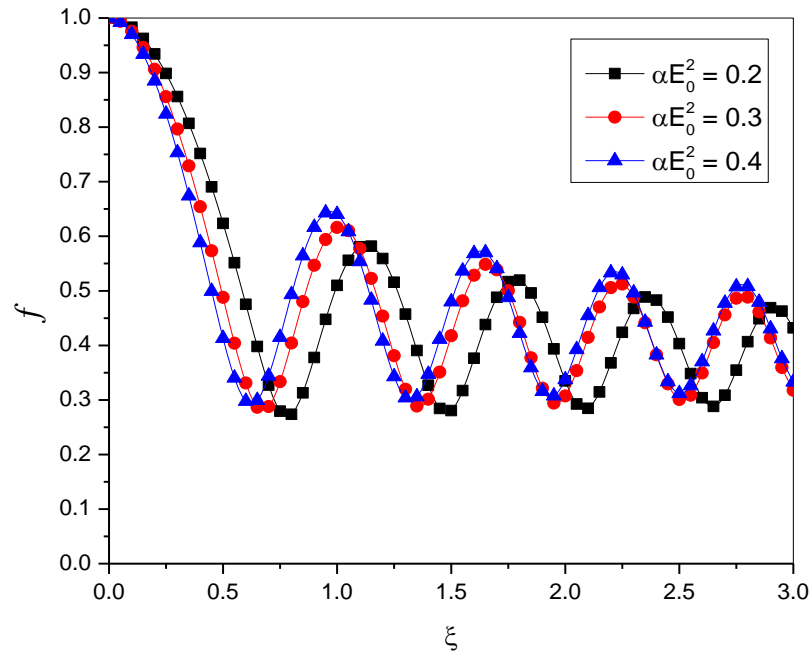


Figure 7.4: Dependence of f on ξ for various values of αE_0^2 . The other parameters are: $\nu/\omega_0 = 0.002$, $\omega_p/\omega_0 = 0.4$, and $b = 0.002$

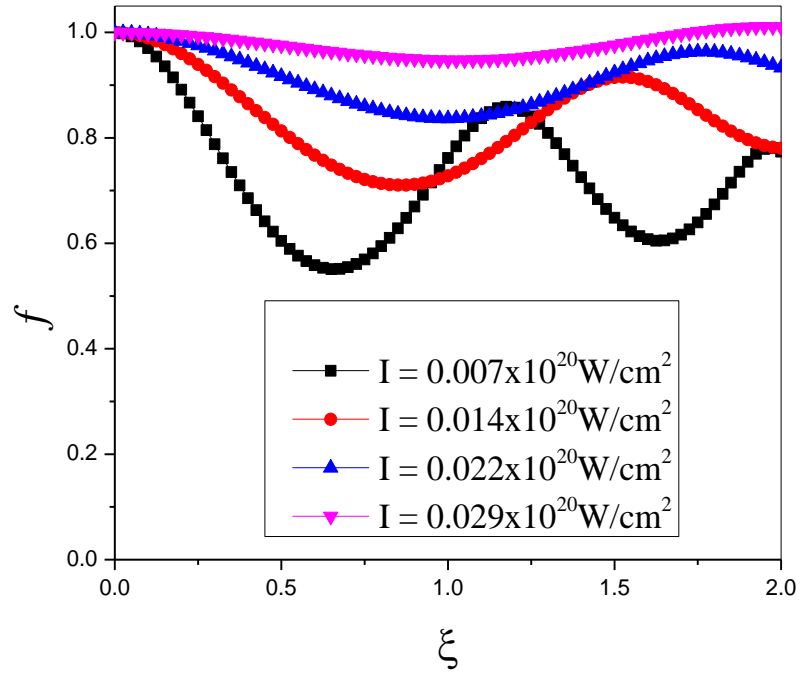


Figure 7.5: Dependence of f on ξ for various values of intensity. The other parameters are: $\nu/\omega_0 = 0.002$, $\omega_p/\omega_0 = 0.6$, and $b = 0.002$

CHAPTER-8

SELF-FOCUSING OF A LASER BEAM IN THE RIPPLED DENSITY MAGNETOPLASMA

8.1 INTRODUCTION

The interaction of high intense laser beams with plasmas gives rise to various wide ranging potential applications including laser-driven acceleration, harmonic generation, x-ray lasers etc. [8,9, 128, 129]. For the success of these applications, it is to be desired that the high intensity laser beam should propagate various Rayleigh lengths without divergence. When such a laser beam interacts with a medium like plasma, it provides oscillatory velocity to the electron, which changes the dielectric constant of the medium [105]. The process of self-focusing has been examined by various authors [116, 43, 117] and is important for the above mentioned applications. The self-focusing is more at relativistic intensity as it generates a quasi-stationary magnetic field [75] and is crucial for propagation of the laser beam over extended distances. For thermal self-focusing to occur, the ion temperature is considered to be important as it seriously influences the laser pulse evolution [87]. The effect of density ramp is such as to shrink the spot size of laser beam so that it becomes more focused while propagating through the plasma. The optimized parameters are found to be crucial for self-focusing as it is enhanced with such parameters. Its ability is further increased by density transition and magnetic field. [22, 85, 97, 102, 80, 100]. Further, the linear absorption destroys the oscillatory character of beam width parameter and thereby makes the self-focusing effect weaker while as the density transition causes sooner and earlier self-focusing [118]. Wani and Kant [130] investigated the relativistic self-focusing of HcosG laser beam in collisionless plasma. They reported that the beam width parameter shows a strong oscillatory behavior and hence the laser beam becomes more focused at lower values of intensity and decentered parameters. Further, the decentered parameter is considered to be essential for self-focusing [90]. Gill *et al.* [81] investigated the relativistic self-focusing by including higher order terms of the dielectric function. They have shown that the magnetic field and hence the higher order terms of dielectric function increase the self-focusing strength.

The density ripple was used to study stimulated Raman scattering of light waves in plasma. The excitation of plasma waves took place under rippled density profile as these waves have nearly the same wavelength as those of density ripple [131]. Further, the rippled density can be used to investigate the phase-matched harmonic generation from plasmas. The efficiency of generation increases rapidly in weak and moderate relativistic regime. However, the phase-matched harmonic generation saturates in strong relativistic regime [132]. Again, Kaur *et al.* [133] found that when ripple period is large, less self-focusing is observed and vice-versa. However, the rippling effect is more pronounced at lower laser intensity. Further, the density ripple increases the length of self-focusing and thus results in decreasing the laser spot size [68]. Keeping in view the ongoing development of high intense lasers, the present paper is aimed to investigate the impact of magnetic field on the self-focusing of laser beam propagating in rippled density plasma. Effect of various optimized parameters is seen on self-focusing in rippled density magnetoplasma. There is an enhancement in self-focusing strength by increasing laser strength and magnetic field to few mega-Gausses. The paper is constituted as follows: in section 8.2, nonlinear dielectric constant is presented. In section 8.3, the basic formulation and the differential equation governing the spot size variation is presented. Section 8.4 is devoted to results and discussions. Finally, the conclusion is added in section 8.5.

8.2 NONLINEAR DIELECTRIC CONSTANT

Consider the Gaussian beam propagation along z direction in magnetoplasma with rippled density profile, $n_0 = n_0^0 + n_{0q} e^{iqz}$, where, n_{0q} is the rippled density. The electric field vector \vec{E} of the laser beam in magnetoplasma can be written as

$$\vec{E} = \vec{A} \exp[i(\omega t - kz)], \quad (8.1)$$

where, \vec{A} is the electric field amplitude, ω is the angular frequency and $k = (\omega/c)\sqrt{\varepsilon_0}$ is the wave number and c is the velocity of light in vacuum. The effective dielectric constant ε is of the form [113]

$$\varepsilon = \varepsilon_0 + \phi(EE^*), \quad (8.2)$$

where, $\varepsilon_0 = 1 - (1 - \omega_{p0}^2 / \omega^2) / (1 - \omega_c / \omega)^2$ represents the linear part and $\phi(EE^*) = \varepsilon_2 AA^*$, $\varepsilon_2 = (1/2)(e/mc\omega)^2 (\omega_{p0} / \omega)^2 / (1 - \omega_c / \omega)^4$, $\omega_{p0}^2 = 4\pi n_0 e^2 / m$ and $\omega_c = eB_0 / mc$ represents the electron cyclotron frequency. Here, ω_{p0} is the plasma frequency, e , m and n_0 being the magnitude of the electronic charge, rest mass and electron density respectively. B_0 is the magnitude of external magnetic field.

8.3 SELF-FOCUSING EQUATIONS

The wave equation for the propagation of laser beam in magnetized plasma is of the form

$$\nabla^2 \vec{E} + \frac{\omega^2}{c^2} (\varepsilon \cdot E) \vec{E} - \nabla (\nabla \cdot \vec{E}) = 0, \quad (8.3)$$

Eq. (8.3) can be written as

$$\frac{\partial^2 E_x}{\partial z^2} + \frac{\partial^2 E_x}{\partial y^2} - \frac{\partial}{\partial x} \left(\frac{\partial E_y}{\partial y} + \frac{\partial E_z}{\partial z} \right) = -\frac{\omega^2}{c^2} (\varepsilon \cdot E)_x, \quad (8.4)$$

$$\frac{\partial^2 E_y}{\partial z^2} + \frac{\partial^2 E_y}{\partial x^2} - \frac{\partial}{\partial y} \left(\frac{\partial E_z}{\partial z} + \frac{\partial E_x}{\partial x} \right) = -\frac{\omega^2}{c^2} (\varepsilon \cdot E)_y, \quad (8.5)$$

$$\frac{\partial^2 E_z}{\partial x^2} + \frac{\partial^2 E_z}{\partial y^2} - \frac{\partial}{\partial z} \left(\frac{\partial E_x}{\partial x} + \frac{\partial E_y}{\partial y} \right) = -\frac{\omega^2}{c^2} (\varepsilon \cdot E)_z. \quad (8.6)$$

In order to solve Eq. (8.3) we suppose the field variations in the z -direction are much larger than in the $x-y$ plane. Therefore, in the zeroth order approximation, the waves are treated as transverse and hence space charge generation is negligible. Therefore one obtains

$$\frac{\partial E_z}{\partial z} \cong -\frac{1}{\varepsilon_{zz}} \left[\varepsilon_{xx} \left(\frac{\partial E_x}{\partial x} + \frac{\partial E_y}{\partial y} \right) + \varepsilon_{xy} \left(\frac{\partial E_y}{\partial x} - \frac{\partial E_x}{\partial y} \right) \right], \quad (8.7)$$

on multiplying Eq. (8.5) by i , adding it to Eq. (8.4) and using Eq. (8.7), we obtain

$$\frac{\partial^2 A}{\partial z^2} + \frac{1}{2} \left(1 + \frac{\varepsilon_0}{\varepsilon_{0zz}} \right) \left(\frac{\partial^2}{\partial x^2} + \frac{\partial^2}{\partial y^2} \right) A + \frac{\omega^2}{c^2} (\varepsilon_0 + \varepsilon_2 AA^*) A = 0, \quad (8.8)$$

where, we have neglected the product of nonlinear part with $\partial^2 A / \partial x^2$ or $\partial^2 A / \partial y^2$. Further,

$$\varepsilon_{0zz} = 1 - \omega_{p0}^2 / \omega^2, \quad \varepsilon_{xz} = \varepsilon_{yz} = \varepsilon_{zx} = \varepsilon_{zy} = 0, \quad \varepsilon_{xx} = \varepsilon_{yy} = 1 - \omega_{p0}^2 / \omega^2 (1 - \omega_c^2 / \omega^2) \quad \text{and}$$

$$\varepsilon_{xy} = -\varepsilon_{yx} = -i(\omega_{p0}^2 / \omega^2)(\omega_c / \omega) / (1 - \omega_c^2 / \omega^2).$$

Now, we assume that $A = A_0 \text{Exp}[i(\omega t - kz)]$, (8.9)

$$\text{with, } k^2 = \frac{\omega^2}{c^2} \left(1 - \frac{\omega_{p1}^2 + \omega_{p2}^2 e^{iqz}}{(\omega - \omega_c)^2} \right)$$

Differentiating Eq. (8.9) twice w. r. t x , y and z respectively, we get

$$\frac{\partial A}{\partial x} = \text{Exp}[i(\omega t - kz)] \frac{\partial A_0}{\partial x}$$

$$\frac{\partial^2 A}{\partial x^2} = \text{Exp}[i(\omega t - kz)] \frac{\partial^2 A_0}{\partial x^2}$$

$$\frac{\partial^2 A}{\partial y^2} = \text{Exp}[i(\omega t - kz)] \frac{\partial^2 A_0}{\partial y^2}$$

Similarly,

$$\begin{aligned} \frac{\partial^2 A}{\partial z^2} = & -\text{Exp}[i(\omega t - kz)] \left[2ik + \frac{qz\omega^2\omega_{p2}^2 e^{iqz}}{kc^2(\omega - \omega_c)^2} \right] \frac{\partial A_0}{\partial z} - A_0 \text{Exp}[i(\omega t - kz)] \frac{qz\omega^2\omega_{p2}^2 e^{iqz}}{kc^2(\omega - \omega_c)^2} \times \\ & \left[1 - \frac{iqz}{2} - \frac{iqz\omega^2\omega_{p2}^2 e^{iqz}}{4k^2c^2(\omega - \omega_c)^2} \right] - A_0 \text{Exp}[i(\omega t - kz)] \left[k^2 - \frac{qz\omega^2\omega_{p2}^2 e^{iqz}}{c^2(\omega - \omega_c)^2} \left(i - \frac{qz\omega^2\omega_{p2}^2 e^{iqz}}{4k^2c^2(\omega - \omega_c)^2} \right) \right]. \end{aligned}$$

Now, substituting the above values in Eq. (8.8) and neglecting $\partial^2 A_0 / \partial z^2$, we get

$$-k \left(\frac{\omega_{p2}}{\omega} \right)^2 \left(1 - \frac{\omega_c}{\omega} \right)^{-2} \left(\frac{2i}{\left(\frac{\omega_{p2}}{\omega} \right)^2} \left(1 - \frac{\omega_c}{\omega} \right)^2 + \frac{qze^{iqz}}{\varepsilon_0} \right) \frac{\partial A_0}{\partial z} + \frac{1}{2} \left(1 + \frac{\varepsilon_0}{\varepsilon_{0zz}} \right) \left(\frac{\partial^2}{\partial x^2} + \frac{\partial^2}{\partial y^2} \right) A_0$$

$$\begin{aligned}
& -k \left(\frac{\omega_{p2}}{\omega} \right)^2 \left(1 - \frac{\omega_c}{\omega} \right)^{-2} \left(\frac{qA_0 e^{iqz}}{\varepsilon_0} \right) \left(1 + \frac{iqz}{2} + \frac{iqz e^{iqz}}{4\varepsilon_0} \left(\frac{\omega_{p2}}{\omega} \right)^2 \left(1 - \frac{\omega_c}{\omega} \right)^{-2} - \frac{i\omega z \sqrt{\varepsilon_0}}{c} \right) \\
& \left(-\frac{\omega q z^2 e^{iqz}}{4c\sqrt{\varepsilon_0}} \left(\frac{\omega_{p2}}{\omega} \right)^2 \left(1 - \frac{\omega_c}{\omega} \right)^{-2} \right) \\
& + \frac{\omega^2}{c^2} (\varepsilon_2 A_0 A_0^*) A_0 = 0, \tag{8.10}
\end{aligned}$$

where, $\omega_{p1}^2 = 4\pi n_0^0 e^2 / m$, $\omega_{p2}^2 = 4\pi n_{0q} e^2 / m$, A_0 is the amplitude and q is the ripple wave number. Now, suggesting a two dimensional Gaussian beam for which $\partial/\partial y = 0$ and using an eikonal $A_0 = A_0^0 \exp(ikS)$, where, k is defined above, A_0^0 and S depend on x and z . Therefore, using these values in the above equation and separating real and imaginary parts of the emerging equation, one obtains

Real part equation is

$$\begin{aligned}
& -\frac{\omega}{c} \left(\frac{\omega_{p2}}{\omega} \right)^2 \left(1 - \frac{\omega_c}{\omega} \right)^{-2} \left[\sin(qz) + \frac{qz}{2} \left(1 - \frac{\omega_c}{\omega} \right)^{-2} \left(\left(\frac{\omega_{p2}}{\omega} \right)^2 \cos(2qz) \right) \right] \frac{\partial A_0^0}{\partial z} \\
& + \frac{\omega^2 A_0^0}{c^2 \left(1 - \frac{\omega_c}{\omega} \right)^2} \left(\frac{\partial S}{\partial z} \right) \left[\cos(qz) + qz \left(\frac{\omega_{p2}}{\omega} \right)^2 \left\{ \begin{aligned} & 2 \left(1 - \frac{\omega_c}{\omega} \right)^2 - \frac{1}{2} \left(\frac{\omega_{p1}}{\omega} \right)^4 \left(1 - \frac{\omega_c}{\omega} \right)^{-2} + \frac{1}{2} \left(\frac{\omega_{p2}}{\omega} \right)^4 \left(1 - \frac{\omega_c}{\omega} \right)^{-2} - 2 \left(\frac{\omega_{p2}}{\omega} \right)^2 \times \\ & \left[\begin{aligned} & \sin(qz) - \frac{1}{4} \left(\frac{\omega_{p1}}{\omega} \right)^4 \left(1 - \frac{\omega_c}{\omega} \right)^{-4} \sin(qz) + \\ & \frac{1}{2} \left(\frac{\omega_{p2}}{\omega} \right)^2 \left(1 - \frac{\omega_c}{\omega} \right)^{-2} \sin(2qz) - \\ & \frac{1}{4} \left(\frac{\omega_{p2}}{\omega} \right)^4 \left(1 - \frac{\omega_c}{\omega} \right)^{-4} \sin(2qz) (\cos(qz) - \sin(qz)) - \\ & \frac{1}{4} \left(\frac{\omega_{p1}}{\omega} \right)^2 \left(1 - \frac{\omega_c}{\omega} \right)^{-2} \left(\frac{\omega_{p2}}{\omega} \right)^2 \left(1 - \frac{\omega_c}{\omega} \right)^{-2} \sin(2qz) \end{aligned} \right] \end{aligned} \right]
\end{aligned}$$

$$+ \frac{1}{2} \left(1 + \frac{\varepsilon_0}{\varepsilon_{0zz}} \right) \left[\frac{\partial^2 A_0^0}{\partial x^2} + \frac{\omega}{c} \left(\frac{\partial A_0^0}{\partial x} \frac{\partial S}{\partial x} + \frac{A_0^0}{2} \frac{\partial^2 S}{\partial x^2} \right) \left(\frac{\omega_{p2}}{\omega} \right)^2 \left(1 - \frac{\omega_c}{\omega} \right)^{-2} \sin(qz) - \right. \\ \left. \frac{\omega^2 A_0^0}{c^2} \left\{ 1 - \left(\frac{\omega_{p1}}{\omega} \right)^2 \left(1 - \frac{\omega_c}{\omega} \right)^{-2} - \left(\frac{\omega_{p2}}{\omega} \right)^2 \left(1 - \frac{\omega_c}{\omega} \right)^{-2} \cos(qz) \right\} \left(\frac{\partial S}{\partial x} \right)^2 \right]$$

$$+ \frac{\omega^2 q S A_0^0}{2c^2 \left(1 - \frac{\omega_c}{\omega} \right)^2} \left(\frac{\omega_{p2}}{\omega} \right)^2 \left[\sin(qz) \left\{ 2 + 2 \left(\frac{\omega_{p1}}{\omega} \right)^2 \left(1 - \frac{\omega_c}{\omega} \right)^{-2} + \frac{1}{2} \left(\frac{\omega_{p1}}{\omega} \right)^4 \left(1 - \frac{\omega_c}{\omega} \right)^{-4} - \right. \right. \\ \left. \left. \frac{1}{2} \left(\frac{\omega_{p2}}{\omega} \right)^4 \left(1 - \frac{\omega_c}{\omega} \right)^{-4} (2 \cos(2qz) + 1) \right\} - \right. \\ \left. q \left(\frac{\omega_{p2}}{\omega} \right)^4 \left(1 - \frac{\omega_c}{\omega} \right)^{-4} \cos(2qz) \cos(qz) \left\{ 1 + \frac{1}{2} \left(\frac{\omega_{p1}}{\omega} \right)^2 \left(1 - \frac{\omega_c}{\omega} \right)^{-2} + \right. \right. \\ \left. \left. \frac{1}{2} \left(\frac{\omega_{p2}}{\omega} \right)^2 \left(1 - \frac{\omega_c}{\omega} \right)^{-2} \cos(qz) \right\} - \right. \\ \left. - qz \left(\frac{\omega_{p2}}{\omega} \right)^2 \left(1 - \frac{\omega_c}{\omega} \right)^{-2} \cos(2qz) \left\{ \frac{1}{4} \left(\frac{\omega_{p1}}{\omega} \right)^4 \left(1 - \frac{\omega_c}{\omega} \right)^{-4} + \right. \right. \\ \left. \left. \frac{1}{2} \left(\frac{\omega_{p2}}{\omega} \right)^2 \left(1 - \frac{\omega_c}{\omega} \right)^{-2} \cos(qz) \right\} - \right. \\ \left. \frac{qz}{4} \left(\frac{\omega_{p2}}{\omega} \right)^6 \left(1 - \frac{\omega_c}{\omega} \right)^{-6} (2 \cos^2(qz) - \sin^3(qz) - 1) \right]$$

$$- \frac{\omega q A_0^0}{2c \left(1 - \frac{\omega_c}{\omega} \right)^2} \left(\frac{\omega_{p2}}{\omega} \right)^2 \left[\left\{ 2 + \left(\frac{\omega_{p1}}{\omega} \right)^2 \left(1 - \frac{\omega_c}{\omega} \right)^{-2} \cos(qz) \right\} + \left(\frac{\omega_{p2}}{\omega} \right)^2 \left(1 - \frac{\omega_c}{\omega} \right)^{-2} \cos(2qz) \right. \\ \left. - qz \left\{ 1 + \frac{3}{4} \left(\frac{\omega_{p1}}{\omega} \right)^2 \left(1 - \frac{\omega_c}{\omega} \right)^{-2} \right\} \left(\frac{\omega_{p2}}{\omega} \right)^2 \left(1 - \frac{\omega_c}{\omega} \right)^{-2} \sin(2qz) + \frac{2\omega z}{c} \sin(qz) \right. \\ \left. - \frac{3qz}{4} \left(\frac{\omega_{p2}}{\omega} \right)^4 \left(1 - \frac{\omega_c}{\omega} \right)^{-4} \sin(3qz) - qz \sin(qz) \left\{ 1 + \frac{1}{2} \left(\frac{\omega_{p1}}{\omega} \right)^2 \left(1 - \frac{\omega_c}{\omega} \right)^{-2} \right\} \right. \\ \left. - \frac{\omega q z^2}{2c} \left(\frac{\omega_{p2}}{\omega} \right)^2 \left(1 - \frac{\omega_c}{\omega} \right)^{-2} \left\{ \cos(2qz) + \left(\frac{\omega_{p1}}{\omega} \right)^2 \left(1 - \frac{\omega_c}{\omega} \right)^{-2} \cos^2(qz) \right\} \right. \\ \left. + \left(\frac{\omega_{p2}}{\omega} \right)^2 \left(1 - \frac{\omega_c}{\omega} \right)^{-2} \cos(3qz) \right]$$

$$+ \frac{\omega^2}{c^2} (\epsilon_2 A_0^0 A^{*0}) A_0^0 = 0 \quad (8.11)$$

And imaginary part equation is

$$\begin{aligned}
& -\frac{\omega}{c} \left(1 - \frac{\omega_c}{\omega}\right)^{-2} \left[2 \left(1 - \frac{\omega_c}{\omega}\right)^2 + \left(\frac{\omega_{p1}}{\omega}\right)^2 - \left(\frac{\omega_{p2}}{\omega}\right)^2 \cos(qz) + qz \left(\frac{\omega_{p2}}{\omega}\right)^2 \sin(qz) \times \right. \\
& \left. \left\{ 1 + \frac{1}{2} \left(\frac{\omega_{p1}}{\omega}\right)^2 \left(1 - \frac{\omega_c}{\omega}\right)^{-2} + \frac{1}{2} \left(\frac{\omega_{p2}}{\omega}\right)^2 \left(1 - \frac{\omega_c}{\omega}\right)^{-2} \cos(qz) \right\} \right] \frac{\partial A_0^0}{\partial z} \\
& + \frac{\omega^2 A_0^0}{2c^2} \left(\frac{\omega_{p2}}{\omega}\right)^2 \left(1 - \frac{\omega_c}{\omega}\right)^{-4} \left(\frac{\partial S}{\partial z} \right) \left[\left(1 - \frac{\omega_c}{\omega}\right)^4 - \frac{1}{4} \left(\frac{\omega_{p1}}{\omega}\right)^4 - \frac{1}{2} \left(\frac{\omega_{p1}}{\omega}\right)^2 \left(\frac{\omega_{p2}}{\omega}\right)^2 \cos(qz) - \right. \\
& \left. \left. \left\{ \frac{1}{2} \left(\frac{\omega_{p2}}{\omega}\right)^2 \left(\cos(2qz) - \frac{1}{2}\right) \right\} \right] \right. \\
& \left. - \frac{\omega^2 A_0^0 q S (\sin(qz) + \cos(qz))}{2c^2 \left(1 - \frac{\omega_c}{\omega}\right)^4 \left(\frac{\omega_{p2}}{\omega}\right)^{-2}} \left[2 \left(1 - \frac{\omega_c}{\omega}\right)^2 + 2 \left(\frac{\omega_{p1}}{\omega}\right)^2 + \frac{1}{2} \left(\frac{\omega_{p1}}{\omega}\right)^4 \left(1 - \frac{\omega_c}{\omega}\right)^{-2} \right. \right. \\
& \left. - \frac{1}{2} \left(\frac{\omega_{p2}}{\omega}\right)^4 \left(1 - \frac{\omega_c}{\omega}\right)^{-2} \cos(2qz) + qz \left(\frac{\omega_{p2}}{\omega}\right)^2 \sin(qz) + \right. \\
& \left. \frac{qz}{2} \left(\frac{\omega_{p2}}{\omega}\right)^4 \left(1 - \frac{\omega_c}{\omega}\right)^{-2} \left\{ 1 + \frac{1}{2} \left(\frac{\omega_{p1}}{\omega}\right)^2 \left(1 - \frac{\omega_c}{\omega}\right)^{-2} \right\} + \right. \\
& \left. qz \left(\frac{\omega_{p1}}{\omega}\right)^2 \left(\frac{\omega_{p2}}{\omega}\right)^2 \sin(qz) \left(1 - \frac{\omega_c}{\omega}\right)^{-2} \left\{ 1 + \frac{1}{4} \left(\frac{\omega_{p1}}{\omega}\right)^2 \left(1 - \frac{\omega_c}{\omega}\right)^{-2} \right\} \right. \\
& \left. + \frac{qz}{4} \left(\frac{\omega_{p2}}{\omega}\right)^6 \left(1 - \frac{\omega_c}{\omega}\right)^{-4} \sin(qz) (3 - \sin^2(qz)) + \right. \\
& \left. \frac{qz}{4} \left(\frac{\omega_{p2}}{\omega}\right)^4 \left(1 - \frac{\omega_c}{\omega}\right)^{-2} \sin(2qz) \left(2 + \left(\frac{\omega_{p1}}{\omega}\right)^2 \left(1 - \frac{\omega_c}{\omega}\right)^{-2} \right) \right]
\end{aligned}$$

$$+ \frac{\omega}{2c} \left(1 - \frac{\omega_c}{\omega}\right)^{-2} \left(1 + \frac{\varepsilon_0}{\varepsilon_{0zz}}\right) \left[\left\{ \left(1 - \frac{\omega_c}{\omega}\right)^2 - \frac{1}{2} \left(\frac{\omega_{p1}}{\omega}\right)^2 - \frac{1}{2} \left(\frac{\omega_{p2}}{\omega}\right)^2 \cos(qz) \right\} \left(2 \frac{\partial A_0^0}{\partial x} \frac{\partial S}{\partial x} + A_0^0 \frac{\partial^2 S}{\partial x^2}\right) \right. \\ \left. + \frac{\omega A_0^0}{c} \left(\frac{\omega_{p2}}{\omega}\right)^2 \sin(qz) \left(\frac{\partial S}{\partial x}\right)^2 \right]$$

$$- \frac{\omega A_0^0 q}{c \left(1 - \frac{\omega_c}{\omega}\right)^4} \left(\frac{\omega_{p2}}{\omega}\right)^2 \left[\sin(qz) \left\{ \left(1 - \frac{\omega_c}{\omega}\right)^2 + \frac{1}{2} \left(\frac{\omega_{p1}}{\omega}\right)^2 + \left(\frac{\omega_{p2}}{\omega}\right)^2 \cos(qz) \right\} - \right. \\ \left. \frac{z\omega}{c} \left(1 - \frac{\omega_c}{\omega}\right)^2 \cos(qz) + qz \cos(qz) \left\{ \left(1 - \frac{\omega_c}{\omega}\right)^2 + \frac{1}{2} \left(\frac{\omega_{p1}}{\omega}\right)^2 \right\} + \right. \\ \left. qz \left(\frac{\omega_{p2}}{\omega}\right)^2 \cos(2qz) \left\{ 1 + \frac{3}{4} \left(\frac{\omega_{p1}}{\omega}\right)^2 \left(1 - \frac{\omega_c}{\omega}\right)^{-2} \right\} \right. \\ \left. - \frac{qz^2 \omega}{2c} \left(\frac{\omega_{p2}}{\omega}\right)^2 \times \left\{ \begin{aligned} &\sin(2qz) + \frac{1}{2} \left(\frac{\omega_{p1}}{\omega}\right)^2 \left(1 - \frac{\omega_c}{\omega}\right)^{-2} \sin(2qz) \\ &+ \left(\frac{\omega_{p2}}{\omega}\right)^2 \left(1 - \frac{\omega_c}{\omega}\right)^{-2} \sin(3qz) \end{aligned} \right\} \right. \\ \left. + \frac{3qz}{4} \left(\frac{\omega_{p2}}{\omega}\right)^4 \left(1 - \frac{\omega_c}{\omega}\right)^{-2} \cos(3qz) \right] = 0$$

(8.12)

Further, $(A_0^0)^2 = (E_{00}^2 / f^2) \exp(-x^2 / r_0^2 f^2)$, r_0 is the spot size of laser beam and $S = (x^2 / 2)\beta(z) + \varphi(z)$, where, $\beta(z) = 2(1 + \varepsilon_0 / \varepsilon_{0zz})^{-1} (1 / f(z)) (\partial f / \partial z)$ and β^{-1} may be regarded as curvature radius of laser beam, φ is a constant, independent of x and $f(z)$ represents the beam width parameter. On substituting these values in Eq. (8.11) and after equating the coefficients of x^2 on both sides of the resulting equation, the expression for beam width parameter is obtained as follows:

$$\begin{aligned}
& -\left(\frac{\omega_{p2}}{\omega}\right)^2 \left(\frac{1}{f}\right)^2 \sqrt{1 - \left(\frac{\omega_{p1}}{\omega}\right)^2 \left(1 - \frac{\omega_c}{\omega}\right)^{-2} - \left(\frac{\omega_{p2}}{\omega}\right)^2 \left(1 - \frac{\omega_c}{\omega}\right)^{-2} \cos(\xi d)} \times \\
& \left[2 \sin(\xi d) + \xi d \left\{ \cos(\xi d) + \frac{1}{2} \left(\frac{\omega_{p1}}{\omega}\right)^2 \left(1 - \frac{\omega_c}{\omega}\right)^{-2} + \frac{1}{2} \left(\frac{\omega_{p2}}{\omega}\right)^2 \left(1 - \frac{\omega_c}{\omega}\right)^{-2} \cos(\xi d) \right\} \right] \left(\frac{\partial f}{\partial \xi} \right) \\
& + \frac{\rho_0^2 \alpha_0^2}{2f^3} \left(1 - \frac{\omega_c}{\omega}\right)^{-2} \left[\left(\frac{\omega_{p1}}{\omega}\right)^2 + \left(\frac{\omega_{p2}}{\omega}\right)^2 \cos(\xi d) \right] \left[\frac{1 - \left(\frac{\omega_{p1}}{\omega}\right)^2 \left(1 - \frac{\omega_c}{\omega}\right)^{-2} - \left(\frac{\omega_{p2}}{\omega}\right)^2 \left(1 - \frac{\omega_c}{\omega}\right)^{-2} \cos(\xi d)}{\left(\frac{\omega_{p2}}{\omega}\right)^2 \left(1 - \frac{\omega_c}{\omega}\right)^{-2} \cos(\xi d)} \right] \\
& + \left[\frac{\partial^2 f}{\partial \xi^2} - \frac{1}{f} \left(\frac{\partial f}{\partial \xi} \right)^2 \right] \left[\frac{1 - \left(\frac{\omega_{p1}}{\omega}\right)^2 - \left(\frac{\omega_{p2}}{\omega}\right)^2 \cos(\xi d)}{2 - \left(\frac{\omega_{p1}}{\omega}\right)^2 \left\{ \left(1 - \frac{\omega_c}{\omega}\right)^{-2} + 1 \right\} - \left(\frac{\omega_{p2}}{\omega}\right)^2 \left\{ 1 + \left(1 - \frac{\omega_c}{\omega}\right)^{-2} \right\} \cos(\xi d)} \right] \times \\
& \left[2 \left(1 - \frac{\omega_c}{\omega}\right)^2 - \frac{1}{2} \left(\frac{\omega_{p1}}{\omega}\right)^4 \left(1 - \frac{\omega_c}{\omega}\right)^{-2} - 2 \left(\frac{\omega_{p2}}{\omega}\right)^2 \cos(\xi d) - \left(\frac{\omega_{p1}}{\omega}\right)^2 \left(\frac{\omega_{p2}}{\omega}\right)^2 \left(1 - \frac{\omega_c}{\omega}\right)^{-2} \cos(\xi d) - \right. \\
& \left. \frac{1}{2} \left(\frac{\omega_{p2}}{\omega}\right)^4 \left(1 - \frac{\omega_c}{\omega}\right)^{-2} \cos(2\xi d) + \frac{\xi d \sin(\xi d)}{4} \left(\frac{\omega_{p2}}{\omega}\right)^2 \left\{ \begin{aligned} & 4 + 4 \left(\frac{\omega_{p2}}{\omega}\right)^2 \left(1 - \frac{\omega_c}{\omega}\right)^{-2} \cos(\xi d) - \\ & \left(\frac{\omega_{p2}}{\omega}\right)^4 \left(1 - \frac{\omega_c}{\omega}\right)^{-4} - \frac{1}{2} \left(\frac{\omega_{p1}}{\omega}\right)^4 \left(1 - \frac{\omega_c}{\omega}\right)^{-4} \\ & - 2 \left(\frac{\omega_{p1}}{\omega}\right)^2 \left(\frac{\omega_{p2}}{\omega}\right)^2 \left(1 - \frac{\omega_c}{\omega}\right)^{-4} \cos(\xi d) \end{aligned} \right\} \right] \\
& + \left(\frac{4}{f} \right) \left(\frac{\partial f}{\partial \xi} \right)^2 \left[\left(1 - \frac{\omega_c}{\omega}\right)^{-2} - \left(\frac{\omega_{p1}}{\omega}\right)^2 - \left(\frac{\omega_{p2}}{\omega}\right)^2 \cos(\xi d) \right] \times \\
& \left[\frac{1 - \left(\frac{\omega_{p1}}{\omega}\right)^2 - \left(\frac{\omega_{p2}}{\omega}\right)^2 \cos(\xi d)}{2 - \left(\frac{\omega_{p1}}{\omega}\right)^2 \left\{ \left(1 - \frac{\omega_c}{\omega}\right)^{-2} + 1 \right\} - \left(\frac{\omega_{p2}}{\omega}\right)^2 \left\{ 1 + \left(1 - \frac{\omega_c}{\omega}\right)^{-2} \right\} \cos(\xi d)} \right]
\end{aligned}$$

$$\begin{aligned}
& + \left(\frac{d}{2} \right) \left(\frac{\omega_{p2}}{\omega} \right)^2 \left(\frac{\partial f}{\partial \xi} \right) \left[\frac{1 - \left(\frac{\omega_{p1}}{\omega} \right)^2 - \left(\frac{\omega_{p2}}{\omega} \right)^2 \cos(\xi d)}{2 - \left(\frac{\omega_{p1}}{\omega} \right)^2 \left\{ 1 + \left(1 - \frac{\omega_c}{\omega} \right)^{-2} \right\} - \left(\frac{\omega_{p2}}{\omega} \right)^2 \left\{ 1 + \left(1 - \frac{\omega_c}{\omega} \right)^{-2} \right\} \cos(\xi d)} \right] \times \\
& \left[\sin(\xi d) \left\{ 2 + 2 \left(\frac{\omega_{p1}}{\omega} \right)^2 \left(1 - \frac{\omega_c}{\omega} \right)^{-2} + \frac{1}{2} \left(\frac{\omega_{p1}}{\omega} \right)^4 \left(1 - \frac{\omega_c}{\omega} \right)^{-4} - \frac{1}{2} \left(\frac{\omega_{p2}}{\omega} \right)^4 \left(1 - \frac{\omega_c}{\omega} \right)^{-4} + \right. \right. \\
& \left. \left. \left(\frac{\omega_{p2}}{\omega} \right)^{-4} \left(1 - \frac{\omega_c}{\omega} \right)^{-4} \sin^2(\xi d) \right\} \right. \\
& \left. - (\xi d \cos(2\xi d)) \left(\frac{\omega_{p2}}{\omega} \right)^2 \left(1 - \frac{\omega_c}{\omega} \right)^{-6} \left\{ \frac{\cos(\xi d)}{2} \left(\frac{\omega_{p2}}{\omega} \right)^2 \left(1 - \frac{\omega_c}{\omega} \right)^2 + \frac{\cos(\xi d)}{4} \left(\frac{\omega_{p2}}{\omega} \right)^2 \left(\frac{\omega_{p1}}{\omega} \right)^2 \right. \right. \\
& \left. \left. + \frac{\sec(2\xi d)}{2} \left(\frac{\omega_{p2}}{\omega} \right)^4 - \frac{3 \cos^2(\xi d)}{4 \sec(2\xi d)} \left(\frac{\omega_{p2}}{\omega} \right)^4 + \frac{\cos^4(\xi d)}{2 \sec(2\xi d)} \left(\frac{\omega_{p2}}{\omega} \right)^4 \right\} \right] \\
& + \left(\frac{1}{2f^3} \right) \left[\left(1 - \frac{\omega_c}{\omega} \right)^{-2} - \left(\frac{\omega_{p1}}{\omega} \right)^2 - \left(\frac{\omega_{p2}}{\omega} \right)^2 \cos(\xi d) \right] \times \\
& \left[\frac{2 - \left(\frac{\omega_{p1}}{\omega} \right)^2 \left\{ 1 + \left(1 - \frac{\omega_c}{\omega} \right)^{-2} \right\} - \left(\frac{\omega_{p2}}{\omega} \right)^2 \left\{ 1 + \left(1 - \frac{\omega_c}{\omega} \right)^{-2} \right\} \cos(\xi d)}{1 - \left(\frac{\omega_{p1}}{\omega} \right)^2 - \left(\frac{\omega_{p2}}{\omega} \right)^2 \cos(\xi d)} \right] = 0,
\end{aligned}
\tag{8.13}$$

where, $\rho_0 = r_0 \omega / c$ is the equilibrium beam radius, $\alpha_0^2 = e^2 E_{00}^2 / m^2 c^2 \omega^2$ represents the initial laser beam intensity (laser strength) parameter, $\xi = z / R_d$ is propagation distance, $R_d = k r_0^2$ represents the diffraction length and $d = q R_d$ represents the normalized ripple wave number. Eq. (8.13) represents the spot size variation of laser beam with the propagation distance.

8.4 RESULTS AND DISCUSSION

Eq. (8.13) represents a nonlinear differential equation which governs the behavior of f with distance ξ in rippled density magnetoplasma. We solved Eq. (8.13) numerically by applying the initial condition at $\xi = 0$, $f = 1$, $(\partial f / \partial \xi) = 0$ and $(\partial^2 f / \partial \xi^2) = 0$ with the typical parameters given as [94]; angular frequency of laser $\omega = 1.778 \times 10^{14} \text{ rad/sec}$, laser beam spot size $r_0 = 40 \mu\text{m}$ and equilibrium plasma density $n_0^0 = 2.55 \times 10^{18} \text{ cm}^{-3}$. By optimizing laser and plasma parameters, we have investigated laser beam dynamics in rippled density magnetoplasma.

Aggarwal *et al.* [94] claimed that the self-focusing of laser beam in rippled density plasma occurs at large ξ values ($\xi = 2.25$ and $\xi = 1.75$). Further, their results reveal that there is a direct dependence of decentered parameter on self-focusing. But, in the present communication, the magnetic field of a few MG gives rise to strong self-focusing in rippled density plasma. Further, the self-focusing occurs earlier at $\xi = 0.12$ as depicted in figure 8.1 which shows the behavior of f with ξ for different values of laser strength parameter. The other parameters are: $\omega_{p1} / \omega = 0.4$, $\omega_{p2} / \omega = 0.15$, $\omega_c / \omega = 0.12$ ($B_0 = 12.19MG$) and $d = 59$ as taken by Lin *et al.* [134]. It is observed that as the laser strength parameter is increased, the nonlinear term dominates the diffraction term and self-focusing occurs earlier at $\xi = 0.12$. The laser spot size gets reduced which in turn decreases the beam width parameter and hence laser beam is self-focused. Figure 8.2 illustrates the variation of f with ξ for different values of λ ; $\lambda = 0.5 \mu\text{m}$, $1.06 \mu\text{m}$ and $1.5 \mu\text{m}$. The laser strength parameter is kept fixed at $\alpha_0 = 0.3$ and the other parameters are same as taken in Figure 8.1. It can be seen from figure 8.2 that the beam width parameter acquires minimum at a very short propagation distance ($\xi = 0.24$) corresponding to $\lambda = 0.5 \mu\text{m}$. Therefore, stronger and earlier self-focusing is achieved for $\lambda = 0.5 \mu\text{m}$ than $1.06 \mu\text{m}$ and $1.5 \mu\text{m}$. Hence, the selection of laser wavelength is also important in achieving earlier focusing of the laser beam. Figure 8.3 depicts the behavior of f with ξ for different values of ω_{p1} / ω . The laser strength parameter is fixed at $\alpha_0 = 0.3$ and the other parameters are same as taken in figure 8.1. It is found that as the electron density increases, the plasma dielectric constant decreases with the

result, the amplitude of laser spot size gets reduced close to the axis of propagation. Consequently, the minimum value of f shifts towards lower value of ξ and the beam focuses in high plasma density region.

Figure 8.4 depicts the behavior of f with ξ for various values of $\omega_{p2}/\omega = 0.15, 0.25$ & 0.3 with $\alpha_0 = 0.2$. The other parameters are same as has been taken in Figure 8.1. It is clear from figure 8.4 that as ω_{p2}/ω increases, self-focusing becomes stronger. It is due to the fact that as ω_{p2}/ω increases, the medium acquires a saturating nonlinearity which limits the energy associated with the electrons of the laser beam. Therefore, the beam width parameter reaches to its minimum value for $\omega_{p2}/\omega = 0.3$ at $\xi = 0.18$. Hence, one would expect the efficient self-focusing because of suitable wavelength of electron density ripple is present in the plasma. Therefore, the outcomes of present analysis are in a good agreement with those of Kaur and Sharma [68]. Where in the effect of density ripple is to decrease the minimum spot size of the laser beam. Figure 8.5 depicts the behavior of f with ξ for various values of magnetic field; $\omega_c/\omega = 0.01, 0.04, 0.08$ & 0.12 (corresponding values of magnetic field are $B_0 = 1.01MG, B_0 = 4.06MG, B_0 = 8.12MG$ and $B_0 = 12.19MG$ respectively). The other remaining parameters have been taken same as in Figure 8.1. The figure shows that it is the magnetic field which has a serious influence on the behavior of beam width parameter. As the magnetic field increases, the nonlinear term begins to control over the diffractive divergence term. It further, changes the propagation characteristics of the medium. Due, to strong interaction between the laser field and magnetic field, the laser beam is more focused. Thus, magnetic field has a significant role in enhancing the self-focusing of laser beam in rippled density plasma. Figure 8.6 illustrates the behavior of f with ξ for various values of normalized ripple wave number; $d = 50, 65$ & 75 with $\alpha_0 = 0.3$. The other parameters are: $d = 59, \omega_{p1}/\omega = 0.4, \omega_{p2}/\omega = 0.15$ and $\omega_c/\omega = 0.12$. It is interesting to note that the beam width parameter shows a different kind of behavior. As we increase the normalized ripple wave number, the beam width parameter decreases gradually at $\xi = 0.12$. Further, due to large ripple wave number, the wavefront curvature continues to focus the laser beam inside the magnetoplasma. Thus, one can say that the self-focusing strength of laser

beam increases in rippled density magnetoplasma. The present analysis results may be useful in laser driven fusion and plasma based accelerators.

8.5 CONCLUSION

In the present communication, we investigated the self-focusing of laser beam in rippled density magnetoplasma. Effect of magnetic field and normalized ripple wave number on self-focusing of a laser beam has been analyzed at various optimized parameters. The differential equation for the beam width parameter has been obtained and the results have been plotted and have been discussed. The results revealed that the magnetic field of a few MG increases the self-focusing capacity of laser beam strongly in rippled density plasma. Further, there is a strong coupling between the magnetic field and laser field. Due to the presence of suitable wavelength of density ripple in plasma, stronger and earlier self-focusing is achieved. The outcomes obtained are expected to be useful in laser driven fusion and plasma based accelerators.

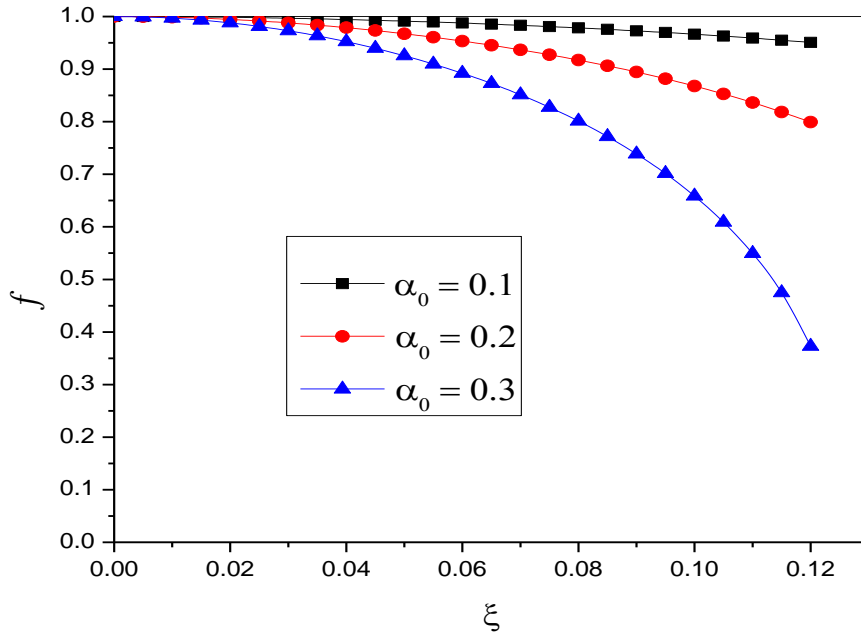


Figure 8.1: Dependence of f on ξ for various values of α_0 . The other parameters are: $d = 59$, $\omega_{p1} / \omega = 0.4$, $\omega_{p2} / \omega = 0.15$ and $\omega_c / \omega = 0.12$.

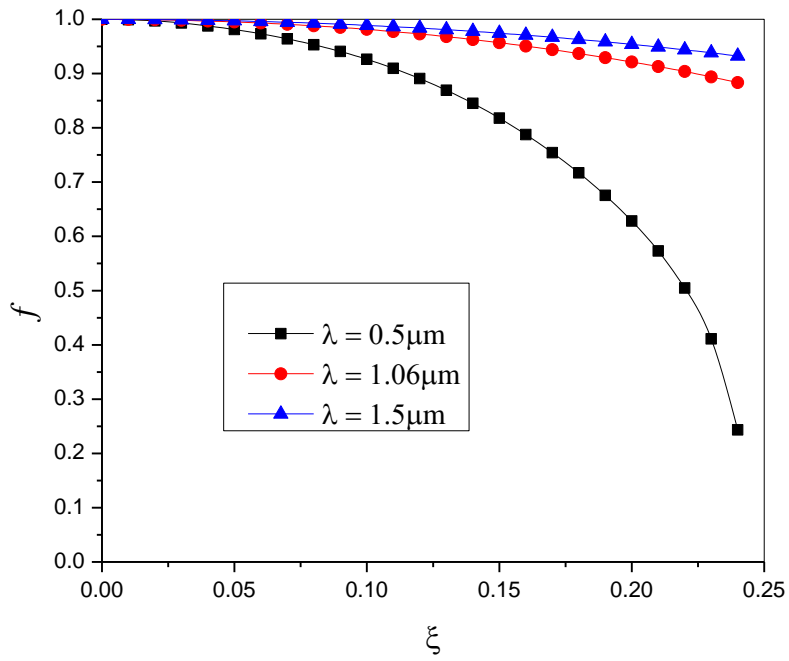


Figure 8.2: Dependence of f on ξ for various values of λ . The other parameters are: $d = 59$, $\omega_{p1} / \omega = 0.4$, $\omega_{p2} / \omega = 0.15$, $\omega_c / \omega = 0.12$ and $\alpha_0 = 0.3$.

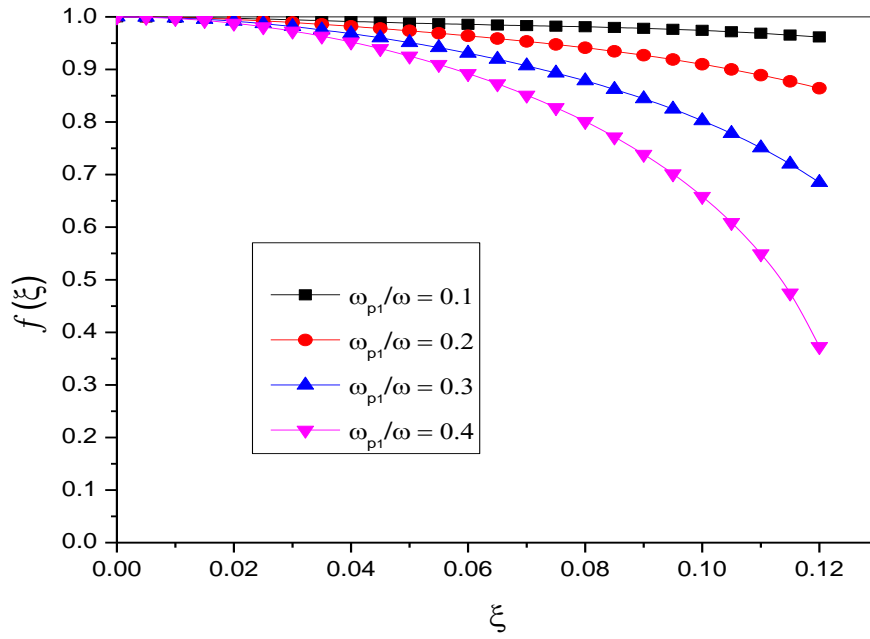


Figure 8.3: Dependence of f on ξ for various values of ω_{p1}/ω . The other parameters are: $d = 59$, $\omega_c/\omega = 0.12$, $\omega_{p2}/\omega = 0.15$ and $\alpha_0 = 0.3$

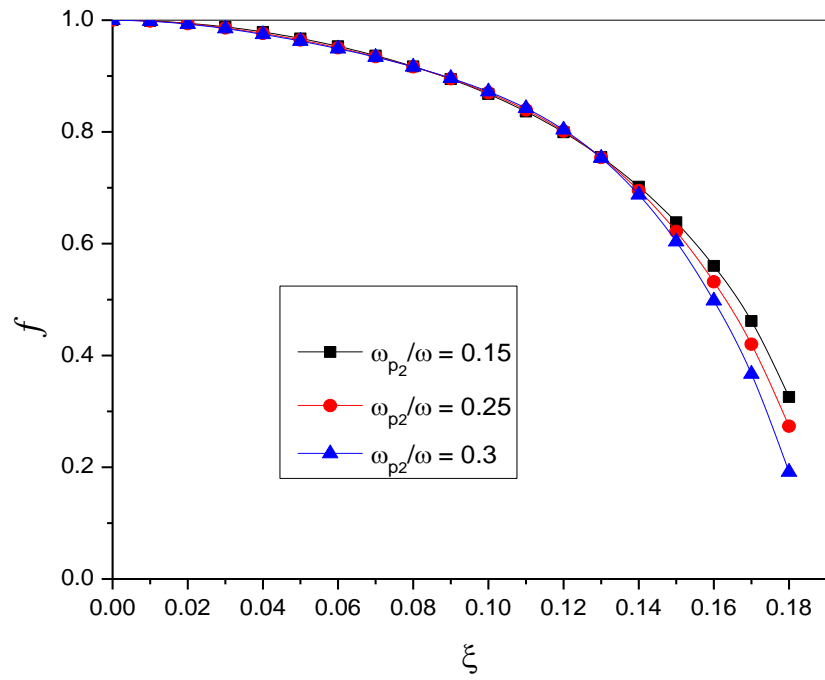


Figure 8.4: Dependence of f on ξ for various values of ω_{p2}/ω . The other parameters are: $d = 59$, $\omega_c/\omega = 0.12$, $\omega_{p1}/\omega = 0.4$ and $\alpha_0 = 0.2$

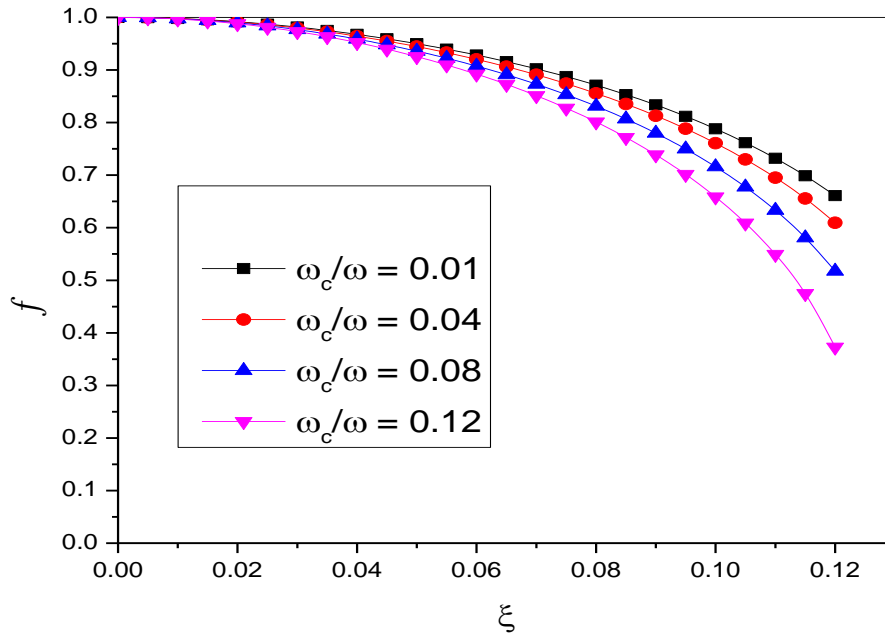


Figure 8.5: Dependence of f on ξ for various values of ω_c/ω . The other parameters are: $d = 59$, $\omega_{p1}/\omega = 0.4$, $\omega_{p2}/\omega = 0.15$ and $\alpha_0 = 0.3$

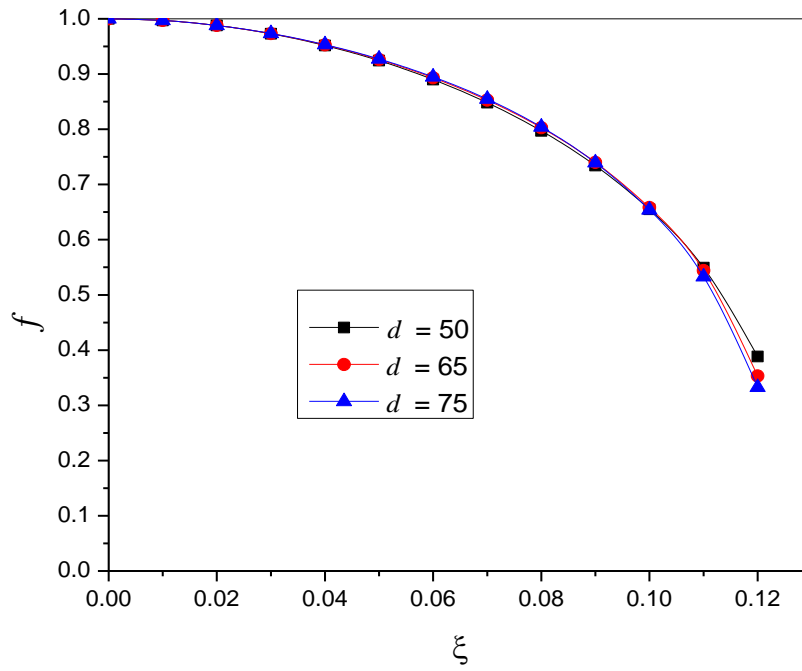


Figure 8.6: Dependence of f on ξ for various values of d . The other parameters are: $\omega_{p1} / \omega = 0.4$, $\omega_{p2} / \omega = 0.15$, $\alpha_0 = 0.3$ and $\omega_c / \omega = 0.12$

CHAPTER-9

SELF-FOCUSING OF HERMITE-COSINE- GAUSSIAN LASER BEAM IN PLASMA UNDER DENSITY TRANSITION

9.1 INTRODUCTION

The self-focusing of laser beams in a nonlinear medium like plasma is a captivating field of research which has an excellence in both theoretical and experimental fields [8, 12]. The intensity of the laser beam, sensitivity of decentered of decentered parameter b and density transition are considered to have a crucial role and having interesting qualities in self-focusing [22, 90]. During the propagation of a laser beam in a Kerr medium, the central parts of the beam give rise to radial compression and the cos-Gaussian beam eventually converts in to a cosh-Gaussian type beam with moderate power [27]. In weakly relativistic and ponderomotive regime, a large value of absorption level weakens the self-focusing effect in the absence of decentered parameter. However, oscillatory self-focusing occurs for a higher value of decentered parameter and all curves are seen to demonstrate self-focusing in a sharp manner [21]. In ponderomotive self-focusing, it is the density ramp that results in sooner and better self-focusing [77]. Furthermore, the quantum effect plays a crucial role in making it earlier and stronger as compared to classical one [84]. Again, apart from quantum effects, the upward ramped density profile results in higher oscillations of beam width parameter and consequently in sooner and better focusing [82]. Nanda *et al.* [91] found that the optimized laser and plasma parameters are equally important to obtain better focusing [93]. Patil *et al.* [135] predicted that the thermal quantum effects are equally important for more oscillations of beam-width parameter. However, it was found that in presence of the multiply charged ions, the nonlinear effects get reduced and hence self-focusing becomes less pronounced [136]. Gupta *et al.* [87] found that it is important to consider the ion temperature for the thermal self-focusing. Furthermore, the upward density transition can accelerate the electron to higher energy over a long propagation distance in comparison to uniform density relativistic plasma [85]. Again, Kant and Wani [118] found that the phenomenon of self-focusing is enhanced by decentered parameter and density transition. Moreover, the oscillatory self-

focusing takes place for decentered parameter $b \leq 2$ [106]. It is to be noted that the optimization of intensity parameter and wavelength can help in obtaining sooner and strong self-focusing [94].

We previously studied the self-focusing of Hermite-cosh-Gaussian beam in plasma and observed that these beams give freedom to mode index (m) and decentered parameter (b). But, it was possible only up to the decentered parameter $b \leq 1$ [119]. Thereafter, Wani and Kant [130] investigated the relativistic self-focusing of HcosG beam in collisionless plasma. They reported that the beam width parameter shows a strong oscillatory behavior and hence the laser beam becomes more focused at lower values of decentered and intensity parameters. However, in the present communication, our purpose is to analyze the impact of upward plasma density ramp profile $n(\xi) = n_0 \tan(\xi/d)$ on self-focusing of HcosG beam propagating in underdense plasma which was not done earlier for such a beam. The importance of the present work lies in the fact that the density transition causes more reduction in the amplitude of spot size of laser beam close to the propagation axis. Therefore, the minimum spot size of the beam decreases and hence modulates the phenomenon of self-focusing. Above all in the present analysis the decentered parameter has a noticeable impact on the propagation of HcosG beam. The present analysis employs WKB and paraxial approximations and is based on the parabolic wave equation approach [114]. The non-linear dielectric constant of plasma is presented in ponderomotive regime. The equations that govern the laser spot size are derived. The computational results in context of plasma density ramp and decentered parameter are discussed and finally a brief conclusion is added.

9.2 FIELD DISTRIBUTION OF HERMITE – COSINE – GAUSSIAN (HcosG) BEAM

Considering the Hermite-cosine-Gaussian (HcosG) laser beam that propagates in the z direction has the field distribution of the form

$$E(x, y, z) = \frac{E_0}{\sqrt{f_1(z)f_2(z)}} H_m\left(\frac{\sqrt{2}x}{r_0 f_1(z)}\right) H_n\left(\frac{\sqrt{2}y}{r_0 f_2(z)}\right) \exp\left[-\left(\frac{x^2}{r_0^2 f_1^2(z)} + \frac{y^2}{r_0^2 f_2^2(z)}\right)\right] \times \cos\left(\frac{\Omega_0 x}{f_1(z)}\right) \cos\left(\frac{\Omega_0 y}{f_2(z)}\right), \quad (9.1)$$

where, H_m and H_n are the m^{th} and n^{th} order Hermite polynomial respectively, E_0 is the constant

amplitude of the electric field, r_0 is the waist width, Ω_0 is the parameter associated with the cosine function, $f_1(z)$ and $f_2(z)$ are the beam width parameters in respective x and y directions.

9.3 NONLINEAR DIELECTRIC CONSTANT

Consider the propagation of HcosG laser beam in plasma whose dielectric constant is characterized of the form [20]

$$\varepsilon = \varepsilon_0 + \phi(EE^*) \quad (9.2)$$

where, $\varepsilon_0 = 1 - \omega_p^2 / \omega^2$ represents the linear part of dielectric constant, $\omega_p^2 = 4\pi n(\xi)e^2 / m$, $n(\xi) = n_0 \tan(\xi / d)$ and $\omega_{p0} = (4\pi n_0 e^2 / m)^{1/2}$ is the plasma frequency, e , m and n_0 being the magnitude of the electronic charge, rest mass and electron density respectively, ξ is the normalized propagation distance and d is a dimensionless adjustable parameter. The other part $\phi(EE^*) = (\omega_{p0}^2 / \omega^2) (1 - \exp(-3m\alpha EE^* / 4M)) \tan(\xi / d)$ represents the nonlinear part of dielectric constant [28], where, $\alpha = e^2 M / 6m_0^2 \omega^2 k_B T_0$ and M is the scatterer mass in the plasma, ω is the frequency of laser used, k_B is the Boltzmann constant and T_0 is the equilibrium temperature.

9.4 SELF-FOCUSING EQUATIONS

The wave equation that governs the propagation of laser beam can be of the following form

$$\nabla^2 \vec{E} - \frac{\varepsilon}{c^2} (-\omega^2 \vec{E}) + \vec{\nabla} \left(\frac{\vec{E} \vec{\nabla} \cdot \varepsilon}{\varepsilon} \right) = 0 \quad (9.3)$$

The last term of equation (9.3) on left hand side is neglected as $k^{-2} \nabla^2 (\ln \varepsilon) \ll 1$, where ' k ' represents the wave number the laser beam. Thus,

$$\nabla^2 \vec{E} + \frac{\omega^2}{c^2} \varepsilon \vec{E} = 0 \quad (9.4)$$

In Cartesian co-ordinate system, we can write this equation as

$$\frac{\partial^2 \vec{E}}{\partial x^2} + \frac{\partial^2 \vec{E}}{\partial y^2} + \frac{\partial^2 \vec{E}}{\partial z^2} + \varepsilon \frac{\omega^2}{c^2} \vec{E} = 0 \quad (9.5)$$

The solution of equation (9.5) is of the following form,

$$\bar{E} = A(x, y, z) \text{Exp}[i(\omega t - kz)] \quad (9.6)$$

$$\text{With } k^2 = \varepsilon_0 \frac{\omega^2}{c^2} = \frac{\omega^2}{c^2} \left(1 - \frac{\omega_{p0}^2}{\omega^2} \tan(\xi / d) \right), \quad (9.6a)$$

where, $\xi = z/R_d$. Now, differentiating equation (9.6) twice w. r. t. 'x, y and z respectively, we get

$$\frac{\partial \bar{E}}{\partial x} = \text{Exp}[i(\omega t - kz)] \frac{\partial A}{\partial x}$$

$$\frac{\partial^2 \bar{E}}{\partial x^2} = \text{Exp}[i(\omega t - kz)] \frac{\partial^2 A}{\partial x^2}$$

$$\frac{\partial \bar{E}}{\partial y} = \text{Exp}[i(\omega t - kz)] \frac{\partial A}{\partial y}$$

$$\frac{\partial^2 \bar{E}}{\partial y^2} = \text{Exp}[i(\omega t - kz)] \frac{\partial^2 A}{\partial y^2}$$

Similarly,

$$\begin{aligned} \frac{\partial^2 \bar{E}}{\partial z^2} = & \text{Exp}[i(\omega t - kz)] \left[\frac{\partial^2 A}{\partial z^2} + \frac{iA \omega_{p0}^2 \text{Sec}^2(z/dR_d)}{2cdR_d \sqrt{\omega^2 - \omega_{p0}^2 \tan(z/dR_d)}} + \frac{iA \omega_{p0}^4 z \text{Sec}^2(z/dR_d)}{4cd^2 R_d^2 (\omega^2 - \omega_{p0}^2 \tan(z/dR_d))^{3/2}} \right] \\ & + \frac{\text{Exp}[i(\omega t - kz)]}{\sqrt{\omega^2 - \omega_{p0}^2 \tan(z/dR_d)}} \left[\frac{iA \omega_{p0}^2 z \text{Sec}^2(z/dR_d) \tan(z/dR_d)}{cd^2 R_d^2} + \frac{iA \omega_{p0}^2 z \text{Sec}^2(z/dR_d)}{2cdR_d} \right. \\ & \left. - \frac{i(\omega^2 - \omega_{p0}^2 \tan(z/dR_d)) \left(\frac{\partial A}{\partial z} \right)}{c} - \frac{i\omega_{p0}^2 z \text{Sec}^2(z/dR_d) \left(\frac{\partial A}{\partial z} \right)}{2cdR_d} \right] \\ & + \frac{A \text{Exp}[i(\omega t - kz)]}{c^2} \left[\frac{\omega_{p0}^2 z \text{Sec}^2(z/dR_d)}{dR_d} - \frac{\omega_{p0}^4 z^2 \text{Sec}^4(z/dR_d)}{4d^2 R_d^2 (\omega^2 - \omega_{p0}^2 \tan(z/dR_d))} \right. \\ & \left. - (\omega^2 - \omega_{p0}^2 \tan(z/dR_d)) \right] \end{aligned}$$

Now, employing the WKB approximation and substituting the above values in Eq. (9.5) and neglecting $(\partial^2 A / \partial z^2)$, we get

$$\begin{aligned}
\frac{\partial^2 A}{\partial x^2} + \frac{\partial^2 A}{\partial y^2} + \frac{\omega^2}{c^2} \Phi(AA^*)A &= \frac{i}{c} \left(\frac{2dR_d(\omega^2 - \omega_{p0}^2 \tan(z/dR_d)) - \omega_{p0}^2 z \sec^2(z/dR_d)}{2dR_d \sqrt{\omega^2 - \omega_{p0}^2 \tan(z/dR_d)}} \right) \left(\frac{\partial A}{\partial z} \right) \\
- \frac{iA \omega_{p0}^2 \sec^2(z/dR_d)}{cdR_d \sqrt{\omega^2 - \omega_{p0}^2 \tan(z/dR_d)}} &\left(1 + \frac{\omega_{p0}^2 z}{4dR_d(\omega^2 - \omega_{p0}^2 \tan(z/dR_d))} + \frac{z \tan(z/dR_d)}{dR_d} \right) \\
- \frac{iA \omega_{p0}^2 \sec^2(z/dR_d)}{cdR_d \sqrt{\omega^2 - \omega_{p0}^2 \tan(z/dR_d)}} &\left(\frac{\omega_{p0}^2 z \tan^2(z/dR_d)}{4dR_d(\omega^2 - \omega_{p0}^2 \tan(z/dR_d))} \right) - \frac{A \omega_{p0}^2 z \sec^2(z/dR_d)}{c^2 dR_d} \\
+ \frac{A \omega_{p0}^4 z^2 \sec^4(z/dR_d)}{4c^2 d^2 R_d^2 (\omega^2 - \omega_{p0}^2 \tan(z/dR_d))} & \quad (9.7)
\end{aligned}$$

To solve equation (9.7) we express A as

$$A(x, y, z) = A_{mn}(x, y, z) \exp[-ikS(x, y, z)] \quad (9.8)$$

Where, $k = (\omega/c)\epsilon_0^{1/2}$ and A_{mn} and S depend on x , y and z . Differentiating equation (9.8) w. r.

t. x , y and z , we get

$$\begin{aligned}
\frac{\partial \bar{A}}{\partial x} &= \text{Exp}[-iKS(x, y, z)] \left[\frac{\partial A_{mn}}{\partial x} - ikA_{mn} \frac{\partial S}{\partial x} \right] \\
\frac{\partial^2 \bar{A}}{\partial x^2} &= \text{Exp}[-iKS(x, y, z)] \left[\frac{\partial^2 A_{mn}}{\partial x^2} - ikA_{mn} \frac{\partial^2 S}{\partial x^2} - 2ik \frac{\partial S}{\partial x} \frac{\partial A_{mn}}{\partial x} - k^2 A_{mn} \left(\frac{\partial S}{\partial x} \right)^2 \right]
\end{aligned}$$

Similarly,

$$\begin{aligned}
\frac{\partial^2 \bar{A}}{\partial y^2} &= \text{Exp}[-iKS(x, y, z)] \left[\frac{\partial^2 A_{mn}}{\partial y^2} - ikA_{mn} \frac{\partial^2 S}{\partial y^2} - 2ik \frac{\partial S}{\partial y} \frac{\partial A_{mn}}{\partial y} - k^2 A_{mn} \left(\frac{\partial S}{\partial y} \right)^2 \right] \\
\frac{\partial \bar{A}}{\partial z} &= \text{Exp}[-iKS(x, y, z)] \left[\frac{\partial A_{mn}}{\partial z} - ikA_{mn} \frac{\partial S}{\partial z} - iSA_{mn} \frac{\partial k}{\partial z} \right]
\end{aligned}$$

Substituting the above values in Eq. (9.7), we get

$$\begin{aligned}
\frac{\partial^2 A_{mn}}{\partial x^2} + \frac{\partial^2 A_{mn}}{\partial y^2} - ikA_{mn} \left(\frac{\partial^2 S}{\partial x^2} + \frac{\partial^2 S}{\partial y^2} \right) - 2ik \left(\frac{\partial S}{\partial x} \frac{\partial A_{mn}}{\partial x} + \frac{\partial S}{\partial y} \frac{\partial A_{mn}}{\partial y} \right) + \frac{\omega^2 \phi(A_{mn}^2) A_{mn}}{c^2} - \\
k^2 A_{mn} \left[\left(\frac{\partial S}{\partial x} \right)^2 + \left(\frac{\partial S}{\partial y} \right)^2 \right] = i \left(\frac{2dR_d k^2 c^2 - \omega_{p0}^2 z \text{Sec}^2(z/dR_d)}{2kc^2 dR_d} \right) \left[\frac{\partial A_{mn}}{\partial z} - ikA_{mn} \frac{\partial S}{\partial z} - iSA_{mn} \frac{\partial k}{\partial z} \right]
\end{aligned}$$

$$\begin{aligned}
& -\frac{iA_{mn}\omega_{p0}^2 \text{Sec}^2(z/dR_d)}{kc^2 dR_d} \left[1 + \frac{z\omega_{p0}^2}{4k^2 c^2 dR_d} + \frac{z \tan(z/dR_d)}{dR_d} - ikz + \frac{z\omega_{p0}^2 \tan^2(z/dR_d)}{4k^2 c^2 dR_d} \right] \\
& + \frac{A_{mn}\omega_{p0}^4 z^2 \text{Sec}^4(z/dR_d)}{4k^2 c^4 d^2 R_d^2}
\end{aligned} \tag{9.9}$$

Now, equating real and imaginary parts of Eq. (9.9), we get

Real part equation is

$$\begin{aligned}
& \frac{1}{\omega^2 A_{mn}} \left(\frac{\partial^2 A_{mn}}{\partial x^2} + \frac{\partial^2 A_{mn}}{\partial y^2} \right) + \frac{\phi(A_{mn}^2)}{\varepsilon_0} = \left(\frac{1}{\omega^2 c^2} \right) \left[k^2 c^2 + \frac{\omega_{p0}^2 z \text{Sec}^2(z/dR_d)}{2dR_d} \right] \left(\frac{\partial S}{\partial z} \right) + \\
& \frac{k^2}{\omega^2} \left[\left(\frac{\partial S}{\partial x} \right)^2 + \left(\frac{\partial S}{\partial y} \right)^2 \right] + \frac{S\omega_{p0}^2 \text{Sec}^2(z/dR_d)}{2\omega^2 c^2 dR_d} \left[\left(1 + \frac{z}{S} \right) \left(\frac{\omega_{p0}^2 z \text{Sec}^2(z/dR_d)}{2dR_d k^2 c^2} \right) - 1 - \frac{2z}{S} \right]
\end{aligned} \tag{9.10}$$

Imaginary part equation is

$$\begin{aligned}
& A_{mn}^2 \left(\frac{\partial^2 S}{\partial x^2} + \frac{\partial^2 S}{\partial y^2} \right) + \frac{\partial S}{\partial x} \frac{\partial A_{mn}^2}{\partial x} + \frac{\partial S}{\partial y} \frac{\partial A_{mn}^2}{\partial y} + \frac{1}{2} \left(1 - \frac{\omega_{p0}^2 z \text{Sec}^2(z/dR_d)}{2dR_d k^2 c^2} \right) \left(\frac{\partial A_{mn}^2}{\partial z} \right) - \\
& \left(\frac{\omega_{p0}^2 A_{mn}^2 \text{Sec}^2(z/dR_d)}{dR_d k^2 c^2} \right) \left[1 + \frac{\omega_{p0}^2 z}{4dR_d k^2 c^2} + \frac{\omega_{p0}^2 z \tan^2(z/dR_d)}{4dR_d k^2 c^2} + \frac{z \tan(z/dR_d)}{dR_d} \right] = 0 \tag{9.11}
\end{aligned}$$

The solutions of equations (9.10) and (9.11) can be written as:

$$\begin{aligned}
A_{mn}^2 = & \frac{E_0^2}{f_1(z)f_2(z)} H_m \left(\frac{\sqrt{2}x}{r_0 f_1(z)} \right) H_n \left(\frac{\sqrt{2}y}{r_0 f_2(z)} \right) \exp \left[- \left(\frac{x^2}{r_0^2 f_1^2(z)} + \frac{y^2}{r_0^2 f_2^2(z)} \right) \right] \times \\
& \cos \left(\frac{\Omega_0 x}{f_1(z)} \right) \cos \left(\frac{\Omega_0 y}{f_2(z)} \right)
\end{aligned} \tag{9.12}$$

And

$$S = \frac{x^2}{2} \beta_1(z) + \frac{y^2}{2} \beta_2(z) + \phi(z) \quad (9.13)$$

Where, $\beta_1(z) = (1/f_1(z))(\partial f_1/\partial z)$ and $\beta_2(z) = (1/f_2(z))(\partial f_2/\partial z)$ represent the curvature of the wavefront in x and y directions respectively. Now, using Eq. (9.12) and Eq. (9.13) in Eq. (9.10) and employing the paraxial approximation, we obtain the expressions for the beam width parameters f_1 and f_2 as follows:

$$\begin{aligned} & \frac{2}{f_1^3} \left(1 - \frac{\omega_{p0}^2}{\omega^2} \tan(\xi/d) \right) - \left(\frac{r_0 \omega}{c} \right)^2 \left(\frac{\omega_{p0}^2}{\omega^2} \right) \left(1 - \frac{\omega_{p0}^2}{\omega^2} \tan(\xi/d) \right) \left(\frac{3m}{2M} \right) \left(1 + \frac{b^2}{2} \right) \times \\ & \frac{(\alpha E_0^2) \tan(\xi/d)}{f_1^2 f_2} \exp \left(-\frac{3m\alpha E_0^2}{4Mf_1 f_2} \right) = \left[1 - \frac{\omega_{p0}^2}{\omega^2} \tan(\xi/d) + \frac{\omega_{p0}^2 \xi \sec^2(\xi/d)}{2d\omega^2} \right] \frac{\partial^2 f_1}{\partial \xi^2} + \\ & \left[1 - \frac{\omega_{p0}^2}{\omega^2} \tan(\xi/d) - \frac{\omega_{p0}^2 \xi \sec^2(\xi/d)}{2d\omega^2} \right] \frac{1}{f_1} \left(\frac{\partial f_1}{\partial \xi} \right)^2 + \frac{\omega_{p0}^2 \sec^2(\xi/d)}{2d\omega^2} \times \\ & \left[\frac{\omega_{p0}^2 \xi \sec^2(\xi/d)}{2d\omega^2 \left(1 - \frac{\omega_{p0}^2}{\omega^2} \tan(\xi/d) \right)} - 1 \right] \left(\frac{\partial f_1}{\partial \xi} \right) \end{aligned} \quad (9.14)$$

And

$$\begin{aligned} & \frac{2}{f_2^3} \left(1 - \frac{\omega_{p0}^2}{\omega^2} \tan(\xi/d) \right) - \left(\frac{r_0 \omega}{c} \right)^2 \left(\frac{\omega_{p0}^2}{\omega^2} \right) \left(1 - \frac{\omega_{p0}^2}{\omega^2} \tan(\xi/d) \right) \left(\frac{3m}{2M} \right) \left(1 + \frac{b^2}{2} \right) \times \\ & \frac{(\alpha E_0^2) \tan(\xi/d)}{f_2^2 f_1} \exp \left(-\frac{3m\alpha E_0^2}{4Mf_1 f_2} \right) = \left[1 - \frac{\omega_{p0}^2}{\omega^2} \tan(\xi/d) + \frac{\omega_{p0}^2 \xi \sec^2(\xi/d)}{2d\omega^2} \right] \frac{\partial^2 f_2}{\partial \xi^2} + \\ & \left[1 - \frac{\omega_{p0}^2}{\omega^2} \tan(\xi/d) - \frac{\omega_{p0}^2 \xi \sec^2(\xi/d)}{2d\omega^2} \right] \frac{1}{f_2} \left(\frac{\partial f_2}{\partial \xi} \right)^2 + \frac{\omega_{p0}^2 \sec^2(\xi/d)}{2d\omega^2} \times \end{aligned}$$

$$\left[\frac{\omega_{p0}^2 \xi \sec^2(\xi/d)}{2d\omega^2 \left(1 - \frac{\omega_{p0}^2}{\omega^2} \tan(\xi/d)\right)} - 1 \right] \left(\frac{\partial f_2}{\partial \xi} \right) \quad (9.15)$$

Where, $b = r_0 \Omega_0$ is called decentered parameter, $\rho_0 = r_0 \omega / c$ is the equilibrium beam radius, $\xi = z / R_d$ is the normalized propagation distance and $R_d = k r_0^2$ represents the diffraction length. Equations (9.14) and (9.15) represent the expressions for the parameters f_1 and f_2 respectively.

9.5 NUMERICAL RESULTS AND DISCUSSION

To compute the above analysis, we solve Eq. (9.14) and Eq. (9.15) by using the initial conditions $[\partial f_1 / \partial \xi]_{\xi=0} = 0, [f_1]_{\xi=0} = 1$ and $[\partial f_2 / \partial \xi]_{\xi=0} = 0, [f_2]_{\xi=0} = 1$ respectively. The various parameters chosen for the purpose of numerical calculations are as follows:

$\omega = 10^{14} \text{ rad/sec}$, $r_0 = 5 \times 10^{-3} \text{ cm}$ and $n_0 = 9.98 \times 10^{17} \text{ cm}^{-3}$ [71]. The diffractive divergence of the laser beam is due to the diffraction term while as self-focusing is due to nonlinear term. Figures 9.1 (a) and 9.1 (b) represent the dependence of f_1 and f_2 with propagation distance for various values of ω_{p0} / ω with $b = 0$ and 1 respectively. The other parameters are $\alpha E_0^2 = 2$, $m/M = 0.02$, $r_0 \omega / c = 50$ and $d = 10$. It is observed from these figures that the beam width parameters attain minimum values at $\xi = 4.3$ (corresponding to $\omega_{p0} / \omega = 0.8$) and $\xi = 2.3$ (corresponding to $\omega_{p0} / \omega = 0.7$) respectively. The amplitude of successive oscillations of f_1 and f_2 decreases and shifts towards lower values of ξ . It means that by considering the ramped density profile and taking in to account the effect of relative plasma density, the self-focusing occurs earlier and becomes stronger. This is due to increase in slope of plasma density curve along the propagation axis. Further, as the laser beam deepens in to the plasma, the plasma dielectric constant decreases rapidly. It is because the electron density depends on the propagation distance. Furthermore, the density ramp causes more reduction in the amplitude of

spot size of laser beam close to the propagation axis. Consequently, the effect gets enhanced and the beam is more focused. However, in uniaxial crystals the HcosG beam spreads in the $x - y$ plane with increasing propagation distance. However, for a short propagation distance its initial beam profile remains invariant [137]. But, in the present communication, it is interesting to note that the oscillatory behavior of f_1 and f_2 is deepened gradually and self-focusing of the laser beam starts acting comparatively at lower values of ξ . Therefore, a desirable self-focusing effect of HcosG beam is observed by exploiting the decentered parameter and hence agrees with the results of Patil *et al.* [73].

Figure 9.2 indicates the variation f_1 and f_2 with ξ for different values of b at $\omega_{p0}/\omega = 0.5$. The other parameters are same as taken in figure 9.1(a). It is evident from figure 9.2 that the beam width parameters attain a minimum value at comparatively lower value of $\xi = 3.15$ corresponding to decentered parameter $b = 1.5$. It is due to the fact that as the decentered parameter is increased, the laser spot size of HcosG beam gets reduced under plasma density ramp. Therefore, the beam converges rapidly and focuses to a smaller spot size. This is because of decentered parameter that changes the self-focusing / defocusing nature of beam in a significant manner. Further, it is the important parameter that has to be optimized to get stronger self-focusing and thus supports the results [90]. Figure 9.3 represents the beam width parameters variation with ξ for various values of αE_0^2 . The decentered parameter is fixed at $b = 1.5$ and the other parameters are same as taken in Figure 9.2. It is obvious from the figure 9.3 that sharp self-focusing is observed at $\xi = 3.15$ (corresponding to $\alpha E_0^2 = 2$). This is because self-focusing term becomes dominant over diffraction term because of the relativistic nonlinearity. It is seen from figure 9.3 that the laser beam becomes self-focused as we increase the initial power of the beam. Hence, in addition to density ramp and decentered parameter, the intensity of laser can be considered to be important in obtaining better focusing of HcosG laser beam.

9.6 CONCLUSION

In the investigation under consideration, we have studied the propagation of Hermite-cosine-Gaussian (HcosG) beam by considering plasma density ramp in a parabolic medium under

paraxial approximation. Our simulation results reveal that the density transition and decentered parameter (b) enhance the self-focusing of HcosG laser beams to a greater extent. It is noticed that the introduction of plasma density ramp makes a remarkable contribution to the process of self-focusing. Moreover, due to increase in the value of intensity of laser beam, self-focusing enhances and shifts towards lower values of normalized distance of propagation. Thus, one may conclude that the optimized laser and plasma parameters have a significant role in improving the focusing of HcosG beam in plasma. The results of present communication could be useful for various applications like plasma-based accelerators and inertial fusion.

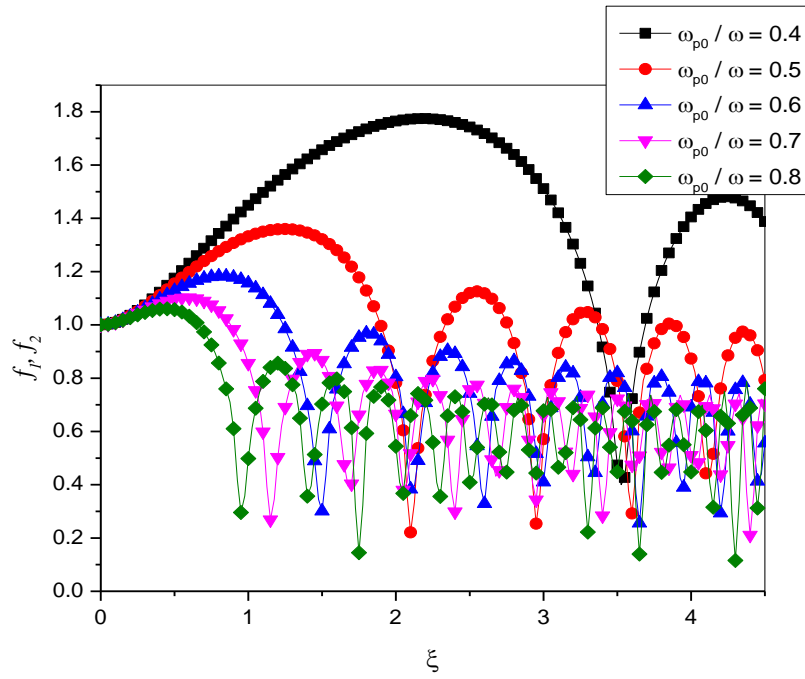


Figure 9.1 (a): Dependence of f_1 and f_2 on ξ for various values of ω_{p0}/ω . The decentered parameter is fixed at $b = 0$ and the other parameters are $\alpha E_0^2 = 2$, $m/M = 0.02$, $r_0 \omega / c = 50$ and $d = 10$

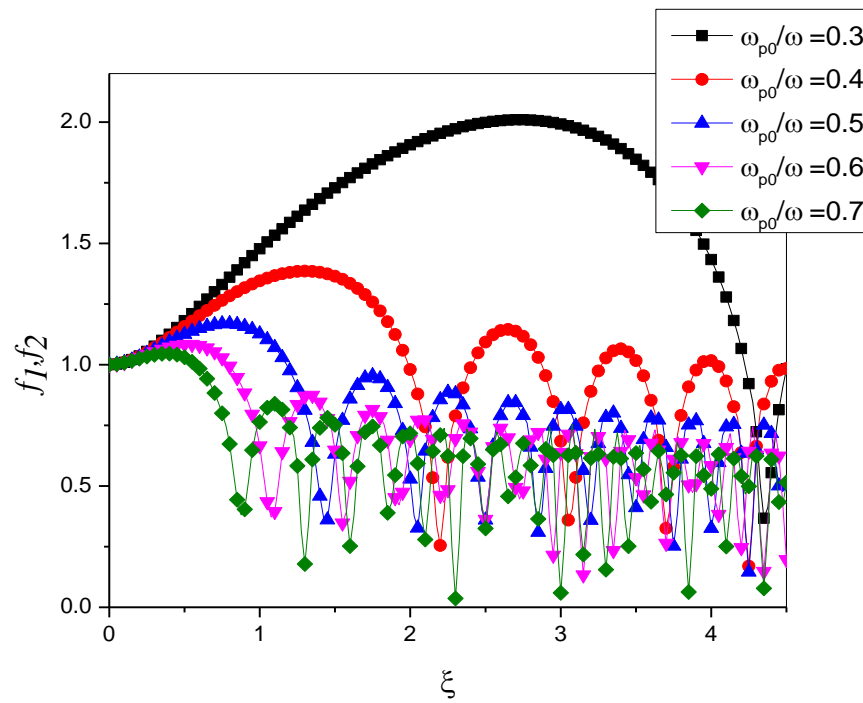


Figure 9.1(b): Dependence of f_1 and f_2 on ξ for various values of ω_{p0}/ω . The decentered parameter is fixed at $b = 1$ and the other parameters are same as taken in Figure 9.1 (a)

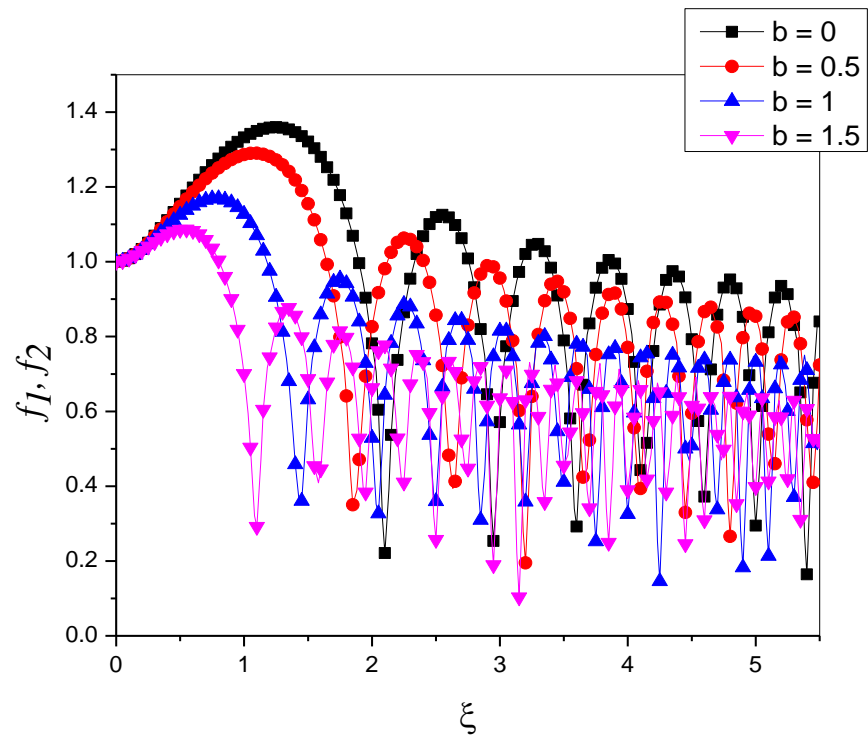


Figure 9.2: Dependence of f_1 and f_2 on ξ for various values of decentered parameter b . The other parameters are: $d = 10$, $\alpha E_0^2 = 2$, $m/M = 0.02$, $r_0 \omega / c = 50$ and $\omega_{p0} / \omega = 0.5$

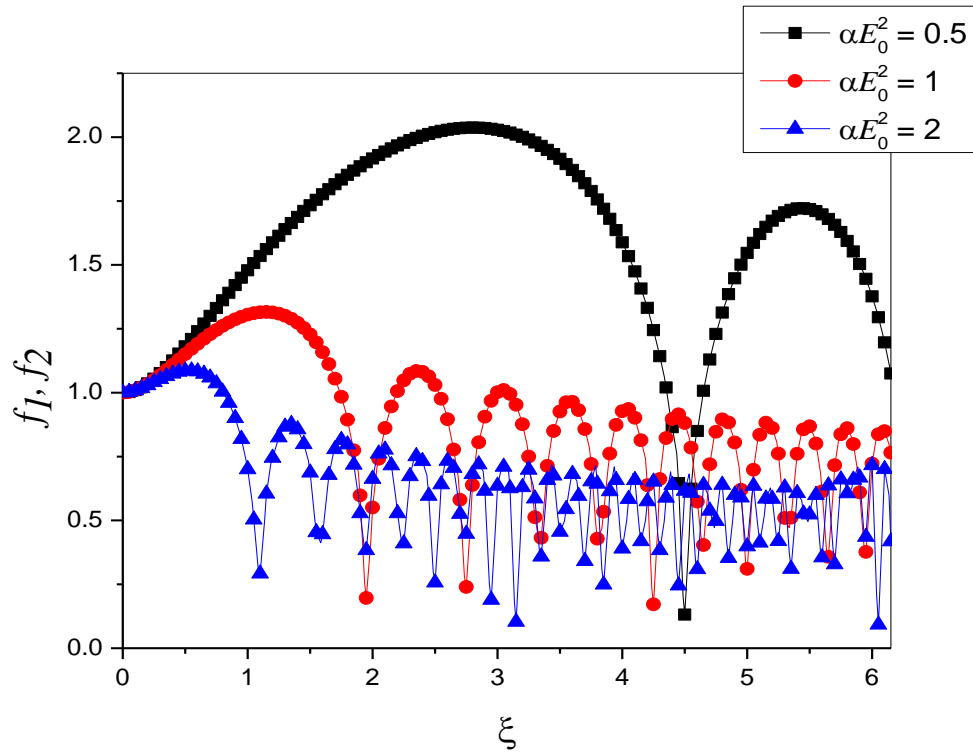


Figure 9.3: Dependence of f_1 and f_2 on ξ for various values of αE_0^2 . The decentered parameter is fixed at $b = 1.5$ and the other parameters are same as taken in Figure 9.2

CHAPTER-10

SUMMARY AND CONCLUSION

The self-focusing of laser beam in plasma is considered to be an important and captivating process that occurs during laser-plasma interaction as it is caused by the change in refractive index which arises due to relativistic mass effect, ponderomotive force, induced plasma diffusion and non-uniform ohmic heating. The up-to-date advances in such laser technology have made the experimentalists to use the pulses focused to extremely high intensities of the order of ($I \geq 10^{20} W/cm^2$). This makes it possible to explore the parameters both in atomic and plasma physics. With the advent of maser, laser and other radiation sources, coherent electromagnetic waves having well defined frequency and phase, have been shown to have wide ranging applications and their interaction with the plasma has been a captivating field of research in recent years. Because of intense electromagnetic radiations, the electron velocity in the plasma becomes quite large as compared to the velocity of light. Therefore, one must take in to account the relativistic mass variation. It therefore leads to self-focusing as the dielectric constant of plasma is an increasing function of the intensity. It is the ponderomotive force of the focused laser which then urges the electrons to move away out of the region having high intensity, reducing the local electron density, and consequently increasing the plasma dielectric function which leads to sooner and even stronger self-focusing. Further, the studies of laser beams with plasmas have attracted the researchers as the waist size is connected to beam width parameter. Therefore, studies of beam width parameters variation becomes an important subject of high power laser beams. Furthermore, a laser beam exhibits oscillatory behavior while propagating in plasma. In order to improve the self-focusing effect, the plasma density transition is introduced.

In the present thesis, we considered the density transition type based self-focusing of a short pulse laser in plasma for HchG, ChG, HcosG, simple Gaussian and chirped Gaussian beams. Due to density transition the spot size of the beam decreases up to a Rayleigh length and does not increase much. By choosing optimized parameters, the combined effect of density ramp, decentered parameter which is a characteristic of cosh-Gaussian beams and linear absorption on the beam width parameter behavior shows that self-focusing occurs sooner, becomes enhanced with shorter propagation distance and then its defocusing takes place. The absorption weakens

the self-focusing effect and density transition sets an earlier and stronger focusing. Therefore, the study of such beams can be analyzed in plasma, but the essential thing is that the plasma density ramp, decentered parameter and absorption coefficient act in such a way that they change the self-focusing or defocusing nature of the beam in a significant manner. Further, due to dominance of self-focusing term over the diffraction term, the self-focusing of HcosG beams occurs in an enhanced manner. However, in uniaxial crystals the HcosG beam spreads in the $x - y$ plane with increasing propagation distance, and its beam profile remains unchanged for a short propagation distance. But, as the decentered parameter is increased, the laser spot size of HcosG beam gets reduced during propagation in plasma under density transition and the beam then converges rapidly and focuses to a smaller spot size. Further, since the laser beam used is highly powerful, the relativistic nonlinear effect emerges from the relativistic mass correction and depends on intensity factor αE_0^2 and relative plasma density ω_{p0} / ω . The nonlinear term is responsible for self-focusing and the divergence of the beam is due to the diffraction term. Further, when the plasma density is increased at relativistic intensities, most of the electrons of the beam having relativistic nature travel with the laser pulse. With the result, a higher current and consequently a higher magnetic field get generated, which further leads to enhancement of self-focusing.

Now, as the initial electron density depends on the distance of propagation. Therefore, as soon as the laser beam passes deeper in to the plasma, the dielectric constant of plasma decreases rapidly. The laser beam then shows an oscillatory behavior and the frequency of oscillation increases, which in turn decreases the amplitude gradually close to the axis of propagation. Therefore, by considering the density transition (ramped density profile) and taking in to account the effect of relative density, the self-focusing process of laser occurs earlier and becomes stronger. Again, with increase in ramp slope of plasma density curve along the propagation axis, the process occurs sooner and hence laser beam is more focused. Further, by increasing the intensity, the diffraction of the propagating beam in a nonlinear medium starts earlier. Thus, one can say that it is the intensity of the beam that controls the behavior of beam width parameter. Again, due to increase in the value of intensity, highly energetic electrons will continue to move forward without loss of energy. Furthermore, the beam width parameter is a function of laser spot size and depends on the intensity of beam. Therefore, the intensity rise results in the reduction of spot size very close to the axis of propagation and the density transition leads the beam width parameter to

decrease with a higher rate. Consequently, the self-focusing of laser beam is enhanced to a greater extent by exploiting the density transition in plasma. Thus the density transition has a crucial role in laser-plasma interaction.

The chirp parameter increases the electron energy and hence momentum so that the electron escapes from the laser beam. The value of chirp parameter decreases with laser intensity and initial electron energy. Although, without chirp, the laser beam shows self-focusing up to a certain critical value but, as the propagation distance increases, it starts to experience defocusing. The chirp parameter minimizes the defocusing and increases the ability of process of self-focusing of laser in plasma. Further, the amplitude of oscillations decreases with the distance of propagation so that sooner, earlier and stronger self-focusing effect is achieved. Also, on increasing the values of negative chirp, the self-focusing at first is strengthened and after attaining a critical value the laser beam defocuses. This is because the frequency of a linear and negative chirped laser beam changes during the propagation in the plasma. The spot size of laser beam depends on ξ and at extended propagation distances the temporal shape of the chirped laser beam will be changed. Therefore, the defocusing of laser beam is weakened and there by the self-focusing effect is strengthened by using chirp. Hence, the chirp parameter plays a significant role in minimizing the defocusing and increasing the ability of process of self-focusing in collisional plasma. Now, for the case of rippled density magnetoplasma, it is the magnetic field that has a serious influence on the beam width parameter variation. As the magnetic field is increased, the nonlinear term begins to control over the diffractive divergence term and the propagation characteristics of the medium are changed. Due, to strong interaction between the magnetic and laser fields, the laser beam is more focused. Thus, one can say that the magnetic field has a significant role in enhancing the self-focusing effect in rippled density plasma. Further, due to large ripple wave number, the wavefront curvature continues to focus the laser beam inside the magnetoplasma. Thus, one can say that the self-focusing strength of laser beam increases in rippled density magnetoplasma.

The present work has direct applications to accelerators based on plasma including laser-driven fusion, inertial confinement fusion, x-ray lasers etc. In such applications, it is important for a highly powerful laser beam to propagate over extended distances without loss of energy so that

an efficient interaction with the plasma is preserved. But during such laser-plasma interactions, the resultant intensity of the laser beam is being affected by instabilities such as scattering processes like stimulated Brillouin scattering and stimulated Raman scattering. These processes can greatly affect the absorption of light in laser produced plasmas because they can prevent light from reaching the critical density region. The laser pulses are very useful in studying the mechanism of powerful terahertz radiation generation from gas targets. The quasi-static transverse currents created by laser field ionization in plasmas are responsible for the THz emission. The chirped laser pulses are used to generate strong THz pulses with amplitudes scaling linearly with the laser amplitude. Thus, density transition is considered to be important in laser plasma interactions, particularly for the self-focusing of short pulse laser in an under dense plasma. Increase in initial density and ramp slope decreases the minimum spot size of the laser beam. The laser and plasma parameters are crucial for self-focusing process in plasmas as it is enhanced with such optimized laser and plasma parameters.

CHAPTER-11

REFERENCES

- [1] Askaryan, G. A., (1962), "Effects of the gradient of strong electromagnetic beam on electrons and atoms", *Sov. Phys. JETP*, **15**, 1088-1090
- [2] Bingham, R., Mendonca, J. T., Shukla, P. K., (2004), "Plasma based charged accelerators", *Plasma Phys. Control Fusion*, **46**, 1-23
- [3] Leemans, W. P., Volfbeyn, P., Guo, K. Z., Chattopadhyay, S., Schroeder, C. B., Shadwick, B. A., Lee, P. B., Wurtele, J. S., Esarey, E., (1998), "Laser-driven plasma based accelerators: wakefield acceleration, channel guiding and laser triggered particle injection", *Phys. Plasmas*, **5**, 1615(9)
- [4] Umstadter, D., (2001), "Review of physics and applications of relativistic plasmas driven by ultra-intense lasers", *Phys. Plasmas*, **8**, 1774-1785
- [5] Sarkisov, G. S., Bychenkov, V. Y., Novikov, V. N., Tikhonchuk, V. T., Maksimchuk, A., Chen, S. Y., Wagner, R., Mourou, G., Umstadter, D., (1999), "Self-focusing, channel formation and high-energy ion generation in interaction of an intense short laser pulse with a He jet", *Phys. Rev. E*, **59**, 7042-7054
- [6] Tabak, M., Hammer, J., Glinsky, M. E., Kruer, W. L., Wilks, S. C., Woodworth, J., Campbell, E. M., Perry, M. D., Mason, R. J., (1994), "Ignition and high gain with ultra-powerful lasers", *Phys. Plasmas*, **1**, 1626-1634
- [7] Regan, S. P., Bradley, D. K., Chirikikh, A. V., Craxton, R. S., Meyerhofer, D. D., Seka, W., Short, R. W., Simon, A., Town, R. P.J., Yaakobi, B., Carroll, J. J., Drake, R. P., (1999), "laser plasma interactions in long-scale-length plasmas under direct-drive national ignition facility conditions", *Phys. Plasmas*, **6**, 2072-2080
- [8] Sprangle, P., Esarey, E., Krall, J., (1996), "Laser driven electron acceleration in vacuum, gases and plasmas", *Phys Plasmas*, **3**, 2183-2190

- [9] Niu, H. Y., He, X. T., Qiao, B., Zhou, C. T., (2008), “Resonant acceleration of electrons by intense circularly polarized Gaussian laser pulses”, *Laser and Particle Beams*, **26**, 51-9
- [10] Lee, J. X., Zang, W. P., Li, Y. D., Tian, J. G., (2009), “Acceleration of electrons by a tightly focused intense laser beam”, *Opt. Exp.*, **17**, 11850-9
- [11] Lourenco, S., Kowarsch, N., Scheid, W., Wang, P. X., (2010), “Acceleration of electrons and electromagnetic fields of highly intense laser pulses”, *Laser and Particle Beams*, **28**, 195-201
- [12] Gupta, D. N., Suk, H., (2006), “Frequency chirp for resonance enhanced electron energy during laser acceleration”, *Phys. Plasmas*, **13**, 044507
- [13] Mulser, P., Bauer, D., (2004), “Fast ignition for fusion pellets with super intense lasers: concepts problems and prospective”, *Laser and Particle Beams*, **22**, 5-12
- [14] Hora, H., (2007), “New aspects for fusion energy using inertial confinement”, *Laser and Particle Beams*, **25**, 37-45
- [15] Winterberg, F., (2008), “Laser for inertial confinement fusion driven by high explosives”, *Laser Part Beams*, **26**, 127-35
- [16] Perkins, F. W., Goldman, M. V., (1981), “Self-focusing of radio waves in an under dense ionosphere”, *J. Geo phys. Res.* **86**, 600-8
- [17] Guzdar, P. N., Chaturvedi, P. K., Papadopoulos, K., Ossakow, S. L., (1998), “The thermal self-focusing instability near the critical surface in the high-latitude ionosphere”, *J. Geo phys. Res.* **103**, 2231-2237
- [18] Gondarenko, N. A., Ossakow, S. L., Milikh, G. M., (2005), “Generation and evolution of density irregularities due to self-focusing in ionospheric modifications”, *J. Geo phys. Res.* **110**, 1978-2012
- [19] Keskinen, M. J., Basu, S., (2003), “Thermal self-focusing instability in the high latitude ionosphere”, *Radio Sci.* **38**, 10953

- [20] Sodha, M. S., Ghatak, A. K., Tripathi, V. K., (1974), "Self-focusing of laser beams in dielectrics, semiconductors and plasmas", Tata- McGraw-Hill, New Delhi
- [21] Gill, T. S., Mahajan, R., Kaur, R., (2011), "Self-focusing of cosh-Gaussian laser beam in a plasma with weakly relativistic and ponderomotive regime", Phys. Plasmas, **18**, 033110-18.
- [22] Kant, N., Wani, M. A., Kumar, A., (2012), "Self-focusing of Hermite-Gaussian laser beams in plasma under plasma density ramp", Optics Commun. **285**, 4483-4487
- [23] Belafhal , A., Ibnchaikh,(2000), "Propagation properties of Hermite-cosh-Gaussian laser Beams", Opt. Commun. **186**, 269-276.
- [24] Patil, S. D., Takale, M. V., Dongare, M. B., (2008), "Propagation of Hermite-cosh-Gaussian laser beams in n-InSb", Opt. Commun. **281**, 4776-4779.
- [25] Patil, S. D., Takale, M. V., Fulari, V. J., Dongare, M. B., (2008), "Propagation of Hermite-cosh-Gaussian laser beams in non-degenerate germanium having space charge neutrality", J. Mod. Opt. **55**, 3529-3535.
- [26] Sobhani, H., Vaziri, M., Rooholamininejad, H., Bahrapour, A. R., (2016), "Nonlinear interaction of intense hypergeometric Gaussian subfamily laser beams in plasma", Opt. & Laser Tech. **81**, 40-45
- [27] Chen, R., Ni, Y., Chu, X., (2011), "Propagation of cos-Gaussian beam in a kerr medium", Opt. & Laser Tech. **43**, 483-487.
- [28] Hora, H., (1969), "self-focusing of laser beams in a plasma by ponderomotive forces", Z. Physik, **226**, 156-159.
- [29] Litvak, A. G., (1970), "Finite-amplitude wave beams in a magnetoactive plasma", Sov. Phys. JETP, **30**, 344-347.
- [30] Sodha, M. S., Tewari, D. P., Ghatak, A. K., Kamal, J., Tripathi, V. K., (1971), "Self-focusing of laser beams in inhomogeneous dielectrics", Opto- electronics, **3**, 157-161

- [31] Sodha, M. S., Khanna, R. K., Tripathi, V. K., (1973), "Self-focusing of a laser beam in a strongly ionized plasma", *Opto- electronics*, **5**, 533-538
- [32] Sodha, M. S., Nayyar, V. P., Tripathi, V. K., (1974), "Asymmetric focusing of a laser beam in TEM₀₁ doughnut mode in a nonlinear dielectric", *Opt. Soc. Am.* **64**, 941-943
- [33] Sodha, M. S., Prasad, S., Tripathi, V. K., (1974), "Nonstationary Self-focusing of a Gaussian pulse in a plasma", *J. Appl. Phys.* **46**, 637-642
- [34] Sodha, M. S., Nayyar, V. P., (1975), "Thermal self-focusing of TEM₀₁ laser beams and ring – shape self-focusing of two specific mixtures of modes", *Opt. Soc. Am.* **65**, 1027-1030
- [35] Siegrist, M. R., (1976), "Self focusing in plasma due to ponderomotive forces and relativistic effects", *Opt. Commun.* **16**, 402-407.
- [36] Nayyar, V. P., (1978), "Self-focusing of a non-Gaussian laser mode in a dense plasma", *J. Appl. Phys.*, **49**, 1114-1118.
- [37] Nayyar, V. P., Soni, V. S., (1979), "Self-focusing and self-defocusing of elliptically shaped Gaussian laser beams in Plasmas", *J. Appl. Phys. D*, **12**, 239-247
- [38] Askaryan, G. A., Mukhamadzhyanov, M. A., (1981), "Nonlinear defocusing of a focused beam: a fine beam from the focus", *JETP Letts.* **33**, 44-48.
- [39] Mori, W. B., Joshi, C., Dawson, J. M., Forslund, D. W., Kindel, J. M., (1988), "Evolution of self-focusing of intense electromagnetic waves in plasma", *Phys. Rev. Letts.* **60**, 1298-1301.
- [40] Kurki-Suonio, T., Morrison, P. J., Tajima, T., (1989), "Self-focusing of an optical beam in a plasma", *Phys. Rev. A*, **40**, 3230-3239.
- [41] Cicchitelli, L., Hora, H., Postle, R., (1990), "Longitudinal field components for laser beams in Vacuum", *Phys. Rev. A*, **41**, 3727-3732.
- [42] Bruce, I. C., Barbara, F., Lasinski, A., Bruce, L., Jullian, C. C., (1991), "Dynamics of ponderomotive self-focusing in plasmas", *Phys. Fluids B*, **3**, 766-775

- [43] Brandi, H. S., Manus, C., Mainfray, G., Lehner, T., Bonnaud, G., (1993), “Relativistic and Ponderomotive self-focusing of a laser beam in a radially inhomogeneous plasma I. Paraxial approximation”, *Phys. Fluids B*, **5**, 3539-3550
- [44] Chen, X. L., Sudan, R. N., (1993), “Two dimensional self-focusing of short intense laser pulse in underdense plasma”, *Phys. Fluids B*, **5**, 1336-1348.
- [45] Bulanov, S. V., Pegoraro, F., Pukhov, A. M., (1995), “Two dimensional regimes of self-focusing, wake field generation and induced focusing of a short intense laser pulse in an underdense plasma”, *Phys. Rev. Letts.* **74**, 710-713.
- [46] Gibbon, P., Jakober, F., Monot, P., Auguste, T., (1996), “Experimental study of relativistic self-focusing and self-channeling of an intense laser pulse in an underdense plasma”, *IEEE Trans. Plasma Sci.* **24**, 343-350.
- [47] Asthana, M. V., Varshney, D., Sodha, M. S., (2000), “Relativistic self-focusing of transmitted laser radiation in plasmas”, *Laser and Particle Beams*, **18**, 101-107
- [48] Hafizi, B., Ting, A., Sprangle, P., Hubbard, R. F., (2000), “Relativistic focusing and ponderomotive channeling of intense laser beams”, *Phys. Rev. E*, **62**, 4120-4125
- [49] Osman, F., Castillo, R., Hora, H., (2000), “Numerical programming of self-focusing at laser-plasma interaction”, *Laser and Particle Beams*, **18**, 59-72.
- [50] Liu, C. S., Tripathi, V.K., (2000), “Laser frequency upshift, self-defocusing, and ring formation in tunnel ionizing gases and plasmas”, *Phys. Plasmas*, **7**, 4360-4363.
- [51] Feit, M. D., Komashko, A. M., Rubenchik, A. M., (2001), “Relativistic self-focusing in underdense plasma”, *Phys. D*, **152**, 705-713.
- [52] Faure, J., Malka, V., Marques, J. R., David, P. G., Amiranoff, F., Taphuoc, K., Rousse, A., (2002), “Effects of pulse duration on self-focusing of ultra-short lasers in underdense Plasmas”, *Phys. Plasmas*, **9**, 756-759.

- [53] Nitikant., Sharma, A. K., (2004), "Effect of pulse slippage on resonant second harmonic generation of a short pulse laser in a plasma", J. Phys. D:Appl. Phys. **37**, 998
- [54] Sharma, A., Verma, M. P., Sodha, M. S., (2004), "Self-focusing of electromagnetic beams in collisional plasmas with nonlinear absorption", Phys. Plasmas, **11**, 4275-4279
- [55] Jha, P., Wadhvani, N., Raj, G., Upadhyaya, A. K., (2004), "Relativistic and ponderomotive effects on laser plasma interaction dynamics", Phys. Plasmas, **11**, 1834-1839
- [56] Kant, N., Sharma, A. K., (2004), "Resonant second-harmonic generation of a short pulse laser in a plasma channel", J. Phys. D: Appl. Phys. **37**, 2395-2398.
- [57] Kant, N., Sharma, A. K., (2005), "Capillary plasma formation by a laser", Phys. Scripta. **71**, 402-405.
- [58] Prakash, G., Sharma, A., Verma, M. P., Sodha, M. S., (2005), "Focusing of an intense Gaussian laser beam in a radially inhomogeneous medium", J. Opt. Soc. Am. B, **22**, 1268-1275
- [59] Varshney, M., Qureshi, K. A., Varshney, D., (2005), "Relativistic self-focusing of a laser beam in an inhomogeneous plasma", Journal of Plasma Phys. **72**, 195-203.
- [60] Saini, N. S., Gill, T. S., (2006), "Self-focusing and self-phase modulation of an elliptic Gaussian laser beam in collision-less magneto-plasma", Laser and Particle Beams, **24**, 447-453
- [61] Kumar, A., Gupta, M. K., Sharma, R. P., (2006), "The effect of a relativistic intense Gaussian laser pulse on the propagation of electron plasma wave", Lasers & Particle Beams, **24**, 403-409.
- [62] Sodha, M. S., Sharma, A., (2006), "Mutual focusing/defocusing of Gaussian electromagnetic beams in collisional plasma", Phys. Plasmas, **13**, 053105-1.
- [63] Gupta, D. N., Suk, H., (2007), "Enhanced focusing of laser beams in semiconductor Plasmas", Appl. Phys. **101**, 043109

- [64] Gupta, D. N., Hur, M. S., Hwang, H., Suk, H., (2007), "Plasma density ramp for relativistic self-focusing of an intense laser", *J. Opt. Soc. Am. B*, **24**, 1155-1159
- [65] Gupta, D. N., Hur, M. S., Suk, H., (2007), "Additional focusing of a high intensity laser beam in a plasma with a density ramp and a magnetic field", *Appl. Phys. Lett.* **91**, 081505
- [66] Agarwal, S. K., Sodha, M. S., (2007), "Steady-state self-focusing of Gaussian electromagnetic beams in an inhomogeneous nonlinear medium: effect of absorption and initial curvature of the beam", *Optik*. **118**, 367-372
- [67] Faisal, M., Verma, M. P., Sodha, M. S., (2008), "self-focusing of electromagnetic pulsed beams in collisional plasmas", *Phys. Plasmas*, **15**, 102301-6
- [68] Kaur, S., Sharma, A. K., (2009), "Self-focusing of a laser pulse in plasma with periodic density ripple", *Laser and Particle Beams*, **27**, 193-199
- [69] Verma, U., Sharma, A. K., (2009), "Effect of self-focusing on the prolongation of laser produced plasma channel", *Laser and Particle Beams*, **27**, 1-7
- [70] Parashar, J., (2009), "Effect of self-focusing on laser third harmonic generation in a clustered gas", *Phys. Scr.* **79**, 015501
- [71] Takale, M.V., Navare, S.T., Patil, S.D., Fulari, V.J., Dongare, M. B., (2009), "Self-focusing and defocusing of TEM_{0p} Hermite-Gaussian laser beams in collision-less Plasma", *Opt. Commun.* **282**, 3157-3162
- [72] Sadighi-Bonabi, R., Habibi, M., Yazdani, E., (2009), "Improving the relativistic self-focusing of intense laser beam in plasma using density transition", *Phys. Plasmas*, **16**, 083105
- [73] Patil, S.D., Navare, S.T., Takale, M.V., Dongare, M. B., (2009), "Self-focusing of cosh-Gaussian laser beams in parabolic medium with linear absorption", *Optics and Lasers in Engineering*, **47**, 604-606
- [74] Xiong, H., Liu, S., Liao, J., Liu, X., (2010), "Self-focusing of laser pulse propagating in magnetized plasma", *Optik*, **121**, 1680-1683

- [75] Singh, A., Walia, K., (2010), "Relativistic self-focusing and self-channeling of Gaussian laser beam in plasma", *Appl. Phys. B*, **101**, 617-622
- [76] Patil, S.D., Takale, M.V., Navare, S. T., Dongare, M. B., (2010), "Focusing of Hermite-cosh-Gaussian laser beams in collision-less magneto plasma", *Laser and Particle Beams*, **28**, 343-349
- [77] Kant, N., Saralch, S., Singh, H., (2011), "Ponderomotive self-focusing of a short laser pulse under a plasma density ramp", *Nukleonika*, **56**, 149-153
- [78] Gill, T. S., Kaur, R., Mahajan, R., (2011), "Relativistic self-focusing and self-phase modulation of cosh Gaussian laser beam in magnetoplasma", *Laser and Particle Beams*, **29**, 183-191.
- [79] Kim, J., Kim, G. J., Yoo, S. H., (2011), "Energy enhancement using an upward density ramp in laser wakefield acceleration", *J. Korean Phys. Soc.* **59**, 3166-3170.
- [80] Navare, S. T., Takale, M. V., Patil, S. D., Fulari, V. J., Dongare, M. B., (2012) "Impact of linear absorption on self-focusing of Gaussian laser beam in collisional plasma", *Optics & Lasers in Eng.* **50**, 1316-1320
- [81] Gill, T. S., Mahajan, R., Kaur, R., Gupta, S., (2012), "Relativistic self-focusing of super-Gaussian laser beam in plasma with transverse magnetic field", *Laser and part. Beams*, **30**, 509
- [82] Habibi, M., Ghamari, F., (2012), "Stationary self-focusing of intense laser beam in cold quantum plasma using ramp density profile", *Phys. Plasmas*, **19**, 103110-6
- [83] Abari, M. E., Shokri, B., (2012), "study of nonlinear ohmic heating and ponderomotive force effects on the self-focusing and defocusing of Gaussian laser beams in collisional underdense plasmas" *Phys. Plasmas*, **19**, 113107-5
- [84] Patil, S. D., Takale, M. V., Navare, S. T., Dongare, M. B., Fulari, V. J., (2013), "Self-focusing of Gaussian laser beam in relativistic cold quantum plasma", *Optik*, **124**, 180-183

- [85] Patil, S.D., Takale, M. V., (2013), “Self-focusing of Gaussian laser beam in weakly relativistic and ponderomotive regime using upward ramp of plasma density”, *Phy. Plasmas*, **20**, 083101-5
- [86] Patil, S.D., Takale, M. V., Fulari, V. J., Gupta, D. N., Suk, H., (2013), “Combined effect of ponderomotive and relativistic self-focusing on laser beam propagation in a plasma”, *Appl. Phys. B*, **111**, 1
- [87] Gupta, D. N., Islam, M. R., Jang, D. G., Suk, H., Jaroszynski, D. A., (2013), “Self-focusing of a high-intensity laser in collisional plasma under weak relativistic-ponderomotive nonlinearity”, *Phy. Plasmas*, **20**, 123103
- [88] Mahajan, R., Gill, T. S., Kaur, R., (2013), “Interaction between parallel Gaussian electromagnetic beams in a plasma with weakly relativistic ponderomotive regime”, *Optik*, **124**, 2686-2690
- [89] Kaur, R., Gill, T. S., Mahajan, R., (2013), “Interaction between parallel Gaussian electromagnetic beams in relativistic magnetoplasma”, *Opt. Commun.* **289**, 127
- [90] Nanda, V., Kant, N., Wani, M. A., (2013), “Sensitiveness of decentered parameter for relativistic self-focusing of Hermite-Cosh-Gaussian laser beam in plasma”, *IEEE Transactions on Plasma Science*, **41**, 2251-2256
- [91] Nanda, V., Kant, N., Wani, M. A., (2013), “Self-focusing of Hermite-cosh Gaussian laser beam in a magnetoplasma with a ramp density profile”, *Phys. Plasmas*, **20**, 113109-7
- [92] Nanda, V., Kant, N., (2014), “Enhanced relativistic self-focusing of Hermite-cosh Gaussian laser beam in plasma under density transition”, *Phys. Plasmas*, **21**, 042101
- [93] Nanda, V., Kant, N., (2014), “Strong self-focusing of a cosh-Gaussian laser beam in collisionless magneto-plasma under plasma density ramp”, *Phys. Plasmas*, **21**, 072111
- [94] Aggarwal, M., Vij, S., Kant, N., (2014), “Propagation of cosh-Gaussian laser beam in plasma with density ripple in relativistic-ponderomotive regime”, *Optik*, **125**, 5081-5084

- [95] Jafari Milani, M. R., Niknam, A. R., Farahbod, A. H., (2014), "Ponderomotive self-focusing of Gaussian laser beam in warm collisional plasma", *Phy. Plasmas*, **21**, 063107
- [96] Malekshahi, M., Dorrnian, D., Askari, H. R., (2014), "Self-focusing of the high intensity ultra short laser pulse propagating through relativistic magnetized plasma", *Opt. Commun.* **332**, 227-232
- [97] Zare, S., Yazdani, E., Razaee, S., Anvari, A., Sadighi-Bonabi, R., (2015), "Relativistic self-focusing of intense laser beam in thermal collisionless quantum plasma with ramped density profile", *Phys. Rev. ST Accel. Beams*, **18**, 041301
- [98] Habibi, M., Ghamari, F., (2015), "Improved focusing of a cosh-Gaussian laser beam in quantum plasma: Higher order paraxial theory", *IEEE Trans. Plasma Sci.* **43**, 2160
- [99] Habibi, M., Ghamari, F., (2015), "Significant enhancement in self-focusing of high-power laser beam through dense plasmas by ramp density profile", *Opt. Soc. Am. B*, **32**, 1429
- [100] Aggarwal, M., Vij, S., Kant, N., (2015), "Self-focusing of quadruple Gaussian laser beam in an inhomogeneous magnetized plasma with ponderomotive nonlinearity: Effect of linear absorption", *Commun. Theor. Phys.* **64**, 565
- [101] Aggarwal, M., Vij, S., Kant, N., (2015), "Propagation of circularly polarized quadruple Gaussian laser beam in magnetoplasma", *Optik*, **126**, 5710
- [102] Aggarwal, M., Kumar, H., Kant, N., (2015), "Propagation of Gaussian laser beam through magnetized cold plasma with increasing density ramp", *Optik*, **127**, 2212
- [103] Varshney, M. A., Sen, S., Shukla, S., Bhargava, V., (2016), "Relativistic nonlinear propagation of rippled Gaussian laser beam in plasma", *Optik*, **127**, 1245-1250
- [104] Eslami, E., Nami, A. E., (2016), "Characteristics of self-focusing of a Gaussian laser pulse under lateral and axial plasma density variations", *IEEE Trans. Plasma Sci.* **44**, 226-231
- [105] Hora, H., (1975), "Theory of relativistic self-focusing of laser radiations in plasmas", *J. Opt. Soc. Am.* **65**, 882-886

- [106] Patil, S. D., Takale, M. V., Navare, S. T., Fulari, V. J., Dongare, M. B., (2012), “Relativistic self-focusing of cosh-Gaussian laser beams in a plasma”, *Opt. and Laser Tech.* **44**, 314-317
- [107] Olumi, M., Maraghechi, B., (2014), “Self-compression of intense short laser pulses in relativistic magnetized plasma”, *Phy. Plasmas*, **21**, 113102-5
- [108] Sati, P., Verma, U., Tripathi, V. K., (2014), “Self-focusing and frequency broadening of laser pulse in water”, *Phys. Plasmas*, **21**, 112110-6
- [109] Kaur, R., Gill, T. S., Mahajan, R., (2011), “Steady state self-focusing, self-modulation of laser beam in an inhomogeneous plasma”, *Optik*, **122**, 375-380
- [110] Casperson, L. W., Hall, D. G., Tovar, A. A., (1997), “Sinusoidal-Gaussian beams in complex optical systems”, *J Opt. Soc. Am. A*, **14**, 3341-8
- [111] Lu, B., Ma, H., Zhang, B., (1999), “propagation properties of cosh-Gaussian beams”, *Opt commun.* **164**, 269-76
- [112] Lu, B., Luo, S., (2000), “Beam propagation factor of hard-edge diffracted cosh-Gaussian beams”, *Opt commun.* **178**, 275-81
- [113] Akhmanov, S. A., Sukhorukov, A. P., Khokhlov, R. V., (1968), “Self-focusing and diffraction of light in a nonlinear medium”, *Sov. Phys. Uspekhi*, **10**, 619-636
- [114] Sodha, M. S., Ghatak, A. K., Tripathi, V. K., (1976), “Self-focusing of lasers in plasmas and semiconductors”, in: E. Wolf, (Ed.), *Progress in Optics. Vol. XIII.* North-Holland, Amsterdam, 169-333
- [115] Gupta, D. N., Hur, M. S., Suk, H., (2006), “Energy exchange during stimulated Raman scattering of a relativistic laser in a plasma”, *J Appl. Phys.* **100**, 103101
- [116] Sodha, M. S., Patel, L. A., Kaushik, S. C., (1979), “Self-focusing of a laser beam in an inhomogeneous plasma”, *Plasma Phys.* **21**, 1

- [117] Niknam, A. R., Hashemzadeh, M., Montazeri, M. M., (2010), “Numerical, investigation of ponderomotive force effect in an underdense plasma with a linear density profile”, IEEE Trans. Plasma Sci. **38**, 2390
- [118] Kant, N., Wani, M. A., (2015), “Density transition based self-focusing of cosh-Gaussian laser beam in plasma with linear absorption”, Commun. Theor. Phys. **64**, 103
- [119] Wani, M. A., Kant, N., (2014), “Self-focusing of Hermite-cosh-Gaussian (HchG) laser beams in plasma under density transition”, Advances in Optics, Article ID942750
- [120] Sadighi- Bonabi, R., Yazdani, E., Habibi, M., Lotfi, E., (2010), “Plasma density ramp for relativistic self-focusing of an intense laser: comment”, J. Opt. Soc. Am. B, **27**, 1731-4
- [121] Niknam, A. R., Hameshemzadeh, M., Shokri, B., (2009), “Weakly relativistic and ponderomotive effects on the density steepening in the interaction of an intense laser pulse with an underdense plasma”, Phys. Plasmas, **16**, 033105
- [122] Chen, X. L., Sudan, R. N., (1993), “Necessary and sufficient conditions for self-focusing of short intense laser pulse in underdense plasma”, Phys. Rev. Lett. **70**, 2082
- [123] Xiong-Ping, X., Lin, Y., (2012), “Effect of higher order axial electron temperature on self-focusing of electromagnetic pulsed laser beam in collisional plasma”, Commun. Theor. Phys. **57**, 873
- [124] Hassoon, K. I., Sharma, A. K., Khamis, R. A., (2010), “Relativistic laser self-focusing in a plasma with transverse magnetic field”, Phys. Scr. **81**, 025505
- [125] Singh, K. P., (2005), “Electron acceleration by a chirped short intense laser pulse in vacuum”, Appl. Phys. Lett. **87**, 254102
- [126] Khachatryan, A. G., Van Goor, F. A., Verschuur, J. W. J., Boller, K. J., (2005), “Effect of frequency variation on electromagnetic pulse interaction with charges and plasma”, Phys. Plasmas **12**, 062116

- [127] Ghotra, H. S., Kant, N., (2015), “Electron acceleration to GeV energy by a chirped laser pulse in vacuum in the presence of azimuthal magnetic field”, *Appl. Phys B*, **120**, 141
- [128] Yu, W., Yu, M. Y., Zhang, J., Xu, Z., (1998), “Harmonic generation by relativistic electrons during irradiance of a solid target by a short pulse ultra-intense laser”, *Phys. Rev. E*, **57**, R2531-R2534
- [129] Sprangle, P., Esarey, E., (1992), “Interaction of ultrahigh laser fields with beams and plasmas”, *Physics Fluids B*, **4**, 2241-2248
- [130] Wani, M. A., Kant, N., (2016), “Investigation of relativistic self-focusing of Hermite–cosine–Gaussian (HcosG) laser beam in collisionless plasma”, *Optik*, **127**, 4705
- [131] Barr, H. C., Chen, F. F., (1987), “Raman scattering in a nearly resonant density ripple”, *Phys. Fluids* **30**, 1180
- [132] Dahiya, D., Sajal, V., Sharma, A. K., (2007), “Phase-matched second and third harmonic generation in plasmas with density ripple”, *Physics of Plasmas*, **14**, 123104.
- [133] Kaur, S., Sharma, A. K., Ryu, C. M., (2008), “Nonlinear propagation of a short-pulse laser in a plasma with density ripple”, *Korean Phys. Soc.* **53**, 3768
- [134] Lin, M. W., Chen, Y. M., Pai, C. H., Kuo, C. C., Lee, K. H., Wang, J., Chen, S. Y., Lin, J. Y., (2006), “Programmable fabrication of spatial structures in a gas jet by laser machining with a spatial light modulator”, *Phys. Plasmas*, **13**, 110701
- [135] Patil, S. D., Takale, M. V., (2013), “Stationary self-focusing of Gaussian laser beam in relativistic thermal quantum plasma”, *Phys. Plasmas*, **20**, 072703
- [136] Misra, S., Mishra, S. K., Sodha, M. S., (2013), “Self-focusing of a Gaussian electromagnetic beam in a multi-ions plasma”, *Phys. Plasmas*, **20**, 103105
- [137] Tang, B., (2009), “Hermite-cosine-Gaussian beams propagating in uniaxial crystals orthogonal to the optical axis”, *J. Opt. Soc. Am. A*, **26**, 2480

- [138] Sodha, M. S., Mishra, S., Agarwal, S. K., (2007), “Self-focusing and cross-focusing of Gaussian electromagnetic beams in fully ionized collisional magnetoplasmas”, *Phys. Plasmas*, **14**, 112302
- [139] Stamper, J., (1991), “Review on spontaneous magnetic fields in laser-produced plasmas: Phenomena and measurements”, *Laser particle beams*, **9**, 841-862
- [140] Kostyukov, I. Y., Shvets, G., Fisch, N., Rax, J., (2002), “Magnetic field generation and electron acceleration in relativistic laser channel”, *Phys. Plasmas*, **9**, 636-648.
- [141] Shukla, P., Stenflo, L., (1989), “Filamentation instability of electromagnetic waves in magnetized plasmas”, *Phys. Fluids B*, **1**, 1926-1928.
- [142] Jha, P., Mishra, R. K., Upadhyaya, A. K., Raj, G., (2006), “Self-focusing of intense laser beam in magnetized plasma”, *Phys. Plasmas*, **13**, 103102
- [143] Jafari, M. J., Jafari Milani, M. R., Niknam, A. R., (2016), “Evolution of a Gaussian laser beam in warm collisional magnetoplasma”, *Phys. Plasmas*, **23**, 073119-10
- [144] Max, C. E., Arons, J., Langdon, A. B., (1974), “Self-modulation and self-focusing of electromagnetic waves in plasmas”, *Phys. Rev. Lett.*, **33**, 209.
- [145] Sodha, M. S., Faisal, M., Verma, M. P., (2009), “Effect of self-focusing on third harmonic generation by a Gaussian beam in a collisional plasma”, *Phys. Plasmas*, **16**, 082304.
- [146] Bharuthram, R., Parashar, J., Tripathi, V. K., (1999), “Transient and time periodic self-focusing of a laser beam in a plasma” *Phys. Plasmas*, **6**, 1611.
- [147] Gupta, D. N., Sharma, A. K., (2002), “Transient self-focusing of an intense short pulse laser in magnetized plasma”, *Phys. Scripta*, **66**, 262.
- [148] Nicholas, D. J., (1982), “Diffraction propagation of a light pulse through a high power laser system”, *Journal of Modern Optics*, **3**, 325-342.

[149] Mingwei, L., Hong, G., Bingju, Z., Liqiang, T., Xiaojuan, L., Yougen, Y., (2006), “Comparison of ponderomotive self-channeling and higher-order relativistic effects on intense laser beams propagating in plasma channels”, *Phys. Letts. A*, **352**, 457.

APPENDIX / LIST OF PUBLICATIONS

1. **Manzoor Ahmad Wani** and Niti Kant, “Self-focusing of Hermite-cosh-Gaussian (HchG) laser beams in plasma under density transition”, *Advances in Optics*, Vol. 2014, Article ID942750
2. Niti Kant and **Manzoor Ahmad Wani**, “Density transition based self-focusing of cosh-Gaussian laser beam in plasma with linear absorption”, *Commun. Theor. Phys.* **64** (2015), 103-107
3. **Manzoor Ahmad Wani** and Niti Kant, “Investigation of relativistic self-focusing of Hermite-cosine-Gaussian (HcosG) laser beam in collisionless plasma”, *Optik*, **127** (2016), 4705-4709
4. **Manzoor Ahmad Wani** and Niti Kant, “Nonlinear propagation of Gaussian laser beam in an inhomogeneous plasma under plasma density ramp”, *Optik*, **127** (2016), 6710-6714
5. **Manzoor Ahmad Wani** and Niti Kant, “Self-focusing / Defocusing of chirped Gaussian laser beam in collisional plasma with linear absorption”, *Commun. Theor. Phys.* **66** (2016), 349-354
6. **Manzoor Ahmad Wani** and Niti Kant, “Self-focusing of a laser beam in the rippled density magnetoplasma”, *Optik*, **128** (2016), 1-7
7. Niti Kant, **Manzoor Ahmad Wani** and Asheel Kumar, “Self-focusing of Hermite-Gaussian laser beams in plasma under plasma density ramp”, *Optics Commun.* **285**, (2012), 4483-4487
8. Vikas Nanda, Niti Kant and **Manzoor Ahmad Wani**, “Sensitiveness of decentered parameter for relativistic self-focusing of Hermite-Cosh-Gaussian laser beam in plasma”, *IEEE Transactions on Plasma Science*, **41**, (2013), 2251-2256
9. Vikas Nanda, Niti Kant and **Manzoor Ahmad Wani**, “Self-focusing of Hermite-cosh Gaussian laser beam in a magnetoplasma with a ramp density profile”, *Phys. Plasmas*, **20**, (2013), 113109-7

CONFERENCE PUBLICATIONS

1. **Manzoor Ahmad Wani** and Niti Kant, “Investigation of relativistic self-focusing of cosh–Gaussian laser beam in plasma using density transition”, ISBN: 978-93-83083-83—1, 82-86, High power coherent radiation generation & its interaction with matter, February 12-14, 2016, SATI, Vidisha (M. P) India.
2. Niti Kant and **Manzoor Ahmad Wani**, “Self-focusing of Hermite-cosine-Gaussian (HcosG) laser beams in plasma”, 11th Kudowa Summer School “Towards Fusion Energy” Kudowa Zdroj, Poland, June 11-15, 2012, p-169 (OP-27).

CONFERENCES ATTENDED

- 1 High power coherent radiation generation & its interaction with matter, February 12-14, 2016, SATI, Vidisha (M. P) India.
- 2 Exploring basic and applied sciences for next generation frontiers (EBAS), November 14-15, 2014, LPU, Phagwara, Punjab India.
- 3 Bhartiya Vigyan Sammelan and Expo (Science for Global Development), October, 11-14, 2012, LPU, Phagwara, Punjab India.
- 4 Science, Technology & Regional Development: Opportunities & Challenges, September, 17-19, 2012, University of Kashmir, Srinagar India.

BIODATA

Name : Manzoor Ahmad Wani
Father's Name : Abdul Aziz Wani
Mother's Name : Saja
Nationality : Indian
Date of Birth : 03. 02. 1982
Permanent Address : Village, Check Wazir Panoo, Tehsil & District Budgam
P. O. Arath, 191111 (Jammu & Kashmir)
Email : manzoorphysics@gmail.com

EDUCATIONAL QUALIFICATION:

Bachelor's degree : B. Sc. (Non-medical)
University : University of Kashmir, Srinagar
Year of award : 2003
Percentage : 59.16
Master's degree : M. Sc. (Physics)
University : University of Kashmir, Srinagar
Year of award : 2006
Percentage : 65.47
Bachelor's of Education : B. Ed.
University : University of Kashmir, Srinagar
Year of award : 2007
Percentage : 65.1

Master of Philosophy : M. Phil (Physics)
University : Lovely Professional University (LPU), Phagwara, Punjab, India
Year of award : 2010
CGPA : 8.57
Equivalent percentage : 77.13%

A Research Proposal
on
DENSITY TRANSITION BASED SELF-FOCUSING OF A SHORT PULSE LASER IN
PLASMA

Submitted to

LOVELY PROFESSIONAL UNIVERSITY

in partial fulfillment of the requirements for the award of degree of

DOCTOR OF PHILOSOPHY (Ph.D.) IN PHYSICS

Submitted by:

Supervised by:

Manzoor Ahmad Wani

Dr.Niti Kant

FACULTY OF TECHNOLOGY AND SCIENCES
LOVELY PROFESSIONAL UNIVERSITY
PUNJAB

INTRODUCTION

The self-focusing of laser beams in nonlinear optical media is a fascinating topic which has inspired theoretical and experimental interest. The self-focusing of laser beam plays an important role in a large no. of ultra-intense laser applications such as laser-driven fusion, laser-driven accelerators, x-ray lasers, electron acceleration in Wakefield, fast igniter concept of inertial confinement fusion etc. These applications require the pulse to propagate over several Rayleigh lengths in order to preserve an efficient interaction with the plasma. Also it is important to note that for above applications preformed plasma channels are required to guide the laser beam beyond the Rayleigh length, after which the beam expands infinitely in vacuum due to natural diffraction. Self-focusing of a laser beam in plasma has been examined by a number of authors. Two different mechanisms have been proposed. Self-focusing due to plasma density variations produced by ponderomotive forces and relativistic self-focusing due to Lorentz factor of the optical constants in the plasma. Self-focusing is very undesirable in laser fusion applications where it could prevent compression of fuel pellets. On the other hand the self-focusing of a laser beam in to a filament would provide an effective method of achieving the high flux densities required to study laser plasma interactions such as generation of electron-positron pairs. The self-focusing of a laser beam in plasma is being treated in terms of the ponderomotive acceleration due to the gradient of light intensity. The focusing of radiation within the first minima of diffraction sets a lower limit to the laser power which is of the order of 1MW for the usual lasers if cut-off density and a plasma temperature of about 10eV are assumed. Also it has been studied that in the presence of a magnetic wiggler of suitable period, a Gaussian laser beam resonantly generates a second harmonic in a plasma. The phase matching conditions for the process are satisfied for a specific value of wiggler period. The self-focusing of the fundamental pulse enhances the intensity of the second harmonic pulse. The harmonic undergoes periodic focusing in the plasma channel created by the fundamental wave.

When an intense laser radiation propagates through plasma the relativistic nonlinearities lead to self-focusing of the laser pulse when the laser power exceeds the critical power. Besides this, ponderomotive nonlinearity leading to plasma density perturbation is also expected to affect the focusing properties of the laser pulse. The intense laser beam sets the plasma electrons in relativistic quiver motion. Consequently, ponderomotive nonlinearity sets in, leading to electron density perturbation inside the plasma. This perturbation is caused due to $\mathbf{V} \times \mathbf{B}$ force that the radiation field exerts on the free plasma electrons. The effects of relativistic nonlinearity on the laser pulse as it traverses through partially stripped plasma have been studied in great detail. However, the effects of ponderomotive nonlinearity along with these effects have not been included. Since both the nonlinearities after the propagation of a laser beam through plasma, so it is important to study their combined effect.

The interaction of lasers with semiconductors has been a fascinating field of research for several decades. Semiconductors provide a compact and less expensive medium to model nonlinear phenomena encountered in laser-produced plasmas. The observation of self-focusing in semiconductors is of great relevance to the

practical applications and possibilities of optical limiting devices. In equilibrium, the temperature of the free carriers is the same as that of the crystal so that the net energy exchange between the carriers and the lattice of the crystal is zero. When an electric field is applied, the free carriers gain energies, which causes the temperature to be higher than that of the crystal in the steady state. For moderate values of the electric field, the increase in the temperature of the carriers is proportional to the square of the electric field. The change in temperature of the carriers leads to corresponding change in the effective mass of carriers. This effect is important for laser self-focusing in semiconductors. The high power laser plasma interaction continues to be a front line area of research. The significant interest is currently focused on laser interaction with atomic clusters. An intense short pulse laser quickly converts them in to plasma balls which expand rapidly under hydrodynamic expansion or coulomb explosion. As the electron density inside an expanding cluster decreases and approaches thrice the critical density, the electron response to the laser is resonantly enhanced and one observes a host of exciting phenomena e.g. strong absorption of laser energy, efficient generation of harmonics, self-focusing and energetic neutron production.

IMPORTANCE OF SELF FOCUSING:

The self- focusing of laser beam plays an important role in a large number of applications such as laser -driven fusion, laser-driven acceleration, x-ray lasers, optical harmonic generation, the production of quasi mono-energetic electron bunches, electron acceleration in wake-field, fast igniter concept of inertial confinement fusion etc. Self-focusing effect imposes a limit on the power that can be transmitted through an optical medium. It means self-focusing reduces the threshold for the occurrence of other nonlinear optical processes. Self-focusing often leads to damage in optical materials so it is a limiting factor in the design of high-power laser systems but it can be harnessed for the design of optical power limiters and switches. The ponderomotive force associated with an intense laser beam expels electrons radially and can lead to cavitation in plasma. Relativistic effects as well as ponderomotive expulsion of electrons modify the refractive index. For laser powers exceeding the critical power, the analysis of relativistic self-focusing indicates that a significant contraction of the spot size and a corresponding increase in intensity is possible. The self-focusing of a laser pulse in plasma with periodic density ripple has also been investigated. The effect of density ripple is to cause overall increase in the self-focusing length. The minimum spot size decreases with the wave number of the ripple. The relativistic self-focusing occurs almost instantaneously in the time of the order of a period of the optical oscillation, while the ponderomotive self-focusing arises later in time because of the motion of plasma from the axis of the beam. It is further observed that the self-focusing length decreases with increase in intensity of the beam. This is due to the fact that at relativistic intensity, a quasi-stationary magnetic field is generated, the pinching effect of which adds to self-focusing.

IMPORTANCE OF PLASMA DENSITY RAMP:

The plasma density ramp plays an important role during laser-plasma interaction. To achieve strong self-focusing, it is important to apply a specific plasma density profile that will have a good impact on the applications of laser-plasma interaction. Self-focusing of laser beam has been investigated under different plasma density ramp profiles. Under plasma density ramp, self-focusing becomes stronger and laser beam can propagate the distance much greater than the Rayleigh length. Under the plasma density ramp the ponderomotive self-focusing of a short laser pulse may acquire a minimum spot size due to the ponderomotive self-focusing. The self-focused laser pulse diffracts and focuses periodically because of the mismatch between the channel size and spot size. By slowly increasing the density, the oscillation amplitude of the laser spot size can be significantly reduced. As the laser propagates through the density ramp region, it sees a slowly narrowing channel. In such a case the oscillation amplitude of the spot size shrinks, while its frequency increases. Therefore, the laser pulse propagating in a plasma density ramp tends to become more focused. If there is no density ramp, the laser pulse is defocused due to the dominance of the diffraction effect. As the plasma density increases, self-focusing effect becomes stronger. It is because as the laser propagates through the density ramp region, it sees a slowly narrowing channel. In such an environment, the oscillation amplitude of the spot size shrinks, while its frequency increases. Also as the equilibrium electron density is an increasing function of the distance of propagation of the laser, the plasma dielectric constant decreases rapidly as the beam penetrates deeper and deeper in to the plasma. Consequently, the self-focusing effect is enhanced and the laser is more focused. However, the minimum plasma density is chosen in the assumption of underdense plasma. The length of plasma density ramp is considered to avoid the maximum defocusing of the laser and better focusing is observed by increasing the length of the density ramp. But the plasma density should not be much larger; otherwise, the laser can be reflected because of the over dense plasma effect. So, plasma density ramp plays an important role to make the self-focusing stronger. This kind of plasma density ramp may be observed in a gas jet plasma experiment.

REVIEW OF LITERATURE:

Interaction of a short pulse laser with plasma has been a fascinating field of research for last few decades. Self-focusing of intense laser light in plasma plays an important role in a large amount of high power laser applications, such as x-ray lasers, x-ray generation, laser-driven acceleration, high harmonic generation etc. Therefore, laser beams have always been an interesting area of research.

The first discussion of self-focusing of laser beams in plasma was published by *Askaryan (1962)*. He considered the energy momentum flux density of the laser beam at self-focusing, where the whole plasma has been expelled and where the pressure is balanced by the plasma pressure profile acting against the centre of the laser beam. Askaryan was able to compare the necessary optical intensities for compensating the gas dynamic pressure.

Hora (1969) studied the self-focusing of laser beams in plasma by ponderomotive forces and treated self-focusing of laser beams in plasma in terms ponderomotive acceleration due to the gradient of light intensity. The focusing of radiation within the first minima of diffraction sets a lower limit to the laser power which is of the order of 1MW for the usual lasers if cut-off density and a plasma temperature of about 10eV are assumed.

Sodha et al. (1974) investigated the self-focusing of a cylindrically symmetric Gaussian electromagnetic pulse in collision-less and collisional plasmas by considering the ponderomotive force and the non-uniform heating (and the consequent redistribution of electrons) as the sources of non-linearity. They considered that the duration of pulse is larger than the characteristic time of non-linearity. They found that the beam is focused in a moving filament. Because of relaxation effects the peak of the pulse is shifted to higher values in case of collisional plasmas and the pulse is severely distorted because of self-focusing; the shift of peak in the case of collision-less plasmas is not significant.

Siegrist (1976) studied self-focusing in plasma due to ponderomotive forces and relativistic effects. The propagation of intense laser pulses in a plasma discussed in terms of a constant shape paraxial-ray approximation. Self-focusing due to ponderomotive forces and relativistic effects investigated. It is found that the stationary self-focusing behaviour of each mechanism treated separately similar with several orders of magnitude difference in critical power. In stationary self-focusing due to the combined mechanisms, complete saturation of ponderomotive self-focusing prevents the occurrence of relativistic effects.

Cohen et al. (1991) investigated the dynamics of ponderomotive self-focusing in plasmas. They calculated the space-time evolution of non-linear self-focusing of a coherent electromagnetic beam in plasma. The parameters are considered for which the dominant non-linearity is the ponderomotive force and the plasma response is hydrostatic. The self-focusing can be important both for high-power lasers in inertial-confinement fusion applications and for heating of magnetically confined plasmas with intense, pulsed free electron lasers.

Hafizi et al. (2000) investigated the relativistic self-focusing and ponderomotive channelling of intense laser beams. The ponderomotive force associated with an intense laser beam expels electrons radially and can lead to cavitations in plasma. Relativistic effects as well as ponderomotive expulsion of electrons modify the refractive index. They derived an envelope equation for the laser spot size, using the source-dependent expansion method with Laguerre-Gaussian Eigen functions, and reduced to quadrature. The envelop equation is valid for arbitrary laser intensity within the long pulse, quasi-static approximation and neglects instabilities. They analyzed that a significant contraction of the spot size and a corresponding increase in intensity is possible for laser powers exceeding the critical power for relativistic self-focusing.

Nitikant and Sharma (2004) have seen the effect of pulse slippage on resonant second harmonic generation of a short pulse laser in plasma. In their work they found that process of second harmonic

generation of an intense short pulse laser in plasma is resonantly enhanced by the application of a magnetic wiggler. The laser imparts an oscillatory velocity to electrons and exerts a longitudinal ponderomotive force on them at $(2\omega_1, 2k_1)$, where ω_1 and k_1 are the frequency and the wave number of the laser, respectively. As the electrons acquire oscillatory velocity at the second harmonic, the wiggler magnetic field beats with it to produce a transverse second harmonic current at $(2\omega_1, 2k_1 + k_0)$, driving the second harmonic electromagnetic radiation. However, the group velocity of the second harmonic wave is greater than that of the fundamental wave, hence, the generated pulse slips out of the main laser pulse and its amplitude saturates

Varsheney et al. (2005) studied the relativistic self-focusing of a laser beam in inhomogeneous plasma. They have presents an analysis of relativistic self-focusing of intense laser radiation in an axially inhomogeneous plasma. The nonlinearity in the dielectric constant arises on account of the relativistic variation of mass for an arbitrary magnitude of intensity. An appropriate expression for the nonlinear dielectric constant has been used in the analysis of laser-beam propagation in the paraxial approximation for a circularly polarized wave. The variations of the beam width parameter with the propagation distance, the self-trapping condition and the critical power have been evaluated. It was seen that the laser beam width tends to attain a constant value depending upon the plasma inhomogeneity and the initial laser intensity. Numerical estimates are made for typical values of the laser–plasma interaction applicable for underdense and overdense plasmas.

Gupta and Suk (2007) studied enhanced focusing of laser beams in semiconductor plasmas, in which the beating of two co-propagating laser beams can resonantly excite a large amplitude plasma wave in a narrow gap semiconductor. The higher ponderomotive force on the electrons due to the plasma beat wave makes the medium highly nonlinear. As a result, the incident laser beam becomes self-focused due to the nonlinearity by the ponderomotive force. Further they showed the self-focusing and spot size evolution of the laser beam in semiconductor plasmas.

Agarwal and Sodha (2007) studied steady-state self-focusing of Gaussian electromagnetic beams in an inhomogeneous nonlinear medium: Effect of absorption and initial curvature of the beam and investigated the effect of linear absorption and initial curvature of an electromagnetic Gaussian beam on focusing/defocusing in an inhomogeneous nonlinear medium. It has been found that the maximum and minimum of the beam width keep decreasing with increase in distance of propagation (or absorption) till the beam becomes very weak and diverges steeply and penetration in an overdense medium also decreases with increasing absorption. Converging beams initially converge and then go in (1) the oscillatory divergence (2) self-focusing or (3) steady divergence mode depending up on the initial values of beam width and axial irradiance. The maximum penetration in an overdense medium has the highest values for $-0.7 < (\partial f/\partial z)_{\text{at } z=0} < 0.4$ and falls sharply, outside these limits.

Takale et al. (2009) studied the self-focusing and defocusing of TEM_{0p} Hermite-Gaussian laser beams in collision-less plasma and found that the nonlinearity in the dielectric constant is mainly due to the

ponderomotive force. They found that the modes with odd p -values defocus and that with even p -values exhibit oscillatory as well as defocusing character of beam width parameters variation during their propagation in collision-less plasma. Further they have used the parabolic wave equation approach for entire theoretical formulation and completed the numerical computation by using fourth order Runge-Kutta method. They obtained the differential equations for beam width parameters under paraxial approximation and observed perfectly synchronized periodic oscillations of beam width parameters in transverse directions in small scale spatial manipulations in optical trap.

Bonabi et al. (2009) studied improving the relativistic self-focusing of intense laser beam in plasma by using density transition. They analyzed the propagation of a Gaussian beam in underdense plasma with upward increasing density ramp and this causes the laser beam to become more focused and penetrations deep into the plasma by reduction of diffraction effect. In their work, they introduced a unique upward density ramp profile which increased self-focusing effect for intense laser system and the transverse variation of the wave packet decreased substantially. They derived an equation of spot size and computational curves were presented for self-focusing in underdense plasma. In the obtained optimized condition they showed that the intense laser beams can be focused down to diameters comparable to the laser wavelength. The closest value reported on focusing down to the Nd-glass laser wavelength which is an important step forward toward the aims proposed with the ambitious project of extreme light infrastructure. The effects of laser intensity on the self-focusing parameters were also investigated. Based on our more reliable derived equations and introducing more effective density profile, a much stronger focusing is observed and it could produce ultrahigh laser irradiance over distances much greater than the Rayleigh length which can be used for various applications.

Patil et al. (2009) studied the self-focusing of Cosh-Gaussian laser beams in a parabolic medium with linear absorption, the field distribution in the medium is expressed in terms of beam width parameter, decentered parameter and absorption coefficient. They established the differential equation for beam width parameter by following WKB and paraxial approximations through parabolic wave equation approach and analytical solution is obtained for the same. The behavior of beam width parameter with the normalized distance of propagation is studied at various values of decentered parameter with different absorption levels in the medium. Their results show that the sharp self-focusing occurs on account of absorption. Further they suggested that depending up on the desirability of self-focusing effect in a particular application, the decentered parameter of Cosh-Gaussian beams can be exploited with appropriate absorption level in a parabolic medium.

Xiong et al. (2010) investigated the influence of arbitrary outside magnetic field on self-focusing of short intense laser pulse propagating in underdense and magnetized cold plasma. They set the outside magnetic field in the plane that includes y and z -axis and used the angle between y -axis and outside magnetic field. Their results show that there is a different effect on self-focusing corresponding to different angle and intensity.

Patil et al. (2010) investigated the focusing of Hermit-Cosh-Gaussian (HChG) laser beams in collision-less magneto-plasma by considering ponderomotive nonlinearity. They presented the dynamics of the combined effects of nonlinearity and spatial diffraction and plotted the beam width parameter with distance of propagation for highlighting the nature of focusing and discussed the effect of mode index and decentered parameter on self-focusing of beams. They found that the self-focusing/defocusing of HChG beams is dependent on the mode index and decentered parameter.

Gill et al. (2010) while studying the propagation of high power electromagnetic beam in relativistic magnetoplasma with higher order paraxial ray theory found that such a theory explains the phenomenon of ring formation in self-focusing followed by bright and dark rings.

Kaur et al. (2011) studied steady state self-focusing, self-modulation of laser beam in an inhomogeneous plasma and found that increasing power density leads to trapping of particle in the potential. Further, they found that by increasing control parameters, strong self-focusing is observed. However, there are no chances for the beam to collapse.

Kant et al. (2011) analyzed the ponderomotive self-focusing of a short laser pulse under a plasma density ramp and found that the ponderomotive self-focusing becomes stronger when plasma density ramp taken into account. They found that, for a given laser spot size, the oscillation amplitude becomes larger for a higher plasma density. By slowly increasing the density, the oscillation amplitude of the laser spot size can be significantly reduced. As the laser propagates through the density ramp region, it sees a slowly narrowing channel. In such a case the oscillation amplitude of the spot size shrinks, while its frequency increases. Therefore, the laser pulse propagating in a plasma density ramp tends to become more focused. If there is no density ramp, the laser pulse is defocused due to the dominance of the diffraction effect. As the plasma density increases, self-focusing effect becomes stronger. Similarly as in case of no density ramp, the beam width parameter does not increase much. After several Rayleigh lengths, the beam width parameter attains a minimum value and maintains it for a long distance. Consequently, the self-focusing effect is enhanced and the laser pulse is more focused.

Navare et al. (2012) investigated the impact of linear absorption on self-focusing of Gaussian laser beam in collisional plasma and concluded that by considering the nonlinearity in dielectric constant mainly due to the elastic electron-ion collision, it is observed that absorption plays a vital role in self-focusing of laser beams, there by weakens the oscillatory behaviour of beam width parameter with the distance of propagation.

Kant et al. (2012) while studying the self-focusing of Hermite- Gaussian laser beams in plasma under plasma density ramp found that the effect of plasma density ramp and initial intensity of the laser beam are important and play a vital role in laser plasma interaction and hence in strong self-focusing of laser beam.

Habibi et al. (2012) studied the stationary self-focusing of intense laser beam in cold quantum plasma using ramp density profile and found that in addition to quantum effects, the density transition causes much higher oscillation and better focusing of laser beam in cold quantum plasma than in classical relativistic case.

Patil et al. (2012) investigated relativistic self-focusing of Cosh-Gaussian laser beams in a plasma and concluded that self-focusing occurs for decentered parameter $b = 0, 1$ and all other curves are seen to exhibit sharp self-focusing for $b = 2$. Further, for such a beam the pinching effect becomes stronger by increasing the values of decentered.

Nanda et al. (2013) investigated the self-focusing of Hermite-Cosh Gaussian laser beam in a magnetoplasma with a ramp density profile and concluded that the presence of plasma density ramp and magnetic field enhances the self-focusing effect to a greater extent.

Mahajan et al. (2013) studied the interaction between two parallel Gaussian electromagnetic beams in a plasma with weakly relativistic ponderomotive regime and concluded that when the axis of two beams are initially parallel along z-axis in the xz plane, oscillatory self-focusing takes place in all the three cases. However, defocusing of two beams is also observed for a chosen set of parameters and the difference increases with increase in propagation distance.

Patil et al. (2013) analysed the self-focusing of Gaussian laser beam in weakly relativistic and ponderomotive regime using upward ramp of plasma density, WKB and paraxial approximations through parabolic equation approach. They found that upward plasma density ramp tends to enhance self-focusing significantly and the beam gets more focused while traversing several Rayleigh lengths as compared with uniform density relativistic plasma.

Kaur et al. (2013) while studying the interaction between parallel Gaussian electromagnetic beams in relativistic magnetoplasma found that self-focusing occurs only at lower values of propagation distance. However, with increase in propagation distance, defocusing of the beam occurs.

Nanda et al. (2013) studied the sensitiveness of decentered parameter for relativistic self-focusing of Hermite-Cosh-Gaussian laser beam in plasma and found that the proper selection of decentered parameter was very much sensitive to self-focusing.

Patil et al. (2013) studied self-focusing of Gaussian laser beam in relativistic cold quantum plasma and observed that quantum effects play vital role in laser plasma interaction. Further while comparing the self-focusing effect in quantum plasma with the classical relativistic case, they found that quantum effects produce better self-focusing than classical ones.

Nanda et al. (2014) while studying the enhanced relativistic self-focusing of Hermite- Cosh Gaussian laser beam in plasma under density transition observed that the proper selection of decentered parameter and presence of density transition results stronger self-focusing of laser beam.

Liu et al. (2014) investigated the electron energy spectrum in circularly polarized laser irradiated overdense plasma and found that the evanescent field profile of a circularly polarized short pulse laser gets significantly modified because of relativistic mass variation and ponderomotive force. While ignoring the space charge field effects, the ponderomotive force pushes the electrons in the skin layer and transfers the quiver energy exactly in to the streaming energy.

Aggarwal et al. (2014) studied the self-focusing of Cosh Gaussian laser beam in plasma with density ripple in relativistic ponderomotive regime under paraxial approximation and concluded that there is decrease in self-focusing of the beam with increase in wavelength, intensity and ripple wave number of the beam. Further, by optimising these parameters, a strong self-focusing is observed.

OBJECTIVES

1. Self-focusing of Hermite-Cosh-Gaussian laser beams in plasma under density transition

ABSTRACT

Self-focusing of Hermite-Cosh-Gaussian (HChG) laser beam in plasma under density transition has been discussed here. The field distribution in the medium is expressed in terms of beam width parameters and decentered parameter. The differential equations for the beam width parameters are established by a parabolic wave equation approach under paraxial approximation. To overcome the defocusing, localized upward plasma density ramp is considered and to discuss the nature of self-focusing, the behaviour of beam width parameters with dimensionless distance of propagation for various values of decentered parameters is examined by numerical estimates. The results are presented graphically and the effect of plasma density ramp and decentered parameter on self-focusing of the beams has been discussed.

Theoretical considerations

We employed the propagation of HChG laser beam along z -axis in the plasma with the field distribution in the following form:

$$E(r, z) = \frac{E_0}{2f} H_m \left(\frac{\sqrt{2}r}{r_0 f} \right) \exp(b^2 / 4) \left\{ \exp \left[- \left(\frac{r}{r_0 f} + \frac{b}{2} \right)^2 \right] + \exp \left[- \left(\frac{r}{r_0 f} - \frac{b}{2} \right)^2 \right] \right\} \quad (1)$$

where m is the mode index associated with the Hermite Polynomial H_m , r_0 is the waist width of Gaussian amplitude distribution, b is the decentered parameter, r is the radial coordinate, E_0 is the amplitude of Gaussian beams for the central position at $r=z=0$, $A_0(r,z)$ is the amplitude of HChG beams in cylindrical coordinates and f is the dimensionless beam-width parameter, which is a measure of both axial intensity and width of the beam.

Nonlinear dielectric constant

Further, we consider propagation of HChG laser beam in a nonlinear medium characterized by dielectric constant of the form

$$\varepsilon = \varepsilon_0 + \Phi(EE^*) \quad (2) \text{ With } \varepsilon_0 = 1 - \omega_p^2 / \omega^2, \omega_p^2 = 4\pi n(\xi) e^2 / m$$

$$\text{And } n(\xi) = n_0 \text{Tan}(\xi / d), \xi = z / R_d \quad (3)$$

$$\varepsilon_0 = 1 - (\omega_{p0}^2 / \omega^2) \text{Tan}(\xi / d), \omega_{p0}^2 = 4\pi n_0 e^2 / m \quad (4)$$

where ε_0 and Φ represents the linear and nonlinear parts of dielectric constant respectively, ω_p is plasma frequency, e is the electronic charge, m be the electron mass, n_0 is the equilibrium electron density, R_d is the diffraction length, ξ is the normalized propagation distance, d is a dimensionless adjustable parameter.

Now, in case of collision-less plasma, the nonlinearity in the dielectric constant is mainly due to ponderomotive force and the nonlinear part of dielectric constant is given by

$$\Phi(AA^*) \approx (1/2)\varepsilon_2 A_0^2 \quad (5) \text{ With } \varepsilon_2 = 2(\omega_p^2 / \omega^2)\alpha; \alpha = e^2 M / 6m^2 \omega^2 K_b T_0$$

Where M is the mass of scatterer in the plasma, ω is the frequency of laser used, K_b is the Boltzmann constant and T_0 is the equilibrium plasma temperature.

Self-focusing

The wave equation governing the propagation of laser beam may be written as

$$\nabla^2 \mathbf{E} + \left(\frac{\omega^2}{c^2} \right) \varepsilon \mathbf{E} + \nabla \left(\frac{E \nabla \varepsilon}{\varepsilon} \right) = 0 \quad (6)$$

The last term of equation (6) on left hand side can be neglected provided that $k^{-2} \nabla^2 (\ln \varepsilon) \ll 1$ where ' k ' represents the wave number. Thus,

$$\nabla^2 \mathbf{E} + \left(\frac{\omega^2}{c^2} \right) \varepsilon \mathbf{E} = 0 \quad (7)$$

Now, employing Wentzel-Kramers-Brillouin (WKB) approximation, equation (7) reduces to a parabolic wave equation as:

$$\frac{i\omega}{c} \left(2\sqrt{1 - \frac{\omega_{p0}^2}{\omega^2} \tan^2(z/dR_d)} - \frac{\frac{\omega_{p0}^2}{\omega^2} z \sec^2(z/dR_d)}{dR_d \sqrt{1 - \frac{\omega_{p0}^2}{\omega^2} \tan^2(z/dR_d)}} \right) \left(\frac{\partial A}{\partial z} \right) - \frac{\frac{\omega_{p0}^2}{\omega^2} A \sec^2(z/dR_d)}{dR_d \sqrt{1 - \frac{\omega_{p0}^2}{\omega^2} \tan^2(z/dR_d)}} - \frac{\frac{\omega_{p0}^2}{\omega^2} A z \sec^2(z/dR_d)}{d^2 R_d^2 \sqrt{1 - \frac{\omega_{p0}^2}{\omega^2} \tan^2(z/dR_d)}} \left(\tan(z/dR_d) + \frac{\frac{\omega_{p0}^2}{\omega^2} \sec^2(z/dR_d)}{4 \left(1 - \frac{\omega_{p0}^2}{\omega^2} \tan^2(z/dR_d) \right)} \right)$$

$$= \frac{\omega^2}{c^2} \left(\frac{\frac{\omega_{p0}^2}{\omega^2} Az \text{Sec}^2(z/dR_d)}{dR_d} - \frac{\left(\frac{\omega_{p0}^2}{\omega^2}\right)^2 Az^2 \text{Sec}^4(z/dR_d)}{4d^2 R_d^2 \left(1 - \frac{\omega_{p0}^2}{\omega^2} \text{Tan}(z/dR_d)\right)} \right)$$

$$\frac{\partial^2 A}{\partial r^2} + \frac{1}{r} \frac{\partial A}{\partial r} + \frac{\omega^2}{c^2} \Phi(AA^*)A \quad (8)$$

To solve equation (8) we express A as

$$A = A_0(r, z) \exp[-iks(r, z)] \quad (9)$$

Where, $k = \frac{\omega}{c} \sqrt{1 - \frac{\omega_{p0}^2}{\omega^2} \text{Tan}(z/dR_d)}$ and ' A_0 ' and ' S ' are real functions of r and z with $S(r, z)$ as eikonal of the beam which determines convergence/divergence of the beam. Substituting for A from equation (9) in equation (8) and equating real and imaginary parts on both sides of the resulting equation, one obtains:

$$\begin{aligned} \frac{c^2}{\omega^2 A_0} \left(\frac{\partial^2 A_0}{\partial r^2} + \frac{1}{r} \frac{\partial A_0}{\partial r} \right) + \Phi(A_0^2) &= \left(2 \left(1 - \frac{\omega_{p0}^2}{\omega^2} \text{Tan}(z/dR_d) \right) - \frac{\omega_{p0}^2}{\omega^2} \frac{z \text{Sec}^2(z/dR_d)}{dR_d} \right) \frac{\partial S}{\partial z} \\ &+ \left(1 - \frac{\omega_{p0}^2}{\omega^2} \text{Tan}(z/dR_d) \right) \left(\frac{\partial S}{\partial r} \right)^2 - \frac{\omega_{p0}^2}{\omega^2} \frac{\text{Sec}^2(z/dR_d)}{dR_d} \left(S + z - \frac{\omega_{p0}^2}{\omega^2} \frac{z \text{Sec}^2(z/dR_d)(S - z/2)}{2dR_d \left(1 - \frac{\omega_{p0}^2}{\omega^2} \text{Tan}(z/dR_d) \right)} \right) \end{aligned} \quad (10)$$

And

$$\begin{aligned} \left(1 - \frac{\omega_{p0}^2}{\omega^2} \frac{z \text{Sec}^2(z/dR_d)}{2dR_d \left(1 - \frac{\omega_{p0}^2}{\omega^2} \text{Tan}(z/dR_d) \right)} \right) \frac{\partial A_0^2}{\partial z} + \frac{\partial S}{\partial r} \frac{\partial A_0^2}{\partial r} + \left(\frac{\partial^2 S}{\partial r^2} + \frac{1}{r} \frac{\partial S}{\partial r} \right) A_0^2 \\ - \left(\frac{\omega_{p0}^2}{\omega^2} \frac{\text{Sec}^2(z/dR_d)}{dR_d \sqrt{1 - \frac{\omega_{p0}^2}{\omega^2} \text{Tan}(z/dR_d)}} + \frac{\omega_{p0}^2}{\omega^2} \frac{z \text{Sec}^2(z/dR_d) \text{Tan}(z/dR_d)}{d^2 R_d^2 \sqrt{1 - \frac{\omega_{p0}^2}{\omega^2} \text{Tan}(z/dR_d)}} \right) A_0^2 \end{aligned}$$

$$-\left(\frac{\omega_{p0}^2}{\omega^2}\right)^2 \left(\frac{z \text{Sec}^4(z/dR_d)}{4d^2 R_d^2 \left(1 - \frac{\omega_{p0}^2}{\omega^2} \text{Tan}(z/dR_d)\right)} \right) A_0^2 = 0 \quad (11)$$

The solutions of equations (10) and (11) for a cylindrically symmetric HChG beam can be written as:

$$S = \frac{r^2}{2} \beta(z) + \Phi(z) \quad (12)$$

And

$$A_0^2 = \frac{E_0^2}{4f^2} H_m^2 \left(\frac{\sqrt{2}r}{r_0 f} \right) \exp(b^2/2) \times \left\{ \exp \left[-2 \left(\frac{r}{r_0 f} + \frac{b}{2} \right)^2 \right] + \exp \left[-2 \left(\frac{r}{r_0 f} - \frac{b}{2} \right)^2 \right] + 2 \exp \left[- \left(\frac{2r^2}{r_0^2 f^2} + \frac{b^2}{2} \right) \right] \right\} \quad (13)$$

$$\text{with } \beta(z) = \frac{1}{f(z)} \frac{\partial f}{\partial z}$$

where $\beta(z)$ is the inverse radius of curvature of wave front and $\Phi(z)$ is the phase shift.

Under the paraxial approximation, we have established the differential equation of the beam-width parameter for the $m=0$ mode as,

$$\begin{aligned} & \left(1 - \frac{\omega_{p0}^2}{\omega^2} \text{Tan}(\xi/d) \right) \left(\frac{6b^2}{(2-b^2)f} \right) + \frac{\alpha E_0^2}{2} \left(\frac{r_0 \omega}{c} \right)^2 \left(\frac{\omega_{p0}^2}{\omega^2} \right) \left(1 - \frac{\omega_{p0}^2}{\omega^2} \text{Tan}(\xi/d) \right) \frac{\text{Tan}(\xi/d)}{f^3} \\ & = \left[\left(\frac{\omega_{p0}^2}{\omega^2} \right) \text{Tan}(\xi/d) + \left(\frac{\omega_{p0}^2}{\omega^2} \right) \frac{\xi \text{Sec}^2(\xi/d)}{2d} - 1 \right] \frac{\partial^2 f}{\partial \xi^2} - \left[\left(\frac{\omega_{p0}^2}{\omega^2} \right) \frac{\xi \text{Sec}^2(\xi/d)}{2d} \right] \frac{1}{f} \left(\frac{\partial f}{\partial \xi} \right)^2 \\ & + \left(\frac{\omega_{p0}^2}{\omega^2} \right) \frac{\text{Sec}^2(\xi/d)}{2d} \left[1 - \left(\frac{\omega_{p0}^2}{\omega^2} \right) \frac{\xi \text{Sec}^2(\xi/d)}{2d \left(1 - \left(\frac{\omega_{p0}^2}{\omega^2} \right) \text{Tan}(\xi/d) \right)} \right] \end{aligned} \quad (14)$$

Equations (14) is the required expression for beam width parameters f .

2. Self-focusing of Hermite-Cosine-Gaussian(HCosG) Laser Beams in Plasma Using density Transition

ABSTRACT

We present the self-focusing of Hermite-Cosine-Gaussian (HCosG) laser beam in plasma under density transition by considering ponderomotive nonlinearity. Analytical formulas for propagation of HCosG beam in plasma are derived. The field distribution in the medium is expressed in terms of beam width parameters and decentered parameter. To overcome the defocusing, localized upward plasma density ramp is considered. To highlight the nature of self-focusing, plot of beam width parameters versus dimensionless distance of propagation will be obtained for different laser and plasma parameters and hence the effect of plasma density ramp and decentered parameter on self-focusing of the beams will be discussed.

THEORETICAL CONSIDERATIONS

Considering the Hermite-Cosine-Gaussian (HCosG) laser beam propagating along z-axis with the field distribution in the following form

$$E(x, y, z) = \frac{E_0}{\sqrt{f_1(z)f_2(z)}} H_m\left(\frac{\sqrt{2}x}{r_0 f_1(z)}\right) H_n\left(\frac{\sqrt{2}y}{r_0 f_2(z)}\right) \exp\left[-\left(\frac{x^2}{r_0^2 f_1^2(z)} + \frac{y^2}{r_0^2 f_2^2(z)}\right)\right] \text{Cos}\left(\frac{\Omega_0 x}{f_1(z)}\right) \text{Cos}\left(\frac{\Omega_0 y}{f_2(z)}\right) \quad (1)$$

Where H_m or H_n is the mth-order or nth order Hermite polynomial, E_0 is the constant amplitude, r_0 is the waist width, Ω_0 is the parameter associated with the cosine function, $f_1(z)$ and $f_2(z)$ are the beam width parameters in x and y directions.

Nonlinear dielectric constant

Further we consider the propagation of HCosG laser beam in plasma characterized by dielectric constant of the form¹⁴

$$\varepsilon = \varepsilon_0 + \Phi(EE^*) \quad (2)$$

With $\varepsilon_0 = 1 - \omega_p^2 / \omega^2$, $\omega_p^2 = 4\pi n(\xi)e^2 / m$

And $n(\xi) = n_0 \text{Tan}(\xi / d)$, $\xi = z / R_d$ (3)

$$\varepsilon_0 = 1 - (\omega_{p0}^2 / \omega^2) \text{Tan}(\xi / d), \omega_{p0}^2 = 4\pi n_0 e^2 / m \quad (4)$$

Where ε_0 and Φ represents the linear and nonlinear parts of dielectric constant respectively, ω_p is plasma frequency, e is the electronic charge, m be the electron mass, n_0 is the equilibrium electron density, R_d is the diffraction length, ξ is the normalized propagation distance, d is a dimensionless adjustable parameter.

Now, in case of collision-less plasma, the nonlinearity in the dielectric constant is mainly due to ponderomotive force and the nonlinear part of dielectric constant is given by¹⁵

$$\Phi(EE^*) = \frac{\omega_{p0}^2}{\omega^2} \left[1 - \exp\left(-\frac{3}{4} \frac{m}{M} \alpha EE^*\right) \right] \text{Tan}(\xi/d) \quad (5)$$

Where $\alpha = e^2 M / 6 m^2 \omega^2 K_b T_0$ and M is the mass of scatterer in the plasma, ω is the frequency of laser used, K_b is the Boltzmann constant and T_0 is the equilibrium plasma temperature.

Self-focusing

The wave equation governing the propagation of laser beam may be written as

$$\nabla^2 \mathbf{E} + \left(\frac{\omega^2}{c^2} \right) \varepsilon \mathbf{E} + \nabla \left(\frac{E \nabla \varepsilon}{\varepsilon} \right) = 0 \quad (6)$$

The last term of equation (5) on left hand side can be neglected provided that $k^{-2} \nabla^2 (\ln \varepsilon) \ll 1$ Where ' k ' represents the wave number. Thus,

$$\nabla^2 \mathbf{E} + \left(\frac{\omega^2}{c^2} \right) \varepsilon \mathbf{E} = 0 \quad (7)$$

This equation is solved by employing Wentzel-Kramers-Brillouin (WKB) approximation.

Employing the WKB approximation, Equation (7) reduces to a parabolic wave equation as:

$$\begin{aligned} \left(\frac{\partial^2 A}{\partial x^2} \right) + \left(\frac{\partial^2 A}{\partial y^2} \right) + \frac{\omega^2}{c^2} \Phi(AA^*) A = \frac{i}{c} \left(\frac{2 dR_d (\omega^2 - \omega_{p0}^2 \text{Tan}(z/dR_d)) - \omega_{p0}^2 z \text{Sec}^2(z/dR_d)}{2 dR_d \sqrt{\omega^2 - \omega_{p0}^2 \text{Tan}(z/dR_d)}} \right) \left(\frac{\partial A}{\partial z} \right) \\ - \frac{i A \omega_{p0}^2 \text{Sec}^2(z/dR_d)}{c dR_d \sqrt{\omega^2 - \omega_{p0}^2 \text{Tan}(z/dR_d)}} \left(1 + \frac{\omega_{p0}^2 z}{4 dR_d (\omega^2 - \omega_{p0}^2 \text{Tan}(z/dR_d))} + \frac{z \text{Tan}(z/dR_d)}{dR_d} \right) \\ - \frac{i A \omega_{p0}^2 \text{Sec}^2(z/dR_d)}{c dR_d \sqrt{\omega^2 - \omega_{p0}^2 \text{Tan}(z/dR_d)}} \left(\frac{z \omega_{p0}^2 \text{Tan}^2(z/dR_d)}{4 dR_d (\omega^2 - \omega_{p0}^2 \text{Tan}(z/dR_d))} \right) - \frac{A \omega_{p0}^2 z \text{Sec}^2(z/dR_d)}{c^2 dR_d} \end{aligned}$$

$$+ \frac{A\omega_{p0}^4 z^2 \text{Sec}^4(z/dR_d)}{4c^2 d^2 R_d^2 (\omega^2 - \omega_{p0}^2 \text{Tan}(z/dR_d))} \quad (8)$$

To solve equation (8) we express A as

$$A(x, y, z) = A_{mn}(x, y, z) \exp[-iks(x, y, z)] \quad (9)$$

$$\text{Where, } k = \frac{\omega}{c} \sqrt{1 - \frac{\omega_{p0}^2}{\omega^2} \text{Tan}(z/dR_d)}$$

Where ‘ A_{mn} ’ and ‘ S ’ are real functions of x , y and z . substituting for $A(x, y, z)$ from equation (9) in equation (8) and equating real and imaginary parts on both sides of the resulting equation, one obtains:

Real part

$$\begin{aligned} \frac{1}{\omega^2 A_{mn}} \left(\frac{\partial^2 A_{mn}}{\partial x^2} + \frac{\partial^2 A_{mn}}{\partial y^2} \right) + \frac{\Phi(A_{mn}^2)}{c^2} &= \left(\frac{\omega^2 - \omega_{p0}^2 \text{Tan}(z/dR_d)}{\omega^2 c^2} \right) \left(\left(\frac{\partial S}{\partial x} \right)^2 + \left(\frac{\partial S}{\partial y} \right)^2 \right) \\ \frac{1}{\omega^2 c^2} \left(\omega^2 - \omega_{p0}^2 \text{Tan}(z/dR_d) + \frac{\omega_{p0}^2 z \text{Sec}^2(z/dR_d)}{2dR_d} \right) \left(\frac{\partial S}{\partial z} \right) &- \frac{\omega_{p0}^2 S \text{Sec}^2(z/dR_d)}{2\omega^2 c^2 dR_d} \left(1 + \frac{2z}{S} \right) \\ + \frac{\omega_{p0}^2 S \text{Sec}^2(z/dR_d)}{2\omega^2 c^2 dR_d} \left(1 + \frac{z}{S} \right) &\left(\frac{\omega_{p0}^2 z \text{Sec}^2(z/dR_d)}{2dR_d (\omega^2 - \omega_{p0}^2 \text{Tan}(z/dR_d))} \right) \end{aligned} \quad (10)$$

Imaginary part

$$\begin{aligned} \left(\frac{\partial^2 S}{\partial x^2} + \frac{\partial^2 S}{\partial y^2} \right) A_{mn}^2 + \left(\frac{\partial A_{mn}^2}{\partial x} \right) \left(\frac{\partial S}{\partial x} \right) + \left(\frac{\partial A_{mn}^2}{\partial y} \right) \left(\frac{\partial S}{\partial y} \right) + \frac{1}{2} \left(1 - \frac{\omega_{p0}^2 z \text{Sec}^2(z/dR_d)}{2dR_d (\omega^2 - \omega_{p0}^2 \text{Tan}(z/dR_d))} \right) \frac{\partial A_{mn}^2}{\partial z} \\ - \frac{\omega_{p0}^2 A_{mn}^2 \text{Sec}^2(z/dR_d)}{dR_d (\omega^2 - \omega_{p0}^2 \text{Tan}(z/dR_d))} \left(1 + \frac{\omega_{p0}^2 z}{4dR_d (\omega^2 - \omega_{p0}^2 \text{Tan}(z/dR_d))} \right) \\ - \frac{\omega_{p0}^2 A_{mn}^2 \text{Sec}^2(z/dR_d)}{dR_d (\omega^2 - \omega_{p0}^2 \text{Tan}(z/dR_d))} \left(\frac{\omega_{p0}^2 z \text{Tan}^2(z/dR_d)}{4dR_d (\omega^2 - \omega_{p0}^2 \text{Tan}(z/dR_d))} + \frac{z \text{Tan}(z/dR_d)}{dR_d} \right) = 0 \end{aligned} \quad (11)$$

The solutions of equations (10) and (11) can be written as:

$$S = \frac{x^2}{2} \beta_1(z) + \frac{y^2}{2} \beta_2(z) + \Phi(z) \quad (12)$$

$$A_{mn}^2 = \frac{E_0^2}{f_1(z)f_2(z)} H_m \left(\frac{\sqrt{2}x}{r_0 f_1(z)} \right) H_n \left(\frac{\sqrt{2}y}{r_0 f_2(z)} \right) \exp \left[- \left(\frac{x^2}{r_0^2 f_1^2(z)} + \frac{y^2}{r_0^2 f_2^2(z)} \right) \right] \text{Cos} \left(\frac{\Omega_0 x}{f_1(z)} \right) \text{Cos} \left(\frac{\Omega_0 y}{f_2(z)} \right) \quad (13)$$

And

$$\beta_1(z) = \frac{1}{f_1(z)} \left(\frac{\partial f_1}{\partial z} \right) \quad ; \quad \beta_2(z) = \frac{1}{f_2(z)} \left(\frac{\partial f_2}{\partial z} \right) \quad (14)$$

Where $\beta_1(z)$ and $\beta_2(z)$ represent the curvature of the wavefront in x and y directions. Now, considering the first mode ($m=0, n=0$) and employing the paraxial approximation to obtain expressions for the beam width parameters f_1 and f_2 as:

$$\begin{aligned} & \left(1 - \frac{\omega_{p0}^2}{\omega^2} \text{Tan}(\xi/d) \right) \left(\frac{2}{f_1^3} \right) - \left(\frac{r_0 \omega}{c} \right)^2 \left(\frac{\omega_{p0}^2}{\omega^2} \right) \left(1 - \frac{\omega_{p0}^2}{\omega^2} \text{Tan}(\xi/d) \right) \left(\frac{3}{2} \right) \left(\frac{m}{M} \right) \left(1 + \frac{b^2}{2} \right) (\alpha E_0^2) \text{Tan}(\xi/d) \frac{1}{f_1^2 f_2} \exp \left(- \frac{3m\alpha E_0^2}{4Mf_1 f_2} \right) \\ & = \left[1 - \left(\frac{\omega_{p0}^2}{\omega^2} \right) \text{Tan}(\xi/d) + \left(\frac{\omega_{p0}^2}{\omega^2} \right) \frac{\xi \text{Sec}^2(\xi/d)}{2d} \right] \frac{\partial^2 f_1}{\partial \xi^2} + \left[1 - \left(\frac{\omega_{p0}^2}{\omega^2} \right) \text{Tan}(\xi/d) - \left(\frac{\omega_{p0}^2}{\omega^2} \right) \frac{\xi \text{Sec}^2(\xi/d)}{2d} \right] \frac{1}{f_1} \left(\frac{\partial f_1}{\partial \xi} \right)^2 \\ & + \left(\frac{\omega_{p0}^2}{\omega^2} \right) \frac{\text{Sec}^2(\xi/d)}{2d} \left[\left(\frac{\omega_{p0}^2}{\omega^2} \right) \frac{\xi \text{Sec}^2(\xi/d)}{2d \left(1 - \frac{\omega_{p0}^2}{\omega^2} \text{Tan}(\xi/d) \right)} - 1 \right] \left(\frac{\partial f_1}{\partial \xi} \right) \end{aligned} \quad (15)$$

And

$$\begin{aligned} & \left(1 - \frac{\omega_{p0}^2}{\omega^2} \text{Tan}(\xi/d) \right) \left(\frac{2}{f_2^3} \right) - \left(\frac{r_0 \omega}{c} \right)^2 \left(\frac{\omega_{p0}^2}{\omega^2} \right) \left(1 - \frac{\omega_{p0}^2}{\omega^2} \text{Tan}(\xi/d) \right) \left(\frac{3}{2} \right) \left(\frac{m}{M} \right) \left(1 + \frac{b^2}{2} \right) (\alpha E_0^2) \text{Tan}(\xi/d) \frac{1}{f_2^2 f_1} \exp \left(- \frac{3m\alpha E_0^2}{4Mf_1 f_2} \right) \\ & = \left[1 - \left(\frac{\omega_{p0}^2}{\omega^2} \right) \text{Tan}(\xi/d) + \left(\frac{\omega_{p0}^2}{\omega^2} \right) \frac{\xi \text{Sec}^2(\xi/d)}{2d} \right] \frac{\partial^2 f_2}{\partial \xi^2} + \left[1 - \left(\frac{\omega_{p0}^2}{\omega^2} \right) \text{Tan}(\xi/d) - \left(\frac{\omega_{p0}^2}{\omega^2} \right) \frac{\xi \text{Sec}^2(\xi/d)}{2d} \right] \frac{1}{f_2} \left(\frac{\partial f_2}{\partial \xi} \right)^2 \\ & + \left(\frac{\omega_{p0}^2}{\omega^2} \right) \frac{\text{Sec}^2(\xi/d)}{2d} \left[\left(\frac{\omega_{p0}^2}{\omega^2} \right) \frac{\xi \text{Sec}^2(\xi/d)}{2d \left(1 - \frac{\omega_{p0}^2}{\omega^2} \text{Tan}(\xi/d) \right)} - 1 \right] \left(\frac{\partial f_2}{\partial \xi} \right) \end{aligned} \quad (16)$$

Where $b = r_0 \Omega_0$ is called decentered parameter and ξ is the dimensionless distance of propagation. Equations (15) and (16) are the required expressions for beam width parameters f_1 and f_2 respectively.

3. Plasma density ramp for Steady-State Self-focusing of Gaussian electromagnetic beams in an inhomogeneous nonlinear medium

ABSTRACT

Steady-state self-focusing of Gaussian electromagnetic beams in an inhomogeneous nonlinear medium under plasma density ramp is discussed here. The differential equation for the beam width parameter is established by a parabolic wave equation approach under paraxial approximation. To discuss the nature of self-focusing, the behaviour of beam width parameters with dimensionless distance of propagation is examined by numerical estimates and the effect of plasma density ramp on self-focusing of the beams is discussed.

Nonlinear dielectric constant

The nonlinear dielectric function ϵ in an isotropic inhomogeneous medium can be expressed as:

$$\epsilon = \epsilon_r(z, EE^*) - i\epsilon_i(z, EE^*) \dots \dots \dots (1)$$

Where in general ϵ_r and ϵ_i are functions of r and the irradiance EE^* (E is the amplitude of the electric vector); in this paper ϵ is assumed to vary only along the z direction.

The saturating nature of ϵ_r may be expressed as

$$\epsilon_r(z, EE^*) = \epsilon_0(z) + \epsilon_s \mu(z) \frac{\epsilon_2 EE^*}{1 + \epsilon_2 EE^*} \dots \dots \dots (2)$$

or,

$$\epsilon_r(z, EE^*) = \epsilon_0(z) + \epsilon_s \mu(z) \left[1 - \exp\left(\frac{-\epsilon_2 EE^*}{\epsilon_s}\right) \right] \dots \dots \dots (3)$$

Where ϵ_0 and μ are functions of z and ϵ_2 and ϵ_s are constants characteristic of the medium and frequency of radiation.

For the case of plasma, the function $\mu(z)$ may be identified with the plasma frequency; in this case

$$\epsilon_0(z) = 1 - \left[\frac{\omega_p^2(0)}{\omega^2} \right] \mu(z) \dots \dots \dots (4)$$

and

$$\varepsilon_i(z) = \mu(z)\varepsilon_i(0).....(5)$$

Where

$$\mu(z) = \left(\frac{\omega_p^2(z)}{\omega_p^2(0)} \right) = \frac{\omega_p^2}{\omega_p^2(0)} \text{ and } \varepsilon_s = \left(\frac{\omega_p^2(z)}{\omega_p^2(0)} \right) = \frac{\omega_p^2(0)}{\omega^2}(6)$$

$$\text{with } \omega_p^2 = 4\pi n(\xi)e^2 / m \quad \text{and} \quad n(\xi) = n_0 \text{Tan}(\xi / d).....(6a)$$

$$\text{Therefore } \omega_p^2 = (4\pi n_0 e^2 / m) \text{Tan}(\xi / d) = \omega_p^2(0) \text{Tan}(\xi / d); \omega_p^2(0) = 4\pi n_0 e^2 / m$$

$$\text{Hence} \quad \mu(z) = \frac{\omega_p^2}{\omega_p^2(0)} = \text{Tan}(\xi / d)$$

ω_p is the plasma frequency, the suffix zero refers to $z=0$ and ω is the wave frequency, ε_i is the characteristic of absorption in the medium and has been considered as independent of the irradiance in this paper; $\mu(z)$ is characteristic of the density of dipoles.

In case of plasmas the saturation of ε_r conforms to all electrons, driven from the axis. In case of Gaussian beam EE^* and hence ε is a function of r^2 , therefore ε can in the paraxial approximation be expanded in powers of r^2 and the series, terminated at the term, having r^2 . Thus

$$\varepsilon_r(z) = \varepsilon_{r0}(z) - r^2 \varepsilon_{r2}(z).....(7)$$

Analysis and Self-focusing

Consider the propagation of laser beam having Gaussian intensity distribution, with z -axis assumed to be in the direction of propagation. The amplitude of the electric vector E satisfies the scalar wave equation

$$\frac{\partial^2 E}{\partial z^2} + \left\{ \frac{\partial^2}{\partial r^2} + \frac{1}{r} \frac{\partial}{\partial r} \right\} E + \frac{\omega^2}{c^2} \varepsilon(r, z) E = 0.....(8)$$

Where c is the speed of light in vacuum.

Eq. (8) can be solved in the paraxial approximation by following the analysis of Akhmanov *et al.* [17] and its extension by Sodha *et al.* [18, 19].

The solution of equation (8) is of the form

$$E(r, z) = A(r, z) \exp \left[-\int_0^z ik(z) dz \right](9)$$

Where $A(r,z)$ is the complex amplitude of the electric field and

$$k^2(z) = \frac{\omega^2}{c^2} \varepsilon_{r_0}(z) \dots \dots \dots (10)$$

Substituting for $E(r,z)$ from Eq. (9) in Eq.(8) and neglecting $(\partial^2 A/\partial z^2)$ in the WKB approximation, one obtains

$$-2ik \frac{\partial A}{\partial z} - iA \frac{\partial k}{\partial z} - k^2 A + \frac{\partial^2 A}{\partial r^2} + \frac{1}{r} \frac{\partial A}{\partial r} + \frac{\omega^2}{c^2} \varepsilon(r, z) A = 0 \dots \dots \dots (11)$$

To solve equation (11) in the paraxial approximation, the complex amplitude $A(r, z)$ may be expressed as

$$A(r, z) = A_0(r, z) \exp[-ik(z)s(r, z)] \dots \dots \dots (12)$$

Where A_0 and S are real and the eikonal S is given by

$$S(r, z) = \frac{r^2}{2} \beta(z) + \Phi(z) \dots \dots \dots (13a)$$

The function $\beta(z)$ may be expressed as

$$\beta(z) = \frac{1}{f(z)} \left(\frac{\partial f}{\partial z} \right) \dots \dots \dots (13b)$$

Where $\beta(z)$ represents the curvature of the wavefront.

Substituting for $A(r,z)$ and S from Eqs. (12) and (13), ε from Eqs. (1) and (7) in Eq. (11) and equating real and imaginary parts on both sides of resulting equation, one obtains:

Real part

$$2 \frac{\partial S}{\partial z} + \left(\frac{\partial S}{\partial r} \right)^2 + \left(\frac{2S}{k} \right) \frac{\partial k}{\partial z} = \frac{1}{k^2 A_0} \left(\frac{\partial^2 A_0}{\partial r^2} + \frac{1}{r} \frac{\partial A_0}{\partial r} \right) - \frac{r^2 \varepsilon_{r_2}(z)}{\varepsilon_{r_0}(z)} \dots \dots \dots (14)$$

Imaginary part

$$\frac{\partial A_0^2}{\partial z} + A_0^2 \left(\frac{\partial^2 S}{\partial r^2} + \frac{1}{r} \frac{\partial S}{\partial r} \right) + \frac{\partial A_0^2}{\partial r} \frac{\partial S}{\partial r} = A_0^2 \left(\frac{-k \tan(z/dR_d) \varepsilon_i(0)}{\varepsilon_{r_0}(z)} - \frac{1}{k} \frac{\partial k}{\partial z} \right) \dots \dots \dots (15)$$

The solution of Eq. (15) is

$$A_0^2(r, z) = Const. \left[\frac{\varepsilon_{r_0}(0)}{\varepsilon_{r_0}(z)} \right]^{1/2} \frac{1}{f^2(z)} \mathfrak{I} \left(\frac{r}{r_0 f(z)} \right) \exp \left[- \int_0^z \frac{\varepsilon_i}{\sqrt{\varepsilon_{r_0}}} \frac{\omega}{c} dz \right]$$

$$= \left(\frac{E_0^2(z)}{f^2(z)} \right) \mathfrak{F} \left(\frac{r}{r_0 f(z)} \right) \dots \dots \dots (16)$$

Where \mathfrak{F} is an arbitrary function and $E_0^2(z)$ is the axial ($r = 0$) irradiance.

For an initially Gaussian beam at $z = 0$

$$EE^* = A_0^2 = E_{00}^2 \exp \left(\frac{-r^2}{r_0^2} \right) \dots \dots \dots (17)$$

Comparing Eqs. (16) and (17) at $z = 0$

$$EE^* = A_0^2(r, \xi) = \frac{E_{00}^2}{f^2(\xi)} \left(\frac{\varepsilon_{r_0}(0)}{\varepsilon_{r_0}(\xi)} \right)^{1/2} \exp \left(\frac{-r^2}{r_0^2 f^2(\xi)} \right) \exp \left[- \int_0^\xi \frac{\varepsilon_i \rho^2 d\xi}{\sqrt{\varepsilon_{r_0}(\xi)}} \right] \dots \dots (18)$$

Where $\xi = (c / \omega r_0^2) z$ and $\rho = (r_0 \omega / c)$ are the dimensionless distance and beam width; the parameter $(\omega r_0^2 / c)$ is known as the Rayleigh length.

Substituting for A_0^2 from Eq. (18) in Eq. (14) and equating the coefficients of r^2 on both sides of the resulting equation, one obtains

$$\frac{\partial^2 f}{\partial \xi^2} = - \frac{\rho^2}{f} \left[\varepsilon'_{r_2} - \frac{1}{\rho^2 f^2} \right] - \frac{1}{2\varepsilon_{r_0}} \left(\frac{\partial f}{\partial \xi} \right) \left(\frac{\partial \varepsilon_{r_0}}{\partial \xi} \right) \dots \dots \dots (19)$$

$$\text{Where } \varepsilon'_{r_2} = r_0^2 f^2 \varepsilon_{r_2} \left(\frac{E_0^2}{f^2} \right) \dots \dots \dots (19a)$$

Thus, with a knowledge of the dependence of ε'_{r_2} on f and on ξ , Eq. (19) could be solved for the beam width parameter f as a function of ξ .

Expanding $A_0^2(r, z)$ from Eq. (16) in a series of r^2 and retaining terms up to r^2 (in the paraxial approximation)

$$EE^* = \frac{E_0^2}{f^2} \left(1 - \frac{r^2}{r_0^2 f^2} \right) \dots \dots \dots (20)$$

Substituting for EE^* from Eq. (20) in Eq. (2) one obtains

$$\varepsilon_{r_0} = \varepsilon_0(z) + \varepsilon_s \text{Tan} \left(z / dR_d \right) \frac{(\varepsilon_2 E_0^2 / f^2)}{1 + (\varepsilon_2 E_0^2 / f^2)} \dots \dots \dots (21)$$

and

$$\varepsilon'_r = \frac{\varepsilon_s \varepsilon_2 E_0^2 \text{Tan}(z/dR_d)}{1 + \varepsilon_2 E_0^2 / f^2} \dots\dots\dots(21a)$$

Using Eq. (21) and (21a) in Eq. (19) we get

$$\frac{\partial^2 f}{\partial \xi^2} = -\frac{\rho^2}{f} \left[\frac{\varepsilon_s \varepsilon_2 E_0^2 \text{Tan}(\xi/d)}{1 + \varepsilon_2 E_0^2 / f^2} - \frac{1}{\rho^2 f^2} \right] + \left[\frac{1}{1 - \varepsilon_s \text{Tan}(\xi/d) + \frac{\varepsilon_s \varepsilon_2 E_0^2 \text{Tan}(\xi/d)}{f^2 + \varepsilon_2 E_0^2}} \right] \times$$

$$\left[\frac{f^2 \text{Sec}^2(\xi/d)}{2d} + \frac{\varepsilon_2 E_0^2 f \text{Tan}(\xi/d)}{f^2 + \varepsilon_2 E_0^2} \left(\frac{\partial f}{\partial \xi} \right) \right] \frac{\varepsilon_s}{f^2 + \varepsilon_2 E_0^2} \left(\frac{\partial f}{\partial \xi} \right) \dots\dots\dots(22)$$

Equation (22) is the required equation for the beam width parameter f .

4. Relativistic self-focusing of Hermite-Gaussian laser beams in plasma with density transition

ABSTRACT

Propagation of Hermite-Gaussian laser beam in a collision-less plasma with density transition has been investigated by taking in to account the relativistic effect. The differential equation for beam width parameter is obtained by using paraxial approach. The spot size of the laser beam decreases as the beam penetrates in to the plasma due to the role of a plasma density ramp. Since the laser beam shows an oscillatory self-focusing and defocusing behavior with the propagation distance. The density ramp could be important for the self-focusing of a high-power laser by choosing the suitable laser and plasma parameters. To reduce the defocusing, localized upward plasma density ramp is introduced, so that the self-focusing becomes stronger. The effect of plasma density ramp and relativistic factor on self-focusing is seen.

5. Effect of plasma density ramp on self-focusing of Cosh-Gaussian laser beams in plasma with linear absorption

ABSTRACT

Propagation of Cosh-Gaussian laser beam in plasma with linear absorption has been investigated by taking in to account the density transition. The differential equation for beam width parameter is obtained by using paraxial approach. To reduce the defocusing, localized upward plasma density ramp is introduced, so that the self-focusing becomes stronger. The effect of plasma density ramp and linear absorption on self-focusing is seen.

6. Effect of linear absorption and plasma density ramp on self-focusing of Gaussian laser beam in collisional plasma.

ABSTRACT

We will investigate the impact of linear absorption on self-focusing of Gaussian laser beam in collisional plasma under plasma density ramp. A second order differential equation of dimensionless beam width parameter will be derived and solved numerically. The effect of plasma density ramp and linear absorption on self-focusing will be discussed.

METHODOLOGY:

1. FORMULATION OF HYPOTHESIS

The hypothesis for the above problems is that we apply plasma density ramp to laser beams in plasma to see its effect on self-focusing. The differential equations for the beam width parameters have to be derived and solved numerically by using MATHEMATICA software. The variation of beam width parameters with normalized propagation distance ξ , has to be plotted in ORIGIN software.

2. SOURCES OF DATA

Theoretical results will be compared with experimental results collected through various research papers.

3. RESEARCH DESIGN:

Theoretical analysis

TOOLS:

MATHEMATICA and ORIGIN software

REFERENCES

- [1] Agarwal, S. K.; Sodha, M. S.; (2007), “Steady-state self-focusing of Gaussian electromagnetic beams in an inhomogeneous nonlinear medium: effect of absorption and initial curvature of the beam”, *Optik*, **118**, 367
- [2] Aggarwal, M.; Vij, S.; Kant, N.; (2014), “Propagation of Cosh Gaussian laser beam in plasma with density ripple in relativistic-ponderomotive regime”, *Optik*, **125**, 5081
- [3] Askaryan, G. A.; (1962), “Effects of the gradient of strong electromagnetic beam on electrons and atoms”, *Sov. Phys. JETP*, **15**, 1088
- [4] Bruce, I.; Cohen, Barbara, F.; Lasinski, A.; Bruce, L.; Jullian, C. Cummings.; (1991), “Dynamics of ponderomotive self-focusing in plasmas”, *Phys. Fluids B*, **3**, 766
- [5] Gill, T. S.; Kaur, R.; Mahajan, R.; (2010), “propagation of high power electromagnetic beam in relativistic magnetoplasma: Higher order paraxial ray theory”, *Phy. Of plasmas*, **17**, 093101
- [6] Gupta, D. N.; Suk, H.; (2007), “Enhanced focusing of laser beams in semiconductor Plasmas”, *Appl. Phys.* **101**, 043109
- [7] Habibi, M.; Ghamari, F.; (2012), “Stationary self-focusing of intense laser beam in cold quantum plasma using ramp density profile”, *Phy. Of Plasmas*, **19**, 103110
- [8] Hafizi, B.; Ting, A.; Sprangle, P.; Hubbard, R. F.; (2000), “Relativistic focusing and ponderomotive channeling of intense laser beams”, *Phys. Rev. E*, **62**, 4120
- [9] Hora, H.; (1969), “self-focusing of laser beams in a plasma by ponderomotive forces”, *Z. Physik.* **226**, 156
- [10] Kant, N.; Saralch, S.; Singh, H.; (2011), “Ponderomotive self-focusing of a short laser pulse under a plasma density ramp”, *Nukleonika*, **56**, 149
- [11] Kant, N.; Wani, M. A.; Kumar, A.; (2012), “Self-focusing of Hermite- Gaussian laser beams in plasma under plasma density ramp”, *Opt.Comm.* **285**, 4483
- [12] Kaur, R.; Gill, T. S.; Mahajan, R.; (2011), “steady state self-focusing, self-modulation of laser beam in an inhomogeneous plasma”, *Optik*, **122**, 375
- [13] Kaur, R.; Gill, T. S.; Mahajan, R.; (2013), “Interaction between parallel Gaussian electromagnetic beams in relativistic magnetoplasma”, *Opt. Commun.* **289**, 127
- [14] Liu, C. S.; Tripathi, V. K.; Shao, X.; Kumar, p.; (2014), “Electron energy spectrum in circularly polarized laser irradiated overdense plasma”, *Phy. Of plasmas*, **21**, 103109

- [15] Mahajan, R.; Gill, T. S.; Kaur, R.; (2013), “Interaction between parallel Gaussian electromagnetic beams in a plasma with weakly relativistic-ponderomotive regime”, *Optik*, **124**, 2686
- [16] Nanda, V.; Kant, N.; Wani, M. A.; (2013), “Self-focusing of Hermite-Cosh Gaussian laser beam in a magnetoplasma with a ramp density profile”, *Phy. of Plasmas*, **20**, 113109
- [17] Nanda, V.; Kant, N.; Wani, M. A.; (2013), “Sensitiveness of decentered parameter for relativistic self-focusing of Hermite-Cosh-Gaussian laser beam in plasma”, *IEEE Trans. on Plasma Sc.* **41**, 2251
- [18] Nanda, V.; Kant, N.; (2014), “Enhanced relativistic self-focusing of Hermite- Cosh Gaussian laser beam in plasma under density transition”, *Phy. of Plasmas*, **21**, 042101
- [19] Navare, S.T.; Takale, M.V.; Patil, S.D.; Fulari, V. J.; Dongare, M. B.; (2012), “Impact of linear absorption on self-focusing of Gaussian laser beam in collisional plasma”, *Opt. and Lasers in Engineering*, **50**, 1316
- [20] Nitikant and Sharma, A.K.; (2004), “Effect of pulse slippage on resonant second harmonic generation of a short pulse laser in a plasma”, *J. Phys. D:Appl. Phys.* **37**, 998
- [21] Patil, S.D.; Navare, S.T.; Takale, M.V.; Dongare, M. B.; (2009), “Self-focusing of Cosh-Gaussian laser beams in parabolic medium with linear absorption”, *Opt. and Lasers in Engineering*, **47**, 604
- [22] Patil, S.D.;Takale, M.V.; Navare, S. T.; Dongare, M. B.; (2010), “Focusing of Hermite-cosh-Gaussian laser beams in collision-less magneto plasma”, *Laser and Particle Beams*, **28**, 343
- [23] Patil, S.D.;Takale, M.V.; (2013), “Self-focusing of Gaussian laser beam in weakly relativistic and ponderomotive regime using upward ramp of plasma density”, *Phy. Of plasmas*, **20**, 083101
- [24]Patil, S.D.;Takale, M.V.; Navare, S. T.; Dongare, M. B.; Fulari, V. J.; (2013), “Self-focusing Gaussian laser beam in relativistic cold quantum plasma”, *Optik*, **124**, 180
- [25] Patil, S.D.;Takale, M.V.; Navare, S. T.; Fulari, V. J.; Dongare, M. B.; (2012), “Relativistic self-focusing Cosh-Gaussian laser beams in a plasma”, *Opt. and Laser Tech.* **44**, 314
- [26] Sadighi-Bonabi, R.; Habibi, M.; Yazdani, E.; (2009), “Improving the relativistic self-focusing of intense laser beam in plasma using density transition”, *Phys. Plasmas*, **16**, 083105
- [27] Siegrist, M. R.; (1976), “Self focusing in plasma due to ponderomotive forces and relativistic effects”, *Opt. Commun.* **16**, 402
- [28] Sodha, M. S.; Prasad, S.; Tripathi, V. K.; (1974), “Nonstationary Self-focusing of a

Gaussian pulse in a plasma”, J. Appl. Phys. **46**, 637

[29] Takale, M.V.; Navare, S.T.; Patil, S.D.; Fulari, V.J.; Dongare, M. B.; (2009), “Self-focusing and defocusing of TEM_{0p}Hermite-Gaussian laser beams in collision-less Plasma”, Opt. Commun. **282**, 3157

[30] Varshney, M.; Qureshi, K. A.; Varshney, D.; (2005), “Relativistic self-focusing of a laser beam in an inhomogeneous plasma”, Journal of Plasma Phys. **72**, 195

[31] Xiong, H.; Liu, S.; Liao, J.; Liu, X.; (2010), “Self-focusing of laser pulse propagating in magnetized plasma”, Optik, **121**, 1680

